Cortical excitability : Prefrontal conditional bistability for parametric working memory in physiological and Alzheimer's Disease conditions & Somatosensory epileptic network activity following neurodevelopmental interneuron mutations

Morgane Leroux

Ph.D. THESIS

for the degree of Doctor of Philosophy in Neuroscience

Cortical excitability: Prefrontal conditional bistability for parametric working memory in physiological and Alzheimer's disease conditions & Somatosensory epileptic network activity following neurodevelopmental interneuron mutations

---

by **Morgane Leroux**

The J. David Gladstone Institutes (GIND, UCSF, U.S.A.)
The Institute of Intelligent Systems and Robotics (UMR7222, Sorbonne Université, France)
Doctoral School n°158 "Brain, Cognition and Behaviour" (Sorbonne Université, France)

Ph.D. thesis committee:

Suliann BEN HAMED, directrice de recherche Institut des Sciences Cognitives M. Jeannerod, Université Claude Bernard Lyon 1 (France)	Reviewer
Valérie CREPEL, directrice de recherche Institut de Neurobiologie de la Méditerranée, Université Aix-Marseille (France)	Reviewer
Thierry BAL, directeur de recherche Institut des Neurosciences Paris-Saclay, Université Paris-Saclay (France)	Examiner
Emmanuel PROCYK, directeur de recherche Stem cell and Brain Research Institute, Université Claude Bernard Lyon 1 (France)	Examiner
Bruno DELORD, professeur universitaire Institut des Systèmes Intelligents et de Robotique, Sorbonne Université (France)	Co-Supervisor
Jeanne PAZ, associate investigator The J. David Gladstone Institutes, University of California San Francisco (U.S.A.)	Co-Supervisor

ISIR INSTITUT DES SYSTÈMES INTELLIGENTS ET DE ROBOTIQUE
SORBONNE UNIVERSITÉ
GLADSTONE INSTITUTES
UCSF University of California San Francisco

“It is because I had fallen very low that I was able to climb so high.”
Junko Tabei, the first woman to climb the peak of Everest on May 16, 1975

***To my friends**,*
who are under no obligation to read this thesis

ACKNOWLEDGEMENTS

This thesis is the result of the last four and a half years of research during which I traveled between the Institute of Intelligent Systems and Robotics, at Sorbonne Université in Paris (France), and the J. David Gladstone Institutes in San Francisco (United States).

As I am sure a lot of my graduate student friends will relate, the process of preparing a Ph.D. is a roller coaster. You perform an experiment filled with hope and innocence, you redo the same experiment because you noticed too late that your recording electrode had an issue, and you redo it a third time because you developed a better stimulation protocol for the purpose of your science. This is how a theoretical 6-month-long experiment becomes a 1.5-year-long one. The downs are tough, but the ups are worth it all. I am really proud of the research I conducted during the past years. But research is not something you do alone in your corner. Whether you are part of my scientific or personal life, I feel grateful for all of you who were by my side during those past years.

First of all, I would like to thank my two advisors, Pr. Bruno Delord and Dr. Jeanne Paz. **Bruno**, thank you for trusting me with this project when I was a Master student. Thank you for the advice and guidance you have provided me over the past years. Thank you also for the meaningful, sometimes philosophical, conversations we shared, particularly at the beginning of my Ph.D. and during the two weeks you spent in San Francisco with David. **Jeanne**, thank you for your unlimited support. Without your confidence in my abilities and encouragement to grow as a scientist and to believe in myself, I would not be the person I am today. Thank you for your valuable ideas and advice for my Ph.D. thesis project. Thank you for challenging me intellectually and trusting me to work on multiple collaborations. But most important, thank you for leading a lab in which major values are prioritized: doing excellent research and celebrating each milestone, small or big, with champagne!

I would like to thank Suliann Ben Hamed, Valérie Crépel, Thierry Bal, and Emmanuel Procyk for accepting to read this thesis and be part of my thesis defense committee. **Suliann** and **Valérie**,

thank you for accepting to review this Ph.D. thesis, and **Thierry** and **Emmanuel**, thank you for your time and guidance during those past four years.

Many thanks to the Gladstone community. I truly realize how lucky I was to evolve in such a stimulating and caring environment. Thank you to the Facility Team who always had a solution to my technical issues, specifically **John** and **Marco** who helped me more than once to open a sealed oxygen tank at 7am. Thank you to the IT Team for making our lives easier.

Deepek, thank you for creating such a great place to work. I will remember the bonfires on the beach in Asilomar, the dance floor on fire during the Holiday Party, and the Halloween costume contest (and the Paz Lab's unfair defeat). **Jennifer**, thank you for your unconditional support, and **Dr. Mahley**, thank you for your guidance and mentoring. **Francoise**, thank you for your perspective and help on so many grant applications and scientific papers. Thank you for our precious discussions over coffee and waffles, your generosity, and friendship.

Pendant mes années d'étude, j'ai pu compter sur le soutien sans faille de ma famille. Merci **Maman** pour tes encouragements, merci de t'être toujours intéressée à ce que j'étudiais et merci de m'avoir soutenu quand j'ai déménagé à Paris puis à San Francisco. **Yvon**, **marraine** et **tonton Jean-Pierre**, merci merci merci pour tout le soutien pendant ces années.

Having one foot on each side of the Atlantic Ocean was challenging on multiple aspects (I don't recommend conducting an international Ph.D. project during the peak of a global pandemic). However, I really think that, in the end, I got the best of both worlds. Wherever I was working in France or in the US, I was supported by amazing human beings.

I am so grateful for all the former and current members of the Paz Lab I got the chance to work with. During all those years, I was surrounded by brilliant scientists, who have bright minds and big hearts. **Irene**, thank you for your warm welcome when I arrived in San Francisco in January 2019, and for making sure I never feel lonely. **Agnieszka** and **Jeremy**, thank you for your kindness and unique humor. **Yuliya**, thank you for our many scientific discussions, but most of all for our non-scientific talks. **Alexis**, thank you for your good mood and the Friday happy

hours. **Britta** and **Clare**, thank you for your many precious advice and kindness. **Isaac** and **Drew**, thank you for the fun moments. **Audrey**, thank you for being such a trustworthy person. **Vivi**, thank you for your contagious energy and generosity.

Thank you for the moments spent with some or all of you: the karaoke nights, the Friday happy hours, the coffee and boba breaks, the gossips at the cubicles, the board game and movie nights, the birthday parties, the scientific retreats in Asilomar, the 'champagne moment' at the Holiday Party, and the Paz Lab retreat in Tahoe. I will cherish these memories for all my life.

Stephanie and **Frances**, Pazettes #2 and #3, but also my grad buddies: thank you a thousand times. I can't imagine what those past years would have looked like if you were not part of them. You taught me how to patch, you were always available to answer my many questions and to help me when the rig was not cooperative. I learned so much from listening to your many amazing scientific presentations. Inside and outside the lab, your friendship was really precious. I loved our weekend trips to Seattle/Portland and Monterey Bay. Stephanie, I will miss our cooking/movie nights. Frances, thank you for all the French food adventures in SF and Palo Alto.

Même en passant la majorité des cinq dernières années à plus de 9000 kilomètres d'eux, j'ai eu la chance de pouvoir compter sur d'incroyables copains et copines!

Merci à mes amis du lycée Victor Hugo, **Cécile**, **Alan**, **Adrien**, **Hugo**, **Marjorie**, **Marianne**, **Gwendal** et **Alexandre**, d'avoir grandi à mes côtés. Peut-être que vous ne vous en rendez pas compte, mais tous les petits moments passés avec vous m'ont aidé à garder les batteries chargées pendant la thèse. Alors, merci pour les soirées, les après-midis jeux de société et les dîners à la crêperie. **Rémi** et **Quentin**, merci pour ces moments de pur bonheur en Mai et Juin 🤘 **Vincent** et **Cha**, que dire après toutes ces années… Merci pour votre amitié sans faille, pour les heures passées au téléphone à se raconter nos vies à l'autre bout du monde et pour les moments partagés quand je rentrais en France.

Charlotte, merci pour les soirées à Brest et à Port-Louis, les vacances en Italie et à Vienne, les festivals Interceltiques, les finales de l'Eurovision, et tous ces repas partagés. **JB**,

merci pour tous nos débats et discussions depuis la L3, parler pendant des soirées entières avec toi au fil des années m'a enrichi d'une manière inimaginable.

David, mon partenaire de début de thèse, je voudrais d'abord te remercier d'avoir été un super binôme de travail! Mais au-delà de ça, ton amitié et ta gentillesse ont été plus que précieuses. **Eléonore**, l'année dernière on s'est littéralement vu aux quatre coins du monde! C'est fou quand même! Merci pour ton accueil en Janvier, les balades à pied et à vélo, les lattes par dizaines et ton écoute de chaque instant. **Nicolas**, à chaque fois que je vois un canard, je pense à toi… Merci d'être toi, tu mérites le meilleur.

Virginie, dire que ce sont les TPs de Neuroscience en M1 qui nous ont rapprochés! Et depuis, on a continué à grandir ensemble. Merci pour ta bienveillance, ta grande tolérance, et tous les repas/goûters/soirées partagées. **Ségolène**, merci pour les nombreux conseils et ton avis toujours réfléchi et posé sur les situations. Merci pour La Réunion, San Diego, Anza-Borrego et Joshua Tree. J'ai déjà hâte de venir te voir aux Pays-Bas! Le monde de la recherche est chanceux de t'avoir, il me tarde de voir les futures découvertes que tu feras.

I would like to finish by thanking "la crème de la crème". You already know everything and, of course, I will never be able to capture your whole awesomeness in just a few lines, but I can try. **Deedee**, you are one of the cleverest people I have ever met. You made me grow on so many different levels. I think we debated for three hours straight in the car when we came back from LA… Probably without noticing, you challenged me to become a better person. Thank you for being so silly, but also so weird and lovely. I will miss you so much Deanna, and I can't wait for our future holidays together around the world. **Mimi**, mille mercis pour l'année passée, mais aussi pour toutes les précédentes. Ton amitié est l'une des choses les plus précieuses. Ta gentillesse, ta bienveillance, ta générosité, ton humour beauf et tous les petits moments partagés remplissent un peu plus mon coeur à chaque fois, merci ♥

CONTENT

SCIENTIFIC ABSTRACT

The prefrontal (PFC) and primary somatosensory (S1) cortices are essential to cardinal cognitive functions. Their correct functional performance requires excitatory/inhibitory excitability balance in cortical networks. Here, we investigated neuronal mechanisms essential to cortical excitability in physiological and pathological conditions in the PFC and S1, in rats and mice.

In Chapter I, we assessed neuronal cellular and network excitability mechanisms underlying parametric working memory (PWM) in the rat PFC. PWM is the ability to manipulate and maintain transient quantitative information (e.g. an object size or a sound amplitude). Graded persistent activity (GPA), the neural substrate of PWM, is characterized by maintained firing frequencies that scale with the signal amplitude to be remembered. Recurrent neural network models show that intrinsic bistability, a neuronal property enabling cellular memorization of events, is required to subserve robust network GPA. A recent model showed that conditional bistability (CB) can arise from calcium-activated non-selective cationic (CAN) conductances, and suggested that such CB could subserve GPA in the PFC. However, this hypothesis has remained unexplored. Using electrophysiological tools in brain slices, we applied a specific model-derived stimulation protocol and provided the first experimental demonstration that CB exists in PFC layer V pyramidal neurons. We showed that CB is boosted by cholinergic (but not dopaminergic, noradrenergic and serotonergic) modulation, via activation of M1 muscarinic receptors, shifting the balance toward after-depolarization and requiring activation of CAN channels. Moreover, we showed that an in vitro analogue of GPA also depends on the muscarinic activation of CAN channels. Altogether, we propose that GPA, underlying PWM, arises from CAN-mediated conditional bistable neurons in recurrent layer V PFC networks.

In Chapter II, we showed how CB is impacted in pathological conditions known to affect working memory (WM). First, we assessed how CB is impacted during aging in wild-type mice and in the 5xFAD mice modeling Alzheimer's disease (AD). We showed that CB exists in the PFC of young adult (2 month-old) wild-type and 5xFAD mice and relies on the cholinergic modulation of CAN channels. Next, we showed that CB declines in 5xFAD mice at 6 month-old in contrast to wild-type mice at 12 month-old. Second, we assessed the effect of a mild traumatic brain injury (TBI) in PFC in young adult rats. We showed that CB is impaired 3 weeks following TBI. We propose that impairment in CB in the PFC may participate in WM loss in AD, TBI and normal aging.

In Chapter III, we investigated neuronal and network consequences of neurodevelopmental gene mutations in S1 in mice. The *Maf* gene family is expressed in inhibitory interneurons and known to be involved in neurogenesis and neuronal migration during neocortical development. Mutations in *Mafb* and *c-Maf* genes in all medial ganglionic eminence-derived interneurons lead to aberrant neuronal excitability, changes in synapse

morphology, altered excitation/inhibition balance, and epileptic activity. However, it remains unknown whether parvalbumin-positive (PV), somatostatin-positive (SST), or both types of interneurons are responsible for S1 network hyperexcitability. We showed that *Mafb* deletion specifically in SST interneurons affects the number of SST interneurons in layers II/III and IV in S1, whereas the *c-Maf* deletion in SST interneurons decreases synaptic excitation and increases in vivo epileptic-like activity in S1 and PFC cortices. In contrast, *Mafb* or *c-Maf* deletions in PV interneurons did not result in changes in neuronal or network excitability or epilepsy. These results suggest that S1 excitation/inhibition imbalance, caused by *Maf* mutations, is mediated by SST interneurons.

RÉSUMÉ SCIENTIFIQUE

L'équilibre entre l'excitabilité et l'inhibition dans les réseaux neuronaux du néocortex est crucial. Dans ce manuscrit, nous avons examiné les mécanismes neuronaux de l'excitabilité corticale dans les conditions physiologiques et pathologiques au travers de deux aires néocorticales, le cortex préfrontal (CPF) et le cortex somatosensoriel primaire (S1), chez le rat et la souris.

Dans une première partie, nous avons étudié les mécanismes de la mémoire de travail paramétrique (MTP), qui permet de maintenir des informations quantitatives transitoires, dans le CPF chez le rat. L'activité persistante gradée (APG), substrat de réseau de la MTP, est caractérisée par une activité de décharge qui se maintient au-delà de la fin d'un stimulus et dont la fréquence est proportionnelle à l'amplitude du signal à retenir. Les modèles de réseaux neuronaux du CPF suggèrent que la bistabilité conditionnelle (BC), une propriété intrinsèque neuronale, peut soutenir l'APG grâce à des conductances cationiques non sélectives activées par le calcium (CAN). À l'aide d'outils électrophysiologiques in vitro, nous avons développé un protocole de stimulation électrique dérivé de notre modèle et nous avons mis en évidence, pour la première fois, l'existence de la BC dans les neurones pyramidaux du CPF. Nous avons démontré que la BC dépend de l'activation des récepteurs cholinergiques muscariniques 1 et des canaux CAN qui génèrent des dépolarisations du potentiel de membrane appelées après-dépolarisations (ADP). De plus, nous avons généré de l'APG en tranche de CPF de rat qui dépend également de l'activation des récepteurs muscarinique 1 et des canaux CAN. Ces résultats soutiennent l'idée que l'APG dépend des neurones bistables conditionnels dans le CPF.

Dans un second temps, nous avons montré comment la BC est affectée dans des conditions pathologiques affectant la mémoire de travail. D'abord, nous avons évalué comment la BC est impactée au cours du vieillissement et dans la maladie d'Alzheimer en utilisant la lignée murine 5xFAD. Nous avons montré que la BC existe dans les neurones du CPF chez les souris contrôles et 5xFAD de 2 mois, et qu'elle dépend de l'activation des canaux CAN par la modulation cholinergique. De plus, nous avons mis en évidence que la BC diminue chez les souris 5xFAD à 6 mois et chez les souris contrôles à 12 mois. Ensuite, nous avons évalué l'effet du traumatisme crânien dans le CPF chez le rat. Nous avons montré que la BC est affectée 3 semaines après le traumatisme. Nos résultats suggèrent que la déficience de BC dans la maladie d'Alzheimer, le vieillissement et après un traumatisme crânien pourrait participer à la perte de mémoire de travail observée dans ces conditions.

Enfin, nous avons étudié les conséquences de mutations de gènes neurodéveloppementaux à l'échelle du neurone et du réseau dans le S1 chez la souris. La famille de gènes *Maf* est exprimée dans les interneurones et connue pour être impliquée dans la neurogenèse et la migration neuronale au cours du développement. Des mutations de *Mafb* et *c-Maf* dans les interneurones entraînent une augmentation de l'excitabilité neuronale, des modifications de morphologie des synapses et un déséquilibre excitation/inhibition du circuit.

Cependant, nous ignorons si ce sont les interneurones de type parvalbumine (PV) ou somatostatine (SST), ou bien les deux, qui sont responsables de l'hyperexcitabilité du réseau du S1. Nous avons observé que, dans les interneurones SST, la délétion de *Mafb* affecte le nombre d'interneurones SST, alors que la délétion de *c-Maf* diminue l'excitation synaptique et augmente l'activité épileptique dans les cortex S1 et CPF in vivo. En revanche, nous n'avons pas observé de modifications de l'excitabilité neuronale ou de réseau à la suite des délétions de *Mafb* ou *c-Maf* dans les interneurones PV. Ces résultats suggèrent que le déséquilibre excitation/inhibition dans le S1, causé par les mutations *Maf*, est médié par les interneurones SST.

SUMMARY FOR BROAD AUDIENCE

In my research project, we assess neuronal components of network excitability of two neocortical regions, the prefrontal cortex (PFC) and the primary somatosensory cortex (S1), in rodents. First, we studied mechanisms underlying working memory, the ability to retain and manipulate information at the time scale of seconds. We showed that excitatory neurons of the PFC exhibit conditional bistability (CB), which allows cellular memorization. We showed that CB requires the activation of cholinergic receptors and TRPC channels. Second, we showed that CB is impaired in rodents modeling Alzheimer's disease and traumatic brain injury, both associated with loss of working memory. Third, we assessed the role of neurodevelopmental genes, *Mafb* and *c-Maf*, in regulating cortical excitability. We showed that, specifically in somatostatin-interneurons, *c-Maf* (but not *Mafb*) deletion impacts neuronal and network excitability, leading to epileptic-like activity in both PFC and S1.

RÉSUMÉ GRAND PUBLIC

Mon projet de recherche s'intéresse aux composants de l'excitabilité du réseau du cortex préfrontal (CPF) et du cortex somatosensoriel primaire (S1) chez le rongeur. Nous avons d'abord étudié les mécanismes de la mémoire de travail, la capacité de rétention d'informations à court terme, dans le CPF. Les neurones excitateurs présentent une forme de mémoire cellulaire, la bistabilité conditionnelle (BC), qui nécessite l'activation de récepteurs et canaux ioniques spécifiques. Cette BC est diminuée chez les rongeurs modèles d'Alzheimer et du traumatisme crânien, deux conditions pathologiques associées à la perte de mémoire de travail. Puis, nous avons évalué le rôle des gènes neurodéveloppementaux *Mafb* et *c-Maf* dans la régulation de l'excitabilité corticale du S1. Dans les interneurones de type somatostatine, la suppression de *c-Maf*, mais pas de *Mafb*, a un impact sur l'excitabilité neuronale et du réseau, conduisant à l'observation d'activité épileptique dans le PFC et le S1.

GENERAL INTRODUCTION

I. Pathophysiological cortical excitability

In this thesis, we are interested in understanding how neuronal excitability influences cortical networks and what are the pathological consequences that can emerge from dysfunctions using rodents as animal models.

In **Chapter I**, we are characterizing *in vitro* the intrinsic properties and neuromodulation mediating conditional bistability in the pyramidal neurons and the network persistent activity that emerge in the prefrontal cortex, in the context of parametric working memory. In **Chapter II**, we are investigating *in vitro* the impact of Alzheimer's disease and mild traumatic brain injury on neuronal bistability in the prefrontal cortex. In **Chapter III**, we are focusing on the changes in synaptic excitability caused by *Maf* gene mutations in inhibitory interneurons in the primary somatosensory cortex and the resulting *in vivo* cortical hyper-excitability.

In this first section of General Introduction, we will present the main components of neuronal and network excitability in the cortex, their role, and how they are affected by pathological dysfunctions. This first part will serve as a general overview before going into more details in the second and third parts.

A. Neuronal excitability

Neurons—the individual elements composing the cortical circuits and more generally the different brain regions—process and transmit information in the form of electrical signals. Their excitability is influenced by both intrinsic properties and synaptic inputs, and it is countered by inhibition. The goal here is to present the non-exhaustive overview of the cellular components influencing neuronal excitability that we will discuss later throughout the Chapters, and highlight different examples of neuronal behaviors in response to increased excitation.

1. Components of excitability

Excitability in neurons—i.e., glutamatergic excitatory or GABAergic inhibitory—corresponds to the generation of action potentials, that are sudden, fast, transitory, and propagating change of the resting membrane potential. Neuronal excitability depends on the interaction between the intrinsic electrical properties inherent to each type of neuron and the received synaptic inputs (Guyton and Hall, 2010).

a) Intrinsic electrical properties

Intrinsic—i.e., passive and active—electrical properties can be measured *in vitro* by performing intracellular recordings of neurons, using the whole-cell patch-clamp method (Fig. 1; Hodgkin, 1964; Huxley, 1964).

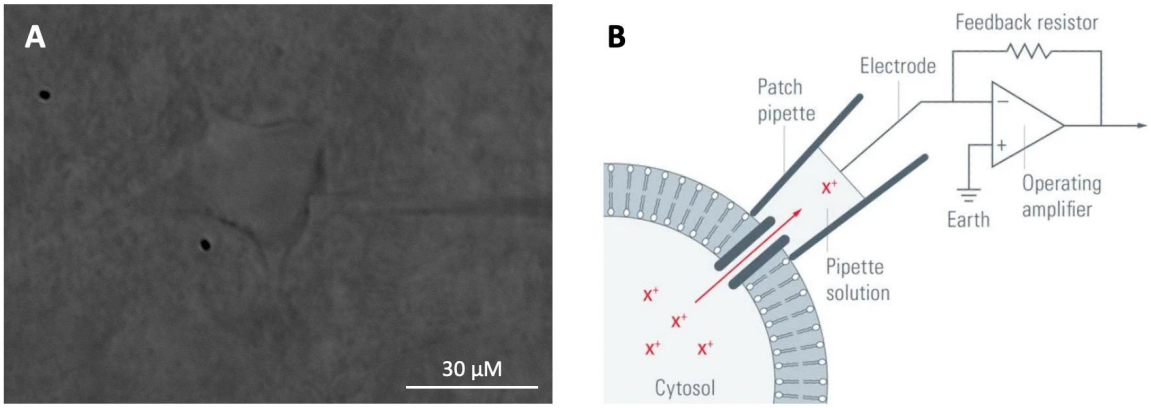

Fig. 1. Whole-cell patch-clamp recordings. A, *Whole-cell patch-clamp recording of a layer V pyramidal neuron in the rat prefrontal cortex. Photo by Morgane Leroux (Paz Lab, Gladstone Institutes).* ***B,*** *General principle: A glass pipette filled with electrolyte solution is tightly sealed onto the neuronal membrane. This creates electrical isolation for a small section of the membrane known as a "patch". As ion channels in this patch open and allow currents to flow, these currents are captured by an electrode connected to a highly sensitive differential amplifier, which enables their precise recording. Schematic from Leica Microsystems website.*

Passive membrane properties influence how the membrane potential changes in response to current across the cell membrane, thus allowing neurons to conduct electrical impulses without the use of voltage-gated ion channels (Sakmann and Neher, 1995). The input resistance, membrane capacitance, and membrane time constant represent the passive membrane properties that we measured in the different projects presented in this thesis in order to understand neuronal excitability in pyramidal neurons in the medial prefrontal cortex (Chapters I and II) and interneurons in the somatosensory cortex (Chapter III). Passive membrane properties are determined *in vitro* by injecting a negative hyperpolarizing current into the neurons (current-clamp mode).

The input resistance (R_{in} in MΩ) is measured using the Ohm's law: $\boldsymbol{R_{in} = (V/I_{inj})*1000}$, I_{inj} being the injected current (in pA) and *V* being the voltage change in response to the injected current (in mV). The input resistance of a neuron reflects, among others, the extent to which membrane channels are open and how easy it is for current to flow across the membrane. Higher is the input resistance, lower is the conductance, meaning that more ionic channels are closed—i.e., not too many ions are leaking from the cell. Thus, neurons with higher input resistance require lower I_{inj} to generate big voltage changes, meaning that they are more excitable.

The membrane capacitance (C_m in pF) is proportional to the neuronal area (*A* in ms*pA) and measured using: $\boldsymbol{C_m = A/V_{pulse}}$, V_{pulse} (in mV) being the voltage injected during the access test at the beginning of *in vitro* intracellular recordings. Higher is the membrane capacitance, bigger

is the area of the recorded neuron, thus the assumption is there are more open channels and the input resistance is lower—i.e., bigger neurons are less excitable.

The membrane time constant (τm in ms) refers to the amount of time it takes for a neuron's membrane potential to change in response to a stimulus and is measured using: $\tau_m = R_{in} * C_m$, which makes it proportional to the neuronal area. Membrane time constant is the time for the potential to reach 63% of its final value in the charging curve during the application of a negative current pulse. Thus, a smaller membrane capacitance leads to a faster time course—i.e., shorter time rise/fall.

Action potential properties are inherent to each individual type of neuron and don't vary. However, they differ from one type of neuron to another, thus affecting differently the excitability of neurons (Guyton and Hall, 2010). Neurons are characterized by an action potential amplitude, duration, and threshold—i.e., rheobase (θ in mV)—, which is the lowest membrane potential value at which an action potential is elicited. Lowest is the threshold, more excitable is the neuron.

Action potential properties result from the presence of **voltage-gated ion channels** in the neuronal membrane. Voltage-gated ion channels are influenced by the membrane potential that determines the rate of transitions between the open and close conformations (Casem, 2016).

Voltage-gated ion channels are capable of producing action potentials because of positive feedback loops between them and the membrane potential. Typically, a rise in the membrane potential can cause ion channels to open, thereby causing a further rise in the membrane potential. The occurrence of an action potential takes place when the positive feedback progresses in an explosive manner (Hodgkin and Huxley, 1952; Purves, 2001).

Voltage-gated sodium channels (VGSCs or Na_v; Wang et al., 2017) are closed at resting membrane potential and open as the membrane potential increases. Channel opening results in a rapid inflow of sodium (Na^+) into the neuron and further depolarization of the membrane potential towards the Nernst equilibrium potential for Na+ (around +65 mV; Eijkelkamp et al., 2012). Then, **voltage-gated potassium channels (VGKCs)** open following strong depolarization—i.e., action potential—and allow exit of potassium (K^+) from the neuron to bring the membrane back towards the Nernst equilibrium potential for K^+ (around -90 mV). Then, VGKCs close to return the membrane to the resting potential (Hodgkin and Huxley, 1952;).

It is important to note that Na_v are responsible for the main transmembrane transport of Na^+ and most of them are blocked by tetrodotoxin (TTX; Narahashi et al., 1960; Narahashi et al., 1964; Wang et al., 2017). Thus, TTX can be used to distinguish overall pre-synaptic activity from post-synaptic responses in extracellular recordings (Pai et al., 2019; Ferguson et al., 2023), as it will be done in Chapter I.

Another type of voltage-gated channels, the **voltage-gated calcium channels (VGCCs)**, are essential for coupling membrane depolarization to the influx of calcium (Ca^{2+}) in all neurons that generate both electrical and chemical signals (Seamans et al., 1997; Catterall, 2011). Low voltage-activated T-type calcium channels (Ca_T) activate rapidly and deactivate slowly, thus they are optimized to contribute to depolarizing currents leading to action potentials (Perez-Reyes, 2003; Cain and Snutch, 2010). In contrast, high voltage-activated L-type calcium channels (Ca_L) activate with slower kinetics and deactivate slowly (Walker and Waard, 1998). Ca_L have a limited contribution to the initiation of action potentials, however they help, among others, to the maintenance of spiking by increasing Ca^{2+} inflow into the neurons (Lipscombe, 2002). We will see later how Ca_L contribute to the maintenance of self-sustained spiking—also called neuronal bistability—in the pyramidal neurons of the PFC.

Calcium-activated channels also contribute to the generation of action potentials because of positive feedback loops between them, the voltage-gated channels, and the membrane potential.

The binding of **calcium-activated non-selective cationic channels (CANs)**—also called transient receptor potential channels (TRPs)—by Ca^{2+} results in Na^+ and Ca^{2+} inflow into the neuron, which further depolarizes the membrane potential and facilitates the generation of action potentials (Haj-Dahmane and Andrade, 1997, 1998; Reboreda et al., 2011; Zylberberg and Strowbridge, 2018; Ratté et al., 2018). In opposition, the binding of **small-conductance calcium-activated potassium channels (SKs)** by Ca^{2+} results in K^+ outflow from the neuron, which hyperpolarizes the membrane potential and limits the generation of action potentials (Vergara et al., 1998; Shah et al., 2017).

Depolarizing and hyperpolarizing currents generated by CANs and calcium-activated potassium channels will be the focus of our Chapters I and II, in which we will question whether these currents contribute to self-sustained spiking in the pyramidal neurons of the mPFC, and to what extent.

b) Synaptic excitability

In addition to cellular intrinsic properties, synaptic transmission adds another level of modulation to the neuronal excitability. Neurons interact with each other by establishing synaptic connections. Depending on the type of neuron, synaptic inputs can transmit excitatory or inhibitory signals.

Glutamatergic excitatory neurons, like the pyramidal neurons discussed in Chapters I and II, release glutamate in the synaptic space to excite surrounding neurons (Purves et al., 2001). Glutamate binds to post-synaptic AMPA receptors and NMDA receptors, which are non-selective cationic channels. Activation of AMPA receptors induces Na+ inflow and K+ outflow, which in

turn overcomes the voltage-dependent magnesium blockade of NMDA receptors. Then, activation of NMDA receptors allows Ca^{2+} entry in addition to Na^{+}/K^{+} flow (Purves et al., 2001). As a result, **excitatory post-synaptic currents (EPSCs)** produce excitatory post-synaptic potentials (EPSPs), and when the summation of EPSPs reaches the action potential threshold, the post-synaptic neurons generate action potentials. Spontaneous EPSCs are an indicator of synaptic excitation in neurons, as it reflects the received excitatory synaptic inputs, and are measured *in vitro* using the voltage-clamp mode at the resting membrane potential and in presence of a $GABA_A$ receptor blocker picrotoxin (Voskobiynyk et al., 2020; Holden et al., 2021; see Chapter III for examples).

In opposition, GABAergic inhibitory neurons, like the somatostatin and parvalbumin-positive interneurons discussed in Chapter III, release GABA in the synaptic space to inhibit surrounding neurons (Purves et al., 2001). GABA binds to post-synaptic GABA receptors, which are chloride (Cl^-) channels. The opening of the channel induces C^- inflow and as a result, **inhibitory post-synaptic currents (IPSCs)** produce inhibitory post-synaptic potentials (IPSPs), inhibiting the generation of action potentials. Spontaneous IPSCs are an indicator of synaptic inhibition in neurons, as it reflects the received inhibitory synaptic inputs, and are measured *in vitro* using the voltage-clamp mode at around 0 mV and in presence of glutamate receptor blockers such as CNQX and APV (Voskobiynyk et al., 2020; Holden et al., 2021; Cho et al., 2023). Note that these AMPA and NMDA receptor blockers can also be used to identify overall post-synaptic responses in extracellular recordings, as it will be done in Chapter I.

2. Different spiking patterns for different roles

The ultimate consequence of the increase in neuronal excitability is the generation of action potentials and different spiking patterns are fundamental for information coding in the brain.

The first difference we can observe is the one between **regular-spiking neurons** (Fig. 2A)—excitatory pyramidal neurons (Subkhankulova, 2010) and inhibitory somatostatin-positive interneurons (Casale et al., 2015)—and **fast-spiking neurons** (Fig. 2B)—inhibitory parvalbumin-positive interneurons (Subkhankulova, 2010; Casale et al., 2015)—within the cortical layers.

Regular-spiking neurons show an ability to fire repetitively at low frequencies (<10 Hz; Subkhankulova, 2010), and some of them display spiking frequency accommodation/adaptation (Fig. 2C). Spike adaptation refers to the progressive slowing of the frequency of discharge of action potentials following an initial higher frequency of spikes during an extended period of excitation—i.e., sustained injections of depolarizing rectangular currents *in vitro* (Ha and Cheong, 2017). It has been shown that calcium-activated potassium and chloride channels are crucial for spike adaptation via generation of a large afterhyperpolarization when neurons are

hyper-activated (Ha and Cheong, 2017). The role of spiking adaptation can be considered as a type of self-inhibition in neurons, thus a 'protective' mechanism to avoid neuronal and ultimately cortical hyper-excitability (Ha and Cheong, 2017).

In contrast, fast-spiking neurons—the most prevalent type of interneurons in the cortex (Rudy et al., 2010)—show stable periodic firing at high frequencies (>10 Hz) without apparent frequency accommodation (Subkhankulova, 2010). Their action potentials are characterized by a large amplitude and short duration (Subkhankulova, 2010). One specific type of VGKC with fast gating kinetics—the K_v3 family—has been demonstrated to be key for the FS phenotype (Erisir et al., 1999; Rudy and McBain, 2001; Lien and Jonas, 2003). The role of the fast-spiking neurons is to provide fast and precise inhibition to the circuit.

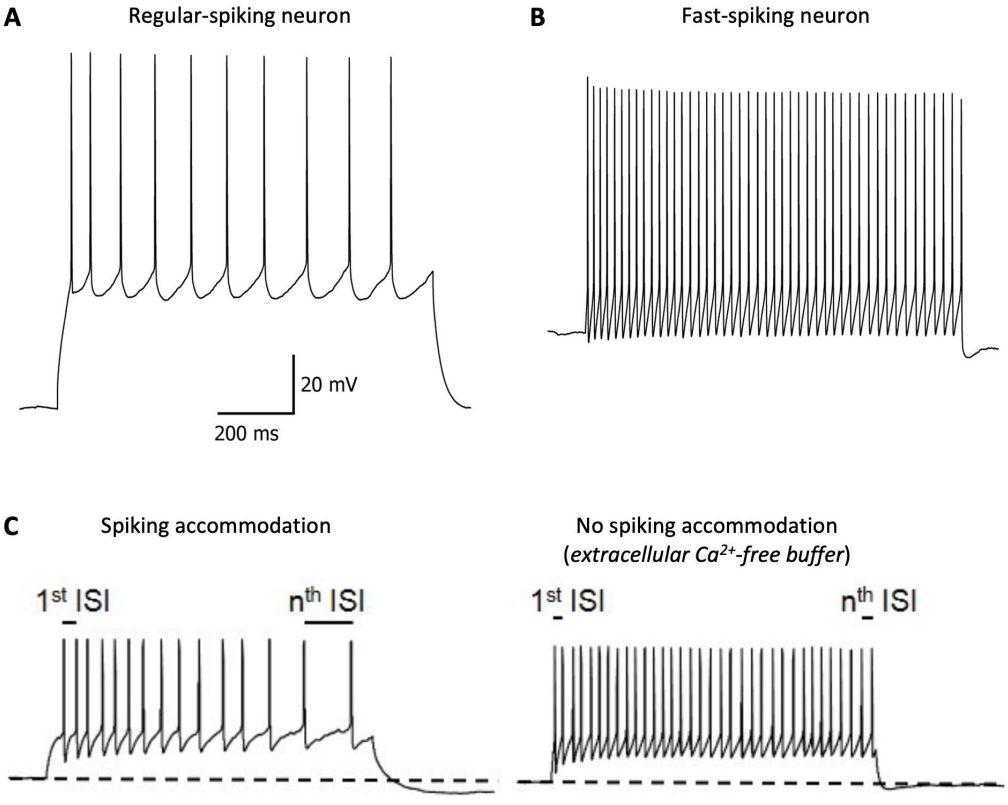

Fig. 2. Examples of regular-spiking and fast-spiking neurons, and spiking accommodation. A and B, *Regular-spiking (A) and fast-spiking neurons (B) form the somatosensory cortex, responding to step current stimulation, in mice. Adapted from Subkhankulova et al. (2010).* ***C,*** *Ca^{2+}-dependent spike frequency adaptation in a regular-spiking neuron in mice. (Left) Thalamocortical neuron with a depolarizing current injection to induce tonic firing in 2.4 mM Ca^{2+} buffer displays the prolongation of inter-spike intervals (ISI). (Right) Replacement of extracellular buffer to Ca^{2+}-free buffer abolishes the spike-frequency adaptation. Adapted from Ha and Cheong (2017).*

In general, neurons function by generating individual action potentials that are relatively isolated, but in several brain regions, neurons can alter their firing pattern from tonic to **bursting**. Bursting—or burst firing—corresponds to periods of rapid action potential spiking followed by quiescent periods much longer than typical inter-spike intervals (Ha and Cheong, 2017).

This firing pattern has many roles and can, among others, enhance neural oscillations and induce neural plasticity. Depending on the brain region and cell type, burst firing has been proven to be dependent on voltage-gated ionic and/or calcium-activated channels (Shao et al., 2021). For example, in the thalamocortical relay neurons (Sieber et al., 2013), Ca_T activation mediates bursts and SK channels rapidly hyperpolarize neurons back to their resting membrane potential, allowing Ca_T to recover from an inactive state and prepare for the next burst (Fig. 3; Perez-Reyes, 2003; Shao et al., 2021). This plays a role in modulation of sensory information processing during sleep (Sieber et al., 2013).

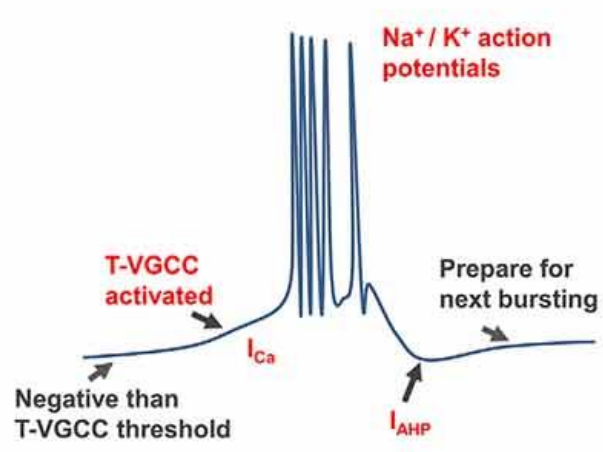

Fig. 3. Example of mechanisms underlying generation and regulation of neuronal bursting. *Schematic of burst firing induced by T-type voltage-gated calcium channels (T-VGCC or Ca_T) activation caused by slight depolarization, T-VGCCs recover from inactivation by the after-hyperpolarization (AHP) to prepare for next bursting. Adapted from Shao et al. (2021).*

Finally, differences can be observed between **monostable** and **bistable neurons** (Rodriguez et al., 2018). Monostable neurons respond to an "all-or-nothing" rule: if they receive a supra-threshold stimulation (θ_{ON}), they elicit action potentials. In opposition, bistable neurons are characterized by a range of stimulation currents at which stable states of quiescence and self-sustained spiking coexist (θ_{OFF} to θ_{ON}). In other words, bistability allows neurons to maintain spiking even after the end of a stimulation, thus to memorize transient information at the cellular scale. This intrinsic neuronal property is thought to be dependent on the activation CAN

channels. The intrinsic properties underlying bistability, and particularly conditional bistability—a newly identified form of bistability crucial for parametric working memory—its neuromodulation, and its effect on cortical excitability will be discussed in the second section of General Introduction and in Chapter II.

B. Cortical excitability

Neurons are part of circuits that are more or less local. For a given neuron, inputs can come from excitatory or inhibitory neurons, within the same cortical layer or a different layer located in the same column, or from a different brain region. All these interactions between excitable neurons serve to the functioning of the brain by creating a balanced cortical excitability.

1. Cortical organization

The neocortex—or commonly called cortex—is divided into a left and a right hemisphere, and each hemisphere separates into four lobes (Fig. 4; Maldonado and Alsayouri, 2023). The **frontal lobe** is crucial for motor function, language (speaking and writing skills) and cognitive processes, such as executive function, decision-making, attention, memory, affect, mood, personality, self-awareness, and social reasoning (Hoffmann, 2013; Pirau, 2022). The **parietal lobe** is responsible for interpreting vision, hearing, motor, sensory, and memory functions (Netter, 2010). The **temporal lobe** helps in understanding spoken and written language, hearing, spatial/visual perception, sensory processing for retention of memories, language, and emotions (Trobe, 2010). Finally, the **occipital lobe** interprets visual information (Rehman, 2022).

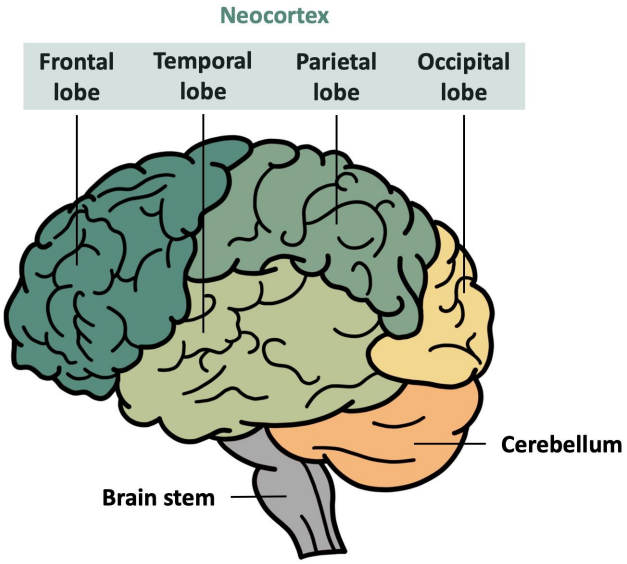

Fig. 4. The human neocortex is divided into four lobes. *It is composed of the frontal lobe (prefrontal cortex, motor cortex, and Broca's area), the parietal lobe (somatosensory cortex, parietal association area, sensory speech area of Wernicke, and Baum's loop), the temporal lobe (auditory Brodmann's areas and Wernicke's area), and the occipital lobe (visual cortices).*

All mammals have a cortex (Fig. 5) that follows a similar but accelerated developpement compared with humans. For example, the brain of mice and rats—the animal models used in these research projects—is stable at the age of three weeks and fully developed by two to three months of age (Semple et al., 2013; Hammelrath et al., 2016). This accelerated brain development compared to humans makes rodents a useful tool to investigate neuronal and cortical excitability, and the associated pathologies.

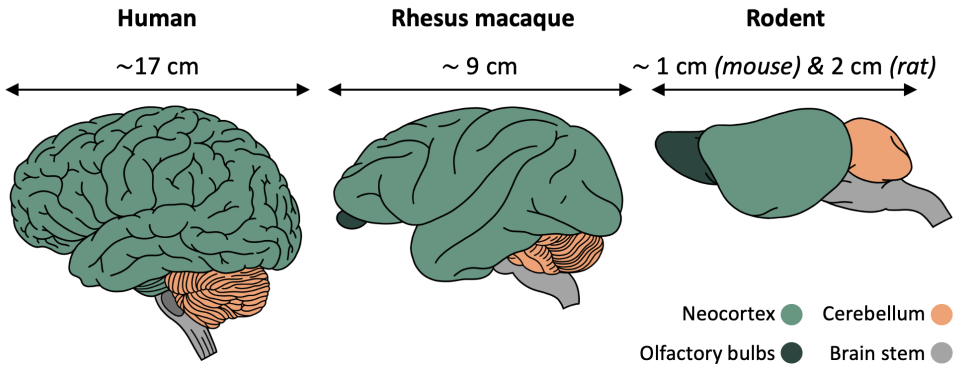

Fig. 5. *Brain size and shape comparison between humans, Rhesus macaques, and rodents.*

The cortex is complex and characterized by a stereotyped organization in layers. This notion was first introduced around the middle of the 19th century and primarily based on its cytoarchitecture—i.e., the distribution and size of pyramidal cell bodies (Meynert, 1868; Brodmann, 1909)—and myeloarchitecture—i.e., the projection pattern of long-range intracortical axons (Fig. 6; Baillarger, 1840; Vogt, 1906).

In a general manner, cortical areas are organized in six different layers, except for the prefrontal cortex which lacks layer IV. In this research project, we will investigate neuronal excitability in layer V from the PFC and layers II/III from the S1. Layers II/III and V—composed of excitatory pyramidal neurons and diverse types of inhibitory interneurons—are both output layers that exchange information with other layers and other neocortical areas (Douglas and Martin, 2004; Douglas and Martin, 2007; Moberg and Takahashi, 2022).

Layer II/III excitatory neurons send projections to layers V, and make major lateral contributions to corticocortical connections between areas at the same level, therefore function to integrate information across cortical areas and hemispheres. Different types of inhibitory interneurons, such as the somatostatin and parvalbumin-positive interneurons, inhibit excitability locally (Luo et al., 2017).

After receiving inputs for layers II/III, **layer V** sends both excitatory and inhibitory projections to layer IV. Also, layer V long-range projecting pyramidal neurons send lateral outputs to other cortical and extracortical regions of the brain, such as the thalamus, striatum, midbrain, and brainstem, at the same level (Douglas and Martin, 2004; Moberg and Takahashi, 2022).

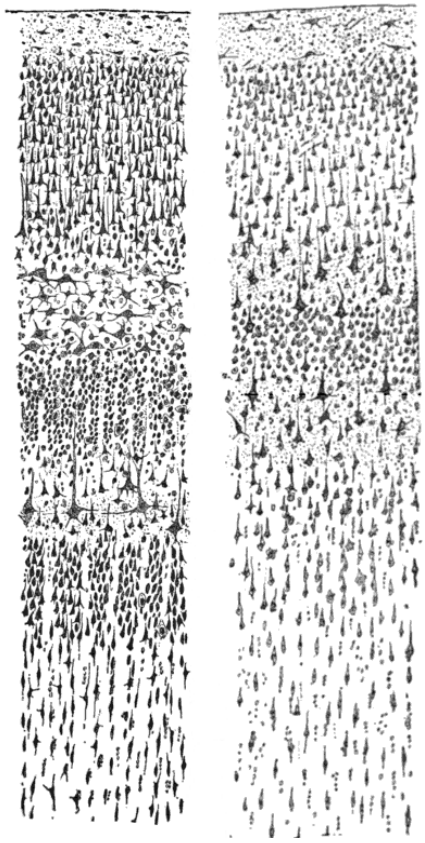

Fig. 6. Drawings of cortical layers by Santiago Ramon y Cajal*, each showing a vertical cross-section, with the surface of the cortex at the top. Left: Nissl-stained visual cortex of a human adult. Right: Nissl-stained motor cortex of a human adult. The Nissl stain shows the cell bodies of neurons (Ramón Y Cajal, 1899).*

2. Excitability & Negative feedbacks at the circuit scale

We can access cortical network excitability by not only looking at the cellular scale, but considering groups of neurons connected to each other to create circuits. There are three main types of neuronal connections: 1) excitatory feedforward connections, 2) inhibitory feedback connections, and 3) lateral connections that are either excitatory or inhibitory (Fig. 7; Bastos et al., 2012).

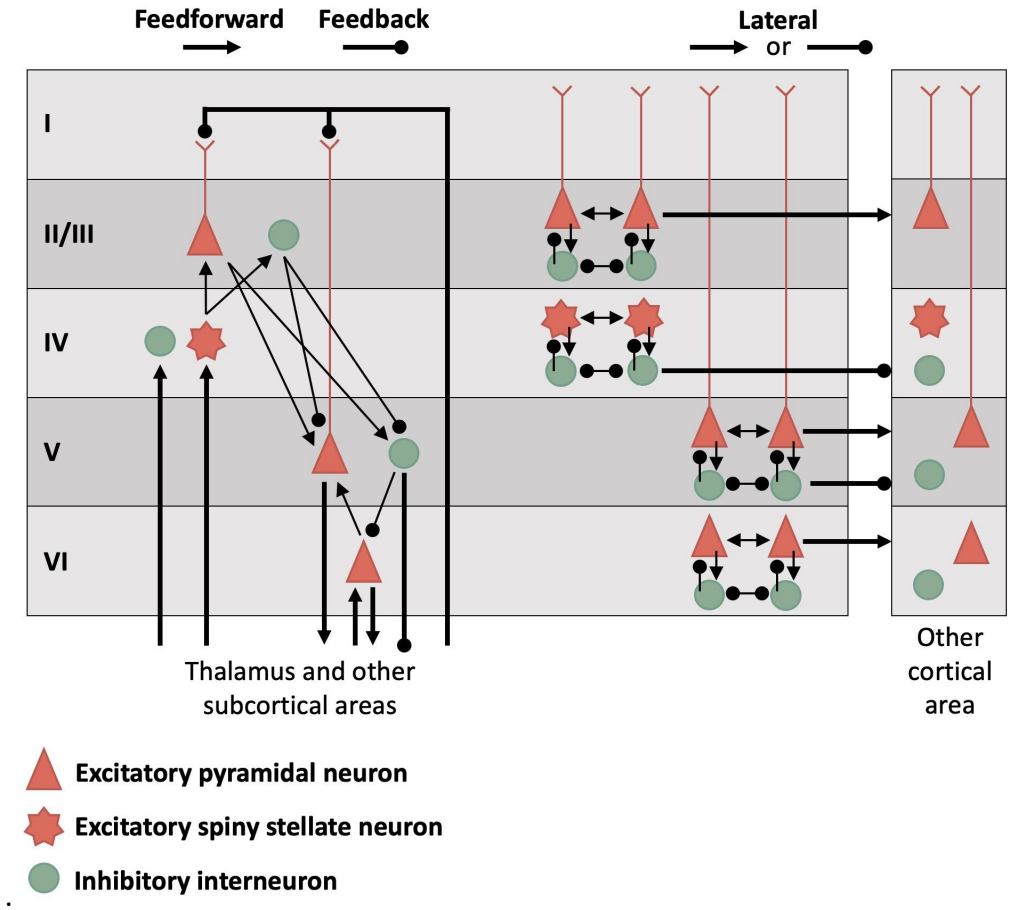

Fig. 7. The canonical cortical microcircuit. *Representation of the most frequently occurring patterns of cortical connectivity—i.e., feedforward, feedback, and lateral connections. Adapted from Bastos et al. (2012).*

The neocortex requires a balanced ratio of excitatory and inhibitory inputs within the circuits. Excitability needs to be sufficient to trigger decision, action, or movement, but it needs to be controlled to avoid hyper-excitability of the circuits.

Feedforward connections between excitatory pyramidal neurons are responsible for input transmission from one cortical area to another, such as the parietal cortex to the prefrontal cortex for context encoding during a working memory task (Greenman et al., 2021). But feedforward excitatory connectivity is also responsible for synaptic reverberation (Wang, 2001). One example is the one occurring in the prefrontal cortex during working memory tasks. When the neurons receive the stimulation—i.e., the information to be remembered—, they send excitatory synaptic inputs to the other neurons in the circuit and a positive feedback loop between the neurons maintains prefrontal cortex activity (Wang, 2001). This synaptic

reverberation phenomenon is crucial for all types of working memory and will be discussed in the second section of General Introduction and in Chapter I.

On the contrary, **negative feedbacks** limit, control, and stop cortical excitability when it is needed. At the local scale, circuits are composed of both excitatory and inhibitory neurons. For example, in cortical layers II/III, complex positive feedforward and negative feedbacks exist between excitatory pyramidal neurons and somatostatin-positive (SST+), parvalbumin-positive (PV+), and vasoactive intestinal polypeptide-expressing (VIP) interneurons neurons (Riedemann, 2019)—this local circuit will be discussed in the third section of General Introduction and Chapter III. Another example at a larger scale is the negative feedback operating between thalamic excitatory neurons that receive sensory inputs, cortical excitatory neurons that are stimulated by thalamic neurons and send projections to the thalamic reticular nucleus (nRT), and inhibitory interneurons neurons located in the nRT (Choe, 2003; Paz et al., 2013). This feedback loop is crucial for modulating sensory processing.

At the circuit level, cortical excitability can be assessed, for example, by recording extracellular multi-unit activity (MUA) and local field potentials (LFPs) *in vivo* using depth electrodes or *in vitro* in slice using multi-electrode arrays—as it will be described in Chapter I. MUA captures neuronal spikes corresponding to one or a small group of neurons around the electrodes. LFPs refer to the electrical potential in the extracellular space surrounding the electrode. If many neurons spike in synchrony, their electrical activity sum up and give rise to changes in LFP amplitude. In order to characterize the emergence of persistent activity in the prefrontal cortex layers, recordings of extracellular activity—MUA and LFPs—will be described in Chapter I.

Larger-scale oscillations measured by electroencephalogram (EEG), will not be discussed in this thesis, however it is important to note that they have a major role in cortical activity and brain function (Sohal et al., 2000; Başar et al., 2001; Paz et al., 2013; Clemente-Perez et al., 2017; Cho et al., 2022).

C. Neuromodulation of the excitability

To function efficiently, the brain constantly evolves and adapts to its environment, and this includes modulation of neuronal excitability. **Neurotransmitters**—that target fast-acting ionic channel receptors—and **neuromodulators**—that target slower G-protein receptors—act on neuronal excitability on a short time-scale.

As we saw above, glutamate and GABA respectively excite and inhibit neuronal excitability by binding ionic channels, which immediately changes the overall positive and negative charges on either side of the membrane. Other common neurotransmitters are serotonin—or 5-hydroxytryptamine (5HT)—and acetylcholine (ACh). 5HT and ACh bind,

respectively, to excitatory $5HT_3$ (Engel et al., 2013) and nicotinic (Radnikow and Feldmeyer, 2018) receptors that increase neuronal excitability and membrane potential depolarization.

Common neuromodulators found in the cortex and subcortical regions are norepinephrine—or noradrenaline (NA; Rho et al., 2018)—and dopamine (DA; Radnikow and Feldmeyer, 2018). But 5HT (Pithadia, 2009) and ACh (Radnikow and Feldmeyer, 2018) also belong to the neuromodulator family as they not only bind to ligand gated ionic channels, but also to G-protein receptors. Like neurotransmitters, neuromodulators are released in the extracellular synaptic space by specific pre-synaptic neurons and the binding to G-protein receptors triggers an intracellular cascade of events in the post-synaptic neuron. For each neuromodulator, its effect is determined by the targeted receptor. For example, NA α_2 receptor binding produces inhibitory effects by limiting the intracellular Ca^{2+} levels in the amygdala, a brain region crucial for fight-or-flight responses (Davies et al., 2004; O'Donnell et al., 2012). One of the many roles of 5HT is to regulate anxiety and stress levels, and activation of $5HT_{1/5}$ and $5HT_{2/3/4/6}$ receptors, respectively, inhibits and excites neurons (Deen et al., 2016; Xiang, 2019). DA regulates, among others, psychomotor functions via D_1-like and D_2-like receptor stimulation that, respectively, stimulates and inhibits adenylate cyclase (Surmeier et al., 2007). Finally, ACh generally has excitatory effects when binds to $M_{1/3/5}$ receptors, through the phospholipase C second messenger pathway, and inhibitory effects when binds to $M_{2/4}$ receptors through adenylate cyclase inhibition (Radnikow and Feldmeyer, 2018).

All the cognitive and behavioral effects associated with NA, 5HT, DA, and Ach will not be described here. However, these neuromodulators are all released in the prefrontal cortex, and their effect on neuronal excitability and precisely on bistability will be discussed in the second section of General Introduction and in Chapter I, questioning their role in working memory processes.

This will not be discussed in this thesis, but we thought important to mention that, on a longer time-scale, **synaptic plasticity** can affect neuronal excitability. For example, in the hippocampus, long-term potentiation (LTP), a process involving persistent strengthening of synapses (bursting), via NMDA and AMPA receptors, leads to a long-lasting increase in signal transmission. LTP is crucial in the context of long-term memorization (Sumi and Harada, 2020).

D. Network excitation/inhibition imbalance

Disruption of neuronal excitability caused by pathological conditions can lead to a multi-scale excitatory/inhibitory imbalance, which can have devastating consequences (Telias and Segal, 2022).

Local brain lesions—affecting one area/region of the brain—can be caused, for example, by a seizure that is a sudden and uncontrolled burst of electrical activity, a stroke that is when the blood supply to the brain is blocked, or a traumatic brain injury, such as when an object violently hits the head.

As a non-exhaustive list of cognitive and behavioral consequences, lesions in the auditory cortex can, specifically, cause buzzing, humming, or ringing sounds (Michelucci, 2019). As a result of a lesion in the Broca area, there is a breakdown between one's thoughts and one's language abilities (Dronkers et al., 2017). Seizures from the primary motor cortex can lead to contralateral unilateral tonic or myotonic activity (Christova et al., 2006). Lesions in the primary visual cortex can cause unilateral or bilateral loss of vision (Hadjikoutis and Sawhney, 2003). Also, after traumatic brain injury to the frontal lobes, some patients suffer from poor impulse control, impaired attention, and working memory loss (Levin and Kraus, 1994). In this manuscript, the effects of a mild traumatic brain injury on the neuronal excitability of the pyramidal neurons in the prefrontal cortex, in the context of working memory, will be discussed in Chapter II.

However, a traumatic brain injury occurring at high speed in a car accident (with brain rotation inside the skull) or a generalized seizure propagating through both hemispheres of the brain can alter multiple cortical and subcortical regions and even the whole brain. Thus, such conditions can damage multiple crucial cognitive capacities (Ackerman, 1992).

Interestingly and in some cases, one of the most efficient ‘repair’ mechanisms after injury is the bilateral arrangement of the brain. The limited specialization of the two hemispheres allows for some flexibility—or compensation—if only one hemisphere is injured; often the other hemisphere can compensate to some degree, depending on the age at which injury occurs (a young, still-developing brain readjusts more readily; Ackerman, 1992).

Other pathologies, such as neurodevelopmental diseases caused by gene mutations can alter the whole brain development and excitability, which also leads to the impairment of multiple cognitive functions.

For example, as part of research funding from the FoxG1 Foundation, I participated in the study of the cognitive consequences of an autism spectrum-like disorder called the FoxG1 syndrome. The FoxG1 syndrome is a rare neurodevelopmental disorder that can be caused by various mutations within the *FOXG1* (Forkhead box G1 protein) gene, which encodes a transcription factor (FOXG1 Foundation). Approximately 700 children have been diagnosed with FoxG1 syndrome, which occurs in both males and females (Florian et al., 2011). Children affected by FOXG1 mutations have an unusually small head size—i.e., microcephaly—by early childhood. The condition is associated with a pattern of brain malformations that includes a thinner corpus callosum and an underdevelopment of the white matter (Kortüm et al., 2011).

Mutations in *FOXG1* lead to severe cognitive disabilities, sleep disturbances, epileptic seizures and limited social interactions, including poor eye contact and a near absence of speech and language skills (Florian et al., 2011). Nowadays, there is no treatment to cure children with the FoxG1 syndrome.

Other autism spectrum disorders, schizophrenia, and Rett syndrome have been also characterized by cortical excitability imbalance causing epileptic seizures, sensory hypersensitivity, repetitive behavior, and/or attention deficits; each symptom being potentially caused by independent mechanisms (Liu et al., 2021; Antoine, 2022).

As we can see from these examples, neurodevelopmental disorders can alter brain morphology, connectivity, and excitability, leading to devastating consequences. In Chapter III, we will discuss the effects on neuronal and network excitability of two mutations of genes implicated in the development and migration of interneurons—*Mafb* and *c-Maf genes*—in the somatosensory cortex.

Other types of pathologies, such as neurodegenerative diseases, can also alter the whole brain excitability (Palop and Mucke, 2021; Kazim et al., 2021). For example, Alzheimer's disease is a progressive disease that starts with molecular and cellular symptoms in local brain areas—such as the hippocampus—but rapidly spreads to other parts of the brain (Rao et al., 2022). Alzheimer is characterized by synaptic impairments, neuromodulation disruption, and neurodegeneration which lead, among others, to loss of long-term and short-term memory, communication and orientation impairments, and changes in personality (Joe and Ringman, 2019). The consequences of Alzheimer's disease on the neuronal excitability of the pyramidal neurons in the prefrontal cortex, in the context of working memory, will be investigated in Chapter II.

In the first part of General Introduction, I described the components of neuronal and cortical excitability. In order to understand what is altered in pathological conditions, it is crucial to know the physiological mechanisms of excitability that underlie neocortical function. In the following parts and chapters, I will investigate the neuronal and circuit mechanisms of two specific cortical regions.

In the second part of General Introduction, I will describe the prefrontal cortex and its cognitive aspect. Particularly, I will describe how the prefrontal cortex excitability can generate working memory (relevant to Chapter I) and what disruptions in pathological conditions—Alzheimer's disease, aging, and after a traumatic brain injury—can affect this crucial role of the prefrontal cortex (relevant to Chapter II).

In the third part of General Introduction, I will describe the primary somatosensory cortex function and how deletions in genes that govern its cortical development affect excitability at the neuronal and network scales (relevant to Chapter III).

II. Medial prefrontal cortex & working memory capacities throughout life

In this second part of General Introduction, we will discuss the many roles of the medial prefrontal cortex, before going into more details about what is known to this date about the neuronal and circuit mechanisms underlying working memory capacities. Special focus will be devoted to parametric working memory, which refers to the ability to retain and manipulate quantitative information, and is still poorly experimentally studied.

This second section of General Introduction will serve to explain the significance behind the projects conducted in Chapters I and II. In Chapter I, we will characterize conditional bistability, the *theoretical* neuronal intrinsic property crucial for graded persistent activity emergence in the medial prefrontal cortex, the neural correlate of parametric working memory. Then, in Chapter II, we will investigate how neuronal mechanisms of parametric working memory are affected in Alzheimer's disease and after traumatic brain injury, two pathological conditions characterized by working memory loss.

A. Medial prefrontal cortex: Center of executive function

1. Medial prefrontal cortex location and connectivity

The medial prefrontal cortex (mPFC) is located on the forward-facing part of the frontal lobes in humans and non-human primates, and deeper in the neocortex behind the olfactory bulbs in rodents (Fig. 8).

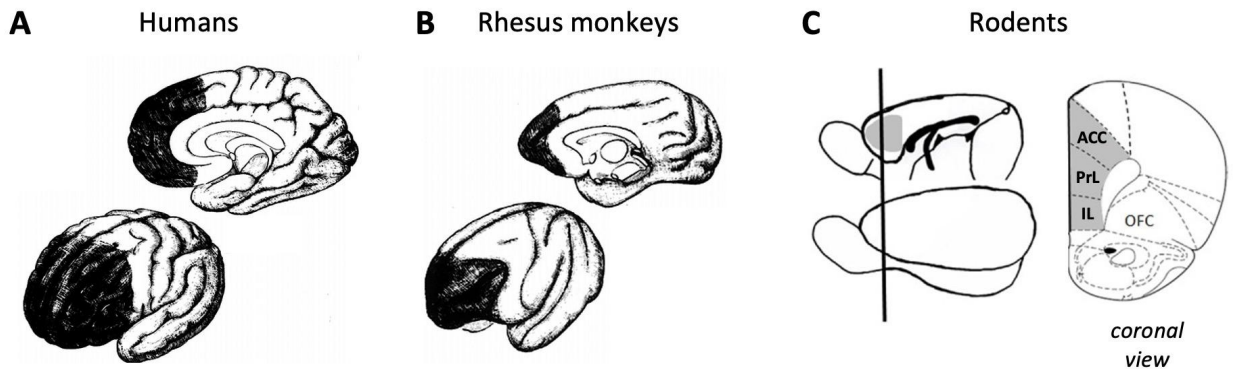

Fig. 8. Location of the medial prefrontal cortex (mPFC) in different mammals. *mPFC in human (A), Rhesus monkey (B), and rodent (C) brains. In (A) and (B), mPFC is represented in black. Adapted from Fuster (2002). In (C), mPFC is represented in gray. Adapted from Bizon et al. (2012).*

If the mPFC is common to all mammals, comparisons between the different groups of animals are complicated by the debate over the homology of prefrontal regions (Seamans et al., 2008; Chudasama, 2011).

In rodents (Fig. 8C), the mPFC is composed of the anterior cingulate cortex (ACC), the prelimbic cortex (PrL), and the infralimbic cortex (IL) (Fig. 15). In non-human primates, there is a real distinction between the mPFC, that is composed of only the PrL and the IL, and the cingulate cortex. Differences in functions between PrL, IL, and ACC will be discussed later.

As part of the neocortex, the mPFC is composed of both excitatory and inhibitory neurons. Excitatory neurons—mainly pyramidal neurons (Fig. 9)—are the largest cell population in the mPFC (80 %; Xu et al., 2019) and are composed of subtypes projecting to intra-cortical or long-distance targets (Bhattacherjee et al., 2019).

In Chapter I, the goal will be to characterize the excitability of pyramidal neurons of the layer V of the mPFC and more precisely, their bistability properties.

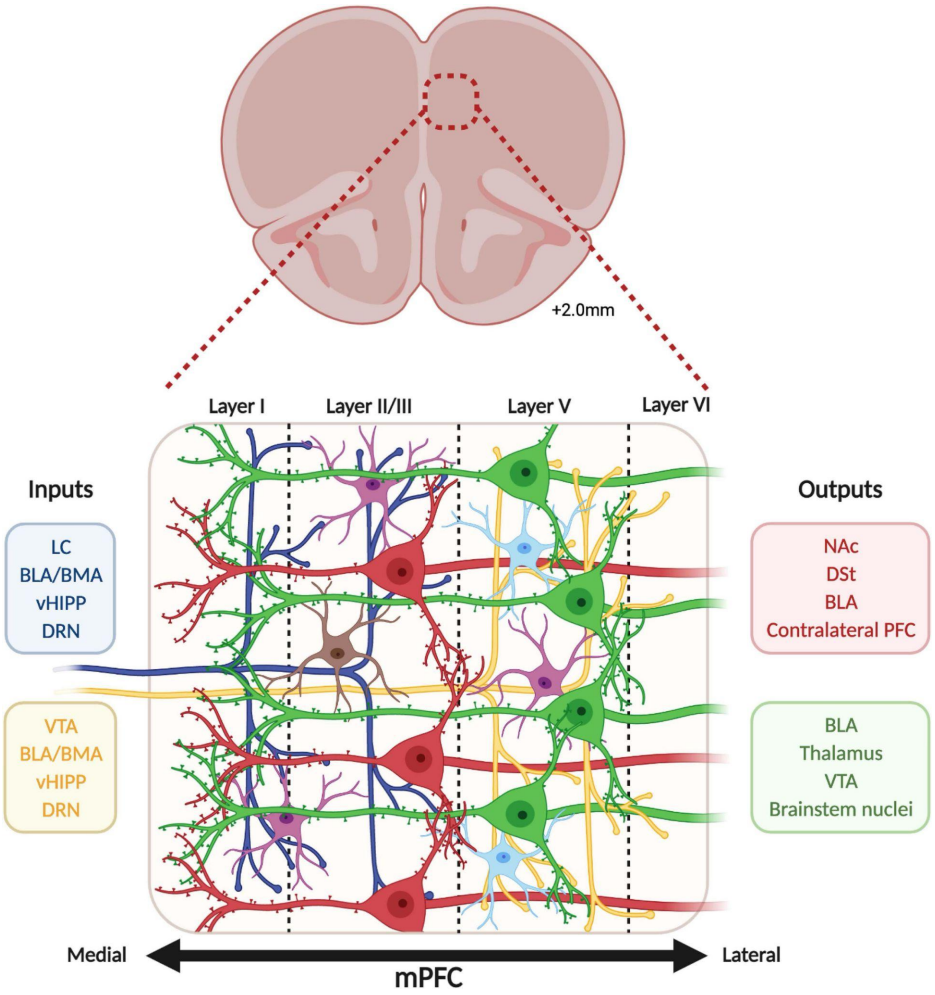

Fig. 9 (previous page). Layer and cellular organization of the medial prefrontal cortex (mPFC). *The mPFC is organized in layers, numbered I (medial, close to the midline) to VI (lateral). Pyramidal glutamate neurons are lying in layers II/III (red), V (green), and VI (not represented), while GABAergic interneurons (somatostatin in purple, parvalbumin in blue, and vasoactive intestinal peptide in brown) are spread in layers I, II/III and V. The mPFC receives layer-specific inputs (dark blue and yellow) from locus coeruleus (LC), basolateral and basomedial amygdala (BLA and BMA), ventral hippocampus (vHIPP), dorsal raphe (DRN) and ventral tegmental area (VTA) while mPFC pyramidal neurons send projections (red and green) to the nucleus accumbens (NAc), dorsal striatum (DSt), BLA, contralateral PFC, thalamus, VTA and brainstem nuclei. From Bittar and Labonté (2021).*

Interestingly, if specific functions have been attributed to most regions of the neocortex—for example, the primary somatosensory cortex and the Broca's area are, respectively, responsible for sensation processing and speech—the mPFC has a less specific kind of function.

The mPFC is connected—receives inputs and sends outputs via the excitatory pyramidal neurons—with almost all the other brain regions (Fig. 10), including the neuromodulatory systems (Fig. 10), which allows the mPFC to play a crucial role in multiple cognitive functions (Bittar and Labonté, 2021).

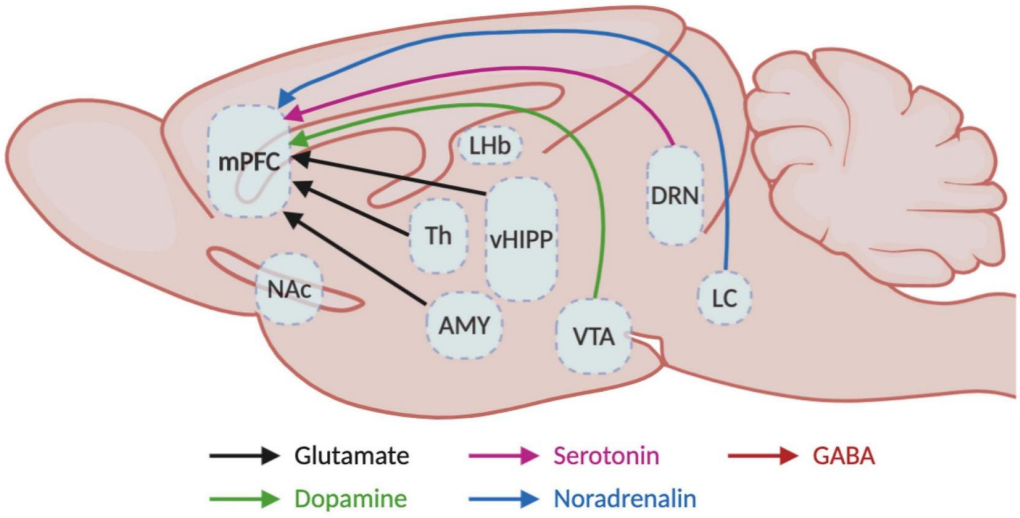

Fig. 10. Medial prefrontal cortex (mPFC) inputs. *Schematic representation of the afferent projections in the mPFC with their respective neurotransmitter systems. Note that the mPFC also receives cholinergic afferent projections from the basal nucleus of Meynert that are not represented here. AMY, amygdala; DRN, dorsal raphe nucleus; LC, locus coeruleus; LHb, lateral habenula; NAc, nucleus accumbens; Th, thalamus; vHIPP, ventral hippocampus; VTA, ventral tegmental area. Adapted from Bittar and Labonté (2021).*

2. The many roles of the medial prefrontal cortex

a) Role in decision-making and adaptive behavior

The general role of the mPFC is to produce the most adaptive response—i.e., an action or emotional response—within a given spatial and emotional context. All frontal areas are strongly interconnected (Paxinos and Watson, 2007), meaning that information about actions, emotions, and stimuli is available to all prefrontal areas (Euston et al., 2012).

The mPFC plays a crucial role in executive function—adaptive behavior and decision-making—, including working memory capacities. If the whole mPFC contributes to executive functions and adaptive behaviors in goal- and reward-directed tasks, there appears to be a dorsal-ventral gradient in rodent mPFC, where major distinctions can be observed between the PrL/IL and ACC regions.

On the one hand, experimental studies conducted with rats showed that the **PrL and IL** cortices are crucial to associate a place/location to a reward in a spatial working memory task (Hok et al., 2005). Usually, about one third of cells in PrL/IL regions show firing rate changes tied to reward and reward expectancy (Pratt and Mizumori, 2001; Burton et al., 2009; Gruber et al., 2010). Moreover, PrL and IL have been shown to be involved in cue/context interactions (Baeg et al., 2001), dynamic coding (Batuev et al., 1990; Baeg et al., 2003), action timing (Narayanan et Laubach, 2006; Narayanan et Laubach, 2009), and planning of intended actions—i.e., decision-making—(Seamans et al 1995), with large trial-to-trial variability (Baeg et al., 2003). This suggests that PrL and IL underlie executive functions at the second time-scale. Rich and Shapiro (2009) showed that the mPFC contributes to the coordination of new memory strategies, which demonstrate flexible behavior. Precisely, they pinpointed differences between PrL and IL suggesting that PrL helps to initiate new adaptive strategies, and IL helps to establish them. In addition, neuronal flexibility in PrL and IL—crucial to organize and modify behavior (Seamans et al 1995; Rich and Shapiro, 2009)—allows retrospective encoding of information during the delay period of a working memory task. The neuronal mechanisms underlying working memory capacities in the mPFC, and particularly PrL and IL, will be discussed in the following section of General Introduction and will be the focus of Chapter I.

On the other hand, **ACC** has a slower pacing of processes. In a decision-making task, ACC tracks the animal's progression through monitoring of choices, outcomes, and contexts, at the block of trials level (Lapish et al., 2008; Hillmam and Bilkey, 2012)—i.e., at the minute time-scale. In addition, Wu et al. (2017) also showed that ACC demonstrates no trial-to-trial variability and is necessary to sustain attention. Moreover, if PrL and IL are responsible for flexibility at the second time-scale, ACC is responsible for long-term changes in strategies (Seamans et al., 1995). However, we can also note that recent work demonstrated a possible role of ACC in short time-scale flexibility (Ratté et al., 2018).

Overall, PrL and IL are the executors in reward-based decision-making tasks, such as working memory tasks. PrL and IL are engaged in motivational factors (Diehl and Redish, 2023) and they integrate predictive relationships between stimuli, actions, and reward (Rich and Shapiro, 2009). PrL and IL are characterized by neuronal flexibility that allows adaptive behavior at the second time-scale (Baeg et al., 2003). In opposition, ACC is the monitor of executive functions. ACC is involved in processing information about active decisions (Diehl and Redish, 2023) and monitors animal performances in decision-making tasks at the minute time-scale (Hillmam and Bilkey, 2012; Fig. 11).

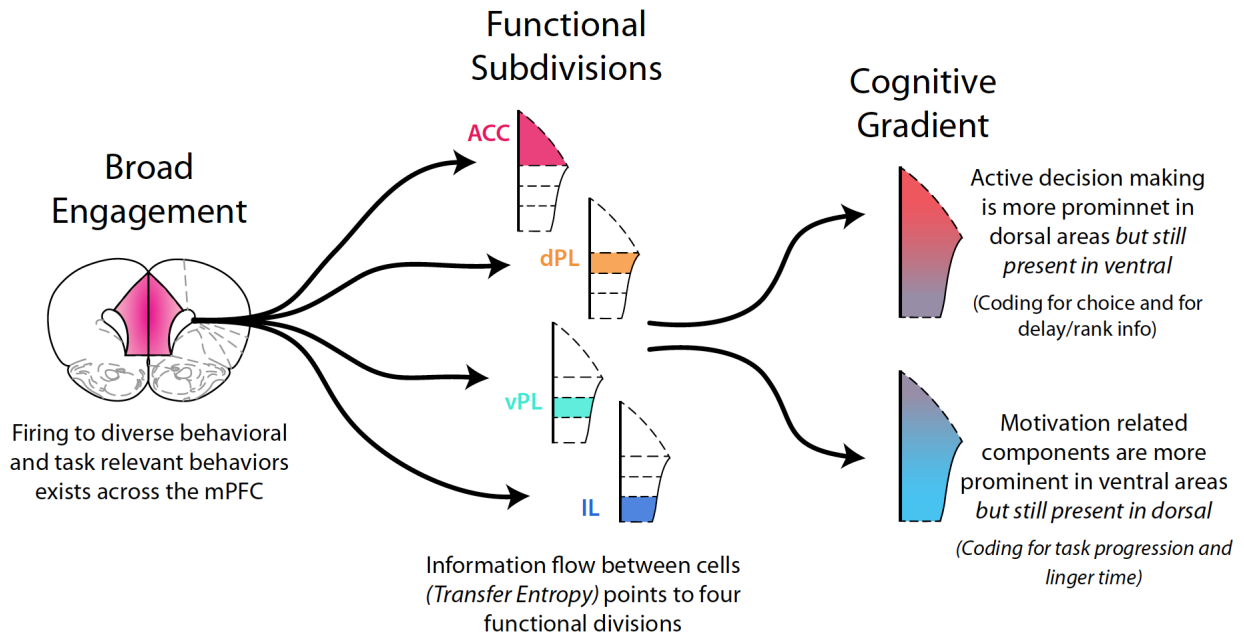

Fig. 11. Functional activity in the medial prefrontal cortex (mPFC). *Functional activity in mPFC exhibits a gradient along the dorso-ventral axis. Neural engagement during active decision processing is more prominent in dorsal regions while motivation related components were more strongly represented in ventral areas. From Diehl and Redish (2023).*

It is interesting to note that if PrL/IL and ACC regions play different roles in goal-directed behaviors, differences also exist in the output responses (Euston et al., 2012).

Based on its connectivity, the **ventral mPFC**—IL and ventral PrL—has been characterized as "visceral motor cortex" (Vogt and Gabriel, 1993). Prominent among its connections are reciprocal projections to and from the amygdala. The ventral mPFC also provides the primary cortical input to the lateral habenula, an area involved in learned responses to pain, stress, anxiety, and reward (Hikosaka, 2010; Li et al., 2011). The ventral mPFC is strongly

interconnected with anterior insular areas, known to be involved in pain perception (Jasmin et al., 2003). The ventral mPFC communicates with the hypothalamus, which mediates intrinsic homeostatic drives, such as hunger and thirst, and coordinates the autonomic and endocrine systems (Paxinos and Mai, 2003). Finally, the ventral mPFC has bidirectional connections with a wide range of neuromodulatory systems, including the dorsal raphe, ventral tegmental area, and locus coeruleus which, among other things, play an important role in adaptive responses to rewarding and stressful events (Schultz, 2001; Maier and Watkins, 2005; Itoi and Sugimoto, 2010; Kranz et al., 2010).

The connections of the **dorsal mPFC**—dorsal PrL and ACC—are similar to those of the ventral mPFC except that the dorsal mPFC has weaker connectivity with emotional and autonomic centers and stronger connectivity with motor and pre-motor areas (Heidbreder and Groenewegen, 2003; Gabbott et al., 2005; Hoover and Vertes, 2007). The dorsal mPFC in rats also projects directly to the spinal cord (Gabbott et al., 2005). To sum up, dorsal mPFC monitors adaptive actions, while adaptive emotional responses are mainly controlled by ventral mPFC (Euston et al., 2012).

b) Other central roles

(1) Social behaviors

The mPFC is also crucial to other cognitive functions and behaviors, including social behavior and **inhibition of inappropriate and impulsive behavior**. It has been shown that the PrL and IL help to prepare upcoming behavior, maintain an appropriate task set, and correct behavior following an error (MacDonald et al., 2000; Garavan et al., 2002). The ACC is involved in conflict detection and evaluative processes indicating when control needs to be more strongly engaged (MacDonald et al., 2000). In a cohort of Alzheimer's patients, reduced gray matter volume in the mPFC and cingulate cortices has been strongly correlated with behavioral disinhibition (Serra et al., 2010)—the inability to inhibit inappropriate behavior, such as impulsivity, poor risk assessments, and disregard for social conventions (Krueger et al., 2011).

Moreover, the mPFC has been shown to regulate **emotional expression**. Patients with bilateral injuries to the mPFC suffer, among others, from a reduced intensity of emotion and can no longer foretell the consequences of what is said and done. However, if only one hemisphere of the mPFC is injured, the other can potentially compensate and avert this social behavioral impairment (Euston et al., 2012).

(2) Long-term memory

Human and animal studies showed that the mPFC is implicated in **long-term memory consolidation and retrieval** (Euston et al., 2012).

Human imaging studies showed that the mPFC is implicated in **memory consolidation**—the process of transforming a labile memory into a more stable, long-lasting form (Müller and Pilzecker, 1900; Lechner et al., 1999)—during sleep. When a group of subjects were deprived of the subsequent night of sleep following word pair learning, scientists observed that, six months after learning, they obtained a lowest test score compared to control subjects. In addition, activity in the mPFC was significantly elevated in control subjects allowed to sleep compared with sleep-deprived subjects.

In rodents, injection of disruptive agents into the mPFC immediately altered learning of various memory tasks led to memory impairments: odor-reward association (Tronel and Sara, 2003; Tronel et al., 2004; Carballo-Marquez et al., 2007), lever-press for reward (Izaki et al., 2000), socially transmitted food preference (Carballo-Marquez et al., 2009), object recognition (Akirav and Maroun, 2005), and the Morris water maze (Leon et al., 2010). Also, interfering with mPFC plasticity immediately after contextual fear conditioning tasks caused deficits in memory retrieval 24 hours to 72 hours later (Runyan et al., 2004).

Specifically, it has been shown there is a critical post-task time-window for consolidation. In mice, disrupting the mPFC one or two hours after learning causes memory impairments because replays for recently learned events in the mPFC can no longer happen, whereas disruption outside this window does not (Izaki et al., 2000; Tronel and Sara, 2003; Takehara-Nishiuchi et al., 2005;Carballo-Marquez et al., 2007; LaLumiere et al., 2010).

Retrieval is the recovery of stored information. Medial PFC is involved in the retrieval of both 'remote' (Bontempi et al., 1999; Frankland et al., 2004; Takashima et al., 2006)—memory spanning several hours or longer (Tronel and Sara, 2003)—and 'recent'—order of tens of minutes (Seamans et al., 1995)—memories (Corcoran and Quirk, 2007); as well as in working memory—spanning hundreds of milliseconds to minutes (Narayanan et al., 2006)—but this will be developed later as it will be the focus of Chapter I.

However, many studies showed greater involvement of the mPFC in remote (vs. recent) memory. Human imaging studies showed a greater activation of the mPFC during the recall of stimuli learned several weeks earlier compared with the recall of recently learned stimuli. Also in mice, imaging studies during spatial and fear memory tests showed that the mPFC is significantly more active during remote retrieval compared with recent (Frankland et al., 2004; Maviel et al., 2004; Teixeira et al., 2006).

In rodents, inactivation of the mPFC led to deficits in retrieval of remote memories while apparently leaving recent memory intact. This effect has been demonstrated across a range of tasks including the radial arm maze (Maviel et al., 2004), the 'win-shift' spatial task in an 8-arm maze (Seamans et al., 1995), the Morris water maze (Teixeira et al., 2006), contextual fear

conditioning (Frankland et al., 2004; Holahan and Routtenberg, 2007), and conditioned taste aversion (Ding et al., 2008).

The greater mPFC activity during remote retrieval can be explained by the greatest dendritic spine growth density—i.e., synaptic plasticity—in mPFC when measured at a remote time point after a task, as compared with a more recent time point (Restivo et al., 2009).

(3) Self-awareness

If the philosophy and neuroscientific questions about the neural basis of consciousness will not be detailed in this thesis, multiple studies suggest that the mPFC might play a role (Michel and Morales, 2019).

In humans, it has been proven that the mPFC is one of the crucial brain regions for the 'default state network' activation when we have nothing in particular in mind. With the mPFC—responsible, among others, for coordinating emotions and thinking—, other brain regions are also activated (Fig. 12): posterior cingulate cortex, precuneus, and angular gyrus (Graner et al., 2013).

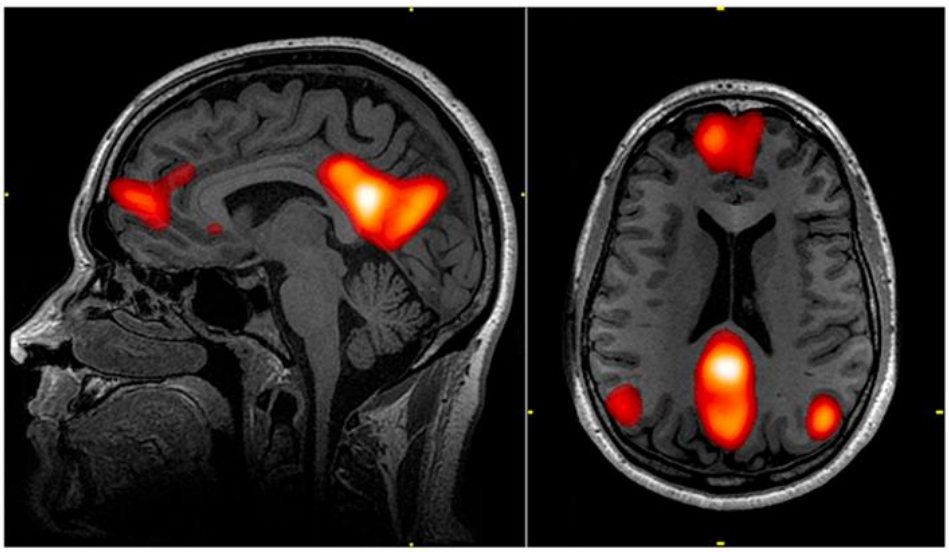

Fig. 12: Locating the self. *Magnetic resonance imaging of areas of the brain in the default mode network. From Graner et al. (2013).*

Now that we discussed the diverse roles of the mPFC, we will focus on its specific role in working memory capacities and what are the neuronal and circuit excitability mechanisms involved.

B. The seat of working memory

Working memory (WM)—i.e., the fundamental ability to access and manipulate transient information for a few seconds—is essential to higher cognitive functions (Baddeley, 1992). Imaging techniques in humans (Courtney et al., 1998; Nyberg, 2002; D'Esposito et al., 2006; Quentin et al., 2019) and extracellular recordings in primates and rodents (Fuster, 1973; Goldman-Rakic, 1995; Yang et al., 2014) have unraveled that the mPFC plays a central role in WM.

1. Spatial and object working memory: The most studied working memory types

WM capacities can easily be assessed *in vivo* in humans and animals using a stereotyped form of behavioral tasks consisting in 1) a phase of presentation of the stimulus/cue/information to remember, 2) a delay of a few seconds during which the animal has to hold in memory the information to remember, 3) a test to assess WM capacities.

Object WM (OWM) is the ability to temporarily store and manipulate binary information—e.g., the presence or absence of an object, the color of an object—and can be tested *in vivo*, for example, by training the animal to remember a specific object (Fig. 13A) or the color of a light source in a delayed match-to-sample experiment (Dudchenko, 2004).

Spatial WM (SWM) is the ability to temporarily store and manipulate spatial information and can be tested *in vivo*, for example, by training the animal to remember which arm of a T-maze does not contain the reward (Fig. 13B; Dudchenko, 2004).

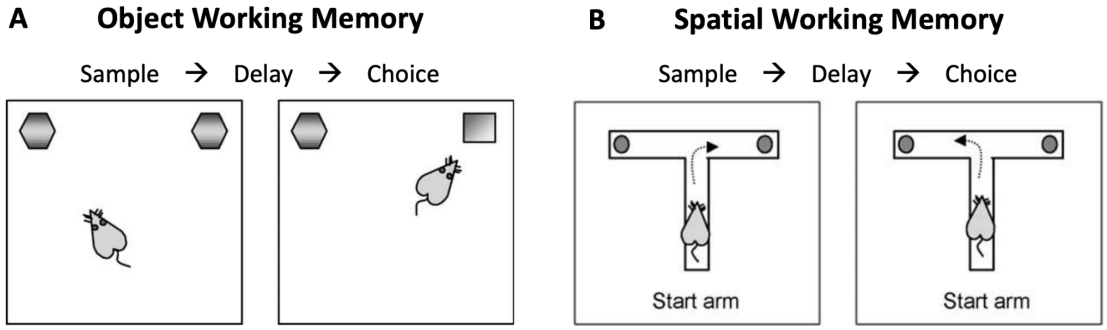

Fig. 13. Examples of Object Working Memory and Spatial Working Memory tasks in rodents. A. *The spontaneous exploration task of Ennaceur and Delacour (1988). A rodent is presented with an object or pair of identical objects which are allowed to explore. Following a delay, the rodent is presented with the previously presented object and a novel object. The rodent tends to demonstrate its memory for the previously presented object by spending more time exploring the novel object.* ***B.*** *Delayed alternation on a T-maze. On the sample run, the rodent is placed on the stem of the T-maze and permitted to enter one of the arms. The rodent may then be removed from the maze for a delay period. After the delay, the rodent is returned to the stem of the maze, and will typically choose the alternate arm of the T-maze. Adapted from Dudchenko (2004).*

It is well established that WM relies on persistent activity (PA)—i.e., the ability of neural networks to maintain neural activity after the end of a stimulation (Fuster and Alexander, 1971). For instance, in OWM, neurons in the PFC show sustained activity for one specific cue—e.g., red light—but not for the other—e.g., green light—(Fuster and Jervey, 1981; Fuster and Jervey, 1982; Fuster et al., 1982). In SWM, self-maintained level activity occurs in PFC neurons that are selective of the spatial position of the triggering cue (Funahashi et al., 1989; Goldman-Rakic, 1995).

The theory is that overall PA, occurring during WM task delay, self-sustains through spiking reverberation in recurrent excitatory loops within the network (Wang, 2001; Compte, 2006). In the neocortex, **four different hypotheses** could explain this theory (Wang, 2001):

- PA could arise from **a large network composed of the cortex and subcortical regions**, such as the thalamocortical loop, or the cortico-striato-thalamo-cortical loop. Consistent with this theory, thalamic (Fuster and Alexander, 1973) and caudate (Hikosaka et al., 1989) neurons exhibit PA.
- PA could be maintained by **reciprocal loops between cortical areas**, such as between the mPFC and the posterior parietal cortex. PA is recorded in these two brain regions, however there is no evidence that this mPFC-Parietal cortex loop is necessary for the generation of PA. On the contrary, in macaques performing an OWM experiment (Miller et al., 1996), it has been shown that the mPFC is capable of sustaining a stimulus-selective persistent activity when the inferotemporal neurons are easily disrupted by distractors.
- PA could be produced by **local excitatory loops within the mPFC**. Goldman-Rakic (1995) proposed a PFC network model in which PA arises from reverberatory excitation and stimulus selectivity is formed by recurrent inhibition. This theory is consistent with the anatomical and electrophysiological data showing extensive horizontal excitatory connections in the mPFC (macaques: Levitt et al., 1993; Kritzer and Goldman-Rakic, 1995; Gonzalez-Burgos, 2000). Moreover, mPFC synapses display short-term plasticity on a time scale of 0.1-10 seconds, which might contribute to increase the synaptic efficacy transiently during a reverberatory activity (rats: Hirsch and Crepel 1990; Hempel et al., 2000).

Theoretical work confirmed that cortical architectures may provide sufficiently excitatory and nonlinear feedback for neocortex dynamics to converge toward PA (attractor dynamics: Cossart et al., 2003; MacLean et al., 2005). However, network excitatory reverberation as the unique cause of network PA emergence is controversial because it fails to robustly account for fundamental aspects of persistent activity: the high irregularity of spiking during the delay period of WM tasks, the large intertrial variability of the discharge, and the ability to encode

parametric information (Seidemann et al., 1996; Koulakov et al., 2002; Compte et al., 2003; Goldman, 2003; Shafi et al., 2007; Barbieri and Brunel, 2008).

- As a non-exclusive alternative that could explain parametric working memory capacities, it has been proposed that PA requires spiking reverberation, but also **intrinsic cellular bistability**. This is the theory we will investigate in my thesis work.

2. Parametric working memory

a) An ubiquitous property among mammals

Parametric WM (PWM) is the ability to temporarily store and manipulate quantitative information—e.g., a numerical value or the perceived magnitude of a physical dimension (the size of an object, the amplitude of a sound, or the frequency of a vibration; Romo et al., 1999).

PWM can be tested *in vivo*, for example, by training the animal to hold in memory the frequency of a mechanical vibration applied to the tip of a finger (macaques; Brody, 2003; Barak et al., 2010) or against the whiskers (rats, Fig. 14; Fassihi et al., 2014). In this type of behavioral task, after the delay, the animal is presented to another cue characterized by a different frequency or amplitude, and the animal has to indicate which one of the first or second cue had the highest frequency/amplitude.

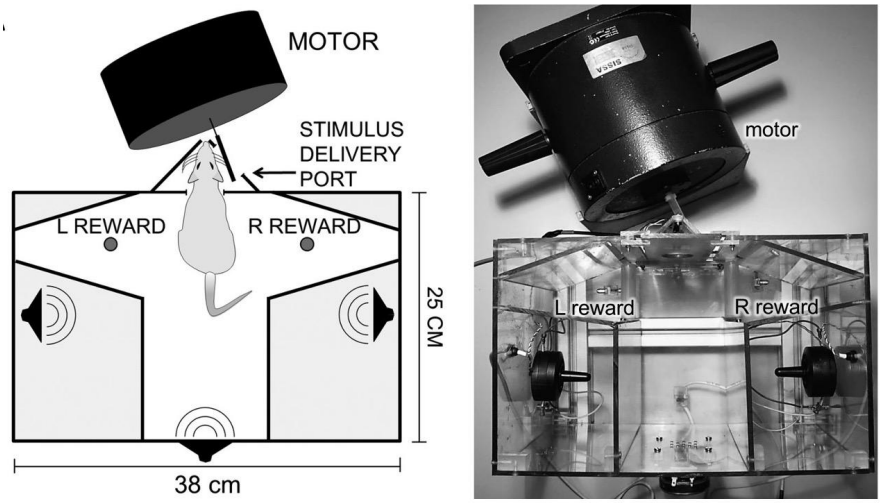

Fig. 14. Example of parametric working memory (PWM) task with rats. *The rat places its head into the stimulus delivery port, then receives two whisker stimulations characterized by two different frequencies and separated by a delay of a few seconds. The rat has to hold in memory the parametric information of the two simulations and indicate which one has the highest or smallest vibration frequency. Left: apparatus schematic. Right: Photograph of the apparatus from above. Adapted from Fassihi et al. (2014).*

We use PWM capacities every day, for example to estimate the amplitude of a sound, the size of an object, or quantities in a general manner Despite the crucial role of PWM in daily life, the mechanisms underlying PWM are still poorly understood. The goal of Chapter I will be to investigate the cellular and circuit excitability mechanisms underlying PWM.

b) Graded persistent activity: The neural correlate of parametric working memory

As we saw above, PA is the network correlate of all types of WM. However, depending on the type of WM studied, this PA has different features. For instance, in monkeys and models, the PA recorded in the mPFC during the delay of a PWM task is called graded persistent activity (GPA; Fig. 15) and scales with the information/cue amplitude to be remembered—for example, higher is the amplitude of a sound to remember, higher is the neuronal firing rate during the delay (Romo et al., 1999; Koulakov et al., 2002, Brdoy et al., 2003; Goldman et al., 2003, Major and Tank, 2004).

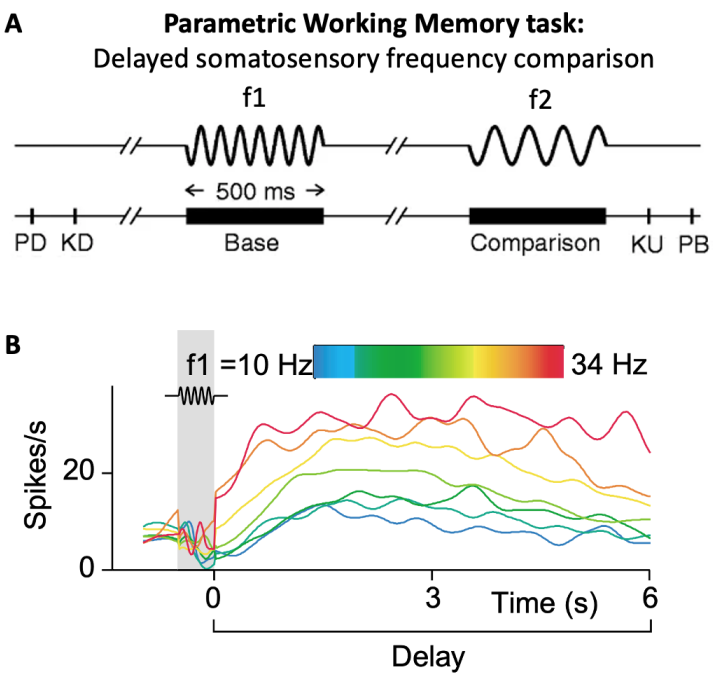

Fig. 15. Graded persistent activity recorded in the prefrontal cortex (PFC) of monkeys during the delay of a parametric working memory task. A. *Sequence of events during parametric discrimination trials. The mechanical probe is lowered on the skin of one digit of the hand (PD); the monkey places his free hand on an immovable key (KD); the probe oscillates vertically, at the base frequency (f1); after a delay, a second mechanical vibration is delivered at the comparison frequency (f2); the monkey releases the key (KU) and presses one of two push-buttons (PB) to indicate whether the comparison frequency was higher or lower than the base. Adapted from Romo et al. (1999).* ***B.*** *Unit recordings of a PFC neuron from a monkey performing a somatosensory vibration delayed match task. Firing rate increases with the frequency of f1, the stimulus being remembered, indicated by different colors. From Major and Tank (2004).*

Theoretical studies showed that, just like PA in OWM and SWM, GPA emergence requires reverberation of activity within recurrent connectivity—the prevailing architecture in local mPFC networks (Seung et al., 2000; Miller et al., 2003; Machens et al. 2005; Machens and Brody, 2008). However, robust emergence of GPA—that doesn't require the fine-tuning in the models—also requires the presence of individual elements (pyramidal neurons or small groups of pyramidal neurons) within the mPFC recurrent neural network model characterized by a bistable behavior (Koulakov et al., 2002; Goldman et al., 2003).

As mentioned in the first section of General Introduction, cellular bistability can be defined as the coexistence of two stable states of quiescence and self-sustaining spiking; in other words, pyramidal neurons that exhibit bistable properties can continue to discharge after the end of an input—i.e., self-sustained spiking. Bistable neurons oppose monostable neurons (M; Fig. 16A) that can not continue to discharge after the end of a stimulation—i.e., two stable states of quiescence and spiking cannot co-exist.

The role of bistable neurons in the emergence of PA in WM has long been criticized because bistability presents features that are rigid, in the context of WM flexibility. Such stereotyped bistable features include independence to background depolarization, requirement for long stimuli (scale of seconds), strong pharmacological manipulations, long and highly regular discharges at high frequency (tens of seconds to minutes), with possibly inactivated spikes (Haj-Dahmane and Andrade, 1997; Egorov et al., 2002; Tahvildari et al., 2008; Zhang and Séguéla, 2010; Gee et al., 2012).

Experiments performed on monkey neurons showed that, under strong neuromodulatory manipulations that upregulates depolarizing spike-triggered conductances, a type of bistability—called absolute bistability (AB; Fig. 16B)—can maintain neuronal self-sustained spiking after receiving a supra-threshold stimulation. However, AB neurons display unrealistic stereotypes discharges inconsistent with WM firing patterns (Compte et al., 2003; Shafi et al., 2007).

If AB cannot explain the emergence of GPA in PWM, a more flexible form of bistability—called conditional bistability (CB; Fig. 16C)—has been proposed by Rodriguez et al. (2018) to be key in that phenomenon in coarse-grained recurrent neural network models (Koulakov et al., 2002; Goldman et al., 2003) and as a plausible biophysical mechanism (Rodriguez et al., 2018).

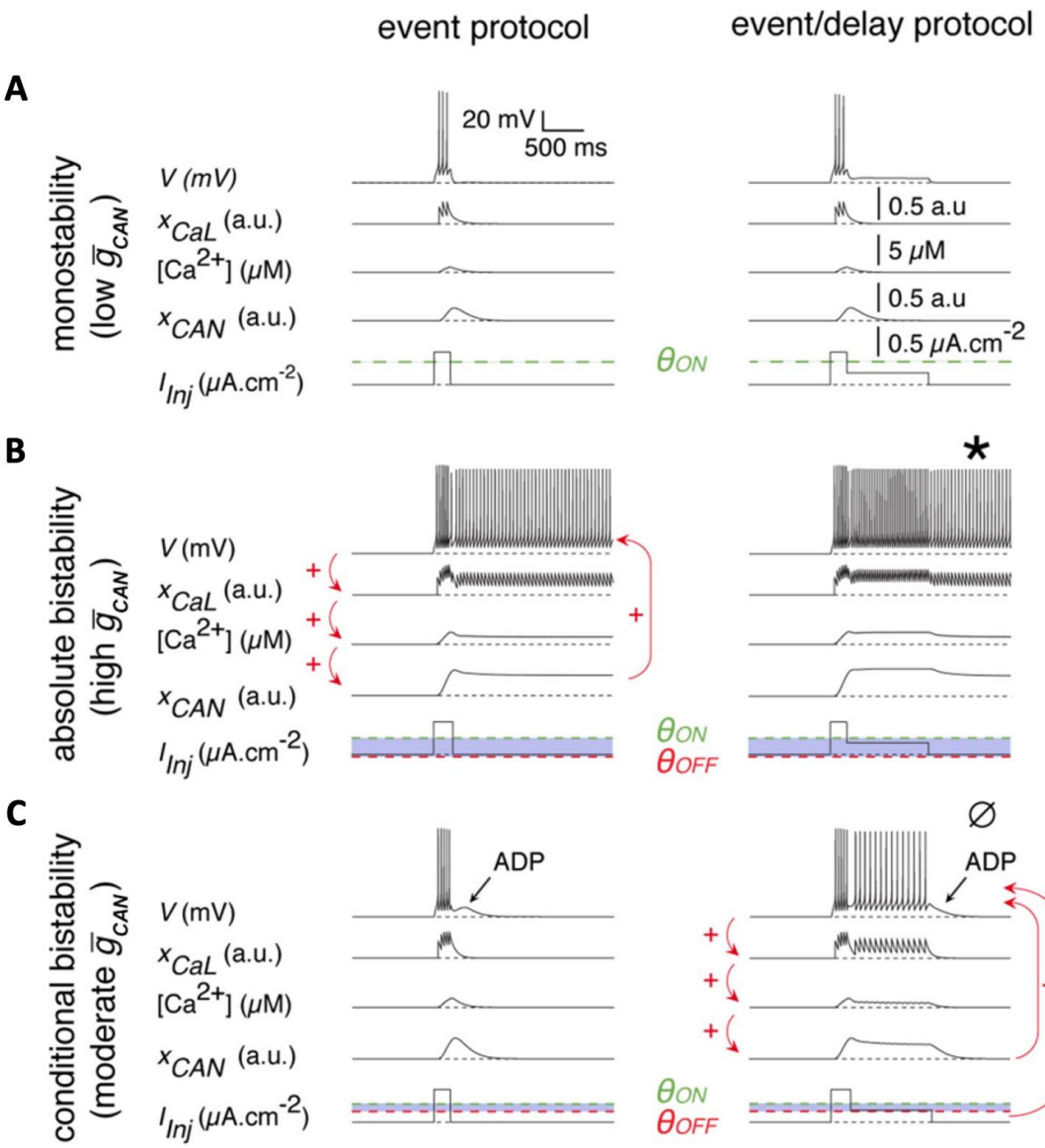

Fig. 16. Conditional bistability is a hidden property in neurons endowed with a suprathreshold conductance in response to standard protocols applied in vitro. *The response of monostable (**A**, gCAN=0.003 mScm^2), absolute bistable (**B**, gCAN=0.03 mScm^2), and conditional bistable (**C**, gCAN=0.02 mScm^2) neuronal models to an event protocol with a 0.2 s suprathreshold current step (left, I_{Inj}) and to the event-delay protocol, in which the event is followed by a subthreshold depolarizing current mimicking background activity in PFC networks during the delay of a working memory task (right, I_{Inj}). Note that the discharge is continuing after the delay stimulus in the absolute bistable neuron (B, star symbol). Note the afterdepolarization (C, ADP, void symbol) following spiking in the conditional bistable neuron. The thresholds for initiating (θ_{ON}) and terminating (θ_{OFF}) spiking are represented as green and red dotted lines, respectively, and the bistability domains are shown in lavender. Red arrows denote the positive feedback loop among spiking, CaL activation (x_{CaL}), increased [Ca^{2+}], and CAN activation (x_{CAN}). Adapted from Rodriguez et al. (2018).*

c) Conditional bistability: The *theoretical* intrinsic property facilitating graded persistent activity

In a recent theoretical study, our team characterized a novel form of spike-mediated bistability called conditional bistability (CB, Fig. 16C). This new type of neuronal bistability demonstrates, in theory, a rich repertoire of cellular mnemonic features, both in *in vitro*-like conditions and under realistic asynchronous synaptic inputs mimicking *in vivo* conditions (Rodriguez et al., 2018). In addition, CB doesn't present stereotyped behaviors such as the ones observed in AB. On the contrary, CB displays functional spikes with low firing frequency (a few hertz, characterizing of regular-spiking neurons) in response to short stimuli, with reasonable durations (Rodriguez et al., 2018).

In contrast to AB, what makes neuronal CB particularly interesting to explain flexible WM mechanisms is that a phasic supra-threshold stimulation—e.g., due to a perceptive, decisional, or motor event—is not sufficient to elicit self-sustained spiking. Hence, under CB, self-sustained spiking also requires a long—tonic—sub-threshold depolarizing stimulation following the initial supra-threshold input. *In vivo*, this tonic pulse may arise from background synaptic inputs due to network PA reverberating within the mPFC (or from connected brain structures) to hold in memory information about the initial event.

Altogether, theoretical neuronal CB could be key in the emergence of flexible WM mechanisms such as GPA, the network correlate of PWM. However, despite many experimental studies addressing self-sustained spiking (Andrade, 1991; Haj-Dahmane and Andrade, 1997; Morisset and Nagy, 1999; Thuault et al., 2013), CB itself has been overlooked, due to the sub-threshold input it requires, and CB has not been demonstrated to exist yet.

According to modeling work, voltage- and calcium-gated ion channels would be key to generate CB (Rodriguez et al., 2018). In addition, experimental studies showed that self-sustained spiking in pyramidal neurons depends on the balance between after-depolarizations (ADP)—i.e., the membrane potential becomes more positive following spiking—and after-hyperpolarizations (AHP)—i.e., the membrane potential becomes more negative following spiking. If the ADP/AHP balance increases, it means that spiking is facilitated and persistent spiking can occur.

Afterpolarizations—i.e., ADP and AHP—can be classified in three different time components: fast (fADP/AHP, characterized in this manuscript by a time constant of tens of ms), medium (mADP/AHP, time constant of ~100-300 ms), and slow (sADP/AHP, time constant of ~500 ms). In the literature, fADP and sADP are known to enhance self-sustained spiking (Haj-Dahmane and Andrade, 1997).

Currents underlying the ADP/AHP balance have been reported to represent excitatory calcium-activated non-selective cationic currents (Haj-Dahmane and Andrade, 1996, 1997,

1998), inhibitory calcium-activated potassium currents (Gulledge et al., 2009) or a combination of both types.

- **Calcium-activated non-selective cationic (CAN) channels**

There is a general consensus that ADP, and particularly sADP, increases are driven by the activation of CAN current-mediated channels (Andrade, 1991; Haj-Dahmane and Andrade, 1997, 1998, 1999). CAN channels are cationic—i.e., calcium and sodium—channels activated by elevation of intracellular concentration of calcium—caused by spiking, activation of Ca_L (Haj-Dahmane and Andrade, 1997), and under the influence of neuromodulation as we will discuss later.

Application of the calcium-channel blocker cadmium, and the use of intracellular calcium buffer BAPTA, lead to the inhibition of fADP (Fig. 17A; Haj-Dahmane and Andrade, 1997). BAPTA application also leads to a decrease in sADP (Fig. 17B, Haj-Dahmane and Andrade, 1998).

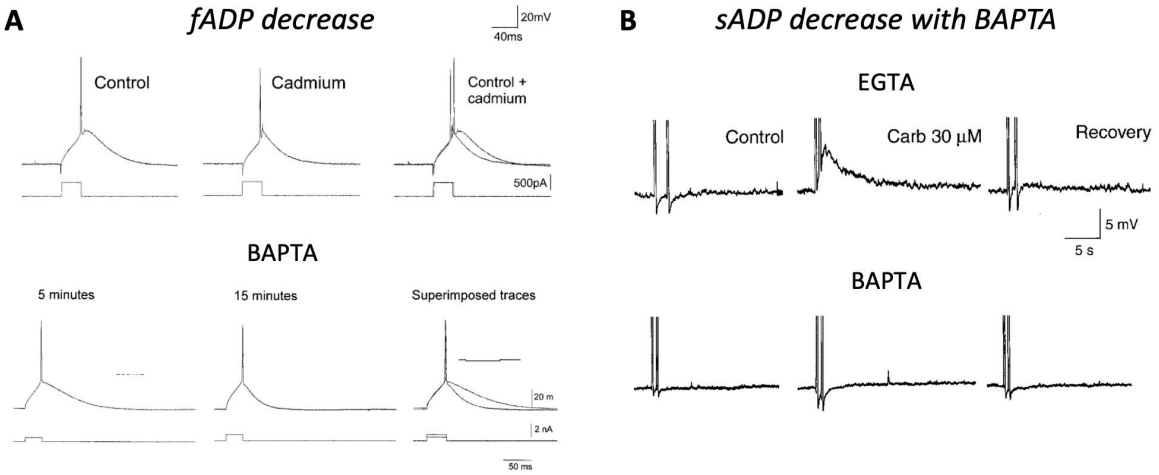

Fig. 17. Blocking calcium channels and buffering intracellular calcium reduces the fast and slow afterdepolarization in rat medial prefrontal cortex. A, *Voltage responses of mPFC pyramidal neurons to a brief suprathreshold stimulus in control condition, in presence of a calcium channel blocker, cadmium (100 mM), and in presence of a calcium buffer, BAPTA (10 mM). Cell resting membrane potential: -72 mV. Adapted from Haj-Dahmane and Andrade, 1997.* ***B,*** *Voltage responses of mPFC pyramidal neurons to a brief stimulus in presence of the low-calcium buffer EGTA (20 µM) and in presence of BAPTA (10 mM). Adapted from Haj-Dahmane and Andrade, 1998.*

More specifically, it has been shown that expression of calcium-activated transient receptor potential canonical (TRPC) channels—e.g., TRPC5 or TRPC6, which are representative of the two main TRPC subfamilies—greatly facilitates the amplitude of currents underlying sADP (I_{sADP}) in pyramidal neurons (Haj-Dahmane and Andrade, 1998; Strübing et al., 2001; Yan et al., 2009).

Also, I_{sADP} is inhibited by flufenamic acid (FFA; Fig. 18)—a widely used TRPC-mediated CAN current blocker.

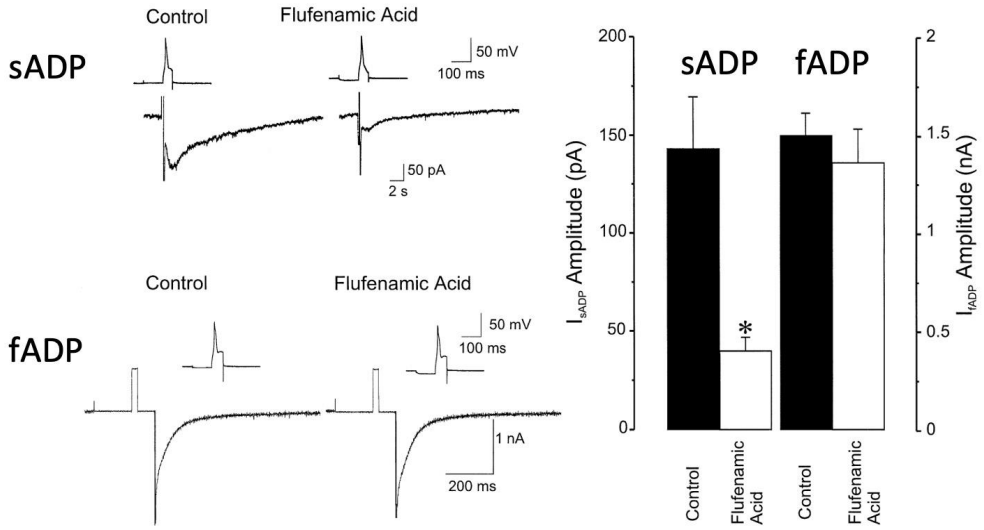

Fig. 18. Flufenamic acid (FFA) decreases slow afterdepolarization (sADP). *FFA selectively blocks the carbachol-induced I_{sADP}. Carbachol-induced I_{sADP} and I_{fADP} were recorded using a `hybrid' current/voltage-clamp protocol in control conditions and in the presence of 100 mM FFA. The insets depict the calcium spikes used to trigger the I_{sADP} and I_{fADP}. Note that the carbachol/cholinergic effect on ADp will be discussed below. Adapted from Haj-Dahmane and Andrade (1999).*

- **Small conductance calcium-activated potassium (SK) channels**

In contrast to CAN channels, SK channels—that are also activated by elevation of the intracellular concentration of calcium during spiking—are responsible for increasing AHP, accomplished through the leak of positively charged potassium ions along their concentration gradient into the extracellular space (Faber and Sah, 2007). This hyperpolarization causes the membrane potential to become more negative and limits spiking, thus PA.

Blocking SK channels with pharmacological agents, such as apamin, reduces AHP and reveals ADPs (Fig. 19).

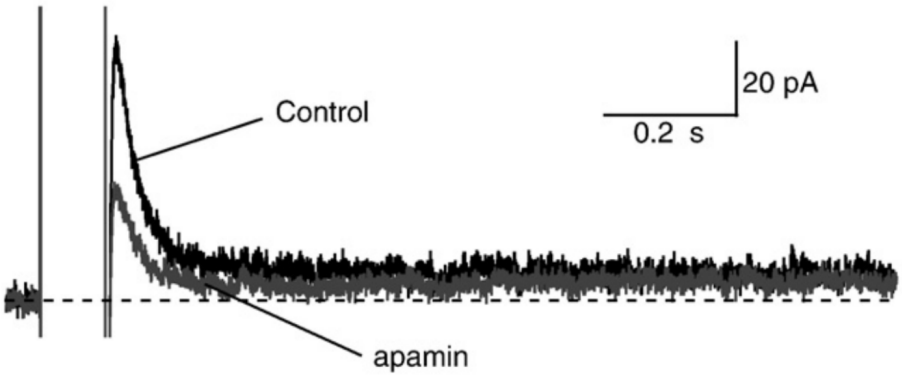

Fig. 19. Effect of apamin of medium afterhyperpolarization currents (I_{mAHP}). *I_{mAHP} evoked by a 100 msec, +50 mV voltage step from a holding potential of −60 mV and recorded at −60 mV is reduced in presence of the SK channels selective blocker apamin (100 nM). From Satake et al. (2008).*

Because the two types of channels described here—CAN and SK—are calcium-activated, it can be challenging to distinguish the specific effect of one or the other type of channels on the afterpolarization potentials. However, only the overall ADP/AHP balance matters to generate self-sustained spiking, and thus CB.

In Chapter I, we will investigate how this ADP/AHP balance is affected in CB in mPFC pyramidal neurons. Then, in Chapter II, we will discuss how it is affected in pathological conditions.

3. The importance of the neuromodulation in neuronal self-sustained-spiking

a) Acetylcholine (ACh)

It is well established that cholinergic inputs to the neocortex play an important role in supporting processes of attention (Phillis, 2005)—required during decision-making tasks, such as PWM.

ACh appears to enhance the strength of input relative to feedback in the cortex. Physiological impact of ACh is twofold: it amplifies the effect of feedforward afferent input to the cortex while simultaneously reducing background activity caused by spontaneous spiking and the spread of activity through excitatory feedback connections within cortical circuits. Consequently, higher ACh levels boost the reactivity to sensory input coming from the thalamus, thereby increasing attention to the surrounding environment and making cortical circuits more sensitive to distinct features of sensory stimuli (Fig. 20; Hasselmo and McGaughy, 2004). Two sets of effects can explain this: **1)** ACh causes depolarization of pyramidal cells, and reduction in spike frequency accommodation, allowing pyramidal cells to respond more robustly to external afferent input (Madison and Nicoll, 1984; Tseng and Haberly, 1989; Barkai

and Hasselmo, 1994), and **2)** ACh depolarizes inhibitory interneurons, decreasing background spiking activity, while suppressing inhibitory synaptic transmission (Patil and Hasselmo, 1999), allowing a stronger response to afferent input due to reduced inhibitory feedback.

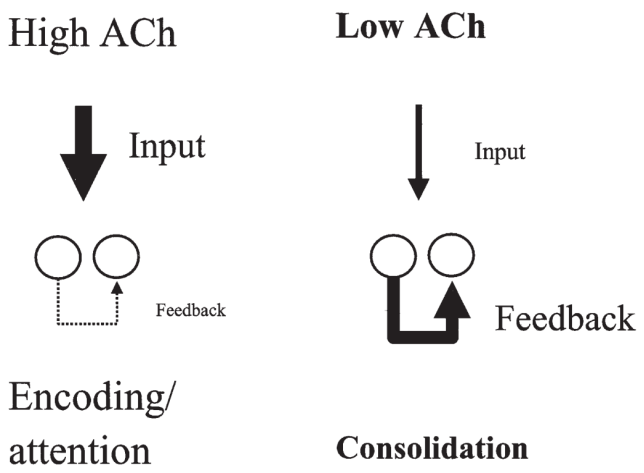

Fig. 20. General theory of acetylcholine (ACh) effects in cortical circuits. *This circuit diagram summarizes the predominant effect of ACh within cortical circuits. High ACh levels cause an increase in the influence of afferent input relative to internal processing. Low ACh levels allow strong feedback relative to weaker afferent input. From Hasselmo and McGaughy (2004).*

More than enhancing depolarization of pyramidal neurons and reducing spiking accommodation, ACh modulates self-sustained spiking (Haj-Dahmane and Andrade, 1996, 1998; Gulledge et al., 2007; Gulledge et al., 2009; Zhang and Séguéla, 2010; Kurowski et al., 2015)—i.e., cellular memorization—, suggesting a crucial role of ACh in CB.

Theoretical work showed that CB emergence in the mPFC depends on the fraction of functional ionic channels in the neurons (Rodriguez et al., 2018) that can be influenced by neuromodulation. Without investigating CB itself, experimental work on self-sustained spiking in cortical neurons indicates that the activation of CAN channels requires neuromodulatory signals such as ACh (Haj-Dahmane and Andrade, 1999; Egorov et al., 2002; Tahvildri et al., 2008).

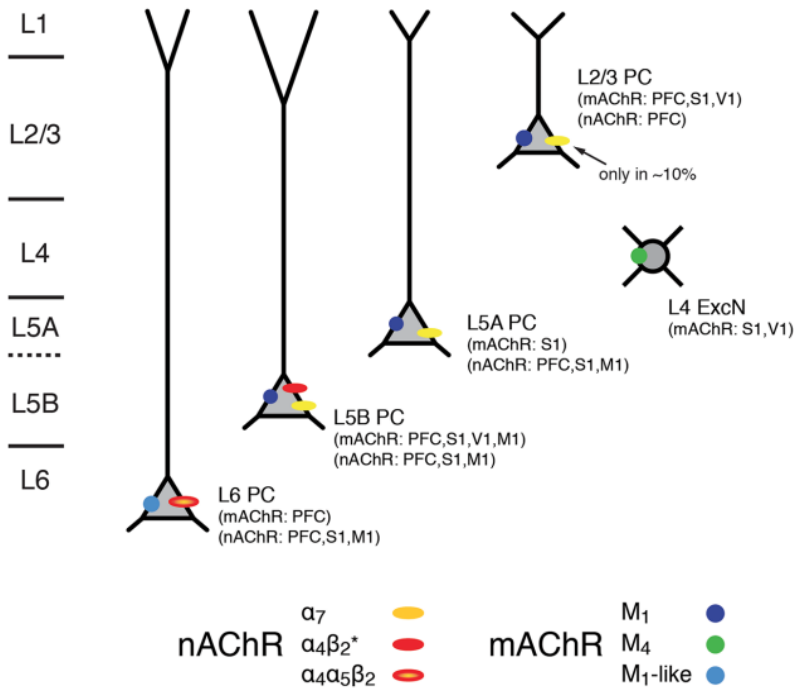

Fig. 21. Expression of cholinergic muscarinic (mAChRs) and nicotinic (nAChRs) receptors in the neocortex. Schematic diagram of the layer- and cell-type specific distribution of nAChRs and mAChRs in the neocortex. Cortical layering is indicated on the left. Pyramidal cells (PC) in layers 2/3, 5A, 5B and 6 are shown. The different brain regions from which the mAChR and nAChR distribution were obtained are given in brackets. From Radnikow and Feldmeyer (2018).

In the layer V pyramidal neurons, both nicotinic and muscarinic cholinergic receptors are expressed (Fig. 21; Radnikow and Feldmeyer, 2018). There is no evidence that nicotinic receptors mediate depolarizations leading to self-sustained spiking (Haj-Dahmane and Andrade, 1996). However, multiple studies have shown that the activation of muscarinic 1 (M1) receptors *in vitro*, via application of carbachol (or oxotremorine/muscarine; Haj-Dahmane and Andrade, 1998), leads to the increase of currents underlying sADP (I_{sADP}; Fig. 22A; Andrade, 1991; Haj-Dahmane et Andrade, 1998, 1999). This afterpotential, once induced, can sustain spiking that greatly outlasts the original stimulus and therefore may serve as a mechanism for the transient storage of memory traces within neuronal networks (Fig. 22B, Andrade, 1991). Specifically, carbachol M1 receptor-binding would increase sADP, through an intracellular mechanism that involves, among others, $G_{q/11}$ and PLC (Yan et al., 2009).

Carbachol-induced I_{sADP} is likely mediated by CAN channels because it is inhibited 1) by FFA (Fig. 18), and 2) by expression of a pore-dead TRPC5 subunit acting as a dominant negative against homomeric and heteromeric TRPC channels (Yan et al., 2009).

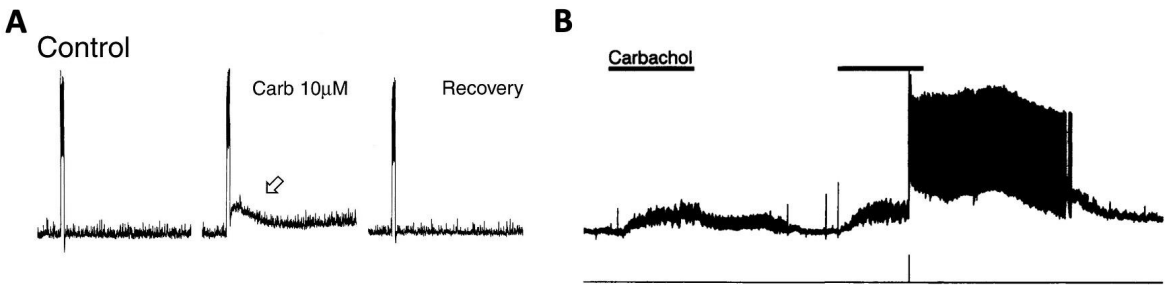

Fig. 22. Activation of muscarinic 1-like (M1) receptors with carbachol increases slow afterdepolarization (sADP), thus persistent activity, and carbachol-induced sADP is inhibited by flufenamic acid (FFA), a blocker of calcium-activated non-selective cationic (CAN) channels. A, *Carbachol (10 μM) induces sADP in pyramidal neurons of the medial prefrontal cortex (mPFC). From Haj-Dahmane and Andrade (1998).* ***B,*** *A single depolarizing current pulse can initiate persistent activity in the presence of carbachol. From Andrade (1991).*

In addition to the activation of Ca_T channels that also allow the activation of CAN channels (Haj-Dahmane and Andrade, 1998), the intracellular cascade of events arising from the binding of ACh to the M1 receptor activates Ca^{2+} release from the endoplasmic reticulum (Dasari et al., 2016). The overall strong increase in intracellular Ca^{2+} levels promotes the activation of CAN channels (Fig. 23).

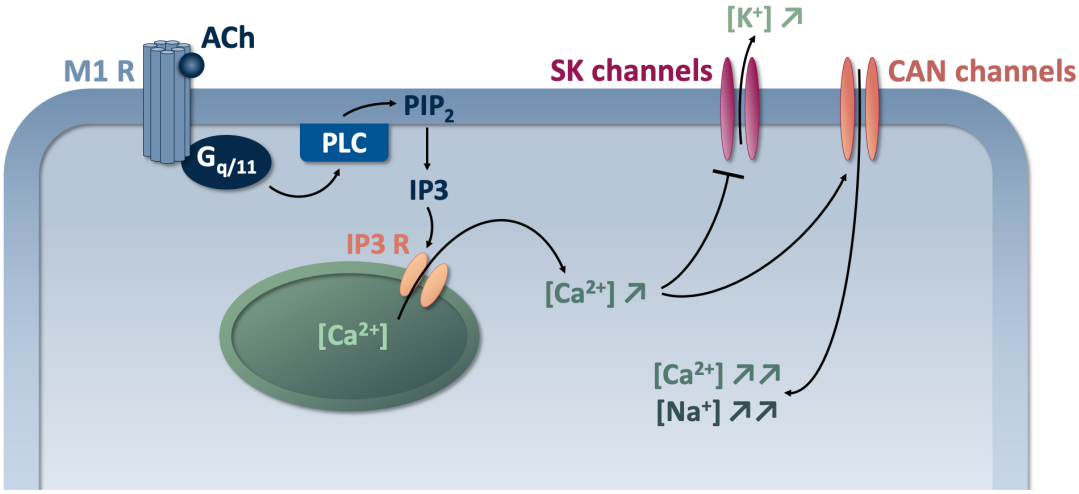

Fig. 23. Summary of the muscarinic 1 (M1)-mediated activation of the CAN channels. *ACh, acetylcholine; M1 R, muscarinic 1-like receptor; Gq/11, G-Protein q/11; PLC, phospholipase C; PIP2, Phosphatidylinositol 4,5-bisphosphate; IP3, inositol trisphosphate; IP3 R, inositol trisphosphate receptors; SK channels, small-conductance calcium-activated potassium channels.*

Altogether, these experimental results on the neuromodulation of ACh on self-sustained spiking—i.e., cellular memorization—and attention mechanisms, added to the theoretical work on the role of the CAN channels in CB, suggest that CB could rely on cholinergic M1 receptor signaling. This hypothesis will be addressed in Chapter I.

b) Other neuromodulators

Although the ACh M1 receptor activation seems to be the predominant source of sADP emergence, it has been proven that other neuromodulators are also capable of coupling to $G_{q/11}$ and inducing PA (Araneda and Andrade, 1991; Greene et al., 1994; Sidiropoulou et al., 2009).

(1) Serotonin (5HT)

In vitro, it has been shown that activation of 5HT receptors leads to depolarization of the membrane potential, via inhibition of the I_{AHP} (Fig. 24; Satake et al., 2008).

Increases in ADP/AHP balance are likely to be caused by the activation of $5HT_2$ receptors—which are associated with an increase in the turnover of inositol phospholipids, shared with a variety of other neurotransmitter receptors including cholinergic M1 and adrenergic α1 receptors (Barnes and Sharp, 1999).

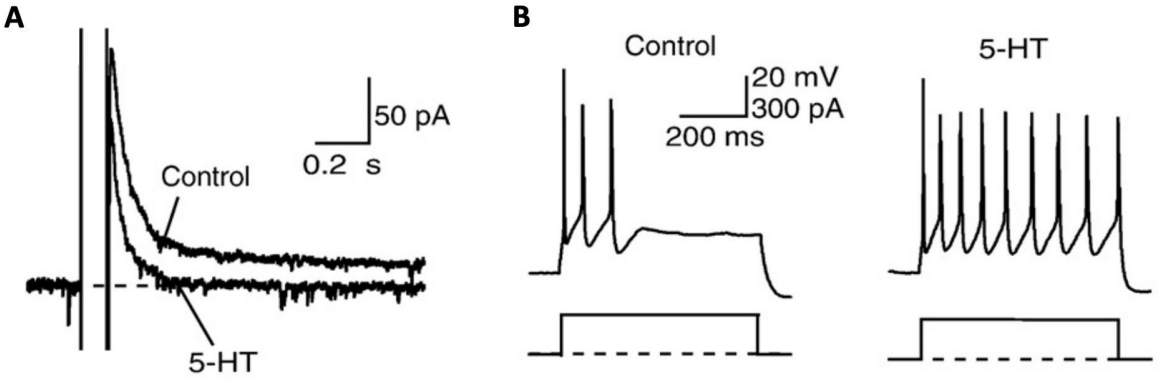

Fig. 24. Serotonin (5HT)-induced suppression of the medium and slow AHP currents (I_{mAHP} and I_{sAHP}) accompanied by reduced spike-frequency adaptation. A, *5HT inhibited the I_{mAHP} and I_{sADP}, which were induced by a 100 msec, +50 mV voltage step from a holding potential of −60 mV and recorded at −60 mV.* ***B,*** *5HT also decreased spike-frequency adaptation. Adapted from Satake et al. (2008).*

Consistently, 5HT applied during periods of sustained PA in pyramidal neurons produces a robust increase in instantaneous spike frequency, through the increase in ADP (Stephens et al., 2018). Moreover, 5HT-induced ADP is greatly reduced when Ca^{2+} is chelated with BAPTA,

meaning that ADPs are gated by intracellular calcium signaling. Stephens et al. (2018) propose that serotonergic—through $5HT_2$ receptors—and cholinergic—through M1 receptors—signaling share common features such as the activation of $G_{q/11}$.

(2) Dopamine (DA)

Various studies demonstrated opposing roles of DA modulation on self-sustained spiking in the mPFC. In the layer V pyramidal neurons, almost all families of dopaminergic receptors are expressed (Fig. 25).

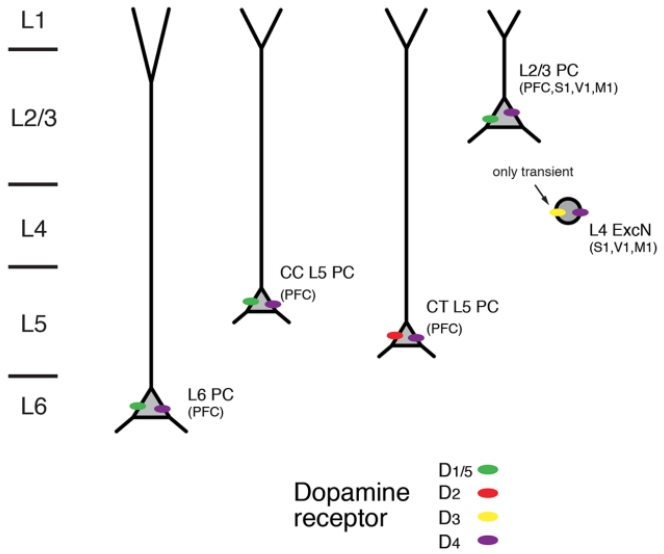

Fig. 25. Expression of dopamine receptors in the neocortex. Schematic diagram of the layer- and cell-type specific distribution of dopamine receptor types in different pyramidal cell types in the neocortex. Data were obtained for pyramidal cells (PC) in layers 2/3, 5, and 6. The different brain regions from which the dopamine receptor distribution were obtained are given in brackets. CC: L5 corticocortical projection targets; CT: L5 corticothalamic projection targets. From Radnikow et al. (2018).

On the one hand, D2/D3 receptor activation mediates inhibition of Ca^{2+}-activated I_{sAHP} (Satake et al. 2008) and overall ADP increases (Gee et al., 2012) in layer V pyramidal neurons, through the activation of CAN channels, among others (Gee et al., 2012).

On the other hand, the effects of D1/D5 receptor activation on PA were the most studied and antagonist effects have been observed. Most studies showed that D1/D5 receptor activation suppresses the high-voltage Ca_L-mediated action potentials (Young and Yang, 2004). Sidiropoulou et al. (2009) demonstrated that D1/D5 receptor activation leads to the sADP

decrease, through the intracellular cascade involving Gs activation, cAMP levels increase, PKA activation, and inhibition of the metabotropic glutamate receptors (mGluR). However, Chen et al. (2007) demonstrated that D1/D5 receptor activation facilitates PA (Fig. 26).

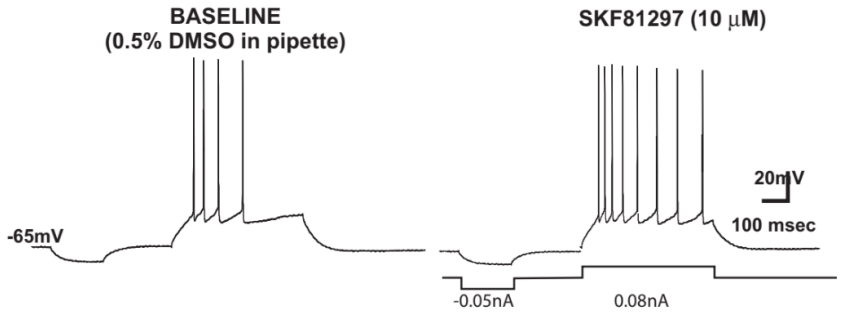

Fig. 26. The D1/5 receptor agonist, SKF81297 (10 μM) enhances spiking. *From Chen et al. (2007).*

(3) Noradrenaline (NA)

Zhang et al. (2013) show that, in some mPFC neurons, NA fails to induce self-sustained spiking (but not carbachol), and in others, NA induces plateau potential and PA (Fig. 27A) via the selective activation of α1 receptors (Fig. 27B) and mGluR5 (Fig. 27C). It has also been shown that NA inhibits Ca^{2+}-activated I_{sAHP} in layer V pyramidal neurons, thus leading to overall increase in ADP (Satake et al. 2008).

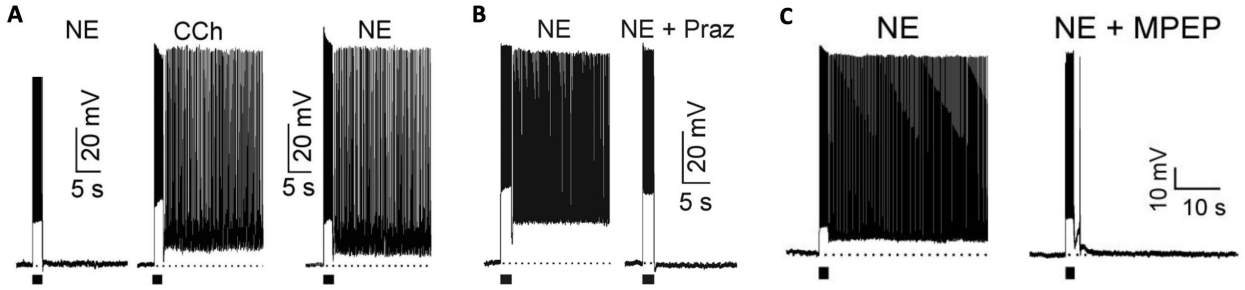

Fig. 27. Norepinephrine (NE) induces persistent firing in pyramidal neurons of the medial prefrontal cortex (mPFC) via activation of α1 adrenoceptors and mGluR5. A. Examples of a mPFC pyramidal neuron non-responsive to NE (10 μM), but sensitive to carbachol (CCh, 10 μM) (left), and a pyramidal neuron characterized by a NE-induced plateau potential and persistent firing following a depolarizing current pulse (right). **B.** NE-evoked persistent firing is blocked by the selective α1 adrenoceptor antagonist, prazosin (2 μM, NE+Praz). **C.** NE-induced persistent firing is blocked by the selective mGluR5 receptor antagonist, 6-methyl-2-(phenylethynyl)pyridine (MPEP, 50 μM). Adapted from Zhang et al. (2013).

In Chapter I, we will investigate how neuromodulation, through ACh, 5HT, DA, and NA, impacts the emergence of CB and GPA in the pyramidal neurons of the layer V of the mPFC.

C. Pathological working memory dysfunction is common

Loss of WM—i.e., difficulty in retaining and manipulating information in the short-term memory (seconds to minutes)—is one of the symptoms of various pathologies and conditions. WM loss can occur in normal aging (Park et al., 2002; Klencklen et al., 2017). It is one of the symptoms of neurodegenerative diseases, such as Alzheimer's Disease and other forms of dementia (Baddeley et al., 1991; Zokaei and Husain, 2019; Rodriguez and Festini, 2022), and neuropsychiatric diseases, including schizophrenia (Eryilmaz et al., 2016; Guo et al., 2018), bipolar disorder (Robinson et al., 2006; Kurtz and Gerraty, 2009; Soraggi-Frez et al., 2017) and attention deficit hyperactivity disorder (Kasper et al., 2012; Ortega et al., 2020). Following traumatic brain injury (Salmond and Sahakian, 2005; Parente et al., 2011; Smith et al., 2015; Manktelow et al., 2017) or stroke (Lugtmeijer et al., 2020), WM capacities can be impaired. Consumption of some medication, such as sedatives (Veselis et al., 2004) and anti-anxiety drugs (Roth et al., 1984), and substance/alcohol abuse (Gould, 2010; Vo et al., 2014; Lechner et al., 2015; Houck and Ewing, 2017) can also affect WM capacities. Moreover, WM disruption can also occur when someone is under chronic stress (Luethi, 2008; Yuan et al., 2016) or is sleep deprived, such as caused by insomnia (Frenda and Fenn, 2016; Peng et al., 2020).

WM loss is devastating for the people impacted and they usually quickly lose their ability to live independently. If we take the example of the PWM, we use this type of WM everyday. A simple representation would be the comparison of two sounds: a sound from a surrounding street characterized by a low amplitude and the firefighter's engine siren characterized by a high amplitude. The normal brain is able to compare the two sounds in a few hundreds of milliseconds or seconds, in order to send information to the body to move to leave the way clear for the coming firefighters. In this situation, a person with WM, and particularly PWM, deficits would be in danger.

People with PWM impairments experience life-threatening situations. In order to be able to develop potential medications and treatments in the future, it is crucial to first understand which WM mechanisms are altered in the brain. To address this goal, and after characterizing cellular and circuit mechanisms underlying PWM in Chapter I, we will identify how these features are affected in Alzheimer's disease and after traumatic brain injury, two pathological conditions affected by WM loss, in Chapter II.

1. Working memory loss in Alzheimer's disease

a) Alzheimer's disease: The most common cause of dementia

Alzheimer's Disease (AD) is a progressive neurodegenerative disease that represents 60 to 70% of all dementia cases (Holtzman et al., 2011). AD is placing a considerable and increasing burden on patients, caregivers, and society, as more people live long enough to become affected. The number of people affected by AD in the US is expected to rise to 13.8 million by 2050 and the worldwide financial burden of the disease is projected to reach $9.12 trillion in the same time-frame, highlighting the critical need for the development of novel therapeutics (Hebert et al., 2013).

To this date, the only few approved drugs to treat AD can only be used for symptomatic treatment of the disease (Marsh and Alifragis, 2018). In order to hopefully one day develop treatments to slow, prevent, or reverse the course of AD, it is important to continue the investigation of cellular and circuit mechanisms responsible for the development of AD. We can distinguish two main types of AD:

Late-onset AD is the most common form of AD and symptoms typically arise after 65 years-old (Isik, 2010). The genetics of this form of AD is an active area of investigation: the ε4 allele of the apolipoprotein E (*APOE*) gene has been identified as the major risk factor for late-onset AD (Corder et al., 1993), however exactly how the different isoforms of *APOE* increase the risk of disease is still not clear and is an active area of investigation (Huang et al., 2004; Mahley et al., 2006).

Early-onset AD or **familial AD (FAD)** arises before 65 years-old and results from inherited mutations in the amyloid precursor protein (APP) and/or the presenilin 1/2 (PS1 and PS2) genes, which code for transmembrane proteins that regulate protein cleavage (Dai et al., 2017). In addition to the genetic factors, epidemiological studies point to depression, traumatic head injury, and cardiovascular and cerebrovascular factors—e.g., cigarette smoking, midlife high blood pressure, obesity, and diabetes—as increasing disease risk (Mayeux and Stern, 2012).

b) Alzheimer's disease symptoms

(1) Behavioral symptoms

AD is characterized by a progressive cognitive decline with a range of behavioral symptoms that typically worsen over time: long and short-term memory—including WM—loss, difficulty with language and communication, impaired decision-making and orientation, decline in visual-spatial skills, challenges with daily tasks, and changes in personality and behavior (Fig. 28).

Fig. 28. Series of self-portraits created over the stages of Alzheimer's disease (AD) by the American artist William Utermohlen, diagnosed with AD in 1995. *From Utermohlen (2008).*

Memory dysfunction is a core defining characteristic of AD. However, long-term and working memory impairments are dissociable in AD. In a study of over 500 AD patients, it has been shown that patients carrying apolipoprotein ε4 alleles (late-onset AD) were older and more likely to present a 'classical' long-term memory deficit than those suffering from FAD and presenting with a constellation of cortical symptomatology, which included WM, language and perceptuospatial deficits (FAD; Panegyres, 2013). People with FAD show deficits in the central executive components of WM (Baddeley et al., 1986; Stopford et al., 2012), resulting in **WM loss** being one of the first symptoms observed in FAD (Saunders and Summers, 2009; Kessels et al., 2010).

Many studies investigated the effect of the disease on object and spatial WM capacities (Burke and Barnes, 2006; Kessels et al., 2010; Klencklen et al., 2012; Murman, 2015; Kronovsek et al., 2021). However, to our knowledge, the consequences of AD on PWM mechanisms are still unknown, so we decided to question whether CB is affected in AD.

(2) Molecular and cellular symptoms

All the AD behavioral symptoms are the consequences of molecular and cellular disruptions spreading to the whole brain as the disease progresses with age. A century ago, post-mortem analysis of human AD brains provided the first clues to the neuronal mechanisms of disease and led to the identification of two molecular hallmark lesions of AD in brain regions that serve memory and cognition (Alzheimer, 1907). AD is characterized by high levels of **insoluble amyloid plaques** (Alzheimer, 1907; Glenner and Wong, 1984). Indeed, it has been shown that mutations in the APP and PS1/2 genes increase the production of amyloid-β (Aβ), which drive the formation of the insoluble fibrils that compose amyloid plaques (Younkin, 1998; Hardy et al., 1998; Sisodia, 1999). Another characteristic of AD are the **neurofibrillary tangles** (NFTs), which are caused by abnormal intracellular accumulation of hyperphosphorylated filaments of tau (Alzheimer, 1907; Chang et al., 2021a, 2021b).

From these two hallmark lesions follow **synaptic disruptions** in neurons as the disease progresses. NFTs, which block the neuron's transport system, harm the synaptic communication between neurons (Brion, 1998; Moloney et al., 2021). Also, oligomeric Aβ triggers synapse dysfunction and induces loss of synapses in the cortex by cholinergic deficiency and glutamate excitotoxicity (Selkoe, 2002). More specifically, it has been shown that soluble Aβ oligomers downregulate post-synaptic M1 receptor function via the binding to adjacent metabotropic glutamate receptor 5 (mGluR5). This leads to a decrease in M1 receptor function and the loss of M1 receptor proteins in the human post-mortem AD cortex. Interestingly, inhibition of Aβ-activated mGluR5 in human organotypic cultures was sufficient to restore M1 receptor function (Yi et al., 2020).

Additionally, research showed that the soluble Aβ oligomers promote the generation of free radicals (oxidative stress) inducing cellular stress and loss of Ca^{2+} homeostasis, and accumulate in the mitochondria triggering dysfunction and **neuronal death** (Kadowaki et al., 2004). As neurons are injured and die throughout the brain, many cortical regions begin to shrink, causing a significant loss of cortex volume (Alves et al., 2023).

Altogether, these neuronal deficiencies in AD suggest that PWM mechanisms and capacities are likely impaired. Alterations of synaptic communication suggest that GPA, the neural correlate of PWM, could not emerge in the PFC, and M1 receptor dysfunction in the cortex suggests that PFC neurons could not exhibit CB. However, these are speculations and have still to be proven. In order to investigate the effect of the progression of AD on PWM mechanisms, we decided to evaluate CB emergence in mPFC neurons at different ages in a mouse model of AD which recapitulates all the symptoms listed below.

c) Animal model of Alzheiner's disease: The 5xFAD mouse line

Transgenic animal models have been critical for understanding the development and progression of AD (Jankowsky and Zheng, 2017). The 5xFAD mouse line, an APP/PS1 double transgenic mouse that coexpresses five FAD mutations (Fig. 29), was created by Oakley et al. (2006) and rapidly recapitulates major features of AD pathology.

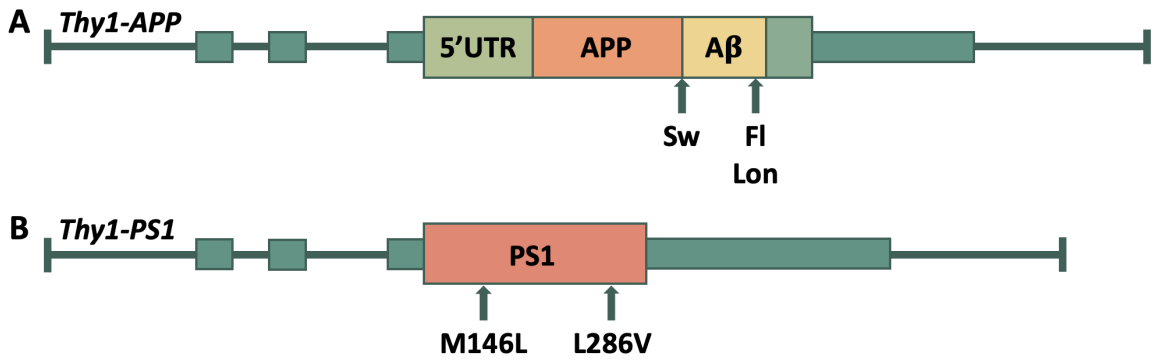

Fig. 29. 5xFAD mouse model (Oakley et al., 2006) coexpresses five FAD mutations. A, *Mutations in the APP cleavage sites: 1) K670N//M671L (Swedish, substitution) which elevates the production of total Aβ, and 2) I716V (Florida, substitution) and 3) V717I (London, substitution) which both increase specifically the generation of* $A\beta_{42}$. ***B,*** *Mutations in subunits of the PS1 cleavage complex: 1) M146L and 2) L286V which elevate specifically* $A\beta_{42}$. *The expression of both transgenes is regulated by neural-specific elements of the mouse Thy1 promoter to drive their overexpression specifically in brain neurons (Moechars, 1996).*

In 5xFAD mice, intraneuronal $A\beta_{42}$ accumulates within neuron soma and neurites starting 1.5 months of age (Oakley et al., 2006). **Aβ plaques deposition** begins at 2 months in the cortex (Oakley et al., 2006), the hippocampus and subcortical structures (Canter et al., 2019; Oblak et al., 2021), and accumulates in an age-dependent manner (Oblak et al., 2021). Elevated soluble oligomeric Aβ levels in the brain are measured starting 4 months (Oblak et al., 2021).

Synaptic degeneration starts at 4 months and significantly drops at 9 months (Oakley et al., 2006). **Neurodegeneration** starts at 3 months of age and is significant at 9 months. The brain regions associated with the highest levels of both intraneuronal $A\beta_{42}$ accumulation and Aβ plaque burden—i.e., cortex, hippocampus, and subiculum—are particularly impacted (Oakley et al., 2006). Cortical layer I is significantly thinner at 9 months, most likely due to the loss of layer V neuron dendrites that project to and ramify in layer I (Oakley et al., 2006).

Spatial **WM** is impaired at 4 months of age (Oakley et al., 2006) and object recognition performance is impacted later in life (Creighton et al., 2019). Long-term memory impairment is detected at 12 months of age (Quintanilla-Sánchez et al., 2023). Findings about exploratory

activity diverge: Oakley et al. observed a normal exploratory behavior (Oakley et al., 2006), however Oblak et al. (2021) measured hyperactivity, using the traveled distance in an open field and home-cage wheel-running assessments. Oakley et al. characterized normal motor function (Oakley et al., 2006), but other teams measured an improvement in motor function compared with WT animals, with a greater latency to fall on the rotarod test starting 6 months (Flanigan et al., 2014; Oblak et al., 2021).

To our knowledge, PWM performance has never been investigated in any mouse model of AD. However, in the 5xFAD mouse line, WM impairments are observed starting at 4 months of age; suggesting a possible decline in PWM capacities and associated cellular and circuit mechanisms over time. Thus, in the first section of Chapter II, we will investigate the effect of AD and aging on neuronal CB in mPFC slices in 5xFAD mice and control littermates at 2, 6, and 12 months of age.

2. Working memory loss after traumatic brain injury

a) Definitions and numbers

Traumatic brain injury (TBI), a form of acquired brain injury, occurs when a sudden trauma causes damage to the brain (National Academies of Sciences, Engineering, and Medicine, 2019). TBI can result from various causes (Fig. 30) and is a major cause of death and disability (National Academies of Sciences, Engineering, and Medicine, 2019).

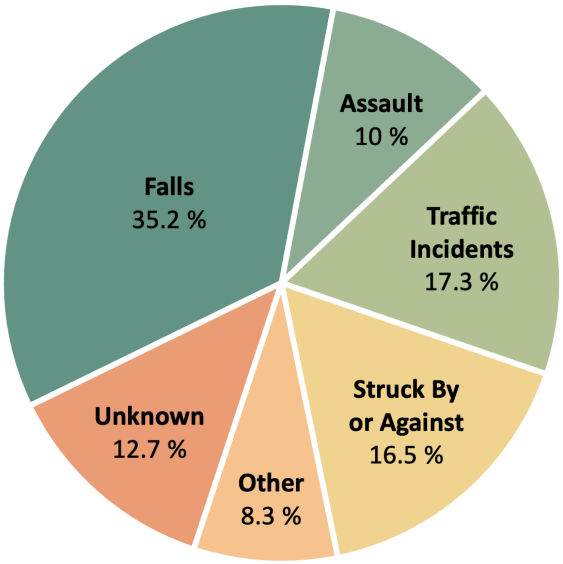

Fig. 30. Leading causes of traumatic brain injury in the United States (in 2013). *Adapted from the Centers for Disease Control and Prevention website.*

Some groups of the population are more susceptible to suffer from TBI.

Professional sports players, such as those in the National Football League in the United States, commonly suffer from TBI. Researchers at Baylor University found that 99 % of former NFL players, 91 % of college football players, and 21 % of high school football players, suffer from chronic traumatic brain injury (Mez et al., 2017).

Head injuries caused by bullet penetration, violent impact, or shock waves from explosive weapons are the main causes of **military TBI** (Kong et al., 2022). It is interesting to note that the term "shell shocked" was created by Myers in 1915 to characterize soldiers suffering from psychological and psychosomatic symptoms resulting from exposure to bombardment in the trenches in the First World War. It was then described as "concussion" or TBI.

Domestic violence by an intimate partner is also a common cause of TBI. From a study on domestic-abuse survivors published in 2002, nearly all respondents had been knocked in the head, with 40 % of them losing consciousness (Jackson et al., 2002). Fortunately, the rate of fatal and nonfatal domestic violence is declining, due to a decline in the marriage rate, decreased domesticity, better access to domestic violence shelters, and improvements in female economic status (Huecker, 2023). However, according to the Centers for Disease Control and Prevention, on average, nearly 20 people per minute are still physically abused by an intimate partner in the United States.

According to the Centers for Disease Control and Prevention website (consulted in 2023), there were over 69,000 TBI-related deaths in the United States in 2021: that is about 190 TBI-related deaths every day. But fortunately, all TBI don't lead to death.

Overall, 69 million people sustain a TBI each year (Dewan et al., 2018), which justifies a real need for understanding the brain changes occurring after injury.

b) Cognitive consequences

Symptoms of a TBI vary depending on the extent of the damage to the brain. A person with a mild TBI may remain conscious or may experience a loss of consciousness for a few seconds or minutes. Other symptoms of mild TBI include headache, confusion, lightheadedness, dizziness, blurred vision or tired eyes, ringing in the ears, bad taste in the mouth, fatigue or lethargy, a change in sleep patterns, behavioral or mood changes, and trouble with memory (including **working memory**), concentration, attention, or thinking (National Academies of Sciences, Engineering, and Medicine, 2019).

A person with a moderate, severe, or chronic TBI may show the same previously cited symptoms, but may also have a migraine, repeated vomiting or nausea, convulsions or seizures, an inability to awaken from sleep, dilation of one or both pupils of the eyes, slurred speech,

weakness or numbness in the extremities, loss of coordination, and increased confusion, restlessness, or agitation (National Academies of Sciences, Engineering, and Medicine, 2019).

As previously explained, disruption of WM capacities is common in aging-related diseases, such as Alzheimer's disease. However, TBI can occur at all ages of life and affect WM capacities prematurely. The frontal lobe, which includes the mPFC and is the seat of WM, is the most common region of traumatic injury (Levin et al., 1987). Thus, in order to develop treatments in the future, it is crucial to identify how the mechanisms are disrupted in the mPFC after TBI.

To address this gap, in the second section of Chapter II, we will use a rodent model of mild traumatic brain injury to assess the impact of injury to the mPFC on CB, a key component in PWM emergence.

III. Mutations of neurodevelopmental genes in interneurons in the primary somatosensory cortex

In this third part of General Introduction, we will describe the neuronal and circuit connectivity in the primary somatosensory cortex, before going into more details about what is known to this date about the cell and network consequences of *Mafb* and *c-Maf* gene mutations in cortical interneurons.

This third section of General Introduction will serve to explain the significance behind the project conducted in Chapter III. *Maf* genes are neurodevelopmental genes known to have prenatal and postnatal roles. In this final chapter, we will characterize the impact of *Mafb* and *c-Maf* mutations in somatostatin and parvalbumin-positive interneurons in the primary somatosensory cortex. More specifically, we will investigate the neuronal intrinsic properties and synaptic excitation of interneurons, as well as the cortical excitability in mouse *Maf* mutants.

A. Primary somatosensory cortex location and connectivity

In humans and other primates, the somatosensory cortex is located in the parietal lobe (Fig. 31) and comprises four distinct regions—also known as Brodmann's areas 1, 2, 3a, and 3b (Purves, 2001). Brodmann's area 3b is commonly called primary somatosensory (S1) cortex.

In rodents, the somatosensory cortex is found in the dorsolateral region of the neocortex (Fig. 31) and divided into the S1—composed of the area representing the whiskers and other parts of the face, the forelimb area (S1FL), the trunk area (S1Tr), and the hindlimb area (S1HL)—and the secondary somatosensory (S2) cortices (Watson et al., 2012).

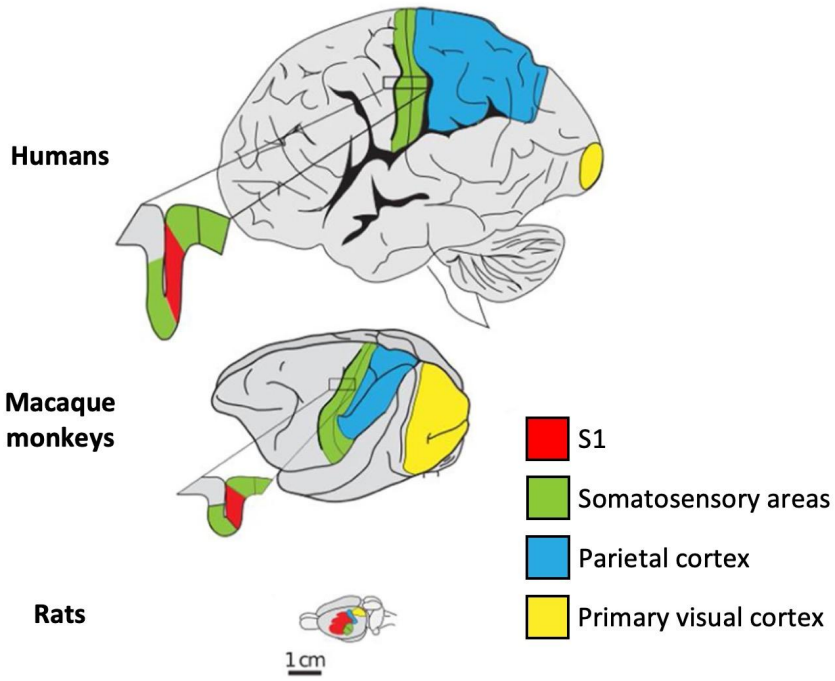

Fig. 31. Location of the primary somatosensory (S1) cortex in humans, macaque monkeys and rats. *Adapted from O'Connor et al. (2021).*

In all species, the somatosensory cortex is connected to the thalamus—a relay station that organizes sensory information routes within the cortex. However several fundamental differences in connectivity patterns between non-human primates (Padberg et al., 2009) and rodents (Carvell and Simons, 1987; Chmielowska et al., 1989; O'Connor et al., 2021) can be noted.

In addition, there are also profound differences in corticocortical connections in mice, rats, and macaque monkeys between homologous fields—i.e., S1/3b area. For example, in mice and rats, the S1 cortex has strong connections with the primary motor cortex (Porter and White, 1983; Smith and Alloway, 2013), while the S1 (area 3b) in macaque monkeys has little to no connections with the primary motor cortex.

Like the other neocortical areas, the S1 cortex is organized in six different layers and composed of excitatory and inhibitory neurons that are responsible for the circuit excitatory/inhibitory balance.

In this section of General Introduction, we want to bring your attention on the local circuit operating between excitatory pyramidal neurons, inhibitory somatostatin-positive (SST+) cortical interneurons (CINs), and inhibitory parvalbumin-positive (PV+) CINs, as these CINs will be the focus of our Chapter III (Fig. 32). Both SST+ and PV+ CINs project direct inhibitory inputs

onto the dendrites of pyramidal neurons, but SST+ CINs also inhibit PV+ CINs. Moreover, we can note that vasoactive intestinal polypeptide-expressing (VIP+) CINs inhibit SST+ interneurons—i.e., VIP+ CINs mediate disinhibitory control by inhibiting inhibitory neurons—but VIP+ CINs will not be studied in Chapter III.

Fig. 32. Example of local circuit between pyramidal neurons, VIP+, SST+, and PV+ cortical interneurons (CINs) in layer II/III. *Intracortical synaptic connections between pyramidal neurons (dark gray), SOM+ CINs (red), PV+ CINs (yellow), VIP+ CINs (blue), and other cortical inputs in L2/3 of a mouse neocortical region, the anterior cingulate cortex. Glu: glutamatergic fibers; ACh: cholinergic fibers; 5-HT: serotonergic fibers; DA: dopaminergic fibers; NA: noradrenergic fibers. From Riedemann (2019).*

In Chapter III, we will investigate how mutations of neurodevelopmental genes in interneurons affect the cortical excitatory/inhibitory balance in the S1 cortex, but the functions of the S1 cortex itself will not be discussed in the project presented in Chapter III.

Here, the S1 cortex will only be used as a generic cortical area and has not been chosen for its specific function on sensory information processing in mammals (Raju, 2022) or the presence of barrels in layer IV of the face somatosensory cortex in mice (Woolsey and Van der Loos, 1970).

B. Pathological development of the neocortex

1. Neurodevelopmental disorders: causes and consequences

Neurodevelopmental disorders—a class of disorders affecting brain development and maturation—are characterized, among others, by an inability to reach cognitive, emotional, and motor developmental milestones.

Neurodevelopmental disorders constitute a serious health problem in our society, affecting >3% of children worldwide (Gilissen et al., 2014). They have a heterogeneous etiology and lead to impaired cognition, communication, adaptive behavior, and psychomotor skills. Neurodevelopmental disorders include autism spectrum disorder (ASD), intellectual disability, attention deficit hyperactivity disorder, schizophrenia, and epilepsy (Tarlungeanu and Novarino, 2018; Niemi et al., 2018).

Neurodevelopmental disorders are associated with many genes and mutations, pointing to a heterogeneous origin of these diseases. The identification of the potential genetic causes of neurodevelopmental disorders is vital for understanding the molecular mechanisms responsible for the onset of these disorders and for the delineation of a genotype–phenotype correlation that could help to monitor the progress of the disorder and to foresee future complications.

2. The *Maf* genes and their roles

The large family of *Maf* genes codes for DNA-binding transcription factors (TF). The TF *Mafb* and *c-Maf* function alone or together to control cell fate and differentiation in bone, epithelial cells, lens, macrophages, and pancreas (Lopez-Pajares et al., 2015; Nishikawa et al., 2010; Soucie et al., 2016).

In the nervous system, *Mafb* and *c-Maf* have multiple functions. For example, *Mafb* is preferentially expressed in a subtype of SST+ CINs (Martinotti cells), where it regulates their migration and axonal projection (Lim et al., 2018), controls embryonic hindbrain regional patterning (Cordes and Barsh, 1994) and promotes the formation of auditory ribbon synapses that are required to activate inner hair cells (Lu et al., 2011; Yu et al., 2013). *c-Maf* has been shown to promote the generation of SST+ CINs (Mi et al., 2018) and is involved in touch receptor differentiation in the peripheral nervous system (Wende et al., 2012).

Mafb and *c-Maf* are particularly intriguing in CIN development because their expression initiates in the medial ganglionic eminence (MGE) subventricular zone (SVZ) and persists in MGE-derived interneurons but not in MGE-derived excitatory projection neurons (Cobos et al., 2006; McKinsey et al., 2013; Zhao et al., 2008, Pai et al., 2019).

SST+ CINs are largely generated before PV+ CINs (Inan et al., 2012; Miyoshi et al., 2007; Pla et al., 2006) and it has been shown that *Mafb* and *c-Maf* control that temporal sequence by restraining the production of SST+ CINs and promoting PV+ CINs fate.

Indeed, mouse conditional double knockout (cDKOs) for *Mafb* and *c-Maf* genes generate excessive SST+ MGE-derived cells, many of which become CINs. As early as E15.5, there is an obvious increase in immature SST+ CINs without any increase in total numbers of MGE-derived CINs (Pai et al., 2019). It is speculated that *Mafb* and *c-Maf*, by serving as a brake on neural differentiation, may regulate cell fate specification (Pai et al., 2019). In addition, *Mafb* and *c-Maf* have distinct functions postnatally in regulating the electrophysiological properties of CINs. (Pai et al., 2019)

3. Electrophysiological consequences of *Maf* mutations in inhibitory interneurons in the primary somatosensory cortex

a) Cellular level

As stated above, *Mafb* and *c-Maf* function together in the MGE to generate PV+ and SST+ neurons through the control of timing and quantity of SST+ CINs that are generated; and *Mafb* and *c-Maf* cDKOs generate significantly less CINs than wild-type mice (Pai et al., 2019).

In addition to neurogenesis and neuronal migration impairment, electrophysiological analyses of adult S1 cortices and *in vitro* assays of neonatal CINs provide evidence that *Mafb* and *c-Maf* have distinct postnatal functions in CIN maturation, synaptogenesis, and activity.

On the one hand, it was found that the spontaneous excitatory post-synaptic currents (sEPSC) amplitudes were smaller in the S1 cortex of *Mafb* conditional knockout (cKO, Fig. 33A), suggesting that *Mafb* promotes excitation of CINs (Pai et al., 2019).

On the other hand, the *c-Maf* cKO CINs had an increased density of excitatory synapses (Fig. 33B) and their sEPSC frequency was enhanced compared with the *Mafb* cKO CINs (Fig. 33A), suggesting that *c-Maf* represses CIN excitation (Pai et al., 2019).

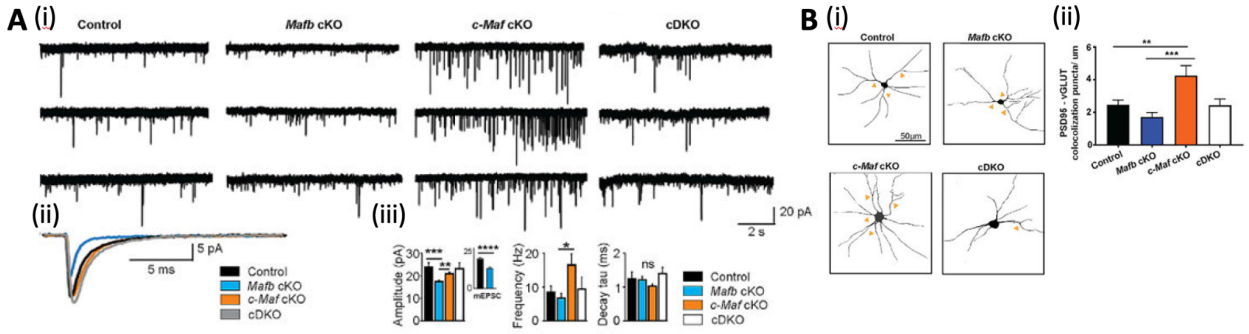

Fig. 33 (previous page). Synaptic excitation of cortical interneurons (CINs) in Mafb cKO, c-Maf cKO, and cDKO mice. A, *Adult whole-cell patch sEPSCs from CINs in the primary somatosensory cortex. (i) Representative traces of spontaneous EPSCs (sEPSCs) in layer 5–6 fast-spiking CINs. (ii) Overlaid average sEPSCs from the representative cells depicted in (A). Note the reduced amplitude of sEPSC specifically in Mafb cKO CINs. (iii) Quantification (means ± SEM) of the amplitude, frequency, and decay time constant of sEPSCs in CINs (V_{hold} = −70 mV). Note the reduced amplitude of sEPSCs in Mafb cKO compared with other genotypes and the enhanced frequency of sEPSCs in c-Maf cKO compared with other genotypes.* ***B,*** *Excitatory synapse quantification on cultured CINs. (i) Representative images of control, Mafb cKO, c-Maf cKO, and cDKO CINs at DIV14. (ii) Quantification (means ± SEM) of excitatory synapses on proximal dendrites. Adapted from Pai et al. (2019).*

Pai et al. (2019) showed that *Mafb* and *c-Maf* mutations mainly affect fast-spiking (FS)—i.e., PV+—CINs, which suggests that these *Maf* genes regulate network excitability mainly by regulating the FS CINs. *Mafb* and *c-Maf* cKOs as well as cDKOs all have reduced firing of PV+ CINs in response to current injections, but *Mafb* and *c-Maf* mutations have distinct effects on synaptic excitation, so it suggests that the opposing roles of *Maf* genes on cortical network excitability mainly result from their distinct effects on the synaptic, rather than intrinsic electric properties of CINs.

b) Circuit level

As we saw in the first part of General Introduction, most cortical excitation is generated by glutamatergic projection neurons (and also thalamic afferents in the S1 cortex), and inhibition is largely generated by locally projecting GABAergic CINs.

Circuit imbalance in the excitation to inhibition (E/I) ratio is one of the mechanisms that contribute to symptoms in neurodevelopmental disorders (Rubenstein and Merzenich, 2003; Chao et al. 2010; Yizhar et al., 2011; Han et al., 2012).

It has been shown that *Mafb* and *c-Maf* mutations in CINs lead to alterations in neocortical circuit excitability. Enhanced S1 circuit excitability recorded in the *Mafb* cKO could be explained by the reduced excitation of CINs and, on the opposite, reduced S1 circuit excitability recorded in the *c-Maf* cKO could be explained by the increased excitation of the CINs (Fig. 34; Pai et al., 2019).

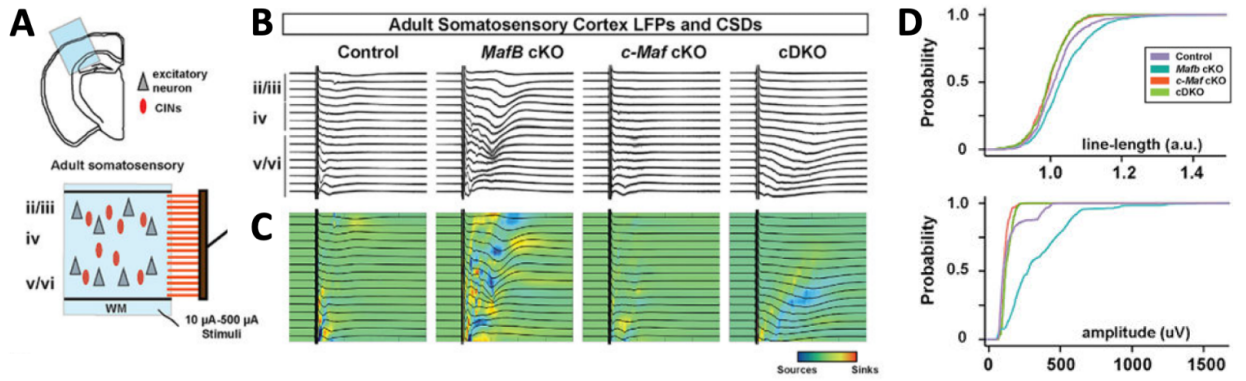

Fig. 34. Local field potential recordings in primary somatosensory cortex (S1) in Mafb cKO, c-Maf cKO, and cDKO mice. A, *Schema depicting the LFP multi-array experiment in the mouse S1.* ***B,*** *Examples of average LFPs (black) for representative control, Mafb cKO, c-Maf cKO, and cDKO slices.* ***C,*** *Current source densities (CSDs) for the average LFPs of the representative slices. Blue indicates a source, and red indicates a sink.* ***D,*** *Bootstrapped cumulative probability distributions of the amplitude and the line-length of the LFP evoked in layers 2/3 (ii/iii) by 500 µA stimulation of the white matter. Note that Mafb cKOs show greater excitability at 500 µA (indicated by greater line-length and amplitude in layers ii/iii compared with all genotypes), whereas c-Maf cKOs show hyporesponsiveness in superficial layers (indicated by reduced line-length and amplitude in layers ii–iii compared with control). Adapted from Pai et al. (2019).*

Neurodevelopmental diseases in which CINs are affected—e.g., autism spectrum disorder (ASD), schizophrenia, and epilepsy—are characterized by disrupted circuit inhibition, resulting in circuit hyperexcitability and less efficient information processing (Rubenstein and Merzenich, 2003; Yizhar et al., 2011; Lim et al., 2018; Sohal and Rubenstein, 2019).

The S1 circuit recordings obtained from *Mafb* or *c-Maf* cKO mice, and cDKOs, by Pai et al. (2019) suggested behavioral consequences. Particularly, results demonstrate a crucial role of *c-Maf* in regulating circuit excitation and increasing overall inhibition in the S1 circuit, thus suggesting a protective mechanism against epilepsy and seizures—conditions characterized by hyperexcitability of the network.

The previous work conducted by our team that investigated the electrophysiological consequences of *Mafb* and *c-Maf* mutations in the S1 CINs didn't distinguish SST+ interneurons from PV+ interneurons. However, these two types of CINs are not characterized by the same neuronal excitability and are not located at the same spot in the S1 local circuitry (Fig. 32).

Thus, in Chapter III, we will study the mechanisms by which transcription factor genes, such as *Mafb* and *c-Maf*, control postnatal neuronal excitability in SST+ and PV+ CINs, and what are the consequences at the network level *in vivo*.

IV. Aims

- **Chapter I:** Characterizing conditional bistability and graded persistent activity, the cellular and circuit mechanisms underlying parametric working memory, in the rat prefrontal cortex

- **Chapter II:** Investigating the impact of Alzheimer's disease and traumatic brain injury, two pathological conditions affected by working memory loss, on conditional bistability in rodent disease models

- **Chapter III:** Identifying the consequences of *Mafb* and *c-Maf* gene mutations in the interneurons of the somatosensory cortex on neuronal and network excitability in mice

CHAPTER I

Physiological mechanisms of the cellular and circuit mechanisms underpinning parametric working memory in the prefrontal cortex

I. Summary

Parametric working memory, the ability to maintain quantitative information, is prominent in the prefrontal cortex (Romo et al., 1999; Brody et al., 2003; Nieder and Mieler, 2004; Fassihi et al., 2014). During parametric working memory, the firing frequency of persistent neural activity monotonously scales with the quantity to be remembered (Romo et al., 1999; Brody et al., 2003; Nieder and Mieler, 2004; Major and Tank, 2004). Accounting for the emergence of such graded persistent activity in prefrontal neural networks has proved complex. Recurrent neural network models suggest that graded persistent activity requires existence of cellular intrinsic bistability to avoid unrealistic tuning of connectivity weights (Koulakov et al., 2002; Goldman, 2003). Bistable neurons either display a stable resting potential or stable spiking, following a transient input triggered by, e.g., an internal signal or an external event. We have theoretically described conditional bistability, a novel form of bistability, whose expression depends on the tonic level of synaptic inputs determined, e.g., by contextual mnemonic, motivational or decision-making working memory-related network activity (Rodriguez et al., 2018). Experimentally, conditional bistability has not been assessed, while being essential to network models displaying parametric working memory (Rodriguez et al., 2018).

Here, using electrophysiological and computational tools, we found that a subset of neurons in the prefrontal cortex exhibits conditional bistability, which depends on calcium-activated cationic non-selective conductances and is upregulated by acetylcholine. Moreover, we find, using extracellular recordings, that network graded persistent activity depends on the same conductances. Together, these results suggest that in behavioral conditions, cellular intrinsic conditional bistability in prefrontal networks underlies graded persistent activity, the neural correlate of parametric working memory.

II. Contributions to the project

Research concept development was done by Jeanne Paz and Bruno Delord. Experimental design was done by Morgane Leroux, David Medernach, Jeanne Paz, and Bruno Delord. Electrophysiological recordings were done by Morgane Leroux. Computational modeling was done by Bruno Delord. Data analysis was done by Morgane Leroux, David Medernach, Jeanne Paz, and Bruno Delord. Writing was done by Morgane Leroux, Jeanne Paz, and Bruno Delord.

III. Manuscript #1. Identification and characterization of intrinsic conditional bistability and network graded persistent activity in the prefrontal cortex of rats

Identification and characterization of intrinsic conditional bistability and network graded persistent activity in the prefrontal cortex of rats

Leroux MA[1,2,3,4], Medernach D[3], Ford JB[1,2], Necula D[1,2,5], Cho FS[1,2,5], Holden SS[1,2,5], Clemente-Perez A[1,2,5], Paz JT[1,4,5,6 #&], Delord B[2,3 #&]

[1]Gladstone Institute of Neurological Disease, Gladstone Institutes, San Francisco CA 94158, USA

[2]The Kavli Institute for Fundamental Neuroscience, and Neurology Department, University of California San Francisco, San Francisco CA 94158, USA

[3]Institut des Systèmes Intelligents et de Robotique (ISIR), Sorbonne University, 4 Place Jussieu, 75005 Paris, France

[4]Brain-Cognition-Behavior Graduate Program, Sorbonne University, 4 Place Jussieu, 75005 Paris, France, Paris, France

[5]Neuroscience Graduate Program, University of California, San Francisco, San Francisco, CA 94158, USA

[&]Co-senior authors. Equally contributed to the supervision of this project

[#]Correspondence to:

jeanne.paz@gladstone.ucsf.edu

bruno.delord@sorbonne-universite.fr

Keywords: Conditional bistability, Graded persistent activity, Prefrontal cortex, Pyramidal neurons, Intrinsic excitability, Electrophysiology, Computational modeling

Funding: This project was funded mainly by the National Science Foundation (NSF) CRCNS grant #1608236 (to JTP) and ANR (to BD). During the study, JTP was also supported by NIH/NINDS grant R01NS096369, DoD grant EP150038, Gladstone Institutes, the Michael Prize, and the Kavli Institute for Fundamental Neuroscience. MAL was supported by the Weill Institute Research Support for Female Learners Impacted by COVID-19 Funding, the Gladstone Institutes,and a FoxG1 Research Fellowship. FSC was supported by NINDS F31 NS111819-01A1, the NSF Graduate Research Fellowship #1144247, and the UCSF Discovery Fellowship. SSH was supported by the AChievement Rewards for College Scientists Scholarship, the Ford Foundation Dissertation Fellowship, NIH grant T32-GM007449, and the Weill Foundation.

Author contributions: Funding acquisition, BD and JTP; Concept Development, BD and JTP; Experimental Design, MAL, DM, BD and JTP; Electrophysiological Recordings, MAL, FSC,

SSH, ACP; Supervision: JTP supervised electrophysiological recordings, BD supervised computational modeling. Data Analysis, MAL, DM, BD, JTP; Computational Modeling, DM and BD; Writing, MAL, DM, BD, JTP. Manuscript editing: all authors.

Competing interests: The authors declare no competing interests.

Data and materials availability: All data and materials described in the manuscript or supplementary materials will be made available upon request.

Acknowledgements: We thank Vivianna DeNittis and Irene Lew for help with animal husbandry, and Francoise Chanut for critical review of the manuscript.

ABSTRACT

Parametric working memory, the ability to maintain quantitative information, is prominent in the prefrontal cortex. During parametric working memory, the firing frequency of persistent neural activity monotonously scales with the quantity to be remembered. Accounting for the emergence of such graded persistent activity in prefrontal neural networks has proved complex. Recurrent neural network models suggest that graded persistent activity requires existence of cellular intrinsic bistability to avoid unrealistic tuning of connectivity weights. Bistable neurons either display a stable resting potential or stable spiking, following a transient input triggered by, e.g., an internal signal or an external event. We have theoretically described conditional bistability, a novel form of bistability, whose expression depends on the tonic level of synaptic inputs determined, e.g., by contextual mnemonic, motivational or decision-making working memory-related network activity. Experimentally, conditional bistability has not been assessed, while being essential to network models displaying parametric working memory. Here, using electrophysiological and computational tools, we found that a subset of neurons in the prefrontal cortex exhibits conditional bistability, which depends on calcium-activated cationic non-selective conductances and is upregulated by acetylcholine. Moreover, we find, using extracellular recordings, that network graded persistent activity depends on the same conductances. Together, these results suggest that in behavioral conditions, cellular intrinsic conditional bistability in prefrontal networks underlies graded persistent activity, the neural correlate of parametric working memory.

INTRODUCTION

Working Memory (WM), the fundamental ability to access and manipulate transient information is essential to higher cognitive functions (Baddeley, 1992). Imaging techniques in humans (Courtney et al., 1998; Nyberg, 2002; D'Esposito et al., 2006; Quentin et al., 2019), as well as extracellular recordings in primates and rodents (Fuster, 1988; Goldman-Rakic, 1995; Yang et al., 2014) have pinpointed the central role of the prefrontal cortex (PFC), among other higher order cortical areas. Understanding how mPFC activity mediates WM represents a major stake since WM dysfunctions are associated with cognitive disorders such as Alzheimer's disease (Šimić et al., 2014; Xu et al., 2019), schizophrenia (Callicot et al., 2000; Yoon et al., 2008; Gao et al., 2019), autism spectrum disorders (Brumback et al., 2017; Xu et al., 2019), and bipolar disorder (Chai et al., 2011).

WM relies on persistent activity (PA), the ability of neural networks to maintain neural activity after the end of a cue (Fuster and Alexander, 1971). Theoretical studies indicate that once triggered, persistent activity self-sustains through spiking reverberation in recurrent networks (Wang, 2001; Compte, 2006). For instance, in object WM (OWM), a spontaneous state at low firing frequency encodes and self-maintained higher firing frequency respectively encode the absence or presence of a cue (Fuster et al., 1982a, 1982b). In spatial WM (SWM), self-maintained level activity occurs in neurons that are selective of the spatial position of the triggering cue (Goldman-Rakic, 1995).

Another form of WM, parametric WM (PWM) the ability to short-term maintain quantitative information has been observed in humans and primates, as well as in rodents (Romo et al., 1999; Brody et al., 2003; Nieder and Mieler, 2004; Fassihi et al., 2014). The remembered quantity may correspond to a numerical value, the perceived magnitude of a physical dimension (e.g., the pitch of a sound; Romo et al., 1999) or the value of an internal signal (e.g., the eye position; Nieder et al., 2004). Persistent neural activity has been observed in the mPFC in PWM, as in OWM and SWM (Romo et al., 1999; Nieder et al., 2004). However, PWM implies a more subtle computation, as it entails graded PA (GPA), i.e., the ability for neurons to self-maintain levels of activity that monotonously scale with the cue parameter to be remembered (Major and Tank, 2004).

Although PWM constitutes an essential form of WM, its mechanisms have largely remained obscure, despite intense research efforts to understand its molecular, cellular and network substrates (Brody et al., 2003; Major and Tank, 2004). This is not surprising as in PWM, GPA ideally implies, from a mathematically point of view, the co-existence of an infinite number of metastable states (frequency levels with null derivative), i.e., a "line attractor" structure that displays much more complex properties than the simple coexistence of two stable fixed point states, as in OWM. In real-world systems, line attractors can be approximated by a finite number of stable states, defined as multi-stability. In practice, multi-stability remains difficult to achieve in models of neuronal systems (Brody et al., 2003), because multiple non-linear positive feed-back loops must be subtly coordinated (compared with bistability in OWM, which requires a single non-linear positive feed-back loop).

Several groups have proposed that PWM arises from network reverberation of activity in neural network models of local recurrent neural circuitry (Brody et al., 2003; Major and Tank,

2004), as was established for OWM or SWM (see above; Wang, 2001; Compte, 2006). Indeed, GPA — the neural correlate of PWM — can arise as an emergent dynamical property of reverberation of activity within recurrent connectivity, the prevailing architecture in local mPFC networks (Seung et al., 2000; Miller et al., 2003; Machens et al. 2005; Machens and Brody, 2008). As for OWM or SWM, this hypothesis is compelling, as cortical architectures apparently provide sufficiently positive and nonlinear synaptic feedback for network dynamics to display attractorial convergence toward persistent self-maintained states of activity (Knierm and Zhang, 2012; Li et al., 2016; Carrillo-Reid et al. 2019; Inagaki et al., 2019).

Unfortunately, in these models, GPA systematically requires fine-tuning of synaptic weights and/or the activation function (i.e., the frequency/intensity (F/I) curve) of individual neurons, typically on the order of 1%, well beneath the typical precision of plastic and/or regulatory signaling processes at work in neurons. Therefore, reverberation of activity in local recurrent neural circuitry cannot solely robustly account for the GPAs observed in PWM in the mPFC. It was later shown that the burden of fine-tuning of neural network architectures can be released, provided that individual elements (neurons or small groups of neurons) of recurrent neural network models are bistable (Koulakov et al., 2002; Goldman, 2003). In these models, the bistability of each individual element is phenomenologically described in terms of firing frequency and a triggered higher frequency of discharge. However, these studies consider coarse-grained mathematical representations of bistability, with neuronal activity phenomenologically described in terms of firing frequency, far from the actual detailed biophysical properties of real neurons.

The possible implication of bistable neurons in the maintenance of persistent activities in WM (Compte, 2006), i.e., in PWM, as well as in OWM (Tegner et al., 2002; Compte, 2006) or SWM (Camperi and Wang, 1998) has been criticized, because WM-related computational processes and persistent activity are highly flexible (e.g., high intertrial variability and irregular spiking; Compte et al., 2003; Shafi et al., 2007), whereas intrinsic cellular bistability generally presents rigid features *in vitro*. Such stereotyped characteristics include a large independence of persistent spiking expression to background depolarization (absolute bistability; AB; Rodriguez et al., 2018), the requirement for long starting (ON) and stopping (OFF) stimuli (seconds), strong pharmacological manipulations, and/or very long and highly regular discharges at high-frequency, with possibly partially inactivated spikes (e.g., Andrade, 1991; Haj-Dahmane and Andrade, 1997; Haj-Dahmane and Andrade, 1998; Egorov et al., 2002; Tahvildari et al., 2008; Zhang and Séguéla, 2010; Gee et al., 2012).

However, some forms of cellular intrinsic bistability with more flexible attributes such as, e.g., short ON stimuli or dependance upon background depolarization, have been described in several cortical areas (Silva et al., 1991; Tahvildari et al., 2008) and specifically in the mPFC (Dembrow et al., 2010; Thuault et al., 2013; Ratté et al., 2018). Such non-stereotyped forms of bistability might be of genuine importance in subserving flexible WM-related computational processes (Compte, 2006; Tegner et al., 2002; Camperi and Wang, 1998). However, the exact nature and specificities of these forms of bistability remains elusive. Indeed, while previous experimental protocols have phenomenologically demonstrated the presence of such flexible forms of bistability (i.e., through the existence of triggered self-sustained spiking), they have not been designed to properly characterize their properties.

In a recent theoretical study, we have characterized a novel form of spike-mediated bistability, conditional bistability (CB), which escapes stereotyped features classically associated with bistability, being triggered by short – phasic – ON pulses (e.g., a few hundreds ms), and displaying low frequency firing (e.g., a few Hz), together with full blown spikes (Rodriguez et al., 2018). CB demonstrates a rich repertoire of mnemonic computations, both in *in vitro*-like conditions and under realistic asynchronous synaptic inputs mimicking *in vivo* conditions (Rodriguez et al., 2018). Moreover, an essential aspect of CB is that, contrarily to AB, a – phasic – supra-threshold pulse (e.g., due to a perceptive, decisional, or motor event) is not sufficient to trigger self-sustained spiking. Hence, under conditional bistability, self-sustained spiking also requires a – tonic – sub-threshold depolarizing pulse following the initial triggering event. In behaving animals, this tonic pulse may arise from background synaptic inputs due to persistent activity reverberating within recurrent networks of the mPFC (or of functionally connected neural structures) to maintain information about the memorized event, or to ongoing motivational, attentional, anticipatory, or executive aspects of WM processes. Thus, CB differs from AB in that its expression conditionally depends upon the functional context in which it exerts its influence, an essential property, given the flexibility required by working memory and executive functions in general. Our study also pinpointed the fact that CB has probably been overlooked, due to the subthreshold input it requires, and we proposed a specific protocol to assess its existence experimentally.

Here, we assess CB experimentally in whole-cell intracellular recordings of deep layer pyramidal neurons in the mPFC in acute brain slices from adult rats and a specific protocol, mimicking a PWM task and derived from our previous study. Doing so, we provide the first experimental evidence that mPFC pyramidal neurons exhibit CB. We unravel how CB is exclusively controlled by cholinergic (ACh) modulation through the regulation of slow CAN conductances. Moreover, we show that cholinergic neuromodulation promotes the active memorization of inputs in a parametric manner –similar to GPA in PWM tasks – and that this memorization depends on slow CAN conductances in layer V mPFC networks. These results suggest that during PWM, slow CAN-mediated CB is essential to recurrent interactions for the emergence of GPA within layer V PFC networks.

METHODS

Experimental animal model

We performed all experiments per protocols approved by the Institutional Animal Care and Use Committee at the University of California, San Francisco and Gladstone Institutes. Precautions were taken to minimize stress and the number of animals used in each set of experiments. Male Sprague-Dawley rats were used for these experiments and ages ranged between 8 and 12 weeks.

Slice preparation

Rats were euthanized with 4 % isoflurane, perfused with ice-cold cutting solution containing 234 mM sucrose, 11 mM glucose, 2.5 mM KCl, 1.25 mM NaH_2PO_4, 10 mM $MgSO_4$, 0.5 mM $CaCl_2$ and 26 mM $NaHCO_3$ equilibrated with 95 % O_2 and 5 % CO_2, pH 7.4, and decapitated. We prepared 250 µm-thick coronal slices containing the mPFC with a Leica VT1200 microtome (Leica Microsystems). We incubated the slices, initially at 32°C for 30 minutes and then at room temperature, in artificial cerebro-spinal fluid (aCSF) containing 126 mM NaCl, 2.5 mM KCl, 1.25 mM NaH_2PO_4, 1 mM $MgSO_4$, 2 mM $CaCl_2$, 26 mM $NaHCO_3$, and 10 mM glucose, equilibrated with 95 % O_2 and 5 % CO_2, pH 7.4 as described (Paz et al., 2011; Paz et al., 2013; Clemente-Perez et al., 2017; Holden et al., 2021; Cho et al., 2022).

Patch-clamp electrophysiology

Recordings were performed as previously described (Paz et al., 2011, Paz et al., 2013, Clemente-Perez et al., 2017, Holden et al., 2021, Cho et al., 2022). We visually identified neurons in layer V of the prelimbic (PL, area 32) and infralimbic (IL, area 25) subdivisions of the mPFC by differential contrast optics with an Olympus microscope (60x objective, NA 1.1, WD 1.5 mm; SKU 1-U2M592). Recording electrodes made of borosilicate glass had a resistance of 2.5-4 MΩ when filled with intracellular solution that contained 10 mM HEPES, 11 mM EGTA, 120 mM K-Gluconate, 11 mM KCl, 1 mM $MgCl_2$ and 1 mM $CaCl_2$, pH adjusted to 7.4 with KOH (290 mOsm). Access resistance was monitored in all the recordings, and cells were included only if the access resistance was lower than 30 MOhm and the change of resistance was lower than 20% over the course of the experiment. We corrected offline the potentials for -15 mV liquid junction potential. All intrinsic and firing properties were recorded in the presence of the synaptic blocker kynurenic acid (2 mM, Sigma) diluted in aCSF.

Extracellular mPFC network activity

Horizontal slices (400 µm) containing mPFC have been placed in an interface chamber at 34 °C and superfused at a rate of 2 mL.min-1 with oxygenated aCSF (same as recipe used for patch-clamp electrophysiology, except supplemented with 0.3 mM glutamine for cellular metabolic support). Extracellular local field potentials (LFPs) and multi-unit activity (MUA)

recordings were obtained with a linear 16-channel multi-electrode array (100 µm inter-electrode spacing, NeuroNexus Technologies) that spanned the six layers of the mPFC. Signals were amplified 10,000 times and band-pass filtered between 100 Hz and 6 kHz for MUA and between 0.001 Hz and 5 kHz for LFPs using the RZ5 signal processor from Tucker-Davis Technologies (TDT, SCR_006495). Position of recording array was visually checked for each recording to confirm position of electrodes in the different mPFC layers. Electrical stimuli (10, 20, 50, 100, 150, 200, 300, 400, 500, and 600 µA) were delivered to the layer V with a pair of tungsten microelectrodes (50-100 kOhm, Ferguson et al., 2023). The stimuli were 100 µs in duration, delivered 9 times with a delay of 8 s between each.

Neuromodulation application

To test the contribution of various neuromodulators, the following drugs were added to the recording aCSF: dopaminergic (DA) D1/D5 receptor agonist SKF-81,297 (10 µM, TOCRIS bioscience), serotonin (5-HT) receptor agonist 5-hydroxytryptamine (30 µM, Sigma), noradrenergic (NA) receptor agonist norepinephrine (10 µM, Sigma), acetylcholine (ACh) muscarinic 1 receptor agonist carbamylcholine, commonly called carbachol (10µM, Sigma), and non-selective CAN channel inhibitor flufenamic acid (FFA, 200 µM, Sigma). The different conditions were assessed as following: No NM (n=29 cells/3 rats), 5HT (n=27 cells/2 rats), DA (n=27 cells/2 rats), NA (n=29 cells/3 rats), ACh (n=29 cells/3 rats), and ACh+FFA (n=27 cells/4 rats).

Identification of conditional bistable neurons

We devised a *conditional bistability protocol*, derived from our previous modeling study (Rodriguez et al., 2018), to classify mPFC pyramidal layer V neurons, according to their type of spiking activity and specifically determine whether they were conditional bistable (CB) neurons, or not. In this protocol, we injected intracellular current steps of increasing intensity, to establish firing frequency / current intensity (F/I) curves and extract their threshold (or rheobase, i.e., the lowest injected current eliciting stable spiking; referred to as θ in the following). The conditional bistability protocol actually consisted of sweeps, each incorporating two stimulations, from which two F/I curves were built and compared. Each sweep thus incorporated 1) a “T1” stimulation consisting of a 5250 ms tonic current pulse, followed by 2) a combined “P/T2” stimulation, where a 250 ms phasic (P) current pulse of supra-threshold intensity (set to generate a 30 Hz spiking rate in each neuron) was immediately preceded a 5000 ms (T2) tonic current pulse (with an intensity similar to that of T1). Sweeps were successively applied with increasing values of the tonic intensity, so that T1-then-P/T2 pairs were intertwined. The tonic current intensity on the first sweep was 0 nA.

This intertwining procedure was devised so as to minimize possible historical dependence that could, e.g., have influenced the F/I obtained from an entire P/T2 protocol (successive sweeps containing only P/T2 stimulations with increasing intensity), if one had previously applied an entire T1 protocol before. Such a possibility could arise from the cumulative evoked spiking upon T1, which could induce, e.g., intrinsic plasticity processes

affecting intrinsic excitability (Turrigiano et al., 2011). Said differently, the intertwined conditional bistability protocol allowed us to compare neuronal spiking in response to T1 and P/T2, within each sweep, in as similar as possible conditions, with regard to previous spiking history of the neuron. The delay separating P/T2 from T1 within a sweep, as well as that separating T1 from P/T2 of the preceding sweep, was 20 seconds. This delay was, in the same manner, devised so as to minimize historical dependence within and across sweeps. This was essential, in particular, to avoid contamination by slow CAN conductance activation (deactivation time constant of the order of 5 seconds; Haj-Dahmane and Andrade, 1998) during previous depolarization (e.g., sweeps or stimulations). These precautions distinguish our study from previous ones (e.g., Ratté et al., 2018), where the background depolarization, applied after the triggering stimulus, is also present before and lies in the sub-threshold voltage range where slow CAN conductances activate (Haj-Dahmane and Andrade, 1997). This point is actually crucial when considering the possible implication of cellular intrinsic bistability in WM (see *Discussion*).

In order to build F/Is, we only considered and compared stable discharge, eliminating discharges consisting of transient spiking. We combined several criteria to that goal. First, spiking had to last at least 500 ms upon tonic pulses, notably to eliminate transient mnemonic discharge after P on P/T2 stimulation (Rodriguez et al., 2018; Fig., 2a). Upon T1 pulses, we discarded spikes during the 250 first ms, so that spiking was considered during the last 5000 ms (i.e., on the same duration as T2 pulses). This allowed to discard the influence of rebound conductance (i.e., the H and low-threshold Ca_T calcium conductances), which could produce a transient surge in spiking frequency during the first 250 ms. In all cases, spiking had to comprise at least two action potentials, which allowed computing firing frequency, unless it was discarded (spikes tagged with a red dot, Fig. 1C). If one of those criteria was not met, we assigned a value of 0 Hz to the considered input intensity and protocol. We excluded isolated sweeps from F/I curves, that is, sweeps upon which spiking occurred in at least upon one of the T1 or T2 pulses and with no discharge on following sweeps (with highest tonic pulse intensities). Such rare events could arise, e.g., from transient, reversible, deflection of the membrane potential (in background slice activity or recording conditions). The firing frequency (F) of selected sweeps was computed as the inverse of the mean of interspike intervals. We considered the first interspike interval as the time difference between the timing of the first spike and the start time of the tonic pulse.

For each neuron, we built the T1 (resp. T2) F/I curves by extracting (I,F) points with firing frequencies F of T1 (resp. T2) pulses with successive pulse intensities. For each F/I curve, we considered a set of (I,F) points including those with non-null firing frequency (obtained using aforementioned criteria) and the last point sweep having no discharge (i.e., the highest injected current giving F = 0 Hz). From that set, we eliminated points with aberrant spiking frequency due to rare, transient variations in neuronal excitability (see above), using a standard outlier method, and then fitted a linear regression model of the set of remaining points, when at least 3 points remained (unless the neuron was discarded from further analysis). In that case, we performed the linear regression on all increasing sets of remaining points (i.e., the first three points, the first four points, and so on) and the best linear regression was kept. This process allowed to best fit the linear part of the F/I curve nearby the threshold, which allowed to best

approximate the spiking threshold. We thus obtained θ_{T1} and θ_{T2}, the threshold of stable discharges upon the F/I curves obtained on T1 and T2 pulses, and built the difference $\Delta\theta = \theta_{T1} - \theta_{T2}$.

A neuron was classified as monostable (M) when $\Delta\theta \leq 0$, that is when spiking during the P pulse was not eliciting more spiking on the subsequent T2 pulse, compared to T1. Here, $\Delta\theta = 0$ indicated no change in the neuron's behavior (as detected by our protocol), while $\Delta\theta < 0$ generally arose because the P pulse elicited spike-induced outward (e.g., AHP) currents which dampened spiking upon the subsequent T2 pulse, compared to T1. By contrast, a neuron was classified as conditional bistable (CB) when $\Delta\theta > 0$, that is when spiking during the P pulse favored more stable spiking on T2, compared to T1 (e.g., by spiking at lower input current intensities and/or spiking more at similar intensities). This typically arose because the P pulse elicited spike-induced inward (e.g., CAN) ionic currents which favored spiking upon the subsequent T2 pulse. We only included visually identified pyramidal neurons with a regular spiking pattern. Using our protocol, we encountered neither absolute bistable (AB, i.e., with positive $\Delta\theta$ and negative θ_{T1}) nor pacemaker (i.e., with negative θ_{T2}) neurons.

Quantification of after-polarization potentials

Membrane potential after-depolarization or after-hyperpolarization (i.e., after-polarizations) were assessed so as to infer which type of spike-triggered ionic currents could be observed in M vs CB neurons and in different neuromodulatory conditions. After-polarization potentials and their possible relationship to the type of discharge (i.e., M vs CB) were extracted as membrane potential modulations at specific times in the protocol. Four different stimulation sweeps were identified as strategic, to assess the currents induced by the P pulse on the discharge type: 1) NS1 (No Spike 1) corresponds to the first sweep of the protocol. No current step is applied (0 pA) upon T1 and T2 and no action potential is generated; 2) NS2 (No Spike 2) is the last sweep (i.e., with the highest current intensity) eliciting no spinking either in T1 T2. In this case, the applied current step remains insufficient to generate action potentials from the recorded neuron, independently from the presence or absence of the preceded 'P' pulse; 3) S1 (Spike 1) is the first sweep with a current intensity sufficient to generate action potentials upon both T1 and T2; 4) S2 (Spike 2) is the sweep situated two current intensity increments above S1 (action potentials are generated upon both T1 and T2). Within 500 ms following the end of the T2 pulse, we classified as fast (F), medium (M) and slow (S) the after-polarization observed in windows 0-50 ms, 50-350 ms, 350-500 ms, respectively. The effect of spiking upon T2 on the subsequent membrane potential was assessed by computing the difference between membrane potentials in S1 and NS2. Positive differences correspond to after-depolarizations (ADP; i.e., depolarizations of the membrane potential following T2) and negative differences to after-hyperpolarizations (AHP; i.e., hyperpolarizations of the membrane potential attributable to T2).

Quantification of the current source densities

Local field potential (LFP) signals from all sixteen recording channels were digitized at 25 kHz, using a 5000 Hz lowpass filter, amplified and stored using a RZ5D processor multichannel workstation (Tucker-Davis Technologies). To better examine the location, direction, and magnitude of currents evoked in response to electrical stimulation, a current source density (CSD) analysis was performed by calculating the second spatial derivative of the LFP (Freeman et al. 1975). When net positive current enters a cell, this creates an extracellular negativity that is reflected in a current “sink,” and appears as a negative deflection in the CSD. Conversely, current “sources” indicate net negative current flowing into a cell and will create positive CSD responses. 6,7-dinitroquinoxaline-2,3-dione (DNQX, 25 μM, Sigma) and (2R)-amino-5-phosphonovaleric acid (APV, 100 μM, Sigma) were used to identify post-synaptic components, while tetrodotoxin (TTX, 5 mM, Sigma) was used to identify pre-synaptic components (Ferguson et al., 2023). CSD peak amplitudes were quantified using trial-averaged responses at each stimulation intensity (9 trials each). Custom MATLAB scripts adapted from Huguenard's laboratory (Ferguson et al., 2023) were used to analyze CSD responses and generate the LFP and CSD plots.

Quantification and Statistical analyses

All numerical values are given as means and error bars are standard error of the mean (SEM) unless stated otherwise. Data analysis was performed with MATLAB (SCR_001622) and GraphPad Prism 7 (SCR_002798). Passive membrane and active electrical properties of the recorded neurons were assessed by non-parametric one-way ANOVA test and Kruskal-Wallis test for post-hoc analysis. Differences between T1 (θ_{T1}) and T2 (θ_{T2}) rheobases in each neuromodulation condition were assessed by Wilcoxon matched-pairs signed rank test. Percentage of CB neurons recorded in different neuromodulation conditions were compared using Chi 2 test with application of the Bonferroni correction (Q = 10%). Threshold differences Δθ, and fast/medium/slow after-polarizations (ADP and AHP) were assessed using Scheirer-Ray-Hare test and Wilcoxon Mann Whitney test for post-hoc analysis. Multi-unit firing rate and CSD pre/post-synaptic responses were assessed using Repeated Measures Two-way ANOVA and Šidák test for post-hoc analysis.

Model of biophysical local recurrent neural network

We built a biophysical model of a single-compartment mPFC layer V pyramidal neuron, using the Hodgkin-Huxley formalism. The membrane potential followed

$$C\frac{dV_{(j)}}{dt} = -I_{Ionic} + I_{Inj}$$

with the ionic current followed

$$I_{Ionic} = I_L + I_{Na} + I_K + I_{CaT} + I_{CaL} + I_{fCAN} + I_{sCAN} + I_{mAHP} + I_{sAHP}$$

in which the leak current was

$$I_L = \overline{g}_L\left(V - V_L\right)$$

where $\overline{g}_L$ was the maximal conductance and V_L the equilibrium potential of the leak current.

The fast sodium underlying the action potential followed

$$I_{Na} = \overline{g}_{Na}\, m_{Na}^3 h_{Na}\left(V - V_{Na}\right)$$

with instantaneous activation, due to its very fast kinetics, and activation voltage-dependance taken from the axon initial segment of mPFC layer 5 pyramidal neurons (Hu et al., 2009), which offered a steep activation and clearcut spike initiation:

$$m_{Na}(V) \equiv m_{Na}^{\infty}(V) = \left(1 + exp(-(V + 30)/9.5)\right)^{-1}$$

and first-order inactivation taken from a previous pyramidal neuron model (Gollomb and Amitai, 1997)

$$\frac{dh_{Na}}{dt} = \frac{\left(h_{Na}^{\infty}(V) - h_{Na}\right)}{\tau_h(V)}$$

with

$$h_{Na}^{\infty}(V) = \ (1 \ + \ exp((V \ + \ 53)/7))^{-1}$$

and

$$\tau_{hNa}(V) = \ 0.37 \ + \ 2.78(1 \ + \ exp((V \ + \ 40.5)/6))^{-1}$$

The fast delayed-rectifier was also derived from that model, with

$$I_K = \overline{g}_K \, n_K^4 \left(V \ - V_K\right)$$

where

$$\frac{dn_K}{dt} = \frac{\left(n_K^{\infty}(V) - n_K\right)}{\tau_n(V)}$$

with

$$n_K^{\infty}(V) = \ (1 \ + \ exp(-\ (V \ + \ 25)/10))^{-1}$$

and

$$\tau_n(V) = \ 0.37 \ + \ 1.85(1 \ + \ exp((V \ + \ 27)/15))^{-1}$$

The low-threshold calcium current was derived from a previous model in thalamo-cortical neurons (Paz et al., 2012)

$$I_{CaT} = \overline{g}_{CaT}\, m_{CaT}^{2} h_{CaT}\left(V - V_{CaT}\right)$$

where

$$\frac{dm_{CaT}}{dt} = \frac{\left(m_{CaT}^{\infty}(V) - m_{CaT}\right)}{\tau_{mCaT}(V)}$$

with

$$m_{CaT}^{\infty}(V) = \left(1 + exp(-(V + 57)/6.2)\right)^{-1}$$

and

$$\tau_{mCaT}(V) = 0.612 + \left(exp\left(-\frac{(V+132)}{16.7}\right) + exp\left(\frac{(V+16.8)}{18.2}\right)\right)^{-1}$$

and

$$\frac{dh_{CaT}}{dt} = \frac{\left(h_{CaT}^{\infty}(V) - h_{CaT}\right)}{\tau_{hCaT}(V)}$$

with

$$h_{CaT}^{\infty}(V) = \left(1 + exp((V + 81)/4)\right)^{-1}$$

and

$$\tau_{hCaT}(V) = \{0.25exp((V + 467)/66.7)\ if\ V < -80\,mV\ \ 7exp(-(V + 22)/10.5)\ if\ V \geq -80\,mV$$

The high-threshold calcium current was taken from our previous model in the mPFC (Rodriguez et al., 2018).

$$I_{CaL} = \overline{g}_{CaL}\, m_{CaL}^{2}\left(V - V_{CaL}\right)$$

where

$$\frac{dm_{CaL}}{dt} = \frac{\left(m_{CaL}^{\infty}(V) - m_{CaL}\right)}{\tau_{mCaL}(V)}$$

with

$$m_{CaL}^{\infty}(V) = \left(1 + exp(-(V + 12)/7)\right)^{-1}$$

and

$$\tau_{mCaL}(V) = 10^{0.6 - 0.02V}$$

Intra-somatic calcium dynamics followed

$$\frac{dCa}{dt} = -\frac{S}{V}\frac{1}{2F}\left(I_{CaT} + I_{CaL}\right) + \frac{Ca_0 - Ca}{\tau_{Ca}}$$

where $\frac{S}{V}$ is the surface to volume ratio, F the Faraday constant, Ca_0 the basal calcium concentration and τ_{Ca} the calcium extrusion/buffering time constant.

The fast calcium-activated non-selective cationic (CAN) current was modeled to mimic its calcium-dependence and fast dynamics (Haj-Dahmane et Andrade, 1997; Haj-Dahmane et Andrade, 1999), as

$$I_{fCAN} = \overline{g}_{fCAN}\, m_{fCAN}\left(V - V_{fCAN}\right)$$

where

$$\frac{dm_{fCAN}}{dt} = \frac{\left(m^{\infty}_{fCAN}(Ca) - m_{fCAN}\right)}{\tau_{fCAN}}$$

with

$$m^{\infty}_{fCAN}(Ca) = \left(1 + exp\left(-\left(Ca - Ca_{h,fCAN}\right)/k_{fCAN}\right)\right)^{-1}$$

The slow CAN current was modeled to mimic its sub-threshold voltage (), calcium-dependence and slow dynamics (Haj-Dahmane and Andrade, 1996; Haj-Dahmane and Andrade, 1998; Haj-Dahmane and Andrade, 1999), as

$$I_{sCAN} = \overline{g}_{sCAN}\, m_{sCAN}\left(V - V_{sCAN}\right)$$

where

$$\frac{dm_{sCAN}}{dt} = \frac{\left(m^{\infty}_{sCAN}(V,Ca) - m_{sCAN}\right)}{\tau_{sCAN}}$$

with

$$m^{\infty}_{sCAN}(V, Ca) = \left(1 + exp\left(-\left(V - V_{h,sCAN}(Ca)\right)/k_{sCAN}\right)\right)^{-1}$$

and the voltage half-activation depending on calcium as

$$V_{h,sCAN}(Ca) = V_{h,sCAN,0} + \Delta V_{h,sCAN} Ca^{n_{sCAN}}$$

The medium after-hyperpolarization (AHP) current was modeled as

$$I_{mAHP} = \overline{g}_{mAHP}\, m_{mAHP}\left(V - V_{mAHP}\right)$$

where

$$\frac{dm_{mAHP}}{dt} = \frac{\left(m^{\infty}_{mAHP}(Ca) - m_{mAHP}\right)}{\tau_{mAHP}}$$

with

$$m^{\infty}_{mAHP}(Ca) = \left(1 + exp\left(-\left(Ca - Ca_{h,mAHP}\right)/k_{mAHP}\right)\right)^{-1}$$

The slow AHP current was modeled as

$$I_{sAHP} = \overline{g}_{sAHP}\, m_{sAHP}\left(V - V_{sAHP}\right)$$

where

$$\frac{dm_{sAHP}}{dt} = \frac{\left(m^{\infty}_{sAHP}(Ca) - m_{sAHP}\right)}{\tau_{sAHP}}$$

with

$$m^{\infty}_{sAHP}(Ca) = \left(1 + exp\left(-\left(Ca - Ca_{h,sAHP}\right)/k_{sAHP}\right)\right)^{-1}$$

Unless stated in the text, default parameters were as following : $C = 1\,\mu F.cm^{-2}$, $\overline{g}_L = 0.0175\,mS.cm^{-2}$, $V_L = -75\,mV$, $\overline{g}_{Na} = 24\,mS.cm^{-2}$, $V_{Na} = 50\,mV$, $\overline{g}_K = 3\,mS.cm^{-2}$, $V_K = -90\,mV$, $\overline{g}_{CaT} = 0.25\,mS.cm^{-2}$, $V_{CaT} = 120\,mV$, $\overline{g}_{CaL} = 0.015\,mS.cm^{-2}$, $V_{CaL} = 150\,mV$, $\frac{S}{V} = 1500\,cm^{-1}$, $Ca_0 = 0.1\,\mu M$, $\tau_{Ca} = 100\,ms$, $V_{fCAN} = -40\,mV$, $\tau_{fCAN} = 34ms$, $V_{sCAN} = -15\,mV$, $\tau_{sCAN} = 5000ms$, $\overline{g}_{mAHP} = 0.1\,mS.cm^{-2}$, $\tau_{mAHP} = 200\,ms$, $V_{mAHP} = -90\,mV$, $\overline{g}_{sAHP} = 0.015\,mS.cm^{-2}$, $\tau_{sAHP} = 15\,s$, $V_{sAHP} = -90\,mV$. Ordinary differential equations were integrated using the forward Euler scheme using a time step of $0.1\,ms$ and a custom MATLAB code.

RESULTS

Assessing conditional bistability properly with a specific stimulation protocol

In order to assess the existence of conditional bistability (CB), we performed whole-cell patch-clamp experiments on rat acute coronal mPFC slices (Fig. 1A), in visually identified layer V pyramidal neurons (Fig. 1B; passive and spiking properties supplementary table 1) and we applied a *conditional bistability protocol* (Fig. 1C; see *Methods* for details), derived from our previous modeling study (Rodriguez et al., 2018). Briefly, this protocol was designed to assess the bistability of recorded neurons, i.e., their ability to exhibit mnemonic activity under the form of a stable state of self-sustained spiking, following a phasic (i.e., 250 ms; P) supra-threshold current pulse mimicking a synaptic barrage signaling a behavioral event (e.g., perceptive, decisional, or motor). The protocol incorporated a second constraint, devised to specifically assess CB. As theoretically unraveled, the expression of CB conditionally depends on the functional context in which it exerts its influence, which is essential with regard to the flexibility required by working memory and executive functions in general (Rodriguez et al., 2018). Specifically, an essential aspect is that, by contrast to AB, self-sustained spiking in CB neurons depends on the presence of a minimal tonic sub-threshold depolarizing drive after the triggering event. In behaving animals, this drive may arise from persistent synaptic reverberation within mPFC recurrent networks, or from related ongoing background (motivational, attentional, anticipatory or decisional, e.g.) activity, during the delay period of working memory tasks.

Thus, in the conditional bistability protocol we devised for the present study, neurons were tested with sweeps that included two successive stimulations, to compare their spiking behavior in response to 1) a tonic current pulse (i.e., the contextual delay drive) alone (no P pulse; stimulation T1) and to 2) a combined stimulation in which the P phasic current pulse immediately preceded a tonic pulse of similar intensity (stimulation P/T2). Applying such sweeps with increasing tonic intensity values allowed to build two frequency / intensity curves and extract the spiking thresholds (i.e., the rheobases) in both conditions, θ_{T1} and θ_{T2}. The threshold difference $\Delta\theta = \theta_{T1} - \theta_{T2}$ then allowed classification of neurons, according to their stability type. Classifying neurons is straightforward when considering theoretical bifurcation diagrams of monostable and bistable neurons. In a monostable neuron (see Fig. 1a; Rodriguez et al., 2018), the threshold for triggering a discharge, θ_{ON} (assessed here by extracting θ_{T2}), is similar to the threshold for terminating that discharge, θ_{OFF} (assessed here by extracting θ_{T1}). In this case, $\Delta\theta = 0$. In our experimental conditions, spiking activity upon the P pulse could sometimes induce the activation of spike-triggered potassium currents (e.g., AHP), which actually decreased spiking activity on P/T2 (compared to T1), i.e., which decreased θ_{T2}, phenomenologically inducing negative $\Delta\theta$. Thus, when $\Delta\theta \leq 0$, the neuron was classified as monostable (M). By contrast, in bistable neurons (see Fig. 1B, C; Rodriguez et al., 2018), θ_{ON} is strictly superior to θ_{OFF}. In the input range $[\theta_{OFF} - \theta_{ON}]$, neurons either exhibit a stable resting membrane potential (i.e., a stable fixed point; in the absence of any supra-threshold trigger) or stable spiking (i.e., a stable limit cycle), once triggered by a supra-threshold pulse, hence the bistability denomination. In our context, the neuron was classified as CB when $\Delta\theta > 0$, i.e., when spiking during the P pulse elicited more spiking on the subsequent T2 pulse, compared to T1 (see *Methods*).

Neuronal conditional bistability in layer V rat mPFC pyramidal neurons

We first assessed the existence of CB in standard aCSF medium, in the absence of any neuromodulator (No NM condition). Applying the conditional bistability protocol to mPFC neurons recorded in this condition unraveled that typically, neurons displayed lower firing frequencies after a P pulse (i.e., upon T2), compared to when P was absent (i.e., T1). Consistently, T2 F/I curves typically situated below their T1 counterparts (Fig. 2A, 1st row from top). Fitting F/I curves, we found that the spiking current threshold was itself right-shifted, with higher values θ_{T2}, compared to θ_{T1} (Fig. 2B, 1st row; p=0.000004, Wilcoxon matched-pairs signed rank test, n=29). Therefore, excitability was decreased when a supra-threshold P pulse was applied before the tonic pulse. This result appeared at first counter-intuitive, as we were expecting *increases* in excitability, rather than decreases, in the context of a study on cellular mnemonic effects. As a consequence, a majority of neurons were classified as monostable (M). Nevertheless, we found that, while most neurons presented large negative $\Delta\theta$, some neurons displayed small positive $\Delta\theta$ (Fig. 2C, 1st row and Fig. 2D). Hence, in this standard condition, a small fraction of neurons were CB (14%; Fig. 2E), i.e., CB neurons (Fig. 2C, 1st row; passive and spike properties were similar in CB and M neurons, Suppl. table 1). Thus, although positive $\Delta\theta$ were small, we found the presence of a minority of CB neurons, consistent with a previous study showing a small fraction of neurons displaying persistent activity in standard conditions in the mPFC (Thuault et al., 2013).

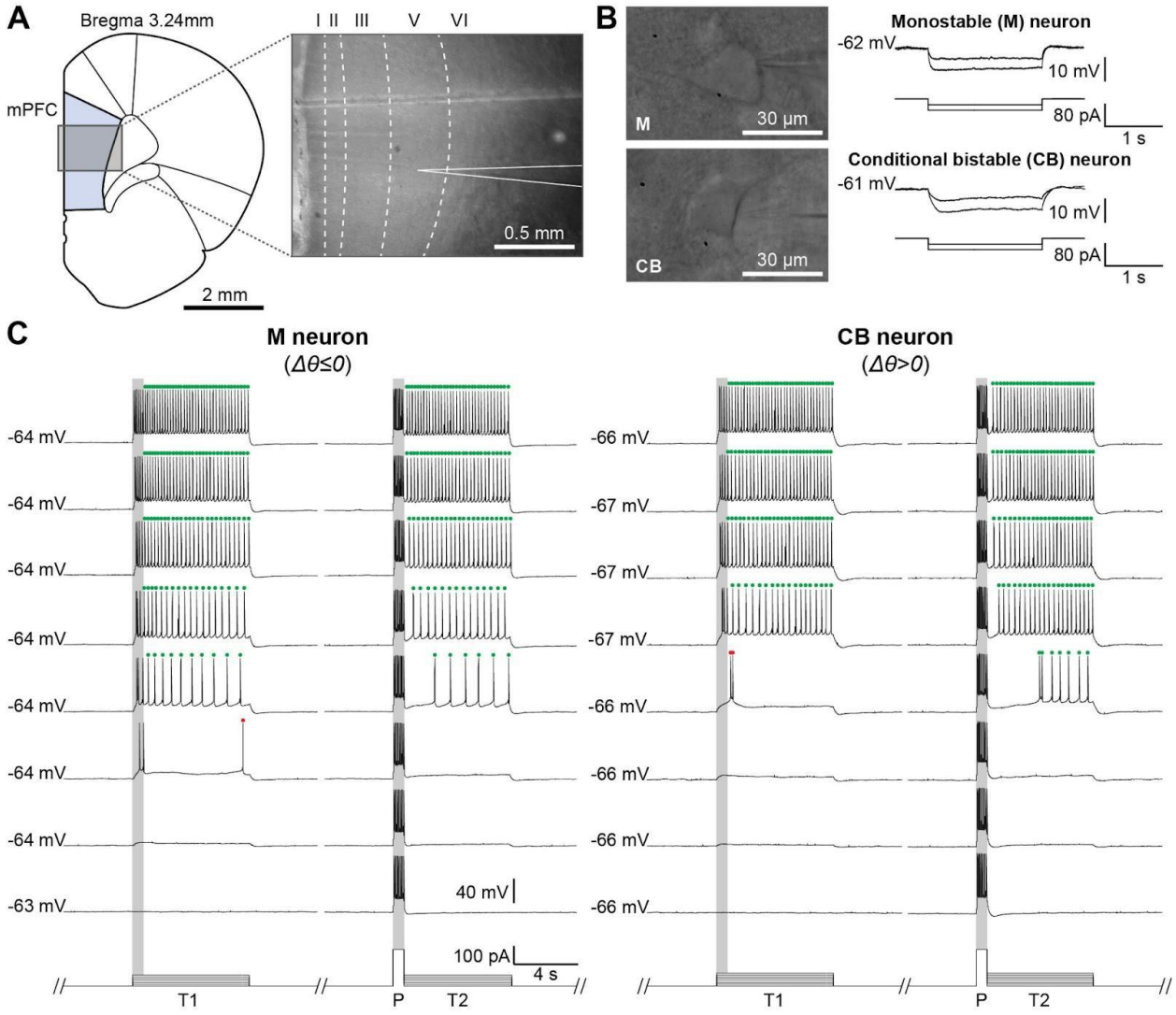

Figure 1. Conditional bistable pyramidal neurons exist in layer V of the prefrontal cortex in rats. A, *Rat acute brain slice of medial prefrontal cortex (mPFC) prepared for whole-cell recordings with stimulation of pyramidal neurons in layer V.* ***B,*** *Left, acute slices of layer V mPFC showing a monostable (M) and a conditional bistable (CB) pyramidal neuron; Right, representative traces of responses to negative current injections.* ***C,*** *Representative traces of responses of a monostable (M, left) neuron and a conditional bistable (CB, right) neuron, in response to the conditional bistability protocol. The protocol comprises sweeps (row organized vertically), which include a tonic T1 pulse stimulation followed by a P/T2 stimulation, formed of a supra-threshold P pulse followed by a T2 pulse (of similar intensity than that of the T1 pulse) (see Methods). Gray zones correspond to the first 250 ms, including the P pulse during the P/T2 stimulation. Only discharges generating more than two action potentials are accounted for (green vs. red, not accounted; see Methods).*

Conditional bistability under dopaminergic, serotonergic and noradrenergic modulation

Serotonergic (Williams et al., 2002, Gonzales-Burgos et al., 2012), dopaminergic (Bezu et al., 2017, Braun et al., 2021) and noradrenergic (Rossetti and Carboni, 2005) systems are known to play a role in working memory. We thus assessed whether CB depends on these neuromodulators. To do so, we applied the same protocol, in the presence of an agonist of one of these major neuromodulators of mPFC: serotonin agonist of 5-hydroxytryptamine receptors (5HT), dopamine agonist of D1/D5 receptors SKF-81297 (DA), noradrenergic agonist receptors norepinephrine (NA), or cholinergic agonist of muscarinic M1-type receptors carbachol (ACh). In these conditions, neurons displayed lower firing frequencies upon T2, i.e., T2 F/I curves situated below T1 ones (Fig. 2A, rows 2-4). However, we found no significant statistical difference between θ_{T1} and θ_{T2} in the presence of the 5HT agonist (p=0.2773, Wilcoxon matched-pairs signed rank test, n=27), DA agonist (p=0.0654, Wilcoxon matched-pairs signed rank test, n=27), and NA agonist (p=0.0776, Wilcoxon matched-pairs signed rank test, n=29) (Fig. 2B, rows 2-4). Accordingly, the distribution of $\Delta\theta$ values appeared more centered (around zero), compared to standard aCSF conditions (Fig. 2C, rows 2-4 and Fig. 2D). Also, the fraction of CB neurons was higher under serotonergic (30%), dopaminergic (37%), and noradrenergic (28%) neuromodulation, compared to the No NM condition (Fig. 2E), although differences were not statistically significant (5HT: adjust. p=0.9111; DA: adjust. p=0.4964; NA: adjust. p=0.9612, Chi 2 test with Bonferroni correction). Thus, while we found that overall excitability after the triggering pulse and CB tendency both appeared somehow increased under these three neuromodulatory influences, the measured effects appeared too subtle to be statistically detected in our setup.

Conditional bistability is enhanced by cholinergic modulation via M1 receptor activation

Cholinergic neuromodulation affects working memory (Zhou et al., 2011; Teles-Grilo Ruivo et al., 2017) and favors persistent spiking mPFC (Haj-Dahmane et Andrade, 1996; Haj-Dahmane et Andrade, 1998; Zhang et Seguela, 2010; Thuault et al., 2013; Ratté et al., 2018) in the rat. We assessed whether cholinergic stimulation could affect conditional bistability. Applying the protocole in presence of the M1-type muscarinic agonist carbachol (ACh) unraveled that globally, neurons displayed larger firing frequencies upon T2 (versus upon T1). Thus, T2 F/I curves typically situated above T1 ones (Fig. 2A, row 5) and we found that θ_{T2} was lower than θ_{T1} (Fig. 2B, row 5; p=6.1e-5, Wilcoxon matched-pairs signed rank test). Thus, in the presence of muscarinic modulation, excitability was increased following a supra-threshold P. Consistently, the distribution of $\Delta\theta$ values was mainly shifted towards positive values (Fig. 2C, row 5) and statistically greater in the ACh condition, compared to those in the absence of neuromodulation, or in the presence of 5HT, DA, or NA agonists (Fig. 2D). Accordingly, the fraction of CB neurons recorded was higher in the presence of the ACh agonist (Fig. 2E), compared to No NM (adjust. p=2.183-9, Chi 2 test with Bonferroni correction), 5HT (adjust. p=1.783e-6, Chi 2 test with Bonferroni correction), DA (adjust. p=1.988e-5, Chi 2 test with Bonferroni correction), and NA (adjust. p=6.179e-7, Chi 2 test with Bonferroni correction) conditions (Fig. 2E). Altogether, these results show that cholinergic modulation via M1-type receptors strongly facilitates conditional bistability.

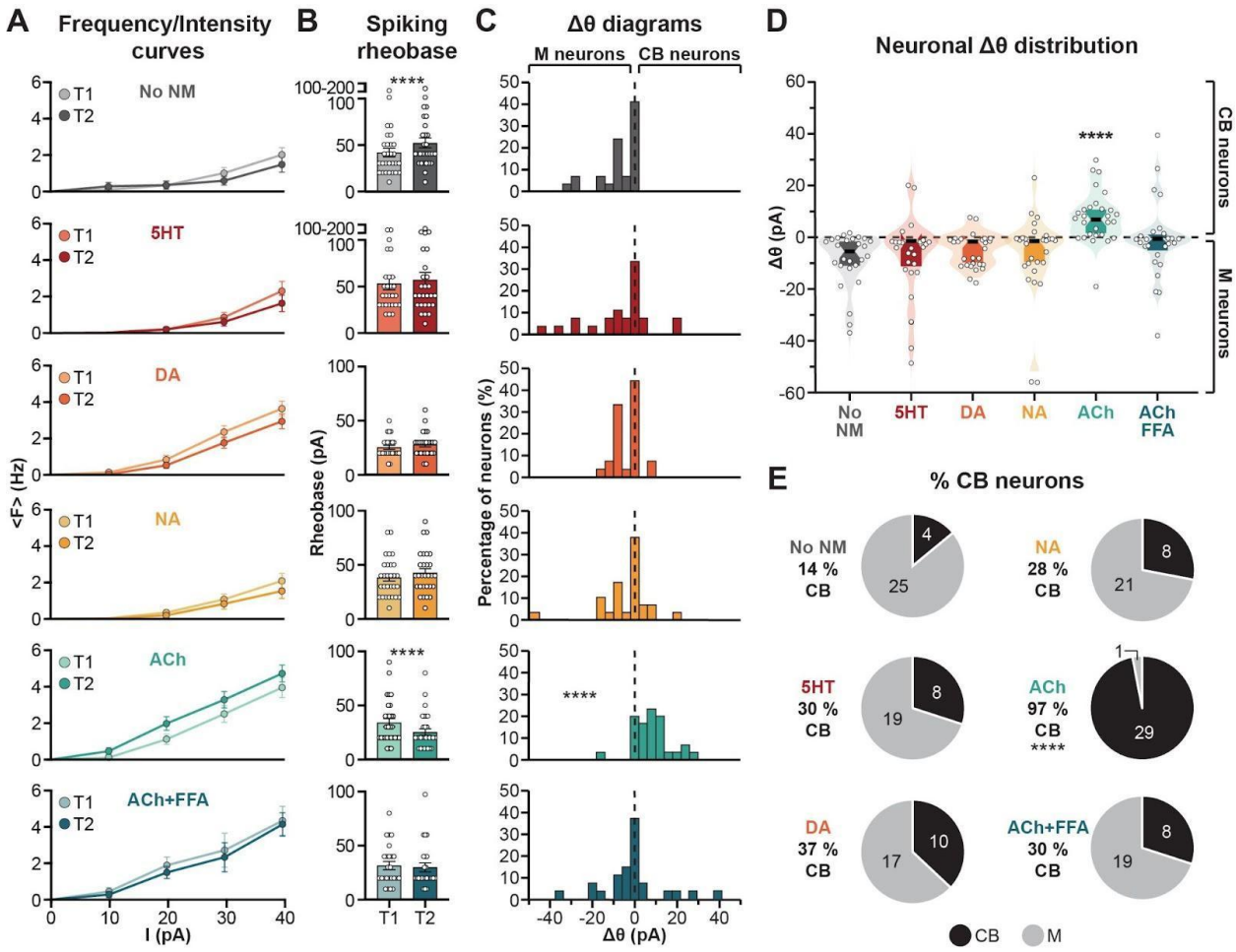

Figure 2. Conditional bistability is modulated by acetylcholine via the activation of M1-type receptors. A*, Frequency-Intensity (F-I) curves and* ***B****, the thresholds for firing of neurons upon T1 (θ_{OFF}) and T2 (θ_{ON}) in absence of neuromodulation (No NM, n=29 cells/3 rats), and under neuromodulation by a serotonergic agonist (5HT, n=27 cells/2 rats), a D1 dopaminergic agonist (SKF-81,297, DA, n=27 cells/2 rats), a noradrenergic agonist (NA, n=29 cells/3 rats), a cholinergic agonist (carbachol, ACh, n=29 cells/3 rats), and a non-selective cationic channel blocker, flufenamic acid (ACh+FFA, n=27 cells/4 rats). Rheobase statistical significance was assessed by Wilcoxon matched-pairs signed rank test analysis (****p<0.0001).* ***C****, Distribution of Δθ values in all conditions. Δθ statistical significance was assessed by Wilcoxon matched-pairs signed rank test analysis (****p<0.0001).* ***D****, Distribution of individual Δθ values for each recorded neuron in the different neuromodulation conditions. Statistical significance was assessed by Scheirer-Ray-Hare test and Wilcoxon Mann Whitney test for the post hoc analysis (****p<0.0001). Violin plot boxes indicate the 75th, 50th and 25th percentiles (upper border, black line, lower line. Dots correspond to individual neurons recorded.* ***E****, Fractions of monostable (M) and conditional bistable (CB) neurons recorded in the different conditions. Statistical significance was assessed by chi 2 test with Bonferroni-Sudak correction (****p<0.0001).*

Cholinergic-modulated conditional bistability depends on CAN channels

In the mPFC, flexible forms of bistability depend on calcium-activated non-selective cationic (CAN) channels (Dembrow et al., 2010; Ratté et al., 2018). Moreover, our previous theoretical work suggests that conditional bistability depends on the activation of calcium-activated non-selective cationic (CAN) channels (Rodriguez et al., 2018). We used flufenamic acid (FFA), a pharmacological blocker of transient receptor potential cation channels (TRPC) channels conveying slow CAN currents (Haj-Dahmane et Andrade, 1999; Zhang et Seguela, 2010; Ratté et al., 2018), to assess the implication of CAN currents in CB. We found that the cholinergic positive modulation on CB was inhibited when FFA was added to the ACh condition (ACh+FFA). Indeed, neurons did not display the larger firing frequencies observed upon T2 (versus T1) in the ACh conduction (Fig. 2A, compare row 6 to row 5). Consistently, no statistical difference between θ_{T1} and θ_{T2} was observed (Fig. 2B, row 6; p=0.5703, Wilcoxon matched-pairs signed rank test), the distribution of $\Delta\theta$ values centered again (Fig. 2C, row 6) and their mean was statistically lower than that in the ACh condition (Fig. 2D). Finally, the fraction of CB neurons was also lower in the ACh+FFA condition, compared to the ACh condition (Fig. 2E; adjust. p=1.783e-6, Chi 2 test with Bonferroni correction). Note, nevertheless, that although the CB fraction under ACh+FFA was not statistically different from that in the No NM condition, it presented a different pattern, with larger positive $\Delta\theta$ values. Altogether, these results suggest that cholinergic modulation of conditional bistability operates through a M1-receptor regulation of the TRPC channels underlying slow CAN currents.

Conditional bistability evoques after-depolarization potentials induced by fast and slow CAN currents

In layer V mPFC pyramidal neurons, persistent spiking and bistability have been related to several spike-mediated, calcium-activated conductances that could participate or modulate conditional bistability. They include two distinct calcium-activated non-selective cationic (CAN) depolarizing conductances promoting persistent spiking and bistability. These conductances differ by their gating kinetics (Haj-Dahmane and Andrade, 1999): a fast CAN (fast CAN) versus a slow CAN current, with activation time constants of the order of a few tens of ms (Haj-Dahmane and Andrade, 1997, 1999) and over a second (Andrade, 1991; Haj-Dahmane and Andrade, 1998, 1999; Ratté et al., 2018), respectively. Following spiking activity, fast and slow CAN conductances produce after-depolarizations (ADP), i.e., depolarizations of the membrane that reveal their presence and kinetics. Besides, spike triggered conductances also include a calcium-activated potassium current, which produces an after-hyperpolarization (AHP) following spiking and displays an activation time constant of the order of 100-200 ms (Haj-Dahmane and Andrade, 1998; Satake et al., 2008; Ratté et al., 2018). This medium AHP (mAHP) current opposes persistent activity and bistability (Haj-Dahmane and Andrade, 1997, 1998) and is typically observed following the stimulation triggering persistent activity (Dembrow et al., 2013; Ratté et al., 2018).

We assessed the possible implication of these three currents in CB. During the persistent activity characterizing CB, fast CAN, mAHP and slow CAN currents are cumulatively activated by successive spikes, while they deactivate after termination of persistent spiking.

Therefore, the membrane potential dynamics following persistent activity, i.e., the after-polarization (either been an after-depolarization (ADP) or after-hyperpolarization (AHP)) reflects the presence of fast CAN, mAHP and slow CAN currents, and may reveal their possible implication in CB. Precisely, these measures were achieved at the end of the T2 pulse of the CB protocol (Fig. 4A) and computed as the relative difference of polarization following persistent spiking minus that observed in its absence (Fig. 4B), to specifically extract CB-related persistent activity spike-mediated currents (Fig. 4C). We specifically defined three components, fast (0-50 ms), medium (50-350 ms), and slow (350-500 ms) after-polarizations, with the idea to quantify the relative strength of the three currents, based on their distinctive kinetics. These observables gave us indications on the after-depolarization / after-hyperpolarization (ADP/AHP) balance. Positive values translated a depolarization of the membrane potential – caused either by an increased activation of ADP currents or a decreased activation of AHP currents — due to CB-related persistent spiking, while negative values indicated decreased ADP and/or increased AHP currents.

The three components of the after-polarization displayed a globally similar pattern in No NM, 5HT, DA and NA conditions (with no statistically significant differences; Fig. 4C, D) with dynamics dominated by 1) a fast after-depolarization that corresponded to the passive decay of the membrane potential and possibly the presence of a fast CAN conductance, followed by 2) a more repolarized after-polarization in medium and slow components revealing the presence of spike-triggered mAHP currents. Note that DA apparently induced a larger ADP during the fast /medium components, possibly due to an increased fast CAN conductance or a decreased medium AHP. Note also that 5HT a larger ADP on the medium and slow components, possibly due to a decreased mAHP or an increased slow CAN conductance, although these effects were globally not significant (except for significant larger depolarization in 5HT, compared to DA, see Fig. Suppl. 1A).

In the presence of ACh, however, the after-depolarization was much higher (compared to No NM), reflecting the activation of spike-triggered depolarizing conductances during persistent activity, i.e., fast CAN and/or slow CAN conductances. Under ACh, also, the additional presence of FFA still left an increased after-depolarization (Fig. 3D and Suppl. Fig. 1A), likely carried by the fast CAN conductance, as FFA selectively inhibits the slow – but not the fast – CAN conductance (Haj-Dahmane et Andrade, 1999). In the medium and slow components this repolarization disappeared in the ACh condition, being replaced by a massive after-depolarization, likely attributable to slow CAN currents, as fast CAN currents had globally vanished during the fast component (being virtually null in the medium component). One cannot formally exclude a cholinergic decrease of mAHP currents that could be masked by the massive activation of slow CAN under cholinergic modulation, which would be consistent with previous reports (Wang and McCormick, 1993; Satake et al., 2008). This cholinergic after-depolarization was fully reversed by FFA. This full FFA reversal contrasted with the partial one observed in the fast component, confirming that the fast CAN current is likely to be enhanced under cholinergic modulation, in addition to the slow CAN current. Altogether, these results suggest that cholinergic modulation induces both increased levels of fast CAN and slow CAN currents during CB-related self-sustained persistent activity.

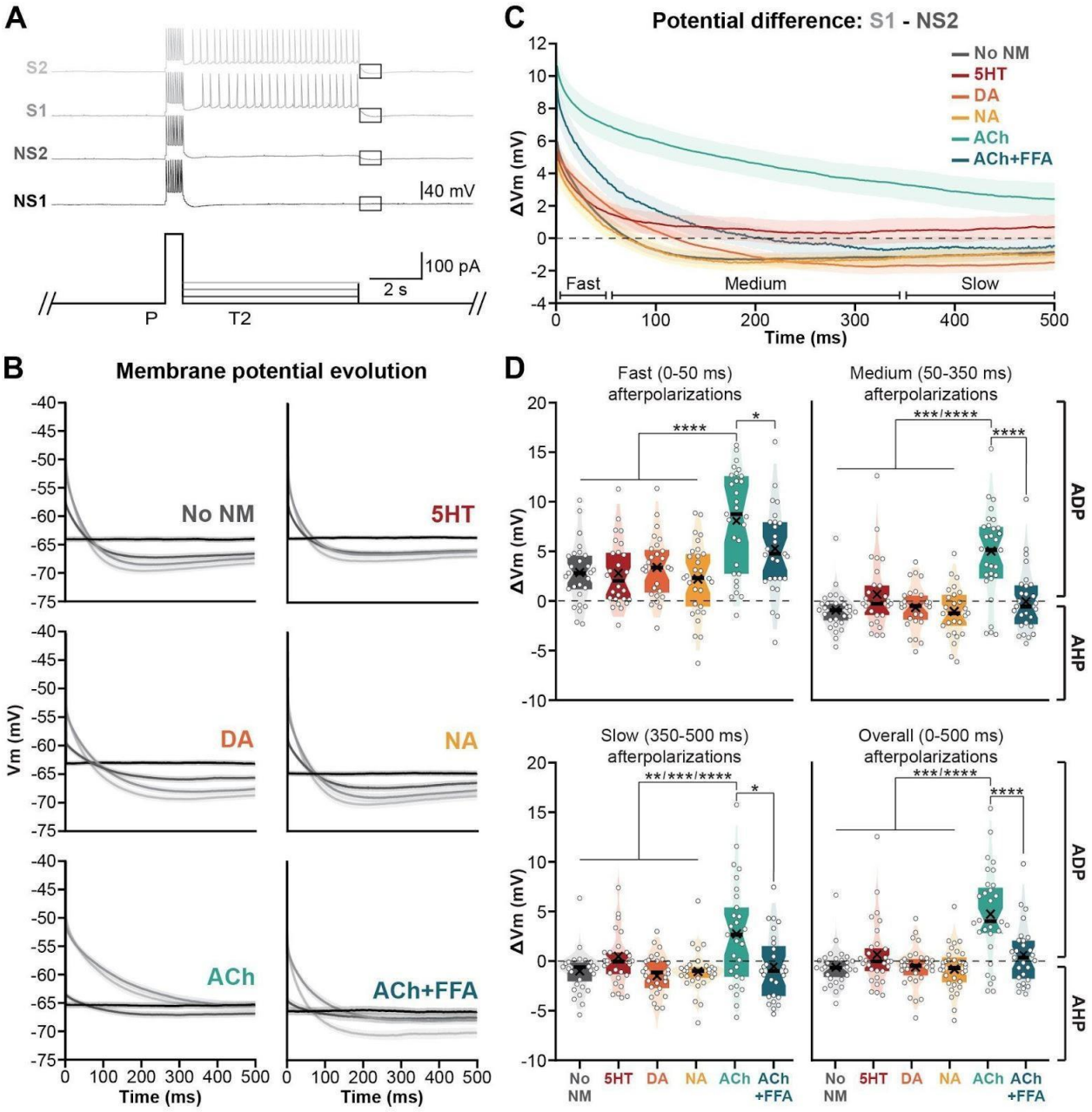

Figure 3. Acetylcholine-dependent conditional bistability is specifically mediated through medium and slow after-depolarization (ADP). A*, Method to identify currents implicated in conditional bistability. Four sweeps of interest were identified in the conditional bistability protocol : NS1 (No Spike 1, first sweep upon which the neuron doesn't fire on T1 and T2); NS2 (No Spike 2, last sweep upon which the neuron doesn't fire on T1 and T2); S1 (Spike 1, first sweep upon which the neuron fires on T1 and T2); and S2 (Spike 2, last sweep upon which the neuron fires on T1 and T2), upon which membrane potentials were extracted during the 500 ms following T2 (black squares).* ***B****, Membrane potential dynamics was averaged across neurons after T2 in the six different neuromodulation conditions.* ***C,*** *Average difference of the membrane potential between sweeps S1 and NS2, after T2 indicates spike-triggered currents activated during CB-related self-sustained persistent activity.* ***D****, Average membrane potential difference in the*

*ranges 0-50 ms (fast after-polarization), 50-350 ms (medium after-polarization), 350-500 ms (slow after-polarization) and across the whole window considered (0-500 ms, overall after-polarization) after T2. On violin plots, boxes indicate the 75th percentile (upper border line), mean (black horizontal line), and 25th percentile (lower border line) of the distribution. Dots correspond to individual neurons recorded. Statistical significance was assessed by Scheirer-Ray-Hare test and Wilcoxon Mann Whitney test for the post hoc analysis (****p<0.0001; ***p<0.001; **p<0.01; *p<0.05).*

Cholinergic-modulated conditional bistability is subserved by both fast and slow CAN conductances in a layer V rat mPFC pyramidal neuron model

To better assess the possible ionic mechanisms underlying CB, we built a Hodgkin-Huxley model of a layer V rat mPFC pyramidal neuron. To do so, we refined our previous model (Rodriguez et al., 2018), by including both the fast CAN and slow CAN conductances, as well as the mAHP, all fitted from *in vitro* data in these neurons (see *Methods*) and applied the conditional bistability protocol employed in our experimental study. Specifically, we explored the effects of cholinergic neuromodulation on layer V rat mPFC pyramidal neurons to understand their possible transitions between monostability and conditional bistability. Experimentally, ACh upregulates both the fast and the slow CAN conductances in layer V rat mPFC pyramidal neurons (Haj-Dahmane and Andrade, 1999). We therefore focused our attention on the causal effect of these two conductances on the type of neuronal excitability.

In the model, we found that when endowed with moderate levels of fast CAN and slow CAN maximal conductances, the model neuron was monostable (Fig. 4A). Indeed, when increasing the tonic pulse intensity, the model neuron either was silent (upper trace) or discharged (lower trace) on both the T1 and T2 pulses. The map in Fig. 4B shows regions in the fast and slow CAN maximal conductances parameter plane, where the neuron is monostable (M), conditionally bistable (CB), absolute bistable (AB), or pacemaker (PM) with $\Delta\theta$ values shown in the CB region for illustrative purposes (see below). In this map, as expected, the neuron displayed in Fig. 4A lies in the M region (Fig. 4B, No NM point). Also, as can be viewed, either increasing fast CAN (i.e., rightward) or slow CAN (i.e., upward), starting from that position, transforms this M neuron into a CB one (Fig. 4B). Thus, in the model, increasing either one of both conductances was sufficient to transform monostable neurons into bistable neurons.

However, experimentally, cholinergic modulation upregulates both conductances (Haj-Dahmane and Andrade, 1999). In the model, an increase of both fast ADP and slow ADP maximal conductances (Fig. 4B, upright diagonal arrow from the No NM point) transformed the M neuron into a CB one, as can be viewed in the map (Fig. 4B, ACh point) and in the example trace (Fig. 4C), which was consistent with our experimental finding that ACh massively transformed M into CB neurons *in vitro* (Fig. 2). Under this scheme, we next considered how the model might help interpret the situation under the ACh+FFA condition. *In vitro*, FFA inhibits the slow CAN conductance but leaves the fast CAN conductance unaffected in layer V rat mPFC pyramidal neurons (Haj-Dahmane et Andrade, 1999), consistent with our observation of a significatively larger fast ADP under ACh+FFA (compared to No NM), likely due to a larger fast CAN maximal conductance (but similar small slow CAN conductance, Fig. 3D and Suppl. Fig.

2A). In our model, adding FFA to ACh corresponds to a decrease of the slow CAN maximal conductance that can be viewed as a downward shift from the ACh point (Fig. 4B, downward arrow). The resulting ACh+FFA neuron still belongs to the CB region, as can be viewed in the map (Fig. 4B, ACh+FFA point) and in the example trace (Fig. 4D). However, considering the biological variability of fast and slow CAN maximal conductances across neurons (i.e., illustrated by large black circles in Fig. 4B), a fraction of neurons should be monostable under ACh+FFA. Moreover, CB neurons lay in the vicinity of the M/CB border, i.e., with very small $\Delta\theta$ values (an order of magnitude lower than those of ACh neurons). Such low $\Delta\theta$ values might not be detected experimentally, compared to the tonic pulse intensity increment used in our protocol, leading to the classification of CB neurons as M neurons. These considerations could account for why, under ACh+FFA, most neurons are M while, at the same time, the CB fraction is larger, compared to that of the No NM condition, although not significantly (Fig. 2C, E).

Altogether, our experimental results are well accounted for by a scheme where the upregulation of both fast and slow CAN conductances participate in the transformation of M neurons into CB neurons under cholinergic neuromodulation.

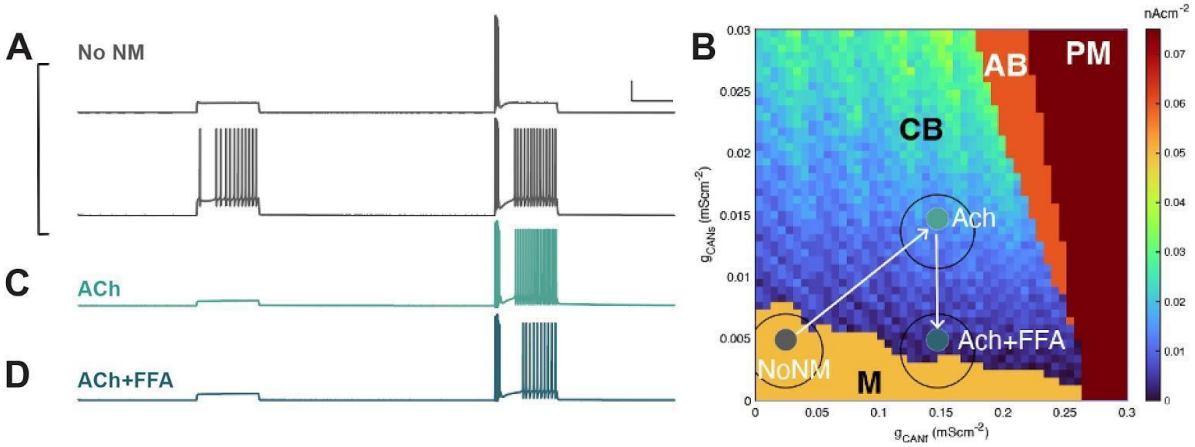

Figure 4. Cholinergic-modulated conditional bistability relies on both fast and slow CAN conductances in a layer V rat mPFC pyramidal neuron model. ***A,*** *Membrane potential of the neuron model with small fast and slow maximal conductances ($g_{fastCAN}$ = 0.0245 mS.cm^{-2}, $g_{slowCAN}$ = 0.0049 mS.cm^{-2}) in response to the conditional bistability protocol, with a tonic pulse intensity of 0.2 (upper trace) and 0.25 (lower trace) and phasic pulse intensity is 0.74 µA.cm^{-2}. The neuron is monostable (M).* ***B,*** *Excitability map in the fast CAN / slow CAN maximal conductances parameter plane showing regions where neurons are monostable (M), conditionally bistable (CB), absolute bistable (AB), and pacemaker (PM). Δθ values are shown in the CB region for illustrative purposes (see text). The position of neurons in the No NM, ACh and ACH+FFA conditions are indicated as colored dots. Large black circles illustrate the possible biological variability of fast and slow CAN maximal conductances in these three conditions.* ***C,*** *Membrane potential of the neuron in A, when fast and slow maximal conductances are increased (g_{fCAN} = 0.147 mS.cm^{-2}, g_{sCAN} = 0.0147 mS.cm^{-2}) to mimic the effect of ACh, in response to the conditional bistability protocol, with a tonic and phasic pulse intensities of 0.08 and 0.56 µA.cm^{-2}. The neuron is conditionally bistable (CB).* ***D,*** *Membrane potential of the neuron in A, when only the fast maximal*

conductances are increased (g_{fCAN} = 0.147 mS.cm^{-2}, g_{sCAN} = 0.0147 mS.cm^{-2}) to mimic the effect of ACh+FFA, in response to the conditional bistability protocol, with a tonic and phasic pulse intensities of 0.11 and 0.56 µA.cm^{-2}. The neuron is still conditionally bistable (CB) but lies at the M/CB border, where experimentally detecting CB might be problematic (see text).

Acetylcholine increases persistent activity in a graded manner at the network level in mPFC through the upregulation of CAN currents

We next investigated whether cholinergic effects at the cellular level, i.e., upregulated CAN currents, as well as enhanced self-sustained persistent spiking and conditional bistability, could affect neural dynamics at the network level in mPFC circuits. To do so, we simultaneously recorded (Suppl. Fig. 2A) the local field potential (LFP; Suppl. Fig. 2B), from which current source density (CSD; Suppl. Fig. 2C) was derived, and extracellular neuronal firing, in superficial (II/III) and deep (V) layers of the mPFC, in response to electrical stimulations applied in layer V, in the No NM, ACh, and ACh+FFA conditions.

First, based on CSD traces, we found that pre-synaptic responses in layers II/III (Suppl. Fig. 2D) and layer V (Suppl. Fig. 2E) were similar in the three neuromodulation conditions tested. This result indicated that following the stimulation, feed-forward synaptic inputs impinging onto local network circuitry in superficial and deep layers were similar, independent of the absence or presence of cholinergic modulation.

We then examined the dynamics of network activity in the seconds following the stimulation, to assess whether local mPFC circuitry could maintain persistent activity (PA), such as that found in the delay period of working memory (WM) tasks in rat mPFC (Yang et al., 2014). We also more specifically assessed whether mPFC local circuitry could display graded persistent activity (GPA), which is found in parametric WM (PWM) tasks in primates (Romo et al., 1999; Brody et al., 2003; Nieder et al., 2004), a form of WM that has been since unraveled in rats (Fassihi et al., 2014). In GPA, the firing frequency of PA monotonously scales with the amplitude of the cue parameter to be encoded and we thus focused on whether PA, if present in our experiment, would scale with the intensity of the electric stimulus.

Here, the overall idea was to study whether the cellular cholinergic effects observed at the cellular level – upregulated CAN currents and enhanced conditional bistability – could promote analogues of PA and GPA, the neural substrates of WM or PWM, in local mPFC circuits. We were particularly interested in whether ACh could enhance GPA, as the cholinergic-induced conditional bistability we unravel in the present study could subserve robust GPA. Indeed, GPA emerges as a generic dynamical property of recurrent neural network models when endowed with bistable units (Koulakov et al., 2002; Goldman et al., 2003), while unrealistic fine-tuning of synaptic weights is required in their absence (Seung et al., 2000; Miller et al., 2003; Machens et al., 2005; Machens and Brody, 2008).

We analyzed the recorded extracellular activity in No NM, ACh, and ACh+FFA conditions in response to electrical stimulations applied in layer V (Fig. 4A). We measured the firing frequency of units in the period 1-5 seconds after the stimulus, to assess whether spiking could

be actively maintained by the network, as opposed to earlier periods (Suppl. Fig. 4A-C), during which network activity reflected a progressive passive decay of activity following the initial spiking surge directly provoked by the stimulus (this initial decay was independent of the neuromodulation condition, consistent with CSD results; Suppl. Fig. 2D, E). We found in the 1-5 second period that the firing frequency of layer V mPFC units displayed different patterns, as a function of the stimulus intensity, depending on the neuromodulation condition (Fig. 4B). Hence, in the No NM condition (Fig.4B, left), the firing frequency of units following the stimulus was very low, below 1 Hz, consistent with spontaneous background activity (Yang et al., 2014). Moreover, most units displayed no dependency to the stimulus intensity. Thus, there was no clear evidence of PA or GPA in the No NM condition. By contrast, when a cholinergic agonist was added to the same slices (Fig. 4B, center), units fired at higher frequencies, in the range 1-10 Hz, consistent with that of PA observed in rats during WM tasks (Yang et al., 2014). Thus, under cholinergic neuromodulation, units appeared able to maintain activity several seconds after the stimulus, i.e., memorize a past incoming feedforward input on layer V mPFC local circuitry. In addition, a large fraction of units (5/11) displayed a monotonic dependance of PA firing frequency with the stimulus intensity, with both positive and negative slopes, a property characterizing GPA in primate prefrontal networks (Brody et al., 2003). Finally, with FFA added to the cholinergic modulation in the slice bath (Fig. 4B, left), the global pattern reversed toward that observed in the no NM condition, with no evidence of PA or GPA.

To get an overview of network dynamics, we pooled all recorded units and examined the dependence of their mean firing frequency upon the stimulus intensity, in each of the three conditions (Fig. 4C). Regarding the ability to memorize the presence of a previous stimulus (i.e., maintain activity after several seconds), we found an overall network activity pattern that was consistent with that observed for individual units. Indeed, in the No NM condition (Fig. 4C, left), the mean mPFC network activity was in agreement with spontaneous background activity during WM tasks, below 1 Hz (Yang et al., 2014), i.e., there was no PA. By contrast, under cholinergic modulation (Fig. 4C, center), mean mPFC activity ranged 2-5 Hz, consistent with functional PA in rat mPFC (Yang et al., 2014). Moreover, this mean firing frequency presented a monotonic positive dependance with the stimulus intensity, as found in GPA in sub-populations of primate prefrontal networks (Jun et al., 2010; Barak et al., 2010). However, in the ACh+FFA condition (Fig. 4C, right), the cholinergic-induced GPA disappeared, indicating that it was dependent on slow CAN currents. Noteworthy, a similar pattern of PA and GPA could be observed in layer V individual and pooled units for the period 0.5-1s (Suppl. Fig. 4D), while we found no evidence of PA or GPA in layer III, with the spiking activity vanishing to background levels after 1s (Suppl. Fig. 4A-E).

Altogether, cholinergic neuromodulation, while not affecting feed-forward synaptic inputs *per se*, is able to promote their active memorization in a parametric manner, which depends on slow CAN conductances in layer V mPFC networks. These results suggest that during PWM, slow CAN-mediated CB is essential to recurrent interactions for the emergence of GPA within layer V PFC networks.

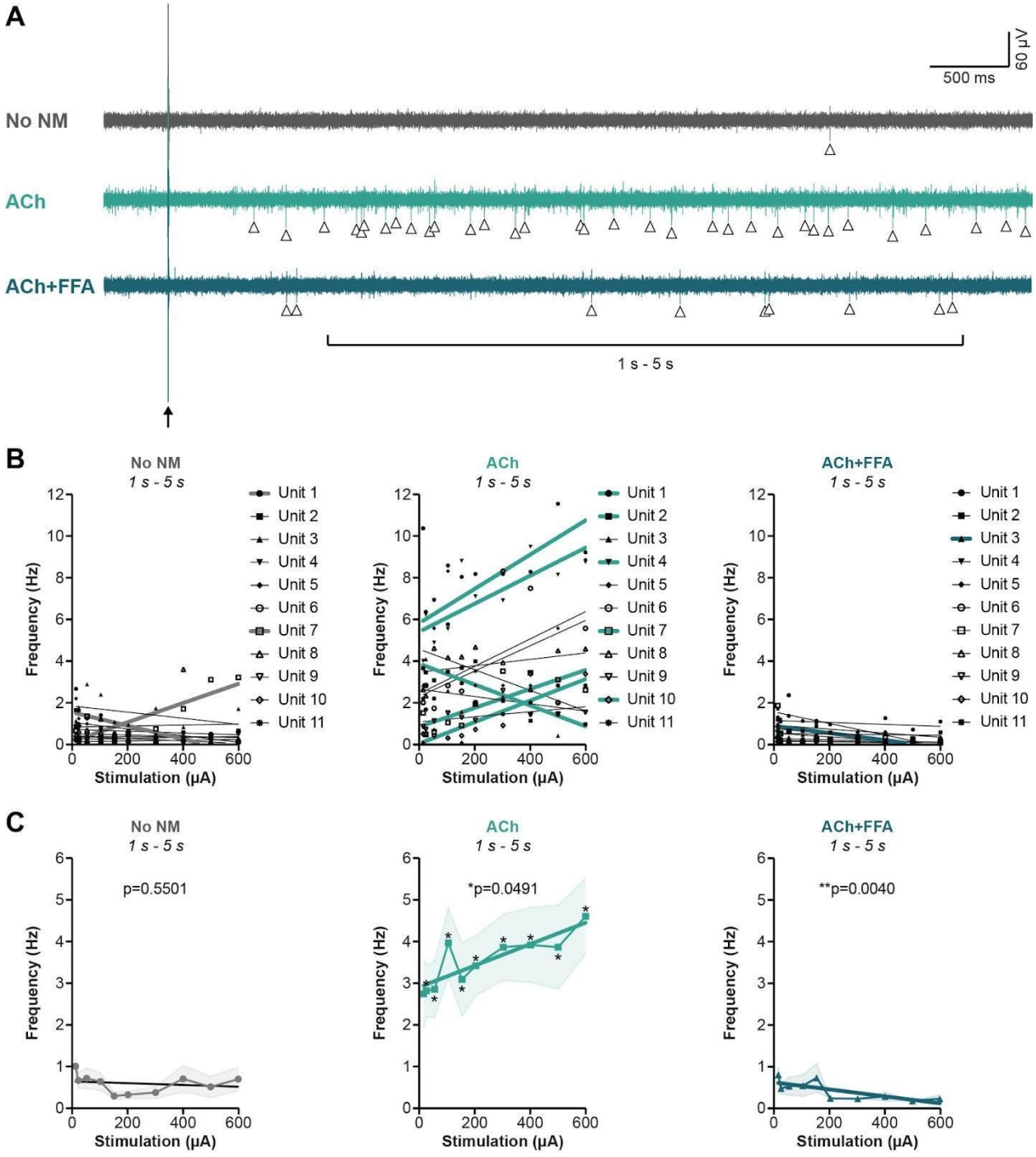

Figure 5. Cholinergic modulation promotes graded persistent activity in mPFC layer V neurons. A, *Representative 5-s-long unit recordings in response to a 200 µA electrical stimulation (black arrow) in the absence of neuromodulation (No NM), under cholinergic modulation (ACh), or under modulation of both ACh and flufenamic acid (ACh+FFA) in mPFC layer V units. Open triangles indicate detected spikes. Data was analyzed for 0-50 ms, 50-350 ms, 350-500 ms, 0.5-1 s, and 1-5 s. Subsequent data analysis is presented here for the 1-5 period. Other periods are presented in Suppl. Figure 4.* ***B,*** *Firing frequency as a function of the stimulus intensity of units for the three conditions. Linear regressions were performed*

and a F test was applied to determine whether the slopes were statistically different from zero (slopes different from zero are bold). ***C****, Mean firing frequency of pooled units as a function of the stimulus intensity for the three conditions. Statistical significance for each stimulus intensity was assessed by Repeated Measures Two-way ANOVA and Šidák test for post-hoc analysis (*p<0.05). Linear regressions were performed and a F test was applied to determine whether the slopes were statistically different from zero (p-values are indicated on each panel and slopes different from zero are bold).*

DISCUSSION

Using *in vitro* recordings and biophysically-constrained models, we unraveled that layer V mPFC pyramidal neurons exhibit conditional bistability (CB), a novel form of bistability. CB existed in a small subset of neurons in all neuromodulatory conditions tested, but became prevalent under cholinergic modulation through M1 receptors. Cholinergic modulation induces both increased levels of fast as well as slow calcium-activated cationic non-selective conductances, which transform monostable neurons into CB neurons. In CB neurons, self-sustained persistent activity is triggered by a transient event but also requires a tonic level of depolarization that may be provided, *in vivo*, by local recurrent synaptic inputs underlying contextual mnemonic, motivational or decision-making, working memory-related network activity. Finally, we demonstrated, through extracellular recordings, that under cholinergic modulation, mPFC layer V local networks exhibit graded persistent activity that depends on slow CAN conductance. Together, these results suggest that during parametric working memory, graded persistent activity arises from recurrent interactions implicating slow CAN-mediated CB in layer V PFC networks.

Existence and characterization of conditional bistability in layer V mPFC pyramidal neurons

Self-sustained spiking following an initial trigger, i.e., intrinsic bistability, constitutes a major hallmark of cellular memory. In many pioneering reports in layer V mPFC pyramidal neurons, bistability was elicited from resting membrane potentials situated around -70 mV (Andrade, 1991; Haj-Dahmane and Andrade, 1996, 1997, 1998; Yan et al., 2009), in the absence of any injected tonic depolarizing current. Accordingly, bistability in these studies should be classified as absolute bistability (AB; Rodriguez et al., 2018). Noteworthy, eliciting bistability from such hyperpolarized resting membrane potential required relatively stringent inducing conditions, i.e., very long inputs at the timescale of seconds (Haj-Dahmane and Andrade, 1998; Yan et al., 2009; Thuault et al., 2013) and/or specific pharmacological manipulation, e.g., strong cholinergic modulation (CCh concentration above 30 µM; Haj-Dahmane and Andrade, 1996, 1998; Yan et al., 2009) or the inhibition of potassium currents (Haj-Dahmane and Andrade, 1997).

However, when elicited from depolarized sub-threshold membrane potential (Sidiropoulou et al., 2009; Dembrow et al., 2010; Thuault et al., 2013; Ratté et al., 2018; Tricoire et al., 2019), typically around or above -60 mV, bistability did not require anymore the relatively unrealistic triggering conditions that were necessary in previous studies. Indeed, bistability could be triggered in the absence (Dembrow et al., 2010; Thuault et al., 2013) or under low levels (CCh 10-20 µM; Dembrow et al., 2010; Ratté et al., 2018) of cholinergic modulation, and following short stimuli, i.e., at the timescale of milliseconds to several hundred milliseconds (Siridopoulou et al., 2009; Dembrow et al., 2010; Gee et al., 2012; Ratté et al., 2018). Thus, bistability in layer V mPFC neurons is actually dependent on depolarizing the membrane resting potential and depends on the presence of a tonic depolarizing injected current, which is consistent with conditional bistability (CB), rather than AB (Rodriguez et al., 2018).

To reconcile these apparently opposing results, we suggest that layer V mPFC pyramidal neurons are predominantly CB, as supported by the voltage-dependence of self-sustained

spiking in recent studies (Siridopoulou et al., 2009; Dembrow et al., 2010; Thuault et al., 2013; Ratté et al., 2018). However, CB neurons may appear as AB neurons (i.e., exhibit self-sustained spiking in the absence of any injected tonic depolarizing current) in conditions in which depolarizing spike-mediated currents are favored over hyperpolarizing ones (e.g., CAN over AHP currents), either by boosting CAN maximal conductance through strong cholinergic neuromodulation (Haj-Dahmane and Andrade, 1996, 1998; Yan et al., 2009), inducing very strong activation levels of CAN conductances (Haj-Dahmane and Andrade, 1998; Yan et al., 2009; Thuault et al., 2013) or by inhibiting potassium currents (Haj-Dahmane and Andrade, 1997).

This hypothesis is supported by the present study, which shows that CB indeed constitutes the prevalent form of bistability, over AB, in layer V mPFC pyramidal neurons (see Methods). Hence, whereas previous studies were only indicative of the possible existence of CB neurons (based on the dependence of bistability upon sub-threshold depolarization; Siridopoulou et al., 2009; Dembrow et al., 2010; Thuault et al., 2013; Ratté et al., 2018), our study explicitly demonstrate their existence, using a dedicated protocol parametrically assessing the effect of depolarization through the building of F/I curves. Leveraging from the protocol allowed to go beyond previous phenomenological observations based on a few isolated traces and get a systematic approach allowing to classify bistability in terms of bifurcation in the framework of dynamical systems theory and, eventually, distinguish CB neurons (Rodriguez et al., 2018).

Our study also departs from previous ones as it dissects bistability in a stricter manner, closer to physiological conditions. Indeed, in previous studies, the tonic current depolarizing the membrane potential is applied after the trigger pulse, as in the present study, but also before the trigger (Dembrow et al., 2010; Ratté et al., 2018). This pre-trigger depolarization may pre-activate the slow CAN conductance, which displays spike-independent voltage activation at sub-threshold potentials, in addition to its spike-triggered, calcium-dependent activation (see below; Haj-Dahmane and Andrade, 1996, 1998, 1999). This possibly accounts for why activating bistability/self-sustained spiking in our study required 5-10 spikes, while even 1 spike was sufficient in these studies (e.g., Fig. 1C; Ratté et al., 2018). Such protocols are problematic because the pre-triggering activation of CAN conductance contaminates its post-triggering activation, jeopardizing the examination of bistability following the trigger. In the context of WM tasks (see below), this point is actually essential, as animals are usually not instructed by explicit contextual inputs that may insure such previous tonic depolarization. By contrast, during WM, network spiking and neuronal depolarization do typically not increase before the cue to be remembered (Inagaki et al., 2019). In that sense, our study likely provides a better account of the actual physiological situation in behaving rodents, by assessing the mechanisms of self-sustained spiking and conditional bistability in a strict fashion, i.e., independently of previous contaminating influences.

Modeling spike-mediated intrinsic bistability

A large array of Hodgkin-Huxley based computational models have assessed different forms of non-spike triggered – “plateau potential” – intrinsic cellular bistabilities, based on either dendritic

calcium-voltage (Booth and Rinzel, 1995) or NMDA-voltage (Major et al., 2008), or between voltage and/or subthreshold conductances (Delord, 1996; Delord et al., 1997; Genet and Delord, 2002; Loewenstein et al., 2005). These mechanisms depart from the bistability we unravel here, which is spike-mediated. By contrast, models of spike-mediated bistability have remained scarce. A spike-mediated form of absolute bistability, based on the positive feedback between the CAN conductance and spike-triggered calcium was previously studied theoretically (Shouval and Gavornik, 2010), but this model does not address conditional bistability. In our more recent theoretical study, we showed how a CAN conductance may underlie conditional bistability (Rodriguez et al., 2018). However, we modeled a generic CAN conductance with a time constant below 100 ms, i.e., mimicking the fast CAN conductance of mPFC layer V pyramidal neurons (Haj-Dahmane et Andrade, 1997).

Here, we refined our model, by fitting passive properties to those of recorded neurons and incorporating both fast and slow CAN conductances, as well medium and slow AHP conductances (see *Methods*). For that reason, the present model offers a major leap in the understanding of the effects of CAN conductances in spike-mediated bistability, compared to previous models (Shouval and Gavornik, 2010; Rodriguez et al., 2018; Ratté et al., 2018). Indeed, it is the first one to consider 1) the dual positive feedback between activation of the slow CAN conductance and sub-threshold voltage, on the one hand, and with spike-triggered calcium influx, on the other hand, and 2) the additional feedback between the activation of the fast CAN conductance and spike-triggered calcium influx.

Ionic mechanisms of conditional bistability in mPFC layer V pyramidal neurons

Moreover, our model takes into account the biophysical effect of acetylcholine on spike-mediated conductances. Cholinergic modulation promotes both fast and slow CAN conductances in layer V rat mPFC pyramidal neurons (Haj-Dahmane and Andrade, 1999). It also reduces AHP currents (Wang and McCormick, 1993), although mainly the slow AHP versus the medium one (Satake et al., 2008). However, exact fine-grained biophysical specificities of this modulation are not experimentally described in sufficient detail (compared to that of CAN, see below), so this effect was not further considered in the present model. Regarding the slow CAN conductance, cholinergic modulation exerts its influence through a systematic increase in maximal conductance (Haj-Dahmane and Andrade, 1999), which was found in our model to be essential in setting excitability, i.e., either M or CB. Also, under cholinergic modulation, the fast CAN conductance presents a combined upregulation of both its maximal conductance and decay time constant, which affects its net magnitude by a factor three (Haj-Dahmane and Andrade, 1999). These effects may participate in the cumulative recruitment of the fast CAN conductance during persistent spiking, which we observe in our study, and therefore promote CB.

In our model, we found that increasing the fast CAN maximal conductance could possibly transform M into CB neurons, as for slow CAN. The ratio of fast to slow CAN maximal conductances effectively required was of the order of ~20, in line with the ratio of corresponding currents found experimentally (Haj-Dahmane and Andrade, 1999). Besides, we observed that increasing the fast CAN time constant in the model could affect neuronal M/CB typology, but

only for time constants in the range of several hundred milliseconds, i.e., above experimentally observed values (i.e., inferior to 100 ms; Haj-Dahmane and Andrade, 1999). This can be understood when considering that neuronal M/CB typology is tested, by definition, in the vicinity of the rheobase, where spiking frequencies are below the minimal frequency at which fast CAN builds up during self-sustained spiking (1/100ms, i.e., 10 Hz). Rather, the cholinergic upregulation of the fast CAN time constant may rapidly exert its effect above rheobasis, at higher spiking frequencies, and increase $\Delta\theta$, the range of input currents where CB expresses (see thickness of the purple region in Fig. 2a and 3 in Rodriguez et al., 2018).

Our data indicate that, during CB-related self-sustained persistent activity, cholinergic modulation induces both increased levels of fast CAN and slow CAN currents. In theory, a slow CAN conductance is not necessary for CB, as indicated by our previous study (CB provided by a fast CAN conductance; Rodriguez et al., 2018). However, the large decrease of the fraction of CB neurons when FFA is added to cholinergic modulation indicates that the slow CAN conductance plays an essential role in supporting conditional bistability, while the fast CAN conductance likely exerts a smaller effect. Indeed, a slow CAN with time constant in the order of seconds appears better adapted to the typical time scale of behavioral contexts in which WM operates (i.e., seconds) and the low frequencies observed during WM (Shafi et al., 2007).

Also, the distinctive implication of fast and slow CAN conductances might arise from differences in their gating dynamics. Indeed, the fast CAN conductance – carried by ion channels distinct from those carrying the slow CAN conductance (Haj-Dahmane and Andrade, 1999) – is calcium- (Haj-Dahmane and Andrade, 1997) but not voltage-dependent (Haj-Dahmane and Andrade, 1999). By contrast, the slow CAN conductance – presumably carried by TCRP5 channels (Sidiropoulou et al., 2009) – presents both voltage activation at subthreshold potentials (Haj-Dahmane and Andrade, 1996, 1998, 1999) and calcium-dependent activation (Gross et al., 2009; Blair et al., 2009; Ratté et al., 2018), which provides an additional computational mechanism subserving the interaction between (e.g., contextual) subthreshold and (e.g., event-driven) spike-induced sources of activation (Andrade, 1991; see the discussion below on functional consequences of this interaction).

Conditional bistability in different rat mPFC cytoarchitectonic subdivisions

At the scale of rodent mPFC subdivisions, bistability has been found in areas 24 (ACC; Haj-Dahmane and Andrade, 1997, 1998, 1999; Zhang et Seguela, 2010; Ratté et al., 2018), 32 (PL; Haj-Dahmane and Andrade, 1998, 1999; Dembrow et al., 2010) and 25 (IL; Haj-Dahmane and Andrade, 1999; Dembrow et al., 2010), indicating that this mnemonic property is ubiquitous in the mPFC.

In an interesting recent study assessing bistability both experimentally and computationally in pyramidal neurons in the ACC (area 24), a cellular model has been developed that incorporates a slow CAN conductance (Ratté et al., 2018). Recordings indicate that bistability is dependent upon the relative depolarization of the resting membrane potential, suggesting that it is conditional (i.e., CB). In this model, CAN activation is instantaneous and dynamics are determined by a slow calcium time constant (~5 seconds). By contrast to the present study, the model does not assess the voltage dependence of bistability in a systematic

manner (i.e., CB), nor the effect of cholinergic modulation. Also, it does not incorporate slow gating dynamics of the CAN conductance, which slowly rises after the Ca^{2+} surge (see Ratté et al., 2018; Fig. 6) nor its sub-threshold voltage dependance. However, it suggests how a low CAN calcium half-activation, by inducing full CAN activation (i.e., saturation), might be central in spike-mediated intrinsic bistability. Indeed, these hypotheses account for why self-sustained spiking can be triggered using short stimuli, 1-5 spikes producing sufficient intracellular calcium concentration to initiate the positive feedback between CAN activation and spike-triggered calcium influx. It also explains how self-sustained spiking resumes after long episodes of hyperpolarization (several seconds to even a minute), as CAN remains saturated for extended periods – the slowly decaying – before calcium crosses down the low CAN calcium half-activation.

While fast triggering of self-sustained activity was also present in our experiments (i.e., 250 ms-long pulses, a few spikes), we did not observe such resistance to hyperpolarization in our neurons. Indeed, while the activation of the slow CAN current could overcome the transient hyperpolarization arising from AHP recruitment following the P pulse trigger (i.e., a few hundred ms to 2 seconds), spiking did not resume upon T1 pulses 20 seconds after the previous self-sustained spiking upon the previous pulse T2 in our protocol (see Methods). In our model, fast triggering was accounted for by sufficiently large CAN maximal conductances and did not require activation saturation. Also, a slow CAN time constant of the order of 5 seconds (Haj-Dahmane and Andrade, 1999) both ensured stable, low frequency, self-sustained spiking (see above), while forbidding it to resume after 10-20 seconds, as in our recordings. Thus, we did not have to incorporate the specific hypotheses of a large calcium time constant and a rapidly saturated calcium activation. Although supported by recordings in ACC neurons (Ratté et al., 2018), such hypotheses are rather unusual in biophysical models of neuronal processes, where calcium time constants typically lie below 100 milliseconds and activation are induced across their full dynamical range.

Moreover, a large calcium time constant is specifically incompatible with the short duration of the calcium-activation of fast CAN conductance found in the ACC and in the prelimbic cortex (PL; area 32; Haj-Dahmane and Andrade, 1997, 1999). The reasons for such a discrepancy may arise from differences in protocols, e.g., the recording method (Ratté et al., 2018), or the age of rats (20-60 in Ratté et al., 2018 versus 63-84 days here). Alternatively, this difference could be accounted for, in ACC neurons, by different sources of calcium displaying small (versus large) time constants, respectively activating fast (versus slow) CAN conductances, within specific micro-domains. Assessing this possibility by incorporating the fast CAN conductance and specific fast/slow calcium signaling could further refine the understanding of the biophysical basis of bistability in the ACC (Ratté et al., 2018).

As another possibility, recordings displaying the fast CAN conductance might have been essentially acquired in the PL (Haj-Dahmane and Andrade, 1997, 1999). This would relieve the inconsistency of co-existing slow calcium dynamics and fast calcium-activated CAN dynamics in ACC neurons. If so, CB might rely on distinct mechanisms in mPFC subdivisions, with slower dynamics in the ACC and a larger resistance to hyperpolarization in the ACC, compared to the PL (see below for possible functional consequences of this temporal distinction).

Other structural determinants of conditional bistability

Here, we did not specifically assess cytoarchitectonic factors that could promote CB. In previous studies, bistability has been found in cortico-cortical neurons (Dembrow et al., 2010), but was preferentially observed in neurons projecting to subcortical structures, such as the thalamus (Gee et al., 2012) or the pons (Dembrow et al., 2010). In parallel, bistability has been observed to correlate with neurons displaying a strong I_H current (Gee et al., 2012; Thuault et al., 2013), which promotes sub-threshold sensitive spike-mediated bistability (Thuault et al., 2013). Conditional bistability may also depend on whether neurons belong to superficial versus deep layers. In the ACC, layer II/III pyramidal neurons display a bistability mediated by calcium-activated CAN currents carried by TRPC5 channels (Zhang and Seguela, 2010), but this bistability is apparently based on plateau-like depolarization (i.e., due to strong positive feedback between sub-threshold potentials and CAN current activation), which is not the case in layer V (Ratté et al., 2018). However, such observations remain rather scarce among the literature, and the role of neuronal types or layers in bistability or CB should be assessed in a deeper fashion.

Neuromodulation of conditional bistability in the mPFC

Here, we found that, remarkably, CB exists in PL/IL areas in all conditions of neuromodulation. The CB fraction was nearly 100% under cholinergic modulation for CB, consistent with the fraction of neurons displaying voltage-dependent bistability in previous studies (Dembrow et al., 2010; Ratté et al., 2018). In other conditions, i.e., in the absence of neuromodulation or in the presence of serotoninergic, dopaminergic and noradrenergic modulation, the CB fraction of neurons was minor but nevertheless substantial (~15-40%), which could be sufficient for the emergence of GPA/PWM in mPFC networks (see below).

In the absence of neuromodulation, CB was present in a very small fraction of neurons, consistent with previous studies showing bistability in the absence of neuromodulation (Thuault et al., 2013; Dembrow et al., 2010). This small fraction was concomitant with very small positive $\Delta\theta$ values, i.e., small sub-threshold range of inputs within which CB can express. Actually, a large fraction of $\Delta\theta$ values lied nearby zero, a region where the balance of spike-mediated depolarizing (CAN) and hyperpolarizing (AHP) currents are balances, and in which transient forms of bistability (Rodriguez et al., 2018; Sarazin et al., bioarxiv) can promote functional neural representations at the network level (Sarazin et al., 2021; Sarazin et al., bioarxiv).

Under serotonergic modulation, the non-significative increase of the CB fraction and the apparition of neurons displaying larger positive $\Delta\theta$ values correlated with a shift of the balance toward depolarizing spike-mediated currents. This effect could arise from a decrease of the mAHP conductance, consistent with the effect of 5-HT_{2a} neuromodulation in the literature (Satake et al., 2008). It could also arise from a 5-HT_{2a} upregulation of the slow CAN conductance, consistent with some previous studies (Araneda et Andrade, 1991; Zhang and Arsenault, 2005; Stephens et al., 2018), although no serotonergic effect on the slow CAN conductance was reported elsewhere (Satake et al., 2008). The situation is actually quite fuzzy, as serotonin is mainly excitatory in mice COM (commissural) neurons (Avesar and Gulledge, 2012), while voltage-dependent bistability – putatively CB – exists in CPn (cortico-pontine)

neurons in rats (Dembrow et al., 2010). Also, the effect of serotonin depends on the type of receptors (5-HT_1 versus 5-HT_2), both present in mPFC neurons (Araneda et Andrade, 1991), and its effect can be opposite in different neuronal subsets when present with dopaminergic modulation (Di Pietro and Seamans, 2011). This complexity possibly accounts for the global larger dispersion of $\Delta\theta$ values we found under serotonergic modulation, with some neurons apparently becoming more monostable and others becoming more CB.

Under dopaminergic modulation, we observed a non-significative increase of the CB fraction, the reduction of negative $\Delta\theta$ values, the appearance of more positive values, and an apparent reduction of $\Delta\theta$ dispersion. Again, these results indicate a shift of the balance toward depolarizing spike-mediated currents. These results are consistent with studies indicating a dopamine-dependent increase in excitability (Yi et al., 2013; Di Pietro and Seamans, 2011). We found that this shift could arise from an increase in the fast CAN conductance, consistent with the dopaminergic modulations of fast ADP in mPFC neurons (Thurley et al., 2008, Buchta et al., 2017), or a decrease in the mAHP conductance, consistent with other several studies (Satake et al., 2008; Yi et al., 2013; Thurley et al., 2008; Buchta et al., 2017). The absence of clear effect on the slow CAN conductance is in line with a complex picture in the literature, with an increase in spike induced sADP (Yi et al., 2013), or no effect (Satake et al., 2008), or the inhibition of metabotropic activated slow CAN-mediated self-sustained spiking by dopamine in mPFC neurons (Sidiropoulou et al., 2009).

Under noradrenergic modulation, modifications were very close to those observed under dopaminergic modifications, both in terms of the fraction of CB neurons or of $\Delta\theta$ distribution. However, we did not detect any difference in terms of putative spike-mediated conductance, compared to when neuromodulation was absent, which contrasted with the apparent fast CAN increase/medium AHP decrease found under dopaminergic conductance. The absence of change in the slow CAN conductance was consistent with previous results (Satake et al., 2008). Besides, the noradrenergic-induced decrease of a slow AHP conductance (Wang and McCormick, 1993; Zhang et Arsenault 2005; Satake et al., 2008) might reconcile these results, accounting for both the non-significative CB fraction increase and the shift of $\Delta\theta$ values toward more positive values, without changes in the fast CAN and mAHP conductances.

In conditions of serotoninergic, dopaminergic and noradrenergic modulation, we found that both the overall excitability and the CB fraction appeared somehow increased, although not statistically significant, compared to the situation where no neuromodulation was applied. Possibly, this partly arises from the fact that we employ a restrictive protocol, compared to previous studies. Indeed, our protocol forbids pre-trigger slow CAN activation, which boosts self-sustained spiking (Dembrow et al., 2010; Ratté et al., 2018). Also, we assess self-sustained spiking in an exhaustive manner, by building F/I curves, which imposes, due to the limited recording time, a minimal current step between successive sweeps. This constraint may force to misclassify CB neurons as monostable, because a $\Delta\theta$ value inferior to that minimal current step will be considered null. Possibly, the phasic application of serotoninergic, dopaminergic and noradrenergic agonists, instead of the tonic application operated here, could provide distinct and/or stronger effects not detected here (Di Pietro and Seamans, 2011; Gulledge and Jaffe, 2001).

Altogether, our results show that cholinergic modulation via M1-type receptors strongly facilitates conditional bistability consistent with its effect on persistent spiking and an unspecified form of voltage-dependent bistability (Andrade, 1991; Ratté et al., 2018). Moreover, our results suggest that cholinergic modulation increases both the fast and slow CAN conductances, and possibly a decrease in AHP currents, consistent with the literature (see above; Wang and McCormick, 1993; Haj-Dahmane et Andrade, 1999; Satake et al., 2008). The present results thus indicate a major effect of cholinergic modulation, compared to the other ones tested. They are consistent with previous theories suggesting that cholinergic modulation is essential in favoring the short-term maintenance of new inputs into persistent activity driven by intrinsic processes, over recurrent attractorial dynamics replaying previously learnt inputs (Hasselmo, 2006). Also, this major effect suggests that CB modulation is principally dependent upon attentional processes. This can be understood, as forming mnemonic CB-promoted memory traces (i.e., persistent activity, see below) in mPFC networks of any event, independent of the filtering operated by attentional processes, would likely reveal problematic both in terms of computational specificity and energetic efficiency.

Possibly, the phasic application of cholinergic, serotonergic, dopaminergic and noradrenergic agonists, instead of the tonic application operated here, could provide distinct and/or stronger effects not detected here (Gulledge and Jaffe, 2001; Gulledge et al., 2007, 2009; Di Pietro and Seamans, 2011). Also, the combined interaction of these neuromodulators, which likely exert their effects altogether in physiological conditions, could upregulate CB in a synergistic manner, with richer and stronger effects, not detected here under the separate application of serotoninergic, dopaminergic and noradrenergic agonists. For instance, dopaminergic and serotonergic modulations induce complex synergistic patterns increasing or decreasing of spike-mediated conductance affecting the gain of excitability in distinct sub-populations of mPFC pyramidal neurons (Di Pietro and Seamans, 2011). Also, cholinergic modulation, when combined with serotoninergic or noradrenergic modulation, produces cumulative synergistically activation of slow CAN conductances (Satake et al., 2008). Future studies should assess how combined neuromodulation effects, closer to physiology, may affect conditional bistability.

Conditional bistability, graded persistent activity and parametric working memory

Here, using extracellular recordings, we find that the ability for mPFC layer V local networks to discharge in a graded persistent manner – as a function of the stimulus intensity – depends on the cholinergic modulation of the slow CAN conductance. Because this modulation massively transforms monostable neurons into CB neurons, we propose that CB is the actual biophysical counter part of coarse-grained rate bistability descriptions that are required in recurrent neural network models to account for graded persistent activity (GPA; Koulakov et al., 2002; Goldman et al., 2003), the neural correlate of parametric working memory (PWM; Romo et al., 1999; Nieder et al., 2004; Fassihi et al., 2014). Indeed, PWM models rely on bistable units that display θ_{OFF} (θ_{T1} in our protocol) distributed across positive intensities, as the CB neurons we unravel in the present study, and they would not maintain parametric working memory with bistable units with null or negative θ_{OFF} values, corresponding to absolute bistable neurons. Under this scheme, the sub-threshold current required to express CB-related self-sustained spiking of

pyramidal neurons would be provided by the recurrent feedback operating through synaptic reverberation in mPFC layer V local circuits during PWM, following an initial stimulus (as well as in our extracellular recordings).

In neural network models displaying GPA/PWM endowed with bistable units, all units were bistable (Koulakov et al., 2002; Goldman et al., 2003). Such a fraction is consistent with that observed under cholinergic modulation (nearby 100%), but much higher than that required to get GPA/PWM in biophysical simulations of mPFC recurrent networks we ran with 50% neurons endowed with conditional bistability (Delord, 2010; Rodriguez, 2017), and even with as low as 25% of bistable neurons. Such fractions allowing GPA/PWM are of the order of what we found experimentally in the absence of neuromodulation or in the presence of serotoninergic, dopaminergic and noradrenergic modulation (~15-40%).

Here, we found global positive GPA encoding (i.e., increasing with stimulus intensity) when pooling units in rat slices *in vitro*. This situation is possibly somehow simpler than that encountered in monkeys *in vivo*, where several sub-populations that are not anatomically separated differentially encode positive and negative task parameters, with no global trend emerging (Jun et al., 2010; Barak et al., 2010). This difference suggests that, possibly, GPA neural representations may differ in rodents and monkeys. Overall, our results suggest that GPA during PWM is indeed based on recurrent synaptic interactions between conditionally bistable neurons in PL/IL areas, and neither on pure synaptic recurrent interactions, which has been discarded by neural network models (Major and Tank, 2004; Brody et al., 2003), nor on intrinsic multi-stability, observed in layer V entorhinal cortex (Egorov et al., 2002), but not in mPFC neurons.

The present results can be related to the results of a previous study using calcium imaging in the rat sensorimotor cortex, which shows that cholinergic modulation of CAN-dependent spiking in pyramidal neurons contributed to sustained responses specifically in layer V circuits (Tricoire et al., 2019). In this study, the sustained response is equivalent to mPFC persistent activity (PA) encountered during object working memory (OWM) or spatial working memory (SWM). However, the dependance of the frequency of this response was not evaluated as a function of the intensity of the stimulus. Our study indicates that the cholinergic modulation of mPFC layer V circuits enable sustained neural responses that are consistent – beyond simple PA – with GPA, when the stimulus intensity is varied. The question arises of whether distinct circuits are responsible for PA and GPA in the mPFC. Our results, considered in conjunction with this previous study (Tricoire et al., 2019), support an alternative possibility whereby both forms of WM correlates may actually be subserved by the same circuits, employed in different conditions, i.e., with fixed intensity stimuli, giving rise to PA in OWM/SWM tasks, versus variable intensity stimuli eliciting GPA in PWM. Said differently, we suggest that circuits in the mPFC could instinctively achieve GPA, and therefore PA, but only one of the two possibilities would be used in a given context, depending on the computational demand. Note that different computational operations could occur in these circuits in the absence of cholinergic modulation, with stimulus intensity setting PA duration rather than firing frequency (Fellous et al., 2003).

Our results show that cholinergic-modulated slow CAN-dependent GPA is specific to deep layers in the mPFC and absent in superficial ones. The question arises whether layer V

might represent a specific substrate dedicated to working memory-related persistent activity in different cortical areas in rats, e.g., in the PL/IL subdivision of the mPFC cortex (present study) or in the sensorimotor cortex (Tricoire et al., 2019). This would be noteworthy, as WM apparently primarily relates on superficial layers in primates (Bastos et al., 2018). However, while we did not find any form of GPA in PL/IL superficial layers, this could be the case in the ACC subdivision of the rat mPFC, where a form of plateau-potential form of bistability is present in superficial layers (Zhang and Seguela, 2010). By contrast, no bistability was observed in superficial layers in the sensorimotor cortex, accounting for the absence of PA (Tricoire et al., 2019). In the present study, the absence of GPA may arise from the absence of bistability (not assessed) or difference in network recurrent dynamics between superficial and deep layers of PL/IL areas.

Conditional bistability and executive functions in the mPFC

As a form of intrinsic cellular memory, CB may alleviate the burden resting on recurrent connectivity for maintaining retrospective as well as prospective persistent activities during working memory, beyond PWM. Hence, bistability is important in other forms of static network attractors (e.g., OWM and SWM; Camperi and Wang, 1998; Tegnér et al., 2002; Compte, 2006). Also, neurons with weak, transient forms of bistability (Rodriguez et al., 2018; Sarazin et al., bioarxiv) promote the expression of dynamic attractors such as neural trajectories (Sarazin et al., 2021; Sarazin et al., bioarxiv).

Moreover, CB offers a unique ability regarding the specificity of neuronal activation, compared to the monostable or absolute bistable forms of excitability assessed hitherto. Indeed, CB, contrarily to other forms of bistability, provides the possibility to generate persistent activity that depends both on phasic events (e.g., percepts, actions, outcomes) and tonic contextual inputs. These tonic inputs may simply signal behaviorally-relevant features related to the context of the task. They may correspond to persistent activity maintaining information about the event itself, such as required for PWM (see above).

The dependence of the slow CAN conductance upon the level of sub-threshold membrane potential provides a supplementary level of complexity by rendering CB expression not only to tonic drives after the event but also before it. Hence, self-sustained spiking of CB neurons may be allowed by tonic inputs from persistent activity maintaining the memory of previous events (which is why we had to separate T1 and P/T2 pulses by 20 seconds long periods, see *Methods*). This possibility allows for the ability to memorize an event only when previous ones have been memorized, i.e., providing a neural basis for working memory representations in sequential tasks. Tonic inputs may also correspond to prospective – ramping – activities. Such activity may recruit self-sustained spiking in CB neurons and allow for the update of anticipatory representations following incoming events. In the same vein, attentional or motivational tonic drives may recruit CB neurons and be updated by ongoing events.

All these possibilities are essential, given the role of rat PL and IL areas in working memory retrospective encoding and dynamic coding (Batuev et al., 1990; Baeg et al., 2003; Yang et al., 2014), action timing (Narayanan et Laubach, 2006, 2009) and action planning (Seamans et al., 1995). In all of these cases, the computational context in which CB exerts its

influence is crucial to generate short-term memories of events and plan upcoming decisions. This feature is appealing, given the importance of cue/context interactions in PL/IL areas (Baeg et al., 2001) and the general requirement for contextual-based flexibility in executive functions such as decision-making and working memory (Seamans et al., 1995).

Besides, CB may exert its effects in different manners in distinct mPFC subdivisions. Indeed, our results, as well as a previous study (Ratté et al., 2018) suggest that CB-related self-sustained spiking lasts over more extended periods of time and is more resistant to hyperpolarization in the ACC, compared to the PL/IL areas. This possibility is functionally attractive due to the distinct functional timescales at which these areas operate in rats, similar to the dissociation seen in primates (Fontanier et al., 2022). Hence, PL/IL areas are involved in solving executive demands at the trial timescale, according to the current strategy (i.e., seconds; Batuev et al., 1990; Baeg et al., 2001, 2003; Yang et al., 2014; Narayanan et Laubach, 2006, 2009). The more labile, i.e., flexible, CB-related self-sustained spiking found in PL/IL areas would constitute a well-designed putative candidate to participate in these working memory operations by facilitating the transient storage of memory traces.

By contrast, ACC is involved in monitoring choices, efforts and outcomes of the current behavioral strategy through sustained attention, by integrating information across trials in working memory tasks (i.e., over minutes; Lapish et al., 2008; Hillmam and Bilkey, 2012; Wu et al., 2017), with no trial-to-trial variability and a large immunity to distraction (Wu et al., 2017). Therefore, ACC CB-related self-sustained spiking with more stability (i.e., lasting over longer periods) and more resistant to hyperpolarization would provide an adapted mechanism for slow-paced monitoring functions, by their ability to integrate the history of activity and code this history onto self-sustained activity.

Thus, the relative stability of cellular CB-mediated self-sustained spiking may constitute an important factor determining the characteristic timescales of network dynamics in different mPFC subdivisions. Altogether, our results suggest that CB is a crucial mechanism that operates in a ubiquitous, generic, and adapted fashion across mPFC subdivisions and the executive functions it subserves.

REFERENCES

Andrade, R. (1991). Cell excitation enhances muscarinic cholinergic responses in rat association cortex. *Brain Research*, *548*(1–2), 81–93. https://doi.org/10.1016/0006-8993(91)91109-e

Araneda, R. C., & Andrade, R. (1991). 5-Hydroxytryptamine2 and 5-hydroxytryptamine1A receptors mediate opposing responses on membrane excitability in rat association cortex. *Neuroscience*, *40*(2), 399–412. https://doi.org/10.1016/0306-4522(91)90128-b

Avesar, D., & Gulledge, A. T. (2012). Selective serotonergic excitation of callosal projection neurons. *Frontiers in Neural Circuits*, *6*. https://doi.org/10.3389/fncir.2012.00012

Baddeley, A. (1992). Working memory. *Science*, *255*(5044), 556–559. https://doi.org/10.1126/science.1736359

Baeg, E. H., Kim, Y. B., Jang, J., Kim, H. T., Mook-Jung, I., & Jung, M. W. (2001). Fast spiking and regular spiking neural correlates of fear conditioning in the medial prefrontal cortex of the rat. *Cerebral Cortex*, *11*(5), 441–451. https://doi.org/10.1093/cercor/11.5.441

Baeg, E. H., Kim, Y., Huh, K., Mook-Jung, I., Kim, H., & Jung, M. W. (2003). Dynamics of population code for working memory in the prefrontal cortex. *Neuron*, *40*(1), 177–188. https://doi.org/10.1016/s0896-6273(03)00597-x

Barak, O., Tsodyks, M., & Romo, R. (2010). Neuronal population coding of parametric working memory. *The Journal of Neuroscience*, *30*(28), 9424–9430. https://doi.org/10.1523/jneurosci.1875-10.2010

Bastos, A. M., Loonis, R., Kornblith, S., Lundqvist, M., & Miller, E. K. (2018). Laminar recordings in frontal cortex suggest distinct layers for maintenance and control of working memory. *Proceedings of the National Academy of Sciences*, *115*(5), 1117–1122. https://doi.org/10.1073/pnas.1710323115

Batuev, A. S., Kursina, N. P., & Shutov, A. P. (1990). Unit activity of the medial wall of the frontal cortex during delayed performance in rats. *Behavioural Brain Research*, *41*(2), 95–102. https://doi.org/10.1016/0166-4328(90)90145-5

Bezu, M., Malikovic, J., Kristofova, M., Engidawork, E., Höger, H., Lubec, G., & Korz, V. (2017). Spatial working memory in male rats: Pre-Experience and task dependent roles of dopamine D1- and D2-Like receptors. *Frontiers in Behavioral Neuroscience*, *11*. https://doi.org/10.3389/fnbeh.2017.00196

Blair, N. T., Kaczmarek, J. S., & Clapham, D. E. (2009). Intracellular calcium strongly potentiates agonist-activated TRPC5 channels. *The Journal of General Physiology*, *133*(5), 525–546. https://doi.org/10.1085/jgp.200810153

Booth, V., & Rinzel, J. (1995). A minimal, compartmental model for a dendritic origin of bistability of motoneuron firing patterns. *Journal of Computational Neuroscience*, *2*(4), 299–312. https://doi.org/10.1007/bf00961442

Braun, U., Harneit, A., Pergola, G., Menara, T., Schäfer, A., Betzel, R. F., Zang, Z., Schweiger, J. I., Zhang, X., Schwarz, K., Chen, J., Blasi, G., Bertolino, A., Durstewitz, D., Pasqualetti, F., Schwarz, E., Meyer-Lindenberg, A., Bassett, D. S., & Tost, H. (2021). Brain network dynamics during working memory are modulated by dopamine and diminished in schizophrenia. *Nature Communications*, *12*(1). https://doi.org/10.1038/s41467-021-23694-9

Brody, C. D., Hernández, A., Zainos, A., & Romo, R. (2003). Timing and neural encoding of somatosensory parametric working memory in macaque prefrontal cortex. *Cerebral Cortex*, *13*(11), 1196–1207. https://doi.org/10.1093/cercor/bhg100

Brumback, A. C., Ellwood, I. T., Kjaerby, C., Iafrati, J., Robinson, S., Lee, A. T., Patel, T., Nagaraj, S., Davatolhagh, M. F., & Sohal, V. S. (2017). Identifying specific prefrontal neurons that contribute to autism-associated abnormalities in physiology and social behavior. *Molecular Psychiatry*, *23*(10), 2078–2089. https://doi.org/10.1038/mp.2017.213

Buchta, W. C., Mahler, S. V., Harlan, B. A., Aston-Jones, G., & Riegel, A. C. (2017). Dopamine terminals from the ventral tegmental area gate intrinsic inhibition in the prefrontal cortex. *Physiological Reports*, *5*(6), e13198. https://doi.org/10.14814/phy2.13198

Callicott, J. H. (2000). Physiological dysfunction of the dorsolateral prefrontal cortex in schizophrenia revisited. *Cerebral Cortex*, *10*(11), 1078–1092. https://doi.org/10.1093/cercor/10.11.1078

Camperi, M., & Wang, X. J. (1998). A model of visuospatial working memory in prefrontal cortex: recurrent network and cellular bistability. *Journal of Computational Neuroscience*, *5*(4), 383–405. https://doi.org/10.1023/a:1008837311948

Carrillo-Reid, L., Han, S., Yang, W., & Akrouh, A. (2019). Controlling visually guided behavior by holographic recalling of cortical ensembles. *Cell*, *178*(2), 447-457.e5. https://doi.org/10.1016/j.cell.2019.05.045

Chai, X. J., Whitfield-Gabrieli, S., Shinn, A. K., Gabrieli, J. D. E., Castanon, A. N., McCarthy, J. M., Cohen, B. M., & Öngür, D. (2011). Abnormal medial prefrontal cortex Resting-State connectivity in bipolar disorder and schizophrenia. *Neuropsychopharmacology*, *36*(10), 2009–2017. https://doi.org/10.1038/npp.2011.88

Cho, F. S., Vainchtein, I. D., Voskobiynyk, Y., Morningstar, A. R., Aparicio, F., Higashikubo, B., Ciesielska, A., Broekaart, D. W. M., Anink, J. J., Van Vliet, E. A., Yu, X., Khakh, B. S., Aronica, E., Molofsky, A. V., & Paz, J. T. (2022). Enhancing GAT-3 in thalamic astrocytes promotes resilience to brain injury in rodents. *Science Translational Medicine*, *14*(652). https://doi.org/10.1126/scitranslmed.abj4310

Clemente-Perez, A., Makinson, S. R., Higashikubo, B., Brovarney, S., Cho, F. S., Urry, A., Holden, S. S., Wimer, M., Dávid, C., Fenno, L. E., Acsády, L., Deisseroth, K., & Paz, J. T. (2017). Distinct thalamic reticular cell types differentially modulate normal and pathological cortical rhythms. *Cell Reports*, *19*(10), 2130–2142. https://doi.org/10.1016/j.celrep.2017.05.044

Compte, A. (2006). Computational and in vitro studies of persistent activity: Edging towards cellular and synaptic mechanisms of working memory. *Neuroscience*, *139*(1), 135–151. https://doi.org/10.1016/j.neuroscience.2005.06.011

Compte, A., Constantinidis, C., Tegnér, J., Raghavachari, S., Chafee, M. V., Goldman-Rakic, P. S., & Wang, X. J. (2003). Temporally irregular mnemonic persistent activity in prefrontal neurons of monkeys during a delayed response task. *Journal of Neurophysiology*, *90*(5), 3441–3454. https://doi.org/10.1152/jn.00949.2002

Courtney, S., Petit, L., Maisog, J. M., Ungerleider, L. G., & Haxby, J. V. (1998). An area specialized for spatial working memory in human frontal cortex. *Science*, *279*(5355), 1347–1351. https://doi.org/10.1126/science.279.5355.1347

Delord, B. (1996). An intrinsic bistable mechanism in neocortical pyramidal neurons might be involved in the generation of sustained discharge patterns related to working memory. *CiNii Research*. https://cir.nii.ac.jp/crid/1571698599754806656

Delord, B. (2010). From intrinsic ionic conductances to temporal computations. *HDR*. https://www.semanticscholar.org/paper/RECHERCHES-(HDR)-FROM-INTRINSIC-IONIC-CONDUCTANCE-Delord/e84c030c73ea8c20405d36349febc43d0fd024d1

Delord, B., Klaassen, A. J., Burnod, Y., Costalat, R., & Guigon, E. (1997). Bistable behaviour in a neocortical neurone model. *Neuroreport*, *8*(4), 1019–1023. https://doi.org/10.1097/00001756-199703030-00040

Dembrow, N. C., Chitwood, R. A., & Johnston, D. (2010). Projection-Specific neuromodulation of medial prefrontal cortex neurons. *The Journal of Neuroscience*, *30*(50), 16922–16937. https://doi.org/10.1523/jneurosci.3644-10.2010

D'Esposito, M., Cooney, J. W., Gazzaley, A., Gibbs, S. E. B., & Postle, B. R. (2006). Is the Prefrontal Cortex Necessary for Delay Task Performance? Evidence from Lesion and fMRI Data. *Journal of the International Neuropsychological Society*, *12*(2), 248–260. https://doi.org/10.1017/s1355617706060322

Di Pietro, N. C., & Seamans, J. K. (2011). Dopamine and Serotonin Interactively Modulate Prefrontal Cortex Neurons In Vitro. *Biological Psychiatry*, *69*(12), 1204–1211. https://doi.org/10.1016/j.biopsych.2010.08.007

Egorov, A. V., Hamam, B., Fransen, E., Hasselmo, M. E., & Alonso, A. (2002). Graded persistent activity in entorhinal cortex neurons. *Nature*, *420*(6912), 173–178. https://doi.org/10.1038/nature01171

Fassihi, A., Akrami, A., Esmaeili, V., & Diamond, M. E. (2014). Tactile perception and working memory in rats and humans. *Proceedings of the National Academy of Sciences of the United States of America*, *111*(6), 2331–2336. https://doi.org/10.1073/pnas.1315171111

Fellous, J., Rudolph, M., Destexhe, A., & Sejnowski, T. J. (2003). Synaptic background noise controls the input/output characteristics of single cells in an in vitro model of in vivo activity. *Neuroscience*, *122*(3), 811–829. https://doi.org/10.1016/j.neuroscience.2003.08.027

Ferguson, B. R., Glick, C., & Huguenard, J. R. (2023). Prefrontal PV interneurons facilitate attention and are linked to attentional dysfunction in a mouse model of absence epilepsy. *eLife*, *12*. https://doi.org/10.7554/elife.78349

Fontanier, V., Sarazin, M., Stoll, F. M., Delord, B., & Procyk, E. (2022). Inhibitory control of frontal metastability sets the temporal signature of cognition. *eLife*, *11*. https://doi.org/10.7554/elife.63795

Fuster, J. M. (1988). Prefrontal Cortex. In *Comparative Neuroscience and Neurobiology* (pp. 107–109). Springer Science. https://link.springer.com/chapter/10.1007/978-1-4899-6776-3_43

Fuster, J. M., & Alexander, G. E. (1971). Neuron activity related to Short-Term memory. *Science*, *173*(3997), 652–654. https://doi.org/10.1126/science.173.3997.652

Fuster, J. M., Bauer, R. H., & Jervey, J. P. (1982). Cellular discharge in the dorsolateral prefrontal cortex of the monkey in cognitive tasks. *Experimental Neurology*, *77*(3), 679–694. https://doi.org/10.1016/0014-4886(82)90238-2

Fuster, J. M., & Jervey, J. P. (1982). Neuronal firing in the inferotemporal cortex of the monkey in a visual memory task. *The Journal of Neuroscience*, *2*(3), 361–375. https://doi.org/10.1523/jneurosci.02-03-00361.1982

Gao, X., Grendel, J., Muhia, M., Castro-Gomez, S., Süsens, U., Isbrandt, D., Kneussel, M., Kuhl, D., & Ohana, O. (2019). Disturbed Prefrontal Cortex Activity in the Absence of Schizophrenia-Like

Behavioral Dysfunction in *Arc/Arg3.1* Deficient Mice. *The Journal of Neuroscience*, *39*(41), 8149–8163. https://doi.org/10.1523/jneurosci.0623-19.2019

Gee, S. M., Ellwood, I. T., Patel, T., Luongo, F., Deisseroth, K., & Sohal, V. S. (2012). Synaptic activity unmasks dopamine D2 receptor modulation of a specific class of layer V pyramidal neurons in prefrontal cortex. *The Journal of Neuroscience*, *32*(14), 4959–4971. https://doi.org/10.1523/jneurosci.5835-11.2012

Genet, S., & Delord, B. (2002). A biophysical model of nonlinear dynamics underlying plateau potentials and calcium spikes in purkinje cell dendrites. *Journal of Neurophysiology*, *88*(5), 2430–2444. https://doi.org/10.1152/jn.00839.2001

Goldman, M. S. (2003). Robust Persistent Neural Activity in a Model Integrator with Multiple Hysteretic Dendrites per Neuron. *Cerebral Cortex*, *13*(11), 1185–1195. https://doi.org/10.1093/cercor/bhg095

Goldman-Rakic, P. S. (1995). Cellular basis of working memory. *Neuron*, *14*(3), 477–485. https://doi.org/10.1016/0896-6273(95)90304-6

González-Burgos, I., Fletes-Vargas, G., González-Tapia, D., González-Ramírez, M. M., Rivera-Cervantes, M., & Martínez-Degollado, M. (2012). Prefrontal serotonin depletion impairs egocentric, but not allocentric working memory in rats. *Neuroscience Research*, *73*(4), 321–327. https://doi.org/10.1016/j.neures.2012.05.003

Gross, S. A., Guzman, G. A., Wissenbach, U., Philipp, S. E., Zhu, M. X., Bruns, D., & Cavalie, A. (2009). TRPC5 is a Ca2+ -activated channel functionally coupled to Ca2+-selective ion channels. *J Biol Chem*, *284*(344), 23–32.

Gulledge, A. T., Bucci, D. J., Zhang, S. S., Matsui, M., & Yeh, H. H. (2009). M1 receptors mediate cholinergic modulation of excitability in neocortical pyramidal neurons. *The Journal of Neuroscience*, *29*(31), 9888–9902. https://doi.org/10.1523/jneurosci.1366-09.2009

Gulledge, A. T., & Jaffe, D. B. (2001). Multiple effects of dopamine on layer V pyramidal cell excitability in rat prefrontal cortex. *Journal of Neurophysiology*, *86*(2), 586–595. https://doi.org/10.1152/jn.2001.86.2.586

Gulledge, A. T., Park, S., Kawaguchi, Y., & Stuart, G. J. (2007). Heterogeneity of phasic cholinergic signaling in neocortical neurons. *Journal of Neurophysiology*, *97*(3), 2215–2229. https://doi.org/10.1152/jn.00493.2006

Haj-Dahmane, S., & Andrade, R. (1996). Muscarinic activation of a Voltage-Dependent cation nonselective current in Rat association cortex. *The Journal of Neuroscience*, *16*(12), 3848–3861. https://doi.org/10.1523/jneurosci.16-12-03848.1996

Haj-Dahmane, S., & Andrade, R. (1997). Calcium-Activated Cation nonselective current contributes to the fast afterdepolarization in rat prefrontal cortex neurons. *Journal of Neurophysiology*, *78*(4), 1983–1989. https://doi.org/10.1152/jn.1997.78.4.1983

Haj-Dahmane, S., & Andrade, R. (1998). Ionic mechanism of the slow afterdepolarization induced by muscarinic receptor activation in rat prefrontal cortex. *Journal of Neurophysiology*, *80*(3), 1197–1210. https://doi.org/10.1152/jn.1998.80.3.1197

Haj-Dahmane, S., & Andrade, R. (1999). Muscarinic receptors regulate two different calcium-dependent non-selective cation currents in rat prefrontal cortex. *European Journal of Neuroscience*, *11*(6), 1973–1980. https://doi.org/10.1046/j.1460-9568.1999.00612.x

Hasselmo, M. E. (2006). The role of acetylcholine in learning and memory. *Current Opinion in Neurobiology*, *16*(6), 710–715. https://doi.org/10.1016/j.conb.2006.09.002

Hillman, K. L., & Bilkey, D. K. (2012). Neural encoding of competitive effort in the anterior cingulate cortex. *Nature Neuroscience*, *15*(9), 1290–1297. https://doi.org/10.1038/nn.3187

Holden, S. S., Grandi, F. C., Aboubakr, O., Higashikubo, B., Cho, F. S., Chang, A., Osorio-Forero, A., Morningstar, A. R., Mathur, V., Kuhn, L. J., Suri, P., Sankaranarayanan, S., Andrews-Zwilling, Y., Tenner, A. J., Lüthi, A., Aronica, E., Corces, M. R., Yednock, T., & Paz, J. T. (2021). Complement factor C1q mediates sleep spindle loss and epileptic spikes after mild brain injury. *Science*, *373*(6560). https://doi.org/10.1126/science.abj2685

Inagaki, H., Fontolan, L., Romani, S., & Svoboda, K. (2019). Discrete attractor dynamics underlies persistent activity in the frontal cortex. *Nature*, *566*(7743), 212–217. https://doi.org/10.1038/s41586-019-0919-7

Jun, J., Miller, P., Hernandez, A., Zainos, A., Lemus, L., Brody, C. D., & Romo, R. (2010). Heterogenous population coding of a Short-Term Memory and Decision task. *The Journal of Neuroscience*, *30*(3), 916–929. https://doi.org/10.1523/jneurosci.2062-09.2010

Knierim, J., & Zhang, K. (2012). Attractor dynamics of spatially correlated neural activity in the limbic system. *Annual Review of Neuroscience*, *35*(1), 267–285. https://doi.org/10.1146/annurev-neuro-062111-150351

Koulakov, A. A., Raghavachari, S., Kepecs, A., & Lisman, J. (2002). Model for a robust neural integrator. *Nature Neuroscience*, *5*(8), 775–782. https://doi.org/10.1038/nn893

Lapish, C. C., Durstewitz, D., Chandler, L. J., & Seamans, J. K. (2008). Successful choice behavior is associated with distinct and coherent network states in anterior cingulate cortex. *Proceedings of the National Academy of Sciences of the United States of America*, *105*(33), 11963–11968. https://doi.org/10.1073/pnas.0804045105

Li, N., Daie, K., Svoboda, K., & Druckmann, S. (2016). Robust neuronal dynamics in premotor cortex during motor planning. *Nature*, *532*(7600), 459–464. https://doi.org/10.1038/nature17643

Loewenstein, Y., Mahon, S., Chadderton, P., Kitamura, K., Sompolinsky, H., Yarom, Y., & Häusser, M. (2005). Bistability of cerebellar Purkinje cells modulated by sensory stimulation. *Nature Neuroscience*, *8*(2), 202–211. https://doi.org/10.1038/nn1393

Machens, C. K., & Brody, C. D. (2008). Design of Continuous Attractor Networks with Monotonic Tuning Using a Symmetry Principle. *Neural Computation*, *20*(2), 452–485. https://doi.org/10.1162/neco.2007.07-06-297

Machens, C. K., Romo, R., & Brody, C. D. (2005). Flexible control of mutual inhibition: a neural model of Two-Interval discrimination. *Science*, *307*(5712), 1121–1124. https://doi.org/10.1126/science.1104171

Major, G., Polsky, A., Denk, W., Schiller, J., & Tank, D. W. (2008). Spatiotemporally graded NMDA Spike/Plateau potentials in basal dendrites of neocortical pyramidal neurons. *Journal of Neurophysiology*, *99*(5), 2584–2601. https://doi.org/10.1152/jn.00011.2008

Major, G., & Tank, D. W. (2004). Persistent neural activity: prevalence and mechanisms. *Current Opinion in Neurobiology*, *14*(6), 675–684. https://doi.org/10.1016/j.conb.2004.10.017

Miller, E. K., Nieder, A., Freedman, D. J., & Wallis, J. D. (2003). Neural correlates of categories and concepts. *Current Opinion in Neurobiology*, *13*(2), 198–203. https://doi.org/10.1016/s0959-4388(03)00037-0

Narayanan, N. S., & Laubach, M. (2006). Top-Down control of motor cortex ensembles by dorsomedial prefrontal cortex. *Neuron*, *52*(5), 921–931. https://doi.org/10.1016/j.neuron.2006.10.021

Narayanan, N. S., & Laubach, M. (2009). Delay Activity in Rodent Frontal Cortex During a Simple Reaction Time Task. *Journal of Neurophysiology*, *101*(6), 2859–2871. https://doi.org/10.1152/jn.90615.2008

Nieder, A., & Miller, E. K. (2004). A parieto-frontal network for visual numerical information in the monkey. *Proceedings of the National Academy of Sciences of the United States of America*, *101*(19), 7457–7462. https://doi.org/10.1073/pnas.0402239101

Nyberg, L. (2002). Levels of processing: A view from functional brain imaging. *Memory*, *10*(5–6), 345–348. https://doi.org/10.1080/09658210244000171

Paz, J. T., Bryant, A. S., Peng, K., Fenno, L. E., Yizhar, O., Frankel, W. N., Deisseroth, K., & Huguenard, J. R. (2011). A new mode of corticothalamic transmission revealed in the Gria4−/− model of absence epilepsy. *Nature Neuroscience*, *14*(9), 1167–1173. https://doi.org/10.1038/nn.2896

Paz, J. T., Davidson, T. J., Frechette, E., Delord, B., Parada, I., Peng, K., Deisseroth, K., & Huguenard, J. R. (2013). Closed-loop optogenetic control of thalamus as a tool for interrupting seizures after cortical injury. *Nature Neuroscience*, *16*(1), 64–70. https://doi.org/10.1038/nn.3269

Quentin, R., J, K., Sallard, E., Fishman, N., Thompson, R., Buch, E. R., & Cohen, L. G. (2019). Differential Brain Mechanisms of Selection and Maintenance of Information during Working Memory. *The Journal of Neuroscience*, *39*(19), 3728–3740. https://doi.org/10.1523/jneurosci.2764-18.2019

Ratté, S., Karnup, S., & Prescott, S. A. (2018). Nonlinear relationship between Spike-Dependent calcium influx and TRPC channel activation enables robust persistent spiking in neurons of the anterior cingulate cortex. *The Journal of Neuroscience*, *38*(7), 1788–1801. https://doi.org/10.1523/jneurosci.0538-17.2018

Rodriguez, G. (2017). Modélisation des bases neuronales de la mémoire de travail paramétrique dans le cortex préfrontal. *Ph.D. Thesis*. https://theses.hal.science/tel-01507598

Rodriguez, G., Sarazin, M., Clemente, A., Holden, S. S., Paz, J. T., & Delord, B. (2018). Conditional bistability, a generic cellular mnemonic mechanism for robust and flexible working memory computations. *The Journal of Neuroscience*, *38*(22), 5209–5219. https://doi.org/10.1523/jneurosci.1992-17.2017

Romo, R., Brody, C. D., Hernandez, A., & Lemus, L. (1999). Neuronal correlates of parametric working memory in the prefrontal cortex. *Nature*, *399*(6735), 470–473. https://doi.org/10.1038/20939

Rossetti, Z. L., & Carboni, S. (2005). Noradrenaline and dopamine elevations in the rat prefrontal cortex in spatial working memory. *The Journal of Neuroscience*, *25*(9), 2322–2329. https://doi.org/10.1523/jneurosci.3038-04.2005

Ruivo, L. M. T., Baker, K. L., Conway, M. W., Kinsley, P., Gilmour, G., Phillips, K. G., Isaac, J. T., Lowry, J., & Mellor, J. R. (2017). Coordinated Acetylcholine Release in Prefrontal Cortex and Hippocampus Is Associated with Arousal and Reward on Distinct Timescales. *Cell Reports*, *18*(4), 905–917. https://doi.org/10.1016/j.celrep.2016.12.085

Sarazin, M., Medernach, D., Naudé, J., & Delord, B. (n.d.). Biophysical control of neural trajectories under disordered brain dynamics. *Bioarxiv*. https://www.biorxiv.org/content/10.1101/2022.07.26.501548v1

Sarazin, M., Victor, J., Medernach, D., Naudé, J., & Delord, B. (2021). Online learning and memory of neural trajectory replays for prefrontal persistent and dynamic representations in the irregular asynchronous state. *Frontiers in Neural Circuits*, *15*. https://doi.org/10.3389/fncir.2021.648538

Satake, T., Mitani, H., Nakagome, K., & Kaneko, K. (2008). Individual and additive effects of neuromodulators on the slow components of afterhyperpolarization currents in layer V pyramidal cells of the rat medial prefrontal cortex. *Brain Research*, *1229*, 47–60. https://doi.org/10.1016/j.brainres.2008.06.098

Seamans, J. K., Floresco, S., & Phillips, A. G. (1995). Functional differences between the prelimbic and anterior cingulate regions of the rat prefrontal cortex. *Behavioral Neuroscience*, *109*(6), 1063–1073. https://doi.org/10.1037/0735-7044.109.6.1063

Seung, H. S., Lee, D. D., Reis, B. Y., & Tank, D. W. (2000). The Autapse: A Simple Illustration of Short-Term Analog Memory Storage by Tuned Synaptic Feedback. *Journal of Computational Neuroscience*, *9*(2), 171–185. https://doi.org/10.1023/a:1008971908649

Shafi, M. M., Zhou, Y., Quintana, J., Chow, C. C., Fuster, J. M., & Bodner, M. (2007). Variability in neuronal activity in primate cortex during working memory tasks. *Neuroscience*, *146*(3), 1082–1108. https://doi.org/10.1016/j.neuroscience.2006.12.072

Shouval, H. Z., & Gavornik, J. P. (2010). A single spiking neuron that can represent interval timing: analysis, plasticity and multi-stability. *Journal of Computational Neuroscience*, *30*(2), 489–499. https://doi.org/10.1007/s10827-010-0273-0

Sidiropoulou, K., Lu, F., Fowler, M., Xiao, R., Phillips, C., Ozkan, E. D., Zhu, M. X., White, F. J., & Cooper, D. (2009). Dopamine modulates an mGluR5-mediated depolarization underlying prefrontal persistent activity. *Nature Neuroscience*, *12*(2), 190–199. https://doi.org/10.1038/nn.2245

Silva, L. R., Amitai, Y., & Connors, B. W. (1991). Intrinsic oscillations of neocortex generated by layer 5 pyramidal neurons. *Science*, *251*(4992), 432–435. https://doi.org/10.1126/science.1824881

Šimić, G., Babić, M., Borovečki, F., & Hof, P. R. (2014). Early failure of the Default-Mode network and the pathogenesis of Alzheimer's disease. *CNS Neuroscience & Therapeutics*, *20*(7), 692–698. https://doi.org/10.1111/cns.12260

Stephens, E. K., Baker, A. L., & Gulledge, A. T. (2018). Mechanisms underlying serotonergic excitation of callosal projection neurons in the mouse medial prefrontal cortex. *Frontiers in Neural Circuits*, *12*. https://doi.org/10.3389/fncir.2018.00002

Tahvildari, B., Alonso, A., & Bourque, C. W. (2008). Ionic Basis of on and off Persistent Activity in Layer III Lateral Entorhinal Cortical Principal Neurons. *Journal of Neurophysiology*, *99*(4), 2006–2011. https://doi.org/10.1152/jn.00911.2007

Tegnér, J., Compte, A., & Wang, X. J. (2002). The dynamical stability of reverberatory neural circuits. *Biological Cybernetics*, *87*(5–6), 471–481. https://doi.org/10.1007/s00422-002-0363-9

Thuault, S., Malleret, G., Constantinople, C. M., Nicholls, R. E., Chen, I., Zhu, J., Panteleyev, A. A., Vronskaya, S., Nolan, M. F., Bruno, R. M., Siegelbaum, S. A., & Kandel, E. R. (2013). Prefrontal cortex HCN1 channels enable intrinsic persistent neural firing and executive memory function. *The Journal of Neuroscience*, *33*(34), 13583–13599. https://doi.org/10.1523/jneurosci.2427-12.2013

Thurley, K., Senn, W., & Lüscher, H. (2008). Dopamine increases the gain of the Input-Output response of rat prefrontal pyramidal neurons. *Journal of Neurophysiology*, *99*(6), 2985–2997. https://doi.org/10.1152/jn.01098.2007

Tricoire, L., Drobac, E., Tsuzuki, K., Gallopin, T., Picaud, S., Cauli, B., Rossier, J., & Lambolez, B. (2019). Bioluminescence calcium imaging of network dynamics and their cholinergic modulation in slices of cerebral cortex from male rats. *Journal of Neuroscience Research*. https://doi.org/10.1002/jnr.24380

Wang, X. J. (2001). Synaptic reverberation underlying mnemonic persistent activity. *Trends in Neurosciences*, *24*(8), 455–463. https://doi.org/10.1016/s0166-2236(00)01868-3

Wang, Z., & McCormick, D. A. (1993). Control of firing mode of corticotectal and corticopontine layer V burst-generating neurons by norepinephrine, acetylcholine, and 1S,3R- ACPD. *The Journal of Neuroscience*, *13*(5), 2199–2216. https://doi.org/10.1523/jneurosci.13-05-02199.1993

Williams, G. V., Rao, S. G., & Goldman-Rakic, P. S. (2002). The Physiological Role of 5-HT2AReceptors in Working Memory. *The Journal of Neuroscience*, *22*(7), 2843–2854. https://doi.org/10.1523/jneurosci.22-07-02843.2002

Wu, D., Deng, H., Xiao, X., Zuo, Y., Sun, J., & Wang, Z. (2017). Persistent Neuronal Activity in Anterior Cingulate Cortex Correlates with Sustained Attention in Rats Regardless of Sensory Modality. *Scientific Reports*, *7*(1). https://doi.org/10.1038/srep43101

Xu, P., Ai, C., Li, Y., Xing, X., & Lu, H. (2019). Medial prefrontal cortex in neurological diseases. *Physiological Genomics*, *51*(9), 432–442. https://doi.org/10.1152/physiolgenomics.00006.2019

Yan, H., Villalobos, C., & Andrade, R. (2009). TRPC channels mediate a muscarinic Receptor-Induced afterdepolarization in cerebral cortex. *The Journal of Neuroscience*, *29*(32), 10038–10046. https://doi.org/10.1523/jneurosci.1042-09.2009

Yang, S., Shi, Y., Wang, Q., Peng, J., & Li, B. (2014). Neuronal representation of working memory in the medial prefrontal cortex of rats. *Molecular Brain*, *7*(1). https://doi.org/10.1186/s13041-014-0061-2

Yi, F., Zhang, X., Yang, C. R., & Li, B. M. (2013). Contribution of dopamine D1/5 receptor modulation of Post-Spike/Burst afterhyperpolarization to enhance neuronal excitability of layer V pyramidal neurons in prepubertal rat prefrontal cortex. *PLOS ONE*, *8*(8), e71880. https://doi.org/10.1371/journal.pone.0071880

Yoon, J., Minzenberg, M., Ursu, S., Walters, R., Wendelken, C., Ragland, J. D., & Carter, C. S. (2008). Association of dorsolateral prefrontal cortex dysfunction with disrupted coordinated brain activity in schizophrenia: relationship with impaired cognition, behavioral disorganization, and global function. *American Journal of Psychiatry*, *165*(8), 1006–1014. https://doi.org/10.1176/appi.ajp.2008.07060945

Zhang, Z., & Arsenault, D. (2005). Gain modulation by serotonin in pyramidal neurons of the rat prefrontal cortex. *The Journal of Physiology*, *566*(2), 379–394. https://doi.org/10.1113/jphysiol.2005.086066

Zhang, Z., & Séguéla, P. (2010). Metabotropic induction of persistent activity in layers II/III of anterior cingulate cortex. *Cerebral Cortex*, *20*(12), 2948–2957. https://doi.org/10.1093/cercor/bhq043

Zhou, X., Qi, X. L., Douglas, K., Palaninathan, K., Kang, H. S., Buccafusco, J. J., Blake, D. T., & Constantinidis, C. (2011). Cholinergic modulation of working memory activity in primate prefrontal cortex. *Journal of Neurophysiology*, *106*(5), 2180–2188. https://doi.org/10.1152/jn.00148.2011

SUPPLEMENTAL TABLES

A **Action potential properties**

Neuronal type	Threshold (mV)	Amplitude (mV)	Half-duration (ms)	# cells
CB	-43.50 ± 1.26	70.25 ± 5.92	2.15 ± 0.26	4
M	-42.24 ± 0.40	68.80 ± 2.25	2.04 ± 0.08	25
Statistics	*n.s.	#n.s.	#n.s.	

B **Passive electric membrane properties**

Neuronal type	Vm (mV)	Rin (MΩ)	τm (ms)	Sag (%)	Cm (pF)	# cells
CB	-63.00 ± 1.73	206.25 ± 32.87	45.00 ± 5.18	25.59 ± 4.70	149.00 ± 56.82	4
M	-62.68 ± 0.65	210.20 ± 17.66	49.32 ± 3.06	23.33 ± 1.97	341.87 ± 43.60	25
Statistics	#n.s.	*n.s.	#n.s.	#n.s.	*n.s.	

Supplemental table 1. Action potential and passive membrane cell properties from neurons recorded in Fig. 1. A, *Active properties—i.e., action potential threshold, height, and half-duration—and* ***B,*** *passive properties—i.e., resting membrane potential, input resistance, membrane time constant, voltage sag, and membrane capacitance—of layer V mPFC neurons recorded in classical aCSF in the absence of neuromodulation (No NM, n = 29 cells / 3 rats). Note that conditional bistable (CB) and monostable (M) neurons have similar passive and active properties. Statistical comparison was assessed by unpaired t test (#n.s.) and nonparametric Mann-Whitney test (*n.s.).*

A **Action potential properties**

Neuromodulation condition	Threshold (mV)	Amplitude (mV)	Half-duration (ms)	T1 Rheobase (pA)	T2 Rheobase (pA)	# cells	# rats
No NM	-42.4 ± 0.4	69.0 ± 2.1	2.06 ± 0.08	41.4 ± 4.6	51.7 ± 5.2	29	3
5HT	-43.7 ± 0.6	68.6 ± 2.1	1.97 ± 0.07	52.7 ± 6.7	57.0 ± 7.9	27	2
DA	-42.7 ± 0.6	67.6 ± 2.0	2.06 ± 0.07	25.4 ± 1.9	28.1 ± 2.2	27	2
NA	-42.6 ± 0.5	69.1 ± 1.4	2.23 ± 0.08	38.3 ± 3.3	42.8 ± 3.6	29	3
ACh	-41.1 ± 0.6	66.1 ± 1.5	2.24 ± 0.09	34.0 ± 3.7	25.3 ±3.0	30	3
ACh+FFA	-42.7 ± 0.7	64.1 ± 2.0	2.51 ± 0.08	31.6 ± 3.8	30.0 ± 4.1	27	4
ANOVA, *post-hoc* Kruskal-Wallis	p=0.0413 (5HT vs. ACh)	n.s.	p=0.0027 (No NM vs. ACh+FFA) p=0.0002 (5HT vs. ACh+FFA) p=0.0060 (DA vs. ACh+FFA)	p=0.000004 (No NM T1 vs. T2) p=0.000061(ACh T1 vs. T2)			
Wilcoxon matched-pairs signed rank test							

B **Passive electric membrane properties**

Neuromodulation condition	Vm (mV)	Rin (MΩ)	τm (ms)	Sag (%)	Cm (pF)	# cells	# rats
No NM	-62.7 ± 0.6	208.8 ± 15.9	48.7 ± 2.7	31.6 ± 3.1	315.3 ± 40.1	29	3
5HT	-61.5 ± 0.7	240.3 ± 16.2	41.6 ± 3.0	16.2 ± 2.5	353.9 ± 44.9	27	2
DA	-60.7 ± 0.6	299.1 ± 19.4	68.7 ± 5.5	25.8 ± 2.1	336.5 ± 59.4	27	2
NA	-62.8 ± 0.8	260.3 ± 22.3	51.8 ± 3.7	24.0 ± 1.8	391.3 ± 50.9	29	3
ACh	-62.7 ± 0.9	290.8 ± 26.8	72.0 ± 4.9	26.1 ± 1.9	353.8 ± 55.8	30	3
ACh+FFA	-62.2 ± 1.0	349.5 ± 26.4	58.6 ± 5.1	20.5 ± 2.4	249.1 ± 53.4	27	4
ANOVA, *post-hoc* Kruskal-Wallis	n.s.	p=0.0187 (No NM vs. DA) p=0.0004 (No NM vs. ACh+FFA)	p=0.0085 (No NM vs. ACh) p=0.0003 (5HT vs. DA) p<0.0001 (5HT vs. ACh) p<0.0446 (NA vs. ACh)	p=0.0036 (No NM vs. 5HT) p=0.0399 (5HT vs. ACh)	n.s.		

Supplemental table 2. Action potential and passive membrane cell properties from neurons recorded in Fig. 1, 2, and 3. (related to Figs. 1-3). A*, Action potential properties in the absence of neuromodulation (No NM, n = 29 cells / 3 rats) and in presence of a serotonin receptor agonist (5-hydroxytryptamine, 5HT, n = 27 cells / 2 rats), a dopamine D1-like receptor agonist (SKF-81,297, DA, n = 27 cells / 2 rats), a noradrenaline receptor agonist (NA, n = 29 cells / 3 rats), a cholinergic receptor agonist (carbachol, ACh, n = 29 cells / 3 rats), and both carbachol and a non-selective cationic channel blocker, flufenamic acid (ACh+FFA, n = 27 cells / 4 rats). Action potential threshold, height and half-duration and the rheobase upon T1 and T2 stimulations were measured in the six neuromodulation conditions. Note the greater rheobase upon T2 (vs. T1) in absence of neuromodulation (No NM) and the lower rheobase upon T2 (vs. T1) in the presence of carbachol (ACh).* ***B****, Passive properties in the presence of No NM, 5HT, DA, NA, ACh, and ACh+FFA. The resting membrane potential (Vm), input resistance (Rin), membrane time constant (τm), voltage sag and membrane capacitance (Cm) were measured in the six neuromodulation conditions. Note the greater membrane time constant (vs. No NM, 5HT and NA) in the presence of carbachol (ACh).*

SUPPLEMENTAL FIGURES

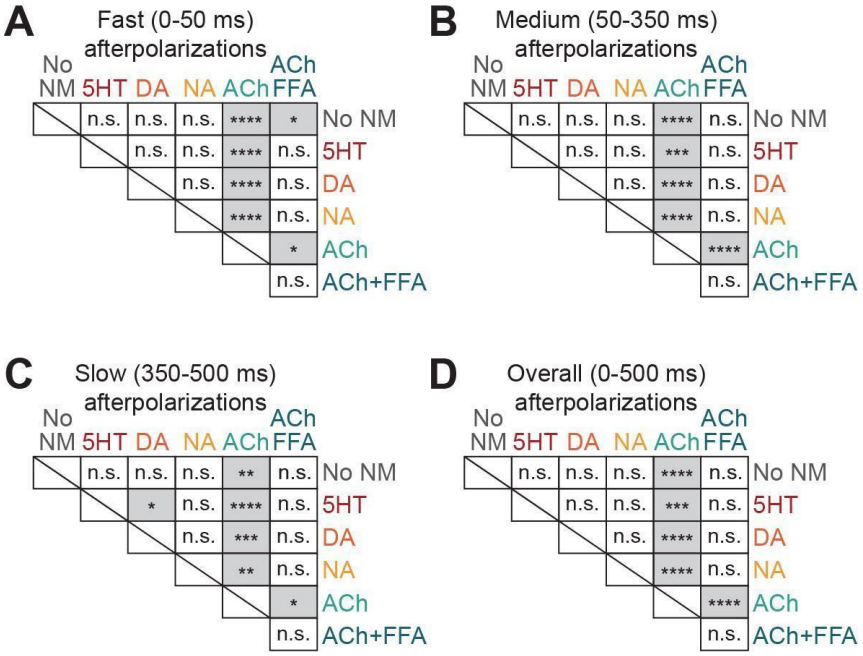

Supplemental Figure 1. Average membrane potential differences. A, *from 0 to 50 ms (fast after-polarizations);* ***B****, from 50 to 350 ms (medium after-polarizations);* ***C****, from 350 to 500 ms (slow after-polarizations); and* ***D****, from 0 to 500 ms (overall after-polarizations) after T2. Note the greater fast, medium, slow, and overall after-polarization in presence of carbachol (ACh). Statistical significance was assessed by Scheirer-Ray-Hare test and Wilcoxon Mann Whitney test for the post hoc analysis (****p<0.0001; ***p<0.001; **p<0.01; *p<0.05; n.s. non significant).*

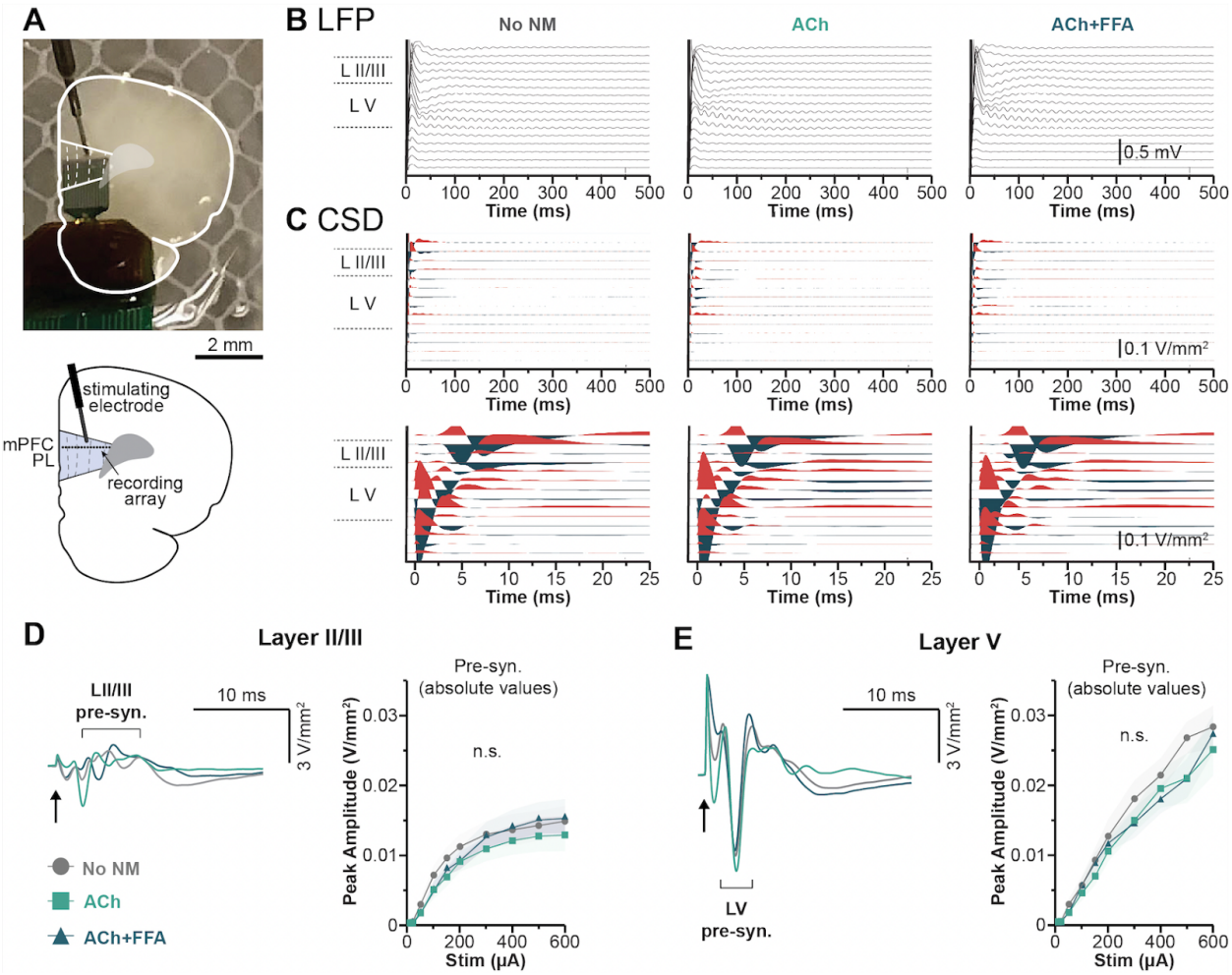

Supplementary Figure 2. Cholinergic modulation does not affect pre-synaptic activity in mPFC superficial and deep layers. A*, Experimental design of LFP recordings in mPFC slices (n = 12).* ***B****, Representative 500-ms-long local field potential (LFP, mV) recordings in response to a 500 µA electrical pulse in the absence of neuromodulation (No NM), and under ACh and ACh+FFA conditions.* ***C****, Representative 500-ms-long (Top) and 25-ms-long (Bottom) current source density (CSD, V/mm2) derived from the LFP recording (Ferguson et al., 2023). CSD traces #3 and #6 were used for layer II/III and layer V response quantification. Pre- and post-synaptic responses were identified using DNQX/APV and TTX (see Suppl. Fig. 3).* ***D****, Representative pre-synaptic response to a 500 µA electrical stimulation (black arrow) and peak amplitude curves (V/mm2) of the pre-synaptic response to electrical stimuli with increasing intensity in layer II/III. Statistical significance for each stimulus intensity was assessed by Repeated Measures Two-way ANOVA and Šidák test for post-hoc analysis (n.s. non significant).* ***E****, Same as E, in layer V.*

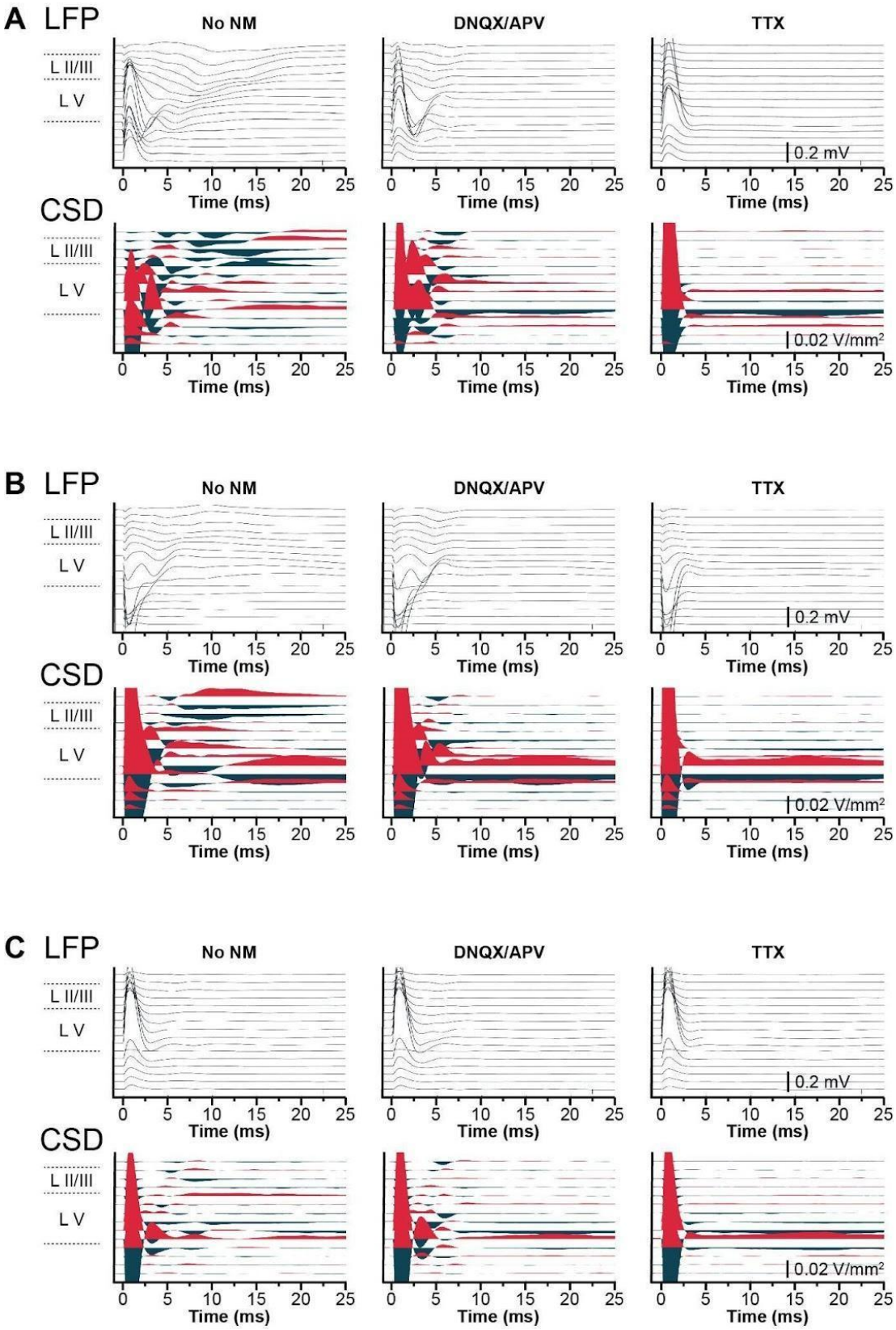
A
LFP
No NM
DNQX/APV
TTX
L II/III
L V
0.2 mV
CSD
L II/III
L V
0.02 V/mm²
Time (ms)
B
LFP
No NM
DNQX/APV
TTX
L II/III
L V
0.2 mV
CSD
L II/III
L V
0.02 V/mm²
Time (ms)
C
LFP
No NM
DNQX/APV
TTX
L II/III
L V
0.2 mV
CSD
L II/III
L V
0.02 V/mm²
Time (ms)

***Supplemental Figure 3 (previous page). DNQX/APV and TTX reduce, respectively, post- and pre-synaptic activity in the mPFC LFP recordings. A**, **B** and **C**, Three representative slices recorded in a classic aCSF, without neuromodulation (No NM, left), after addition of DNQX and APV (middle), and TTX (right). Top, Representative local field potential (LFP) recordings in response to a 0.1 ms 200 µA electrical pulse. Bottom, Representative current source density (CSD) traces (sinks in dark green and sources in red). Post-synaptic activity was determined by the reduction of the late CSD components by DNQX and APX, and pre-synaptic activity was determined by reduction of the fast CSD components following the stimulation by TTX. Data are shown as averages over 9 trials in each condition. These experiments served to identify evoked pre- and post-synaptic responses for CSD analysis in Fig. 5.*

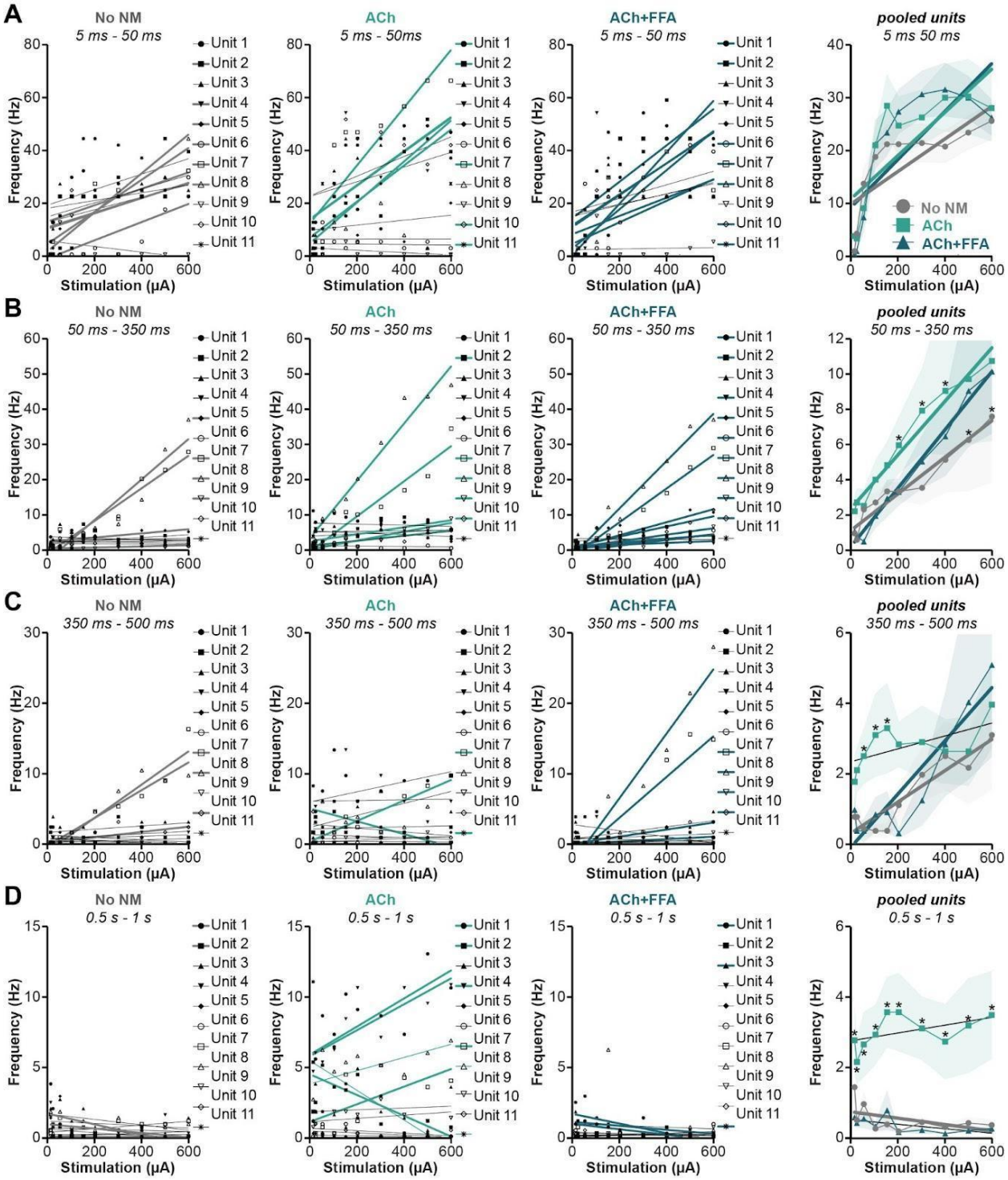

Supplementary Figure 4. Dependance of firing rate on the stimulus intensity in mPFC layer V during early periods. A, *Dependance of firing rate on the stimulus intensity of individual units in the No NM, ACh, and ACh+FFA conditions (three first panels) and of pooled units under the three conditions (last panel) in the 0-50 ms period following the stimulus. For individual units and pooled units, linear regressions were performed and a F test was applied to determine whether the slopes were statistically*

*different from zero (slopes different from zero are bold). For pooled units, statistical significance between conditions for each stimulus intensity was assessed by Repeated Measures Two-way ANOVA and Šidák test for post-hoc analysis (*p<0.05).* ***B****, Same as A for the 50-350 ms period.* ***C****, Same as A for the 350-500 ms period.* ***D****, Same as A for the 500-1000 ms period.*

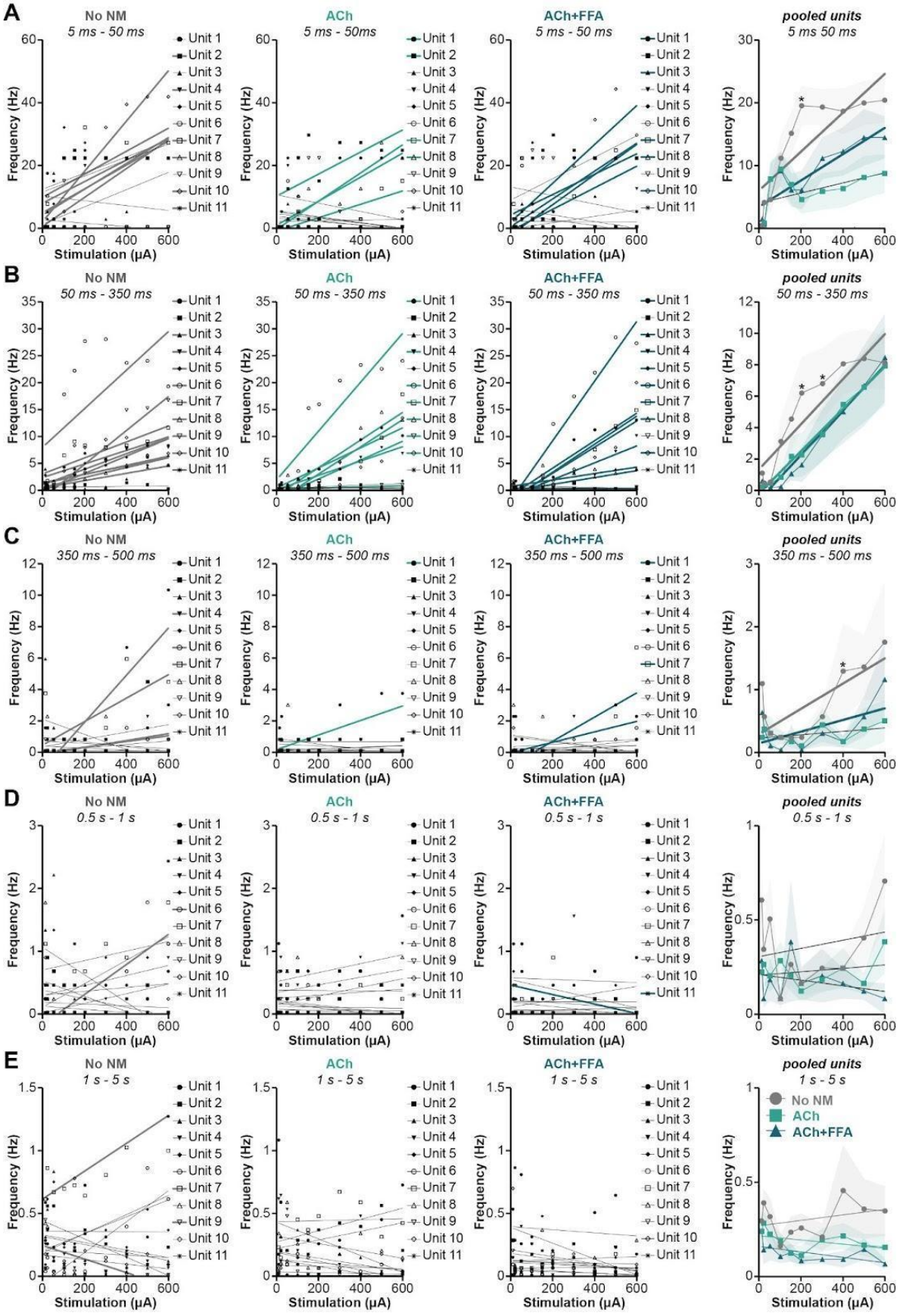
A
No NM
5 ms - 50 ms
ACh
5 ms - 50ms
ACh+FFA
5 ms - 50 ms
pooled units
5 ms 50 ms
B
No NM
50 ms - 350 ms
ACh
50 ms - 350 ms
ACh+FFA
50 ms - 350 ms
pooled units
50 ms - 350 ms
C
No NM
350 ms - 500 ms
ACh
350 ms - 500 ms
ACh+FFA
350 ms - 500 ms
pooled units
350 ms - 500 ms
D
No NM
0.5 s - 1 s
ACh
0.5 s - 1 s
ACh+FFA
0.5 s - 1 s
pooled units
0.5 s - 1 s
E
No NM
1 s - 5 s
ACh
1 s - 5 s
ACh+FFA
1 s - 5 s
pooled units
1 s - 5 s
Unit 1
Unit 2
Unit 3
Unit 4
Unit 5
Unit 6
Unit 7
Unit 8
Unit 9
Unit 10
Unit 11
Frequency (Hz)
Stimulation (µA)
No NM
ACh
ACh+FFA

Supplementary Figure 5 (previous page). Dependance of firing rate on the stimulus intensity in mPFC layers II/III during all periods. A, *Dependance of firing rate on the stimulus intensity of individual units in the No NM, ACh,, and ACh+FFA conditions (three first panels) and of pooled units under the three conditions (last panel) in the 0-50 ms period following the stimulus. For individual units and pooled units, linear regressions were performed and a F test was applied to determine whether the slopes were statistically different from zero (slopes different from zero are bold). For pooled units, statistical significance between conditions for each stimulus intensity was assessed by Repeated Measures Two-way ANOVA and Šidák test for post-hoc analysis (*p<0.05).* ***B****, Same as A for the 50-350 ms period.* ***C****, Same as A for the 350-500 ms period.* ***D****, Same as A for the 0.5-1 s period.* ***E****, Same as A for the 1-5 s period.*

CHAPTER II

Pathological disruption of the mechanisms underpinning parametric working memory in the prefrontal cortex

I. Alzheimer's disease and aging affect conditional bistability in mice

A. Summary

Alzheimer's disease (AD) is the most common type of dementia (Holtzman et al., 2011). One of the earliest symptoms of AD is the loss of working memory (Saunders and Summers, 2009; Kessels et al., 2010), the capacity to maintain transient information for seconds to minutes (Baddeley et al., 1991). Working memory can be disrupted as a normal part of aging (Murman, 2015). Although object and spatial working memory have been extensively studied (Burke and Barnes, 2006; Kessels et al., 2010; Klencklen et al., 2012; Murman, 2015; Kronovsek et al., 2021), parametric working memory, which allows memorization of quantitative information (Romo et al., 1999; Brody et al., 2003; Nieder and Miller, 2004; Fassihi et al., 2014), has remained less elusive. Previous modeling and experimental work show that, to emerge *in vivo*, parametric working memory requires synaptic reverberation in recurrent networks and conditional bistable neurons in the prefrontal cortex (Rodriguez et al., 2018; Leroux et al., manuscript #1). Conditional bistability, a form of cellular intrinsic memory that requires contextual inputs to memorize events and depends on the cholinergic modulation of calcium-activated non-selective cationic channels, might constitute the bistability required in parametric working memory (Leroux et al., manuscript #1). Here, we used the 5xFAD mouse model of AD and wild-type littermates, to investigate conditional bistability at two, six, and 12 months of age. Using patch-clamp electrophysiology, we found that, in layer V pyramidal neurons of the prefrontal cortex, conditional bistability is similar in two-months old 5xFAD and WT mice, but reduced in 5xFAD mice at six months of age, whereas in WT mice, conditional bistability only declines at 12 months of age. These results show that conditional bistability is lost earlier in mice modeling AD, and suggest that, like object and spatial working memory, parametric mnemonic capacities may be affected early in AD.

B. Contributions to the project

Research concept development was done by Morgane Leroux, Jeanne Paz, and Bruno Delord. Experimental design was done by Morgane Leroux and Jeanne Paz. Electrophysiological recordings were done by Morgane Leroux. Data analysis was done by Morgane Leroux, David Medernach, Jeanne Paz, and Bruno Delord. Writing was done by Morgane Leroux, Bruno Delord, and Jeanne Paz.

C. Manuscript #2. Neuronal conditional bistability is impaired in a mouse model of Alzheimer's disease and in aging

Neuronal conditional bistability is impaired in a mouse model of Alzheimer's disease and in aging

Leroux MA[1,2,3,4], DeNittis V[1,2], Ford JB[1,2], Medernach D[3], Necula D[1,2,5], Delord B[2,3 #&], Paz JT[1,4,5,6 #&]

Affiliations:

[1]Gladstone Institute of Neurological Disease, Gladstone Institutes, San Francisco CA 94158, USA

[2]The Kavli Institute for Fundamental Neuroscience, and Neurology Department, University of California San Francisco, San Francisco CA 94158, USA

[3]Institut des Systèmes Intelligents et de Robotique (ISIR), Sorbonne University, 4 Place Jussieu, 75005 Paris, France

[4]Brain-Cognition-Behavior Graduate Program, Sorbonne University, 4 Place Jussieu, 75005 Paris, France, Paris, France

[5]Neuroscience Graduate Program, University of California, San Francisco, San Francisco, CA 94158, USA

[&]Co-senior authors. Equally contributed to the supervision of this project

[#]Correspondence to:

jeanne.paz@gladstone.ucsf.edu

bruno.delord@sorbonne-universite.fr

Keywords: Conditional bistability, Prefrontal cortex, Pyramidal neurons, Intrinsic excitability, Electrophysiology, Alzheimer's disease, Aging

Funding: This project was funded mainly by the National Science Foundation (NSF) CRCNS grant #1608236 (to JTP) and ANR (to BD). During the study, JTP was also supported by NIH/NINDS grant R01NS096369, DoD grant EP150038, Gladstone Institutes, the Michael Prize, and the Kavli Institute for Fundamental Neuroscience. MAL was supported by the Weill Institute Research Support for Female Learners Impacted by COVID-19 Funding, the Gladstone Institutes,and a FoxG1 Research Fellowship.

Author contributions: Funding acquisition, BD and JTP; Concept Development, MAL, BD and JTP; Experimental Design, MAL, DM, BD and JTP; Electrophysiological Recordings, MAL and VD; Data Analysis, MAL, JBF, DN, DM, BD, JTP; Supervision, JTP supervised

electrophysiological recordings and data analysis; Writing, MAL, BD, JTP. Manuscript editing: all authors.

Competing interests: The authors declare no competing interests.

Data and materials availability: All data and materials described in the manuscript or supplementary materials will be made available upon request.

Acknowledgements: We thank Irene Lew for help with animal husbandry, and Francoise Chanut for critical review of the manuscript.

ABSTRACT

Alzheimer's disease (AD) is the most common type of dementia. One of the earliest symptoms of AD is the loss of working memory, the capacity to maintain transient information for seconds to minutes. Working memory can be disrupted as a normal part of aging. Although object and spatial working memory have been extensively studied, parametric working memory, which allows memorization of quantitative information, has remained less elusive. Previous modeling and experimental work show that, to emerge *in vivo*, parametric working memory requires synaptic reverberation in recurrent networks and conditional bistable neurons in the prefrontal cortex. Conditional bistability, a form of cellular intrinsic memory that requires contextual inputs to memorize events and depends on the cholinergic modulation of calcium-activated non-selective cationic channels, might constitute the bistability required in parametric working memory. Here, we used the 5xFAD mouse model of AD and wild-type littermates, to investigate conditional bistability at two, six, and 12 months of age. Using *patch-clamp* electrophysiology, we found that, in layer V pyramidal neurons of the prefrontal cortex, conditional bistability is similar in two-months old 5xFAD and WT mice, but reduced in 5xFAD mice at six months of age, whereas in WT mice, conditional bistability only declines at 12 months of age. These results show that conditional bistability is lost earlier in mice modeling AD, and suggest that, like object and spatial working memory, parametric mnemonic capacities may be affected early in AD.

INTRODUCTION

Alzheimer's disease (AD) is a progressive neurodegenerative disease that represents 60 to 70% of all dementia cases worldwide (Holtzman et al., 2011). AD currently impacts an estimated 44 million people worldwide, and by 2050, this number is projected to double (Dumurgier and Sabia, 2020). Although the effects of AD on loss of long-term memory have been extensively investigated (Carlesimo and Oscar-Berman, 1992; Fleischman and Gabrieli, 1999), one of the first symptoms to manifest in AD is loss of working memory (WM; Baddeley et al., 1991; Saunders and Summers, 2009; Kessels et al., 2010), that can also occur late in life during aging (Murman, 2015).

WM is the fundamental ability to retain and manipulate transient information (Fuster and Alexander, 1971). Various studies have characterized AD- and, more generally, age-related changes in different types of WM, such as object and spatial WM (Burke and Barnes, 2006; Kessels et al., 2010; Klencklen et al., 2012; Murman, 2015; Kronovsek et al., 2021), but to our knowledge, the effects of AD and aging on parametric working memory (PWM) are still unknown. PWM retains quantitative information such as numbers, the amplitude of a sound, or the size of an object (Romo et al., 1999; Brody et al., 2003; Nieder and Miller, 2004; Fassihi et al., 2014).

An example of PWM would be the comparison of two sounds: a sound from a surrounding street characterized by a low amplitude and the firefighter's engine siren characterized by a high amplitude. The brain is able to compare the two sounds in a few hundreds of milliseconds or seconds, in order to send information to the body to move to leave the way clear for the coming firefighters. Thus, people with impairments in PWM can experience life-threatening situations contributing to losing the ability to live independently (Smebye et al., 2015). Although treating PWM loss would not prevent AD or aging, it would greatly improve the quality of life of elderly people and AD patients. This is all the more important since, like we said, WM loss is one of the first symptoms in AD (Saunders and Summers, 2009; Kessels et al., 2010). However, there is currently no treatment to slow down or treat PWM loss, mainly because of a poor understanding of the cellular mechanisms underlying PWM.

PWM is characterized by the emergence of graded persistent activity (GPA), the ability of cortical networks to self-maintain levels of activity that monotonously scale with the cue parameter to be remembered, in the prefrontal cortex (PFC; Major and Tank, 2004). Modeling studies suggested that GPA arises from synaptic reverberation of activity within recurrent networks such as those found in the PFC, provided they are endowed with bistable units (Koulakov et al., 2002; Goldman, 2003). However, in these models, GPA needed systematic fine-tuning of synaptic weights and/or the activation function—i.e., the frequency/intensity (F/I) curve—of individual neurons on the order of 1%, much below the ordinary accuracy of plastic and/or regulatory signaling processes at work in neurons. Because these models are unrealistic on a WM plasticity point of vue, we proposed that GPA may arise in the PFC, without fine-tuning of the parameters, if the networks are endowed with conditional bistable (CB) neurons (Rodriguez et al., 2018). CB is an intrinsic property and a novel form of spike-mediated bistability, which allows cellular memorization of supra-threshold events through self-sustained spiking, in the presence of sub-threshold contextual inputs (Rodriguez et al., 2018).

In animals performing a PWM task, the triggering event is the quantitative information to remember and the tonic pulse arises from background synaptic inputs due to persistent activity reverberating within recurrent networks of the PFC, or of functionally connected neural structures, to maintain information about the memorized information, or to ongoing motivational, attentional, anticipatory, or executive aspects of WM processes. Using electrophysiological tools, our team recently demonstrated for the first time that CB exists in the layer V of the medial PFC (mPFC) in healthy two month-old rats (Leroux et al., manuscript #1). We performed an exhaustive neuromodulation study and showed that CB is mildly impacted by serotonergic, dopaminergic, and adrenergic modulation, while it is heavily modulated by acetylcholine via the activation of muscarinic 1 (M1)-type receptors (Leroux et al., manuscript #1). In addition, and as predicted by the theoretical modeling work (Rodriguez et al., 2018), using electrophysiology, we demonstrated that CB is mediated by cholinergic up-regulation and spike-mediated (Ca^{2+}) activation of calcium-activated non-selective cationic (CAN) channels. Importantly, we were able to record *in vitro* collective activity that resembles GPA in laver V mPFC networks, and we showed that its emergence also depends on the activation of M1 receptors and CAN channels (Leroux et al., manuscript #1), suggesting that CB may constitute the form of bistability required for GPA.

These results on the neuronal mechanisms underlying PWM (Leroux et al., manuscript #1) and the importance and precocity of WM loss in AD patients (Saunders and Summers, 2009; Kessels et al., 2010) lead us to question whether CB is affected in AD in an age-dependent manner, as the cholinergic system is disrupted in AD patients (Bowen et al., 1976; Whitehouse et al., 1982; Rylett et al., 1983; Nilsson et al., 1986). Particularly, it has been shown that soluble Aβ oligomers downregulate post-synaptic M1R function and lead to the loss of M1R proteins in the human post-mortem AD cortex (Yi et al., 2020). To investigate whether CB is down-regulated in AD, we used the 5xFAD mouse model of AD (Oakley et al., 2006) that is characterized by cholinergic M1 receptor function impairment starting six months of age (Yi et al., 2020) and recapitulates most of AD symptoms known to this date in an accelerated manner: amyloid plaque deposition starts at two months of age (Oakley et al., 2006; Canter et al., 2019; Oblak et al., 2021), synaptic degeneration starts at four months of age (Oakley et al., 2006), WM impairment starts at four months of age (Oakley et al., 2006) and worsens with age (Creighton et al., 2019), neuronal loss becomes significant at nine months of age (Oakley et al., 2006), and long-term memory impairment is detected at 12 months of age (Quintanilla-Sánchez et al., 2023). To investigate potential differences in CB between 5xFAD and wild-type (WT) littermates, we performed patch-clamp recordings of the pyramidal neurons from the mPFC layer V of 5xFAD and WT littermate mice at two, six, and 12 months of age. First, we showed that mPFC pyramidal neurons from healthy two month-old mice exhibit cholinergic-dependent CB when stimulated using the *bistability* protocol we previously devised (Leroux et al., manuscript #1). Second, we showed that, in WT mice, CB also correlates with the activation of fast and slow after-depolarizations (ADP), which are underlied by fast and slow CAN conductances. Third, we found that CB is impaired in aging at 12 months of age in WT mice compared with two and six months-old WT mice. Fourth, we found that CB is impaired earlier (at six-months of age) in 5xFAD mice modeling AD. Altogether, our study pinpoints the critical time window between two and six months in 5xFAD mice during which the neuronal mechanisms responsible for CB are disrupted.

METHODS

Experimental animal model

We performed all experiments per protocols approved by the Institutional Animal Care and Use Committee at the University of California, San Francisco and Gladstone Institutes. Precautions were taken to minimize stress and the number of animals used in each set of experiments. Male 5xFAD (#034848-JAX) and C57BL/6J control wild-type littermate mice were used for these experiments and ages ranged between two and 12 months.

Slice preparation

Mice were euthanized with 4 % isoflurane, perfused with ice-cold cutting solution containing 234 mM sucrose, 11 mM glucose, 2.5 mM KCl, 1.25 mM NaH_2PO_4, 10 mM $MgSO_4$, 0.5 mM $CaCl_2$ and 26 mM $NaHCO_3$ equilibrated with 95 % O_2 and 5 % CO_2, pH 7.4, and decapitated. We prepared 250 µm-thick coronal slices containing the mPFC with a Leica VT1200 microtome (Leica Microsystems). We incubated the slices, initially at 32 °C for 30 minutes and then at room temperature, in artificial cerebro-spinal fluid (aCSF) containing 126 mM NaCl, 2.5 mM KCl, 1.25 mM NaH_2PO_4, 1 mM $MgSO_4$, 2 mM $CaCl_2$, 26 mM $NaHCO_3$, and 10 mM glucose, equilibrated with 95 % O_2 and 5 % CO_2, pH 7.4 as described (Paz et al., 2011, Paz et al., 2013, Clemente-Perez et al., 2017, Cho et al., 2017; Holden et al., 2021, Cho et al., 2022).

Patch-clamp electrophysiology

Recordings were performed as previously described (Paz et al., 2011, Paz et al., 2013, Clemente-Perez et al., 2017, Holden et al., 2021, Cho et al., 2022). We visually identified neurons in the layer V of the mPFC by differential contrast optics with an Olympus microscope (60x objective, NA 1.1, WD 1.5 mm; SKU 1-U2M592). Recording electrodes made of borosilicate glass had a resistance of 2.5-4 MΩ when filled with intracellular solution that contained 10 mM HEPES, 11 mM EGTA, 120 mM K-Gluconate, 11 mM KCl, 1 mM $MgCl_2$ and 1 mM $CaCl_2$, pH adjusted to 7.4 with KOH (290 mOsm). Access resistance was monitored in all the recordings, and cells were included only if the access resistance was lower than 30 MOhm and the change of resistance was lower than 20% over the course of the experiment. We corrected offline the potentials for -15 mV liquid junction potential. All intrinsic and firing properties were recorded in the presence of the synaptic blocker kynurenic acid (2 mM, Sigma) diluted in aCSF.

Neuromodulator application

To test the contribution of cholinergic modulation, acetylcholine (ACh) muscarinic 1 receptor agonist carbamylcholine, commonly called carbachol (10µM, Sigma) was diluted in aCSF.

Identification of conditional bistable neurons

We used a *bistability* protocol derived from our previous modeling study (Rodriguez et al., 2018) and experimental study (Leroux et al., manuscript #1) to classify mPFC pyramidal layer V neurons, according to their type of spiking activity and specifically determine whether they were conditional bistable (CB) neurons, or not. In the *bistability* protocol, we injected intracellular current steps of increasing amplitude to establish firing frequency/current intensity (F/I) curves. We extracted the threshold (or rheobase) of each F/I curve—i.e., the lowest injected current eliciting stable spiking referred to as "θ" in this paper. The *bistability* protocol actually incorporated two protocols from which two F/I curves were built and compared. These two protocols included: 1) a protocol referred to as "Tonic 1" (T1), consisting of a 5250 ms current pulse, and 2) a protocol referred to as 'Phasic/Tonic 2' (PT2), consisting of a 5000 ms "tonic" (T2) current pulse immediately preceded by a brief (250 ms) "phasic" (P) current pulse of supra-threshold intensity chosen to generate a 30-Hz spiking rate. The *bistability* stimulation protocol was the same as described in Leroux et al. manuscript #1, and the same method was applied to identify CB neurons. Please, refer to the previous paper (Leroux et al., manuscript #1) for details.

Quantification of after-polarization potentials

The same method to quantify after-polarization potentials as the one described in Leroux et al. (manuscript #1). Briefly, we measured a potential difference after spiking which can be interpreted as the following. Positive differences correspond to the presence of currents underlying after-depolarizations (ADP; i.e., depolarizations of the membrane potential following T2) and negative differences to currents underlying after-hyperpolarizations (AHP; i.e., hyperpolarizations of the membrane potential attributable to T2). Please, refer to the previous paper (Leroux et al., manuscript #1) for more Method details.

Quantification and Statistical analyses

All numerical values are given as means and error bars are standard error of the mean (SEM) unless stated otherwise. Data analysis was performed with MATLAB (SCR_001622) and GraphPad Prism 7 (SCR_002798). Passive membrane and active electrical properties of the recorded neurons were assessed by non-parametric one-way ANOVA test and Kruskal-Wallis test for *post-hoc* analysis. Differences between T1 (θ_{OFF}) and T2 (θ_{ON}) rheobases in each neuromodulation condition were assessed by Wilcoxon matched-pairs signed rank test. Percentage of CB neurons recorded in different genotypes, ages, and neuromodulation conditions were compared using Chi 2 test with application of the Bonferroni correction (Q = 10%). Fast, medium, and slow after-polarizations (ADP and AHP) were assessed using Scheirer-Ray-Hare test and Wilcoxon Mann Whitney test for *post-hoc* analysis.

RESULTS

Neuronal conditional bistability in layer V mouse mPFC pyramidal neurons

To determine the existence of conditional bistability (CB) in mice, we performed whole-cell patch-clamp experiments on acute coronal mPFC slices from young adult (two month-old) mice. Neurons were visually identified as layer V pyramidal neurons, and the *bistability* protocol was applied as described in Leroux et al. (manuscript #1). The protocol aimed to evaluate the ability of recorded neurons to exhibit CB, meaning a mnemonic activity in the form of a stable state of self-sustained—i.e., persistent—spiking, following a phasic supra-threshold current pulse (P) mimicking a synaptic barrage associated with a behavioral event (e.g., perception, decision-making, or motor response).

In our devised *bistability* protocol (Leroux et al., manuscript #1), neurons were subjected to sweeps consisting of two successive stimulations to compare their spiking behavior in two conditions: 1) a tonic current pulse alone (T1), which represents the contextual reverberative activity in the networks, and 2) a combined stimulation where the P phasic current pulse was preceded by a tonic pulse of similar intensity (T2). We created two frequency/intensity curves using these sweeps with rising tonic intensity values, and we determined the spiking thresholds θ_{OFF} and θ_{ON} (rheobases) obtained, respectively, upon T1 and T2 stimulations. Then, the difference between these thresholds, $\Delta\theta = \theta_{OFF} - \theta_{ON}$, enabled the classification of neurons based on their stability type. In a monostable neuron (Rodriguez et al., 2018), the threshold for initiating a discharge upon T2, θ_{ON}, is similar or bigger than the threshold for initiating a discharge upon T1, θ_{OFF}. In this case, $\Delta\theta = 0$. In a CB neuron (Rodriguez et al., 2018), the threshold for initiating a discharge upon T2, θ_{ON}, is smaller than the threshold for initiating a discharge upon T1, θ_{OFF}. In this case, $\Delta\theta > 0$.

In our previous experimental study, we demonstrated that CB exists in the pyramidal neurons of the mPFC in healthy two month-old rats (Leroux et al., manuscript #1). To investigate whether mouse pyramidal neurons also exhibit such intrinsic property allowing cellular memorization of events, we examined the presence of CB in two month-old control mice (WT) using aCSF medium without any neuromodulator (referred to as the No NM condition). By applying the *bistability* protocol to mPFC neurons recorded in this condition, we observed that, on average, θ_{OFF} (θ measured upon T1) was lower than θ_{ON} (θ measured upon T2; Fig. 1A.; $p = 0.0011$, Wilcoxon matched-pairs signed rank test). Therefore, the spiking frequency of the neurons decreased when a supra-threshold P pulse was administered before the tonic pulse. Consequently, the majority of neurons were classified as monostable (M; Fig. 1B). However, we identified that a proportion of neurons exhibited CB (Fig. 1B; 38%), which we refer to as CB neurons. Passive and spike properties were comparable in CB and M neurons (Supplementary table 1). Therefore, this result is consistent with a previous study demonstrating the existence of neurons displaying persistent activity in standard conditions in the mouse mPFC (Thuault et al., 2013) and shows that CB is an ubiquitous property in rodents (Leroux et al., manuscript #1).

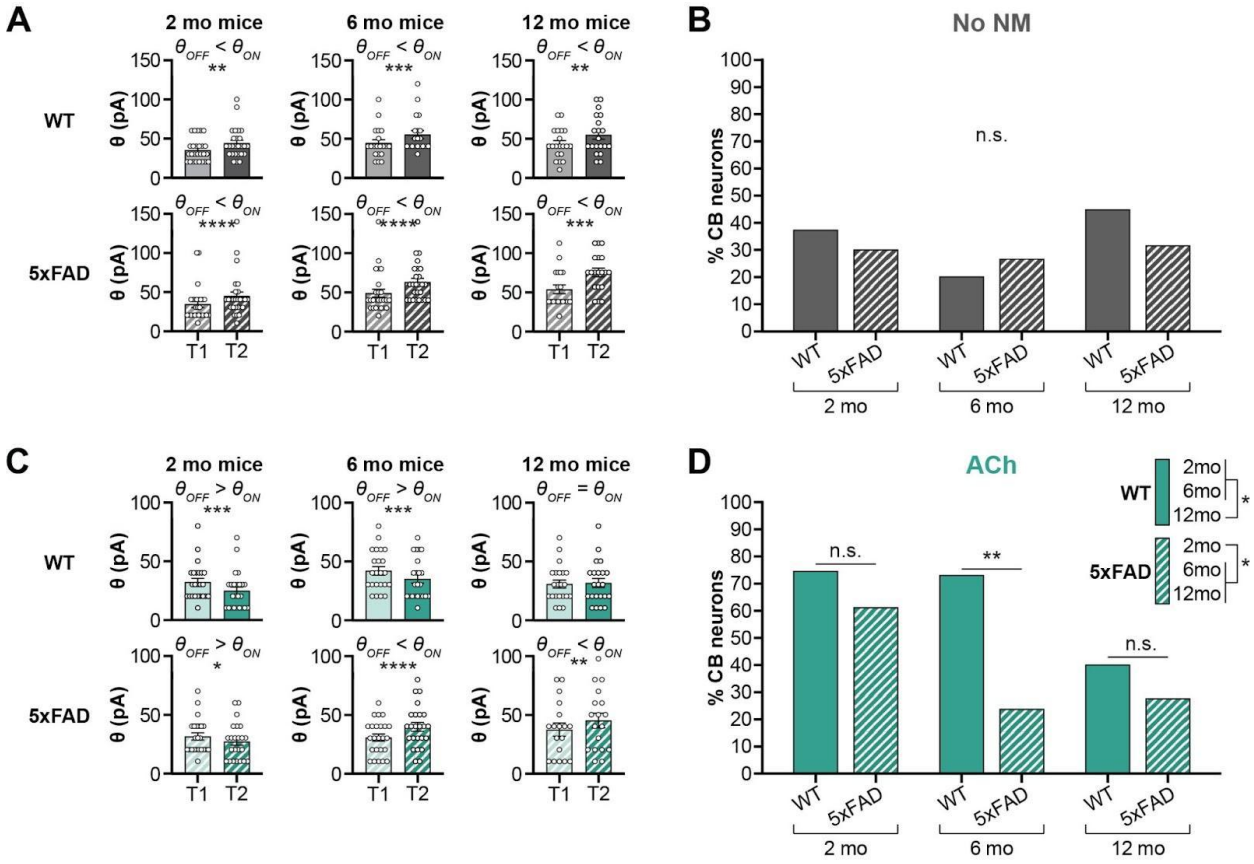

Figure 1. Conditional bistability is modulated by acetylcholine via the activation of M1-type receptors and is impaired earlier in 5xFAD mice compared to wild-type littermates. A*, Thresholds for firing of neurons upon T1 (θ_{OFF}) and T2 (θ_{ON}) in absence of neuromodulation (No NM). Rheobase statistical significance was assessed by Wilcoxon matched-pairs signed rank test analysis (**p<0.01; ***p<0.001; ****p<0.0001; n.s. non significant). 2mo WT, n=26 cells/4 mice; 2mo 5xFAD, n=27 cells/4 mice; 6mo WT, n=22 cells/3 mice; 6mo 5xFAD, n=26 cells/3 mice; 12mo WT, n=20 cells/2 mice; 12mo 5xFAD, n=19 cells/3 mice. **B**, Fractions of monostable (M) and conditional bistable (CB) neurons recorded in absence of neuromodulation (No NM). Statistical significance was assessed by chi 2 test with Bonferroni-Sudak correction (n.s. non significant). **C**, Thresholds for firing of neurons upon T1 (θ_{OFF}) and T2 (θ_{ON}) under neuromodulation by carbachol (ACh). Statistical significance was assessed by Wilcoxon matched-pairs signed rank test analysis (****p<0.0001; ***p<0.001; **p<0.01; *p<0.05; n.s. non significant). 2mo WT, n=24 cells/3 mice; 2mo 5xFAD, n=23 cells/3 mice; 6mo WT, n=23 cells/3 mice; 6mo 5xFAD, n=24 cells/3 mice; 12mo WT, n=22 cells/3 mice; 12mo 5xFAD, n=18 cells/4 mice. **D**. Fractions of M and CB neurons recorded in presence of carbachol (ACh). Statistical significance was assessed by chi 2 test with Bonferroni-Sudak correction (*p<0.05; **p<0.01; n.s. non significant).*

Conditional bistability is enhanced by cholinergic modulation via muscarinic M1 receptor

The impact of cholinergic neuromodulation on working memory has been established in previous studies in mice (Ruivo et al., 2017). Acetylcholine (ACh) also up-regulates self-sustained spiking in the rodent mPFC (Haj-Dahmane and Andrade, 1996, 1998, 1999; Zhang et Seguela, 2010; Thuault et al., 2013; Ratté et al., 2018). To investigate whether cholinergic stimulation affects CB, and specifically in mice, we conducted experiments with the M1-type muscarinic agonist carbachol (referred to as the ACh condition) in two month-old WT mice. By applying the *bistability* protocol in the presence of carbachol, we observed that, overall, θ_{ON} was lower than θ_{OFF} (Fig. 1C; p=0.0006, Wilcoxon matched-pairs signed rank test). Therefore, in the presence of muscarinic modulation, triggered self-sustained spiking was up-regulated. Consistently, the fraction of recorded CB neurons was greater in the presence of the ACh agonist (Fig. 1D, 75%) compared to No NM (adjusted p=0.0153, Chi 2 test with Bonferroni correction). These findings demonstrate that cholinergic modulation through M1-type receptors (M1 R) strongly facilitates CB in mice, as demonstrated in rats (Leroux et al., manuscript #1).

Decline in conditional bistability occurs with aging and is accelerated in 5xFAD mice

To test whether CB is affected by aging in WT and 5xFAD mice, we conducted experiments without neuromodulation (No NM) and in presence of carbachol (ACh) in mice of two, six, and 12 months of age. When measured without neuromodulation, no effect of genotype or age on $\Delta\theta$ (Fig. 1A), nor the fraction of CB neurons recorded (Fig. 1B) was observed, and no difference in passive membrane (Table 1, top) nor action potential (Table 2, top) properties were measured. These observations suggest that CB is not impacted by the genotype or the age of the mice when the recordings are not performed under cholinergic modulation.

Passive electric membrane properties

NM condition	Age (mo)	Genotype	Vm (mV)	Rin (MΩ)	τm (ms)	Sag (%)	Cm (pF)	# cells	# mice
No NM	2	WT	-64.3 ± 1.0	366.3 ± 25.5	42.6 ± 4.1	13.3 ± 2.2	226.6 ± 30.9	26	4
		5xFAD	-66.1 ± 0.9	330.6 ± 25.7	34.7 ± 2.0	16.2 ± 2.6	169.0 ± 19.9	27	4
	6	WT	-65.9 ± 0.6	360.2 ± 30.5	35.4 ± 2.7	12.4 ± 1.8	271.5 ± 37.9	22	3
		5xFAD	-67.5 ± 0.8	324.0 ± 21.8	31.4 ± 2.1	8.0 ± 2.1	240.5 ± 27.8	26	3
	12	WT	-65.5 ± 1.0	283.8 ± 37.9	28.3 ± 2.2	15.1 ± 2.9	183.6 ± 33.2	20	2
		5xFAD	-65.6 ± 0.9	397.4 ± 36.1	37.1 ± 3.5	6.0 ± 2.0	228.4 ± 39.1	19	3
ANOVA *post-hoc* Kruskal-Wallis			n.s.	n.s.	n.s.	n.s.	n.s.		
ACh	2	WT	-63.1 ± 1.1	396.9 ± 28.9	53.9 ± 5.4	14.6 ± 2.6	193.0 ± 34.9	24	3
		5xFAD	-65.9 ± 1.1	369.0 ± 31.7	44.5 ± 3.4	20.1 ± 2.6	153.9 ± 36.1	23	3
	6	WT	-67.4 ± 1.0	346.7 ± 32.9	41.1 ± 3.4	20.4 ± 3.1	156.1 ± 33.0	23	3
		5xFAD	-66.8 ± 0.9	462.0 ± 32.4	47.1 ± 3.7	13.3 ± 2.0	102.5 ± 12.5	24	3
	12	WT	-62.7 ± 1.3	426.1 ± 40.2	49.7 ± 4.7	15.9 ± 2.8	161.2 ± 36.6	22	3
		5xFAD	-65.2 ± 1.4	443.8 ± 48.5	43.3 ± 3.5	11.2 ± 3.4	194.6 ± 77.4	18	4
ANOVA *post-hoc* Kruskal-Wallis			n.s.	n.s.	n.s.	n.s.	n.s.		

Table 1 (previous page). Passive membrane properties from neurons recorded in the absence of neuromodulation (No NM, top) and in presence of a carbachol (ACh, bottom): *resting membrane potential (Vm), input resistance (Rin), membrane time constant (τm), voltage sag, and membrane capacitance (Cm). Statistical analysis: non-parametric one-way ANOVA test and Kruskal-Wallis test for post-hoc analysis. n.s., non significant.*

First, in presence of carbachol, we observed that recorded neurons from six month-old WT mice were characterized by a θ_{ON} lower than θ_{OFF} (Fig. 1C; p=0.0005, Wilcoxon matched-pairs signed rank test), similar to two month-old WT mice. Accordingly, the fraction of CB neurons recorded in the layer V mPFC from 6 month-old WT mice (Fig. 1D; 74%) was similar to two month-old WT mice (Fig. 1D; 75%). By contrast, in 12 month-old WT mice, θ_{OFF} and θ_{ON} were statistically similar on average (Fig. 1C; p=0.8407, Wilcoxon matched-pairs signed rank test). Therefore, at 12 month-old, the discharge of WT neurons was statistically unchanged upon T1 and T2, independently of whether a supra-threshold phasic pulse was administered before the tonic pulse. Therefore, the fraction of CB neurons recorded in 12 month-old WT mice was lower (Fig. 1D, 41%), compared to that of two month-old (Fig. 1D; 75%; adjusted p=0.0199, Chi 2 test with Bonferroni correction) and six month-old (adjusted p=0.0199, Chi 2 test with Bonferroni correction) mice.

Active electric membrane properties

NM condition	Age (mo)	Genotype	Threshold (mV)	Amplitude (mV)	Half-duration (ms)	T1 Rheobase (pA)	T2 Rheobase (pA)	# cells	# mice
No NM	2	WT	-45.2 ± 0.9	63.4 ± 1.7	2.44 ± 0.09	35.0 ± 2.8	43.9 ± 3.8	26	4
		5xFAD	-43.3 ± 0.9	58.9 ± 1.4	2.17 ± 0.06	34.1 ± 4.2	44.4 ± 5.2	27	4
	6	WT	-45.0 ± 1.1	61.6 ± 3.2	2.66 ± 0.14	44.5 ± 4.5	56.8 ± 5.1	22	3
		5xFAD	-45.3 ± 0.9	62.8 ± 2.4	2.37 ± 0.10	48.8 ± 5.1	56.1 ± 3.7	26	3
	12	WT	-43.5 ± 0.8	67.3 ± 2.8	2.18 ± 0.09	43.0 ± 4.3	54.5 ± 5.6	20	2
		5xFAD	-43.1 ± 0.8	60.4 ± 2.0	2.29 ± 0.12	28.4 ± 3.0	40.0 ± 3.0	19	3
ANOVA *post-hoc* Kruskal-Wallis			n.s.	n.s.	n.s.	n.s.	n.s.		
ACh	2	WT	-45.5 ± 0.7	58.2 ± 2.4	2.37 ± 0.14	40.0 ± 3.7	24.6 ± 3.3	24	3
		5xFAD	-44.9 ± 0.8	63.2 ± 2.0	2.48 ± 0.10	38.3 ± 3.4	27.4 ± 3.5	23	3
	6	WT	-44.0 ± 0.7	65.3 ± 3.0	2.48 ± 0.09	41.7 ± 3.6	32.2 ± 3.4	23	3
		5xFAD	-45.8 ± 0.9	60.4 ± 2.1	2.75 ± 0.13	30.4 ± 3.0	40.0 ± 3.7	24	3
	12	WT	-42.4 ± 0.7	63.9 ± 2.0	2.28 ± 0.08	30.5 ± 3.4	38.2 ± 4.7	22	3
		5xFAD	-44.8 ± 0.9	65.8 ± 2.0	2.21 ± 0.11	34.8 ± 4.6	43.9 ± 5.6	18	4
ANOVA *post-hoc* Kruskal-Wallis			n.s.	n.s.	n.s.	n.s.	n.s.		

Table 2. Active membrane properties from neurons recorded in the absence of neuromodulation (No NM, top) and in presence of carbachol (ACh, bottom): *action potential threshold, amplitude, half-duration, and rheobase upon T1 and T2 stimulations. Statistical analysis: non-parametric one-way ANOVA test and Kruskal-Wallis test for post-hoc analysis. n.s., non significant.*

Second, in two month-old 5xFAD mice, θ_{ON} was lower than θ_{OFF} (Fig. 1C; p=0.0382, Wilcoxon matched-pairs signed rank test), indicating triggered self-sustained spiking, similarly to two month-old WT mice. Accordingly, the fraction of recorded CB neurons in two month-old 5xAFD (Fig. 1D; 61%) mice was statistically similar to two month-old WT mice (Fig. 1D; 75%). But in six month-old and 12 month-old 5xFAD mice, on average, θ_{ON} was greater than θ_{OFF} (Fig. 1C; respectively, p=6.1e-5 and p=0.0049, Wilcoxon matched-pairs signed rank test), meaning that the triggered self-sustained spiking present at two month-old disappeared at six and 12 month-old in 5xFAD neurons. Accordingly, the fractions of CB neurons recorded in six month-old (Fig. 1D; 25%) and 12 month-old (Fig. 1D; 28%) 5xFAD mice were lower than that at two month-old 5xFAD mice (Fig. 1D; 61%; respectively, adjusted p=0.0199 and p=0.0199, Chi 2 test with Bonferroni correction).

Altogether, these results demonstrate that, under cholinergic modulation through M1-type receptors, CB is reduced in WT mice at 12 months of age, and earlier, at 6 months of age, in 5xFAD mice. These effects are unlikely to be caused neither by changes in passive membrane (Table 1, bottom), nor action potential (Table 2, bottom) properties, as they were similar between the different genotypes and age groups.

After-depolarization currents, required for conditional bistability, disappear at 6 months of age in neurons from 5xFAD mice

The involvement of specific currents in persistent spiking and bistability in layer V mPFC pyramidal neurons has been established (Andrade, 1991; Haj-Dahmane and Andrade, 1997, 1998, 1999; Ratté et al., 2018). These currents, that include two distinct calcium-activated non-selective cationic (CAN) depolarizing currents, differ in their gating kinetics (Haj-Dahmane and Andrade, 1999), with a fast CAN current and a slow CAN current having activation time constants of, respectively, a few tens of milliseconds (Haj-Dahmane and Andrade, 1997, 1999) and over a second (Andrade, 1991; Haj-Dahmane and Andrade, 1998, 1999; Ratté et al., 2018). Following spiking activity, these currents generate after-depolarizations (ADP), which can be observed as depolarizations of the membrane potential. Additionally, there is a calcium-activated potassium current that produces an after-hyperpolarization (AHP) after spiking activity. The AHP has an activation time constant of approximately 100-200 ms (Haj-Dahmane and Andrade, 1998; Satake et al., 2008; Ratté et al., 2018). The medium AHP current opposes persistent activity and bistability (Haj-Dahmane and Andrade, 1997, 1998) and is typically observed following stimulation that triggers persistent activity (Dembrow et al., 2013; Ratté et al., 2018).

In this study, we examined the potential involvement of these three currents in CB and how they are affected in 5xFAD mice and aging. During CB-related persistent activity, the fast CAN, medium AHP, and slow CAN currents are collectively activated by successive spikes and deactivated after the termination of persistent spiking. Therefore, the after-polarization of the membrane potential following persistent activity, which can be either an ADP or an AHP, reflects the presence of these currents and may indicate their role in CB. We specifically focused on three components: the fast (0-50 ms), medium (50-350 ms), and slow (350-500 ms)

after-polarizations (Leroux et al., manuscript #1). These components allowed us to quantify the relative amplitude of the three currents based on their distinctive kinetics and assess the ADP/AHP balance. Positive values (Fig. 2A) indicated a depolarization of the membrane potential caused by increased activation of ADP currents or decreased activation of AHP currents during CB-related persistent spiking, while negative values (Fig. 2A) indicated decreased ADP and/or increased AHP currents (refer to the Methods section for more details; Leroux et al., manuscript #1).

In the absence of any neuromodulation (Fig. 2B-D, the after-polarizations measured in two, six, and 12 month-old WT and 5xFAD mice are characterized by smaller amplitudes—positive or negative—compared when under cholinergic modulation (Fig. 2E-G), suggesting that without neuromodulation less CAN and AHP currents are activated.

Under cholinergic modulation, the fast ADP was similar between recorded neurons in two, six, and 12 month-old WT and 5xFAD mice (Fig. 2E-G; fast, F graphs), suggesting that, in presence of carbachol, fast ADP cannot on its own account for the differences in fractions of CB neurons observed in two, six, and 12 month-old 5xFAD mice (Fig. 1D). Overall, without neuromodulation (Fig. 2B-D) or in presence of carbachol (Fig. 2E-G), the medium, slow and average after-polarizations are more hyperpolarized in two, six, and 12 month-old 5xFAD than in WT mice, which suggests that in 5xFAD neurons either slow CAN currents are inhibited or medium AHP currents are facilitated, independently of the neuromodulation. But this effect appears significant in six month-old mice, under cholinergic modulation, WT neurons—characterized by a high fraction of CB—exhibit medium and slow ADPs, which underlie triggered self-sustained spiking, and 5xFAD neurons—characterized by a low fraction of CB—exhibit medium and slow AHPs, which inhibit persistent spiking.

Altogether, these findings suggest that cholinergic modulation increases levels of CAN currents during CB-related self-sustained activity in mice, as demonstrated in rats (Leroux et al., manuscript #1). But the medium and slow after-hyperpolarizations in six and 12 month-old 5xFAD neurons inhibit cholinergic-mediated CB to emerge.

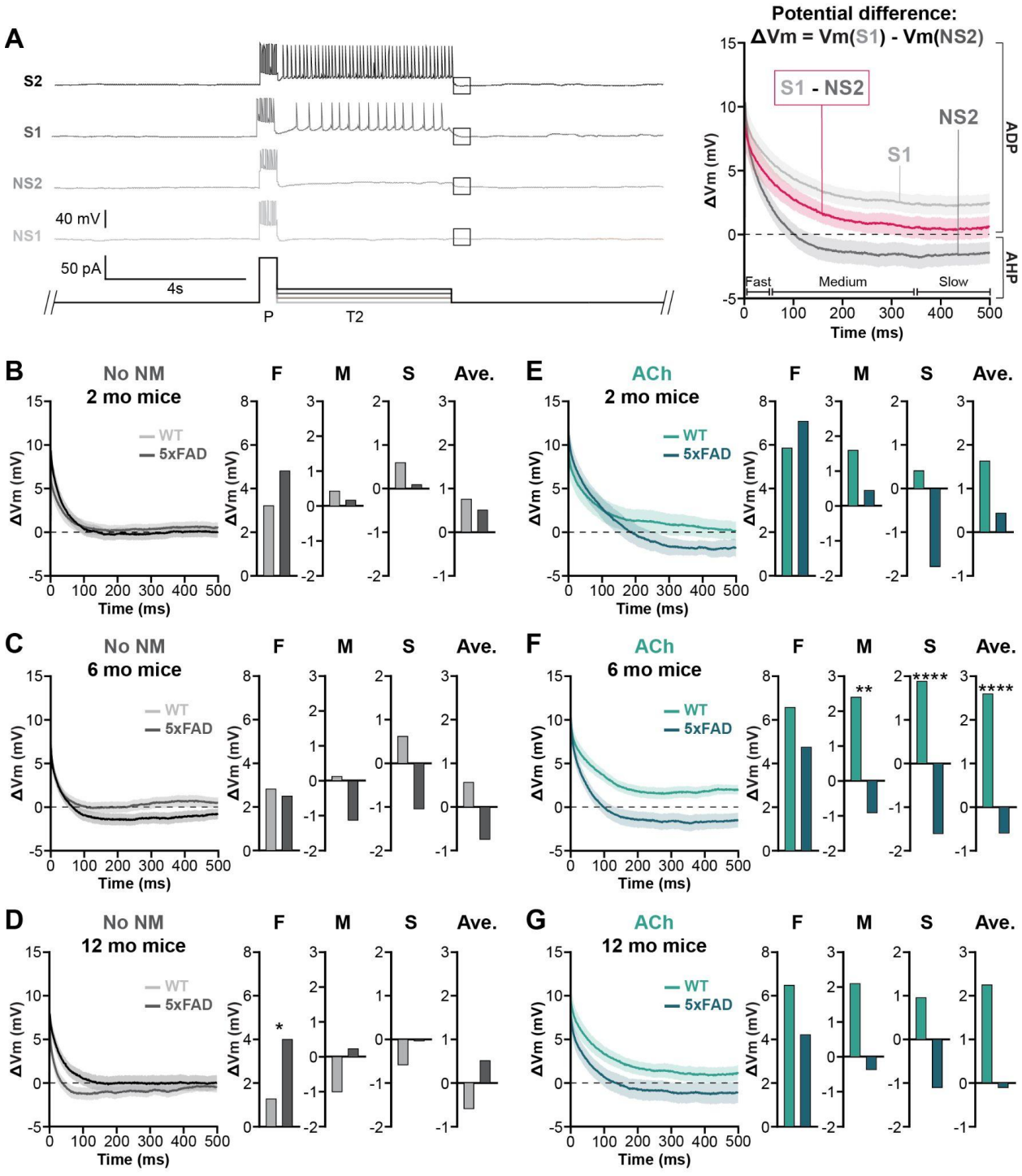

Figure 2. Acetylcholine-dependent conditional bistability impairment in 6-month-old 5xFAD mice is explained by a decrease in after-depolarization (ADP). A*, Method to identify currents implicated in CB. Left, Four sweeps of interest were identified in the bistability protocol: NS1 (No Spike 1, first sweep upon which the neuron doesn't fire on T1 and T2); NS2 (No Spike 2, last sweep upon which the neuron doesn't fire on T1 and T2); S1 (Spike 1, first sweep upon which the neuron fires on T1 and T2); and S2 (Spike 2, last sweep upon which the neuron fires on T1 and T2), upon which membrane potentials were extracted during the 500 ms following T2 (black squares). Right, Average difference of the membrane*

potential between sweeps S1 and NS2, after T2 indicates spike-triggered currents activated during CB-related self-sustained persistent activity. ***B-D****, Average membrane potential difference in absence of any neuromodulation (No NM) in WT and 5xFAD two month-old (2 mo, B), six month-old (6 mo, C), and 12 month-old (12 mo, D) slices.* ***E-G****, Average membrane potential difference under cholinergic modulation (ACh) in WT and 5xFAD two month-old (2 mo, E), six month-old (6 mo, F), and 12 month-old (12 mo, G) slices. Statistical significance was assessed by Scheirer-Ray-Hare test and Wilcoxon Mann Whitney test for the post hoc analysis on average membrane potential difference in the ranges 0-50 ms (fast after-polarization, F), 50-350 ms (medium after-polarization, M), 350-500 ms (slow after-polarization, S), and across the whole window considered (0-500 ms, average after-polarization, Ave.) after T2. (****p<0.0001; **p<0.01; *p<0.05).*

DISCUSSION

Using *in vitro* whole-cell patch-clamp recordings, we unraveled that conditional bistability (CB), a neuronal intrinsic property allowing triggered self-sustained spiking, exists in the pyramidal neurons of the layer V mPFC of adult mice. We also showed that CB is acetylcholine-dependent and mediated through increases in fast and slow after-depolarizations. Moreover, we demonstrated that CB is decreased in aging at 12 months of age in WT mice, and earlier in 5xFAD mice at six months of age.

Discovery of conditional bistability in mice

In this study, we used the previously described electrical *bistability* protocol (Leroux et al., manuscript #1) to assess *in vitro* whether, in mice, pyramidal neurons of the layer V mPFC can exhibit the intrinsic property called conditional bistability (CB). For the first time, to our knowledge, we showed that CB does exist in the mouse mPFC. CB is a neuronal property allowing cellular memorization of an event, or information to remember, at the neuronal scale. Interestingly, in our previous study, we found that, under cholinergic modulation, 97% of layer V mPFC pyramidal neurons in rats exhibited CB (Leroux et al., manuscript #1), which is more than the 75% found in mice. This difference is not surprising as evidence shows that rats have better executive functions than mice and present a more complex behavior (Whishaw et al., 2001; Snyder et al., 2009; Ellenbroek and Youn, 2016). But, depending on the behavioral task, it has been shown that mice can perform as good as rats—e.g., in adaptive decision-making tasks (Jaramillo and Zador, 2014).

Our previous experimental work performed in rats (Leroux et al., manuscript #1) suggests that GPA, the neural correlate of parametric working memory (PWM), depends on CB. To this date, PWM capacities have been investigated in rodents only using rats as animal models. PWM tasks (Fassihi et al., 2014) consist in the comparison of two pieces of information separated by a delay of a few seconds and characterized by different intensities (the frequency of a mechanical vibration against the whiskers, for example). Many studies already proved that young adult healthy mice have object WM and spatial WM capacities (Dudchenko, 2004). However, in order to affirm that mice also have *in vivo* PWM capacities, it will be necessary, in the future, to train mice to similar behavioral PWM tasks than the ones used with rats.

Conditional bistability in mice depends on cholinergic activation of muscarinic 1-type receptor, as in rats

We found that an agonist of the muscarinic 1-type receptors (M1 R), carbachol, significantly facilitates neuronal CB emergence in healthy young adult mice (75% of CB neurons). This result in mice is in agreement with what we previously found in rats (Leroux et al., manuscript #1). Despite the lack of *in vivo* data proving PWM capacities in mice, we show that both types of rodents exhibit CB in the pyramidal neurons of the layer V mPFC, and depend on the same M1 receptor-dependent neuromodulation.

Moreover, we showed in Leroux et al. (manuscript #1) that acetylcholine-dependent CB is mediated through the activation of calcium-activated non-selective cationic (CAN) channels in rats. These channels are responsible for fast (tens of milliseconds) and slow (over a second) CAN currents that produce depolarizations of the membrane potential following spiking, called after-depolarizations (ADP), which facilitate neuronal self-sustained spiking.

In overall, neurons recorded *in vitro* in young adult healthy mice confirmed our previous results from rats (Leroux et al., manuscript #1). Without neuromodulation, AHP currents are stronger and CB is absent in the majority of recorded neurons. However, when neurons are recorded in presence of M1 R agonist, the majority of the neurons show a CB behavior when the *bistability* protocol is applied, meaning that a massive activation of the CAN currents counteracts the AHP currents. We found that cholinergic modulation mediates CB via increases of both fast and slow CAN currents.

In our previous *in vitro* study (Leroux et al., manuscript #1), using an electrical stimulation protocol in slice, we were able to observe GPA-like activities, the neural correlate of PWM, in the mPFC. This result was consistent with *in vivo* studies showing PWM capacities of rats (Fassihi et al., 2014). Moreover, we demonstrated that GPA depends on acetylcholine- and ADP-dependent CB to emerge in mPFC networks. In order to affirm that mice also have parametric capacities at the network level and GPA can emerge in the mPFC circuit in mice, it will be necessary, in the future, to apply the same electrical stimulation protocol in mouse mPFC slice than the one used in Leroux et al. (manuscript #1).

Conditional bistability is impacted in aging

Aging is associated with a variety of cognitive changes in humans (Murman, 2015) but also in mice. Among others, starting six months of age, C57BL/6J WT mice become more anxious and a social interaction impairment starts to appear compared with two month-old mice (Shoji et al., 2016); cognitive capacities continue to decline later in life. Moreover, long-term memory capacities are also altered. Long-term memory, in a contextual fear-conditioning paradigm, declines starting 12 month-old (Shoji et al., 2016), and worsens by 18 month-old (Yanai and Endo, 2021). Spatial memory in the Morris Water Maze is altered starting at six month-old (Hendrickx et al., 2022), but significantly worsens at 12 (Yanai and Endo, 2021; Hendrickx et al., 2022).

Another important cognitive decline observed in aged mice is the loss of WM capacities. Weiss et al. (1999) showed that WT mice perform poorly in a Y-maze, assessing spatial WM, at 16 month-old and 24 month-old compared with 4 month-old mice. Also, Yang et al. (2019) demonstrated that, at 3-5 mo, mice perform correctly novel object recognition task, but object WM capacities are impaired at 19-21 months of age.

In our study, we found that, in presence of carbachol, the fraction of recorded neurons exhibiting CB is significantly decreased in WT mice at 12 month-old compared with two month-old and six month-old WT mice. This result could be explained by the decrease in slow ADP in 12 month-old compared with six month-old mice. Thus, at this age, slow ADP currents would not be sufficient to elicit self-sustained spiking, and hence CB.

M1 R binding by a ligand (acetylcholine or carbachol) leads to the activation of CAN channels through an intracellular cascade of enzyme/protein activations, which involve protein Gq and inositol triphosphate (IP3; Caulfield, 1993; Felder, 1995). Therefore, the decline of the fraction CB at 12 month-old could be explained by an impairment in M1 R expression and/or function, CAN channel expression/function, or molecular species taking part to the intracellular signaling cascade—e.g., second messengers, kinases/phosphatases. It has been shown that aged rats (22-26 month-old) are characterized by a significant decrease of M1 R density in the cortex compared with 3-6 month-old and 15-17 month-old rats (Schwarz et al., 1990). Therefore, we suggest that CB impairment in 12 month-old mice is not caused by a decline in M1 R expression. Rather, the decrease in the amplitude of slow CAN currents and in the fraction of CB neurons might arise from dysregulation of signaling downstream of M1 R or of CAN channels themselves during aging and, in fine, affect functional network dynamics it underlies—e.g., network persistent activity, including GPA, which underlies cellular memorization of information during the delay of object WM, spatial WM, and PWM (Romo et al., 1999; Nieder et al., 2004; Major and Tank, 2004).

Signaling elements involved in decreased conditional bistability in 5xFAD mice

Loss of WM is one of the first symptoms to appear in AD (Baddeley et al., 1991; Saunders and Summers, 2009; Kessels et al., 2010) and people with WM impairments can experience life-threatening situations and quickly lose their ability to live independently (Smebye et al., 2015). Despite its crucial role in daily life, little is known about PWM in AD. Here, and in our previous study (Leroux et al., manuscript #1), we showed that CB, likely subserving GPA, the neural correlate of PWM, depends on the specific cholinergic M1 R activation to generate ADP and facilitate self-sustained spiking in rodents.

AD is characterized, among others, by a disruption of the cholinergic system: 1) significant decline in activity of choline acetyltransferase in the neocortex (Bowen et al., 1976), 2) reduced uptake choline in the cortex (Rylett et al., 1983), 3) reduced release of ACh into the synapse (Nilsson et al., 1986), and 4) degeneration of cholinergic projections from the nucleus basalis of Meynert (Whitehouse et al., 1982). Thus, we wondered whether acetylcholine-dependent CB is impacted in AD, and if *in vitro* application of a cholinergic M1 R agonist in mPFC slice is sufficient to elicit CB.

If various studies showed that the level of M1 R remains unchanged in different regions of the AD brain compared with normal aged brain (Kellar et al., 1987; Flynn et al., 1991; Pearce and Potter, 1991; Hampel et al., 2018); others found that M1 R expression is impaired in AD brains (Shiozaki et al., 2001) and the coupling of the M1 R to G proteins is significantly reduced (Tsang et al., 2006; Janíčková et al., 2013). It has also been shown that M1 R function is impaired in AD brains (Yi et al., 2020) and expression of crucial genes in the M1R/CAN intracellular cascade proteins was decreased: excitatory cortical neurons from post-mortem human AD brains showed a decreased M1/3 R gene expression, a decreased TRPC5 (CAN) gene expression, decreased Protein G genes (29/75 tested) expression, and decrease IP3 kinase gene expression (Zhou et al., 2020). These results suggest that, at the end of life of AD patients, elements of the neuronal machinery necessary to generate CB is disrupted. However,

whether dysregulation of M1 R, downstream signaling, or CAN/TRPC channels is responsible for the downregulation of CB in 5xFAD mice remains obscure. Moreover, insight on the timeline when these changes occur remains to be elucidated. As a therapeutic future possibility, it may be possible to act on these pathways, in a specific time window, to rescue neuronal CB and, consequently, executive functions it is involved in.

Age-dependence of the decrease of conditional bistability in 5xFAD mice

To investigate the effect of AD on conditional bistability, we used the 5xFAD mouse line (Oakley et al., 2006), as an AD animal model. 5xFAD mice recapitulate almost all human AD symptoms. They present Aβ plaques deposition beginning two months of age in deep cortical layers (Oakley et al., 2006). Synaptic degeneration starts at four month-old and peaks starting nine month-old (Oakley et al., 2006). Loss of pyramidal neurons in cortical layer V is observed starting nine month-old (Oakley et al., 2006) and neurite dystrophy is detected at 10-12 month-old (Condello et al., 2015). These molecular and cellular changes are associated with functional consequences, including WM impairments. Spatial WM deficits are observed in four, six, and 12 month-old 5xFAD mice (Oakley et al., 2006; Fertan and Brown, 2022). Object WM is affected in six month-old (Yi et al., 2020) and 12 month-old 5xFAD mice (Creighton et al., 2019). Thus, we decided to investigate the time course of CB, essential to GPA, the neural correlate of PWM, in two, six, and 12 month-old 5xFAD mice.

In two month-old 5xFAD mice, the fraction of CB neurons recorded in presence of cholinergic modulation was high and similar to the one in two month-old WT mice. Surprisingly, the two month-old 5xFAD neurons presented a negative slow after-polarization (AHP), meaning that the self-sustained spiking and CB should be limited. However, this slow AHP, measured in the 350-500 ms time window, was apparently not sufficient to limit CB. Several possibilities could underlie this elevated CB fraction. First, the slightly stronger fast ADP, mediated by fast CAN conductance, is a putative candidate. Also, the slow CAN conductance might actually be substantial, despite being dominated by AHP in the 350-500 ms window. Hence, it may in part subserve the strong fast ADP—in addition to the fast CAN conductance—and be responsible for the slight ADP found in the 50-350 ms time window. Also, possibly, the slow CAN conductance might exert its effects at longer times (after 500 ms). In all these cases, the slow CAN conductance, possibly displaying different (faster or slower) dynamics, compared to in WT mice, might be sufficiently strong to ensure the positive feedback required for self-sustained spiking and CB. Alternatively, the increased fast ADP may correspond to the presence of an upregulated fast CAN conductance—i.e., through some compensatory process—which would provide the required positive feedback. Further explorations of these possibilities are necessary in the future.

In 5xFAD mice, Aβ plaques deposition starts at two month-old (Oakley et al., 2006). Yi et al. (2020) showed that soluble Aβ oligomers downregulate post-synaptic M1 R function via the binding to adjacent metabotropic glutamate receptor 5 (mGluR5), which leads to the decrease in M1 R function in the post-mortem human temporal cortex from AD patients. They also showed that the inhibition of Aβ-activated mGluR5 restores M1 R function in human organotypic cultures

(Yi et al., 2020). Thus, the loss of M1 R function possibly starts at two month-old in 5xFAD mice. This could explain why CAN currents are down-regulated, due to these molecular interactions, but quantitatively not to the point of decreasing the fraction of CB neurons.

In six month-old 5xFAD mice, the fraction of CB neurons recorded in presence of cholinergic modulation was significantly lower than that of two month-old 5xFAD mice and of six month-old WT mice. This reduced fraction might be explained by reduced fast and/or slow CAN conductances, or by an increased AHP conductance, responsible for the reduced fast ADP, as well as for the medium and slow AHP. In principle, these changes in CAN/AHP conductances could be explained by impairment in M1 R expression and/or function, intracellular pathways or of the regulatory state of ionic channels themselves.

At six month-old in 5xFAD mice, Aβ plaques deposition significantly increased compared with two month-old mice (Oakley et al., 2006) and M1 R function is impacted (Yi et al., 2020). Also, in 7 month-old 5xFAD mice, single nucleus RNA sequencing (snRNA-seq, Zhou et al., 2020) analysis showed that a subset of cortical neurons presented a decreased expression of M1 R gene (2 neuronal clusters out of 5) and some Protein G genes (3 neuronal clusters out of 5). But snRNA-seq analysis didn't show changes in expression of TRPC5/6 (CAN channels) gene, nor IP3 kinase gene (Zhou et al., 2020). Therefore, the decline in CB in six month-old 5xFAD mice is likely caused mainly by deficiencies in M1 R function but it might also arise from changes in the regulatory state of CAN channels, once expressed, or from expression or regulation of AHP channels.

In addition to neuronal CB impairment, synaptic degeneration starts at four months in 5xFAD mice, so at six month-old it is likely that synaptic reverberation within the mPFC networks would be affected. Altogether, CB and synaptic input dysfunctions might heavily dampen the collective neural dynamics responsible for the emergence of GPA, the neural correlate of PWM, in six month-old 5xFAD mice. Interestingly, Yi et al. (2020) showed that restoration of M1 R function in 5xFAD mice, via the inhibition of Aβ-activated mGluR5, also increased object WM performance in six month-old 5xFAD mice. Object WM implies a less subtle computation than PWM, only requiring synaptic reverberation within local recurrent mPFC networks, to produce non-graded persistent activity. Thus, AD might affect, through intrinsic and/or synaptic dysregulations, the collective neural dynamics responsible for the whole repertoire of WM functions.

Age-dependent pyramidal neuron loss is correlated with levels of intraneuronal $A\beta_{42}$ and Aβ plaque burden and becomes significant at 9 months of age (Oakley et al., 2006). Nevertheless, we were able to record mPFC pyramidal neurons in 12 month-old 5xFAD mice and apply our *bistability* protocol. In 12 month-old 5xFAD mice, the fraction of CB neurons recorded in presence of carbachol was similar to the one in six month-old 5xFAD mice and significantly lower than two month-old 5xFAD mice. The 12 month-old 5xFAD neurons presented similar fast, medium, and slow after-polarizations than six month-old 5xFAD neurons. Thus, medium and show AHP currents were stronger than ADPs and were caused by increased activation of the AHP channels and/or deactivation of the slow CAN channels.

In 12 month-old 5xFAD, specific activation of M1 R with carbachol fails to elicit CB. The impairment observed in M1 R and Protein G gene expression at seven month-old in 5xAFD probably continues to progress. Moreover, as observed in post-mortem human AD brains, we suggest that the expression of TRPC5/6 (CAN channels) and IP3 kinase genes is reduced by the age of 12 months in 5xFAD mice (Zhou et al., 2020), down-regulating CAN conductances, self-sustained spiking and CB. In addition, synaptic degeneration peaks starting at nine month-old (Oakley et al., 2006) and neurite dystrophy is detected at 10-12 month-old (Condello et al., 2015) in 5xFAD mice. Thus, it is unlikely that in the mPFC of 5xFAD, networks could generate GPA, and perform PWM.

Specific M1 R agonists as a promising future possible treatment for Alzheimer's disease

Altogether, these results suggest that CB depends on M1 R activation and that the disruption of M1 R function, or gene expression, and/or of downstream signaling pathways lead to the down-regulation of CB. Early in the disease progression—around 6/7 month-old in 5xFAD—, the M1 R expression itself is not impaired, but its function is altered. Later as the disease progresses, the gene expression coding for M1 R is disrupted, with other genes coding for crucial intracellular elements, such as TRPC5/6 (CAN), Protein G, and IP3.

In 5xFAD mice, between two and six months of age, there is a critical moment from which M1 R function declines and the specific activation of M1 R is no longer sufficient to generate self-sustained spiking. Drugs allowing to restore M1 R function and/or specifically restore molecular kinetics within downstreal intracellular signaling pathway or the maximal conductance or gating dynamics of CAN and/or AHP conductances could offer potential future treatments to restore PWM mechanisms early in the progression of disease.

REFERENCES

Baddeley, A. D., Bressi, S., Della Sala, S., Logie, R. H., & Spinnler, H. (1991). The decline of working memory in Alzheimer's disease. A longitudinal study. *Brain*, *114*(6), 2521–2542. https://doi.org/10.1093/brain/114.6.2521

Bowen, D. G., Smith, C. A., White, P. J., & Davison, A. (1976). Neurotransmitter-related enzymes and indices of hypoxia in senile dementia and other abiotrophies. *Brain*, *99*(3), 459–496. https://doi.org/10.1093/brain/99.3.459

Brody, C. D., Romo, R., & Kepecs, A. (2003). Basic mechanisms for graded persistent activity: discrete attractors, continuous attractors, and dynamic representations. *Current Opinion in Neurobiology*, *13*(2), 204–211. https://doi.org/10.1016/s0959-4388(03)00050-3

Burke, S. N., & Barnes, C. A. (2006). Neural plasticity in the ageing brain. *Nature Reviews Neuroscience*, *7*(1), 30–40. https://doi.org/10.1038/nrn1809

Canter, R. G., Huang, W., Choi, H., Wang, J., Watson, L. M., Yao, C. G., Abdurrob, F., Bousleiman, S. M., Young, J. Z., Bennett, D. A., Delalle, I., Chung, K., & Tsai, L. (2019). 3D mapping reveals network-specific amyloid progression and subcortical susceptibility in mice. *Communications Biology*, *2*(1). https://doi.org/10.1038/s42003-019-0599-8

Carlesimo, G. A., & Oscar-Berman, M. (1992). Memory deficits in Alzheimer's patients: A comprehensive review. *Neuropsychology Review*, *3*(2), 119–169. https://doi.org/10.1007/bf01108841

Caulfield, M. P. (1993). Muscarinic Receptors—Characterization, coupling and function. *Pharmacol Ther.*, *58*(3), 319–379. https://doi.org/10.1016/0163-7258(93)90027-b

Cho, F. S., Clemente, A., Holden, S. S., & Paz, J. T. (2017). Thalamic Models of Seizures In Vitro. In *Models of Seizures and Epilepsy* (2nd ed., pp. 273–284). https://doi.org/10.1016/b978-0-12-804066-9.00019-5

Cho, F. S., Vainchtein, I. D., Voskobiynyk, Y., Morningstar, A. R., Aparicio, F. J., Higashikubo, B., Ciesielska, A., Broekaart, D. W. M., Anink, J. J., Van Vliet, E. A., Yu, X., Khakh, B. S., Aronica, E., Molofsky, A. V., & Paz, J. T. (2022). Enhancing GAT-3 in thalamic astrocytes promotes resilience to brain injury in rodents. *Science Translational Medicine*, *14*(652). https://doi.org/10.1126/scitranslmed.abj4310

Clemente-Perez, A., Makinson, S. R., Higashikubo, B., Brovarney, S., Cho, F. S., Urry, A., Holden, S. S., Wimer, M., Dávid, C., Fenno, L. E., Acsády, L., Deisseroth, K., & Paz, J. T. (2017). Distinct Thalamic Reticular Cell Types Differentially Modulate Normal and Pathological Cortical Rhythms. *Cell Reports*, *19*(10), 2130–2142. https://doi.org/10.1016/j.celrep.2017.05.044

Condello, C., Yuan, P., Schain, A. J., & Grutzendler, J. (2015). Microglia constitute a barrier that prevents neurotoxic protofibrillar Aβ42 hotspots around plaques. *Nature Communications*, *6*(1). https://doi.org/10.1038/ncomms7176

Creighton, S. D., Mendell, A. L., Palmer, D., Kalisch, B. E., MacLusky, N. J., Prado, V. F., Prado, M. a. M., & Winters, B. D. (2019). Dissociable cognitive impairments in two strains of transgenic Alzheimer's disease mice revealed by a battery of object-based tests. *Scientific Reports*, *9*(1). https://doi.org/10.1038/s41598-018-37312-0

Dudchenko, P. A. (2004). An overview of the tasks used to test working memory in rodents. *Neuroscience & Biobehavioral Reviews*, *28*(7), 699–709. https://doi.org/10.1016/j.neubiorev.2004.09.002

Dumurgier, J., & Sabia, S. (2020, February 1). [Epidemiology of Alzheimer's disease: latest trends]. Rev Prat. https://pubmed.ncbi.nlm.nih.gov/32877124/#:~:text=Abstract&text=Alzheimer's%20disease%20(AD)%20is%20the,225.000%20new%20patients%20each%20year.

Ellenbroek, B., & Youn, J. (2016). Rodent models in neuroscience research: is it a rat race? *Dis Model Mech*, *9*(10), 1079–1087. https://pubmed.ncbi.nlm.nih.gov/27736744/

Fassihi, A., Akrami, A., Esmaeili, V., & Diamond, M. E. (2014). Tactile perception and working memory in rats and humans. *Proceedings of the National Academy of Sciences of the United States of America*, *111*(6), 2331–2336. https://doi.org/10.1073/pnas.1315171111

Felder, C. C. (1995). Muscarinic acetylcholine receptors: signal transduction through multiple effectors. *FASEB J.*, *9*(8), 619–625. https://pubmed.ncbi.nlm.nih.gov/7768353/

Fertan, E., & Brown, R. J. C. (2022). Age-related deficits in working memory in 5xFAD mice in the Hebb-Williams maze. *Behavioural Brain Research*, *424*, 113806. https://doi.org/10.1016/j.bbr.2022.113806

Fleischman, D. A., & Gabrieli, J. D. E. (1999). Long-term memory in Alzheimer's disease. *Current Opinion in Neurobiology*, *9*(2), 240–244. https://doi.org/10.1016/s0959-4388(99)80034-8

Flynn, D. D., Weinstein, D. E., & Mash, D. C. (1991). Loss of high-affinity agonist binding to M1 muscarinic receptors in Alzheimer's disease: Implications for the failure of cholinergic replacement therapies. *Annals of Neurology*, *29*(3), 256–262. https://doi.org/10.1002/ana.410290305

Fuster, J. M., & Alexander, G. E. (1971). Neuron Activity Related to Short-Term Memory. *Science*, *173*(3997), 652–654. https://doi.org/10.1126/science.173.3997.652

Haj-Dahmane, S., & Andrade, R. B. (1996). Muscarinic Activation of a Voltage-Dependent Cation Nonselective Current in Rat Association Cortex. *The Journal of Neuroscience*, *16*(12), 3848–3861. https://doi.org/10.1523/jneurosci.16-12-03848.1996

Haj-Dahmane, S., & Andrade, R. B. (1998). Ionic Mechanism of the Slow Afterdepolarization Induced by Muscarinic Receptor Activation in Rat Prefrontal Cortex. *Journal of Neurophysiology*, *80*(3), 1197–1210. https://doi.org/10.1152/jn.1998.80.3.1197

Haj-Dahmane, S., & Andrade, R. B. (1999). Muscarinic receptors regulate two different calcium-dependent non-selective cation currents in rat prefrontal cortex. *European Journal of Neuroscience*, *11*(6), 1973–1980. https://doi.org/10.1046/j.1460-9568.1999.00612.x

Hampel, H., Mesulam, M., Cuello, A. C., Farlow, M. R., Giacobini, E., Grossberg, G. T., Khachaturian, A. S., Vergallo, A., Cavedo, E., Snyder, P. J., & Khachaturian, Z. S. (2018). The cholinergic system in the pathophysiology and treatment of Alzheimer's disease. *Brain*, *141*(7), 1917–1933. https://doi.org/10.1093/brain/awy132

Hendrickx, J. O., De Moudt, S., Calus, E., De Deyn, P. P., Van Dam, D., & De Meyer, G. R. (2022). Age-related cognitive decline in spatial learning and memory of C57BL/6J mice. *Behavioural Brain Research*, *418*, 113649. https://doi.org/10.1016/j.bbr.2021.113649

Holden, S. S., Grandi, F. C., Aboubakr, O., Higashikubo, B., Cho, F. S., Chang, A. C., Osorio-Forero, A., Morningstar, A. R., Mathur, V., Kuhn, L. J., Suri, P., Sankaranarayanan, S., Andrews-Zwilling, Y., Tenner, A. J., Lüthi, A., Aronica, E., Corces, M. R., Yednock, T., & Paz, J. T. (2021). Complement factor C1q mediates sleep spindle loss and epileptic spikes after mild brain injury. *Science*, *373*(6560). https://doi.org/10.1126/science.abj2685

Holtzman, D. M., Morris, J. C., & Goate, A. (2011). Alzheimer's Disease: The Challenge of the Second Century. *Science Translational Medicine*, *3*(77). https://doi.org/10.1126/scitranslmed.3002369

Janickova, H., Rudajev, V., Zimčík, P., Jakubík, J., Tanila, H., El-Fakahany, E. E., & Doležal, V. (2013). Uncoupling of M1 muscarinic receptor/G-protein interaction by amyloid β1–42. *Neuropharmacology*, *67*, 272–283. https://doi.org/10.1016/j.neuropharm.2012.11.014

Jaramillo, S., & Zador, A. M. (2014). Mice and rats achieve similar levels of performance in an adaptive decision-making task. *Frontiers in Systems Neuroscience*, *8*. https://doi.org/10.3389/fnsys.2014.00173

Kellar, K. J., Whitehouse, P. J., Martino-Barrows, A. M., Marcus, K. A., & Price, D. L. (1987). Muscarinic and nicotinic cholinergic binding sites in alzheimer's disease cerebral cortex. *Brain Research*, *436*(1), 62–68. https://doi.org/10.1016/0006-8993(87)91556-3

Kessels, R. P. C., Meulenbroek, O., Fernández, G., & Rikkert, M. G. M. O. (2010). Spatial Working Memory in Aging and Mild Cognitive Impairment: Effects of Task Load and Contextual Cueing. *Aging Neuropsychology and Cognition*, *17*(5), 556–574. https://doi.org/10.1080/13825585.2010.481354

Klencklen, G., Després, O., & Dufour, A. (2012). What do we know about aging and spatial cognition? Reviews and perspectives. *Ageing Research Reviews*, *11*(1), 123–135. https://doi.org/10.1016/j.arr.2011.10.001

Kronovsek, T., Hermand, E., Berthoz, A., Castilla, A., Gallou-Guyot, M., Daviet, J., & Perrochon, A. (2021). Age-related decline in visuo-spatial working memory is reflected by dorsolateral prefrontal activation and cognitive capabilities. *Behavioural Brain Research*, *398*, 112981. https://doi.org/10.1016/j.bbr.2020.112981

Major, G., & Tank, D. W. (2004). Persistent neural activity: prevalence and mechanisms. *Current Opinion in Neurobiology*, *14*(6), 675–684. https://doi.org/10.1016/j.conb.2004.10.017

Medeiros, R., Kitazawa, M., Caccamo, A., Baglietto-Vargas, D., Estrada-Hernandez, T., Cribbs, D. H., Fisher, A., & LaFerla, F. M. (2011). Loss of Muscarinic M1 Receptor Exacerbates Alzheimer's Disease–Like Pathology and Cognitive Decline. *American Journal of Pathology*, *179*(2), 980–991. https://doi.org/10.1016/j.ajpath.2011.04.041

Murman, D. L. (2015). The Impact of Age on Cognition. *Seminars in Hearing*, *36*(03), 111–121. https://doi.org/10.1055/s-0035-1555115

Nieder, A., & Miller, E. K. (2004). A parieto-frontal network for visual numerical information in the monkey. *Proceedings of the National Academy of Sciences of the United States of America*, *101*(19), 7457–7462. https://doi.org/10.1073/pnas.0402239101

Nilsson, L. M., Nordberg, A., Hardy, J., Wester, P., & Winblad, B. (1986). Physostigmine restores3H-acetylcholine efflux from Alzheimer brain slices to normal level. *Journal of Neural Transmission*, *67*(3–4), 275–285. https://doi.org/10.1007/bf01243353

Oakley, H. D., Cole, S. R., Logan, S., Maus, E., Shao, P., Craft, J., Guillozet-Bongaarts, A. L., Ohno, M., Disterhoft, J. F., Van Eldik, L. J., Berry, R. J., & Vassar, R. (2006). Intraneuronal β-Amyloid Aggregates, Neurodegeneration, and Neuron Loss in Transgenic Mice with Five Familial Alzheimer's Disease Mutations: Potential Factors in Amyloid Plaque Formation. *The Journal of Neuroscience*, *26*(40), 10129–10140. https://doi.org/10.1523/jneurosci.1202-06.2006

Oblak, A. L., Lin, P. H., Kotredes, K. P., Pandey, R. P., Garceau, D., Williams, H. G., Uyar, A., O'Rourke, R. W., O'Rourke, S., Ingraham, C. M., Bednarczyk, D., Belanger, M., Cope, Z. A., Little, G. J.,

Williams, S. G., Ash, C., Bleckert, A., Ragan, T., Logsdon, B. A., . . . Lamb, B. T. (2021). Comprehensive Evaluation of the 5XFAD Mouse Model for Preclinical Testing Applications: A MODEL-AD Study. *Frontiers in Aging Neuroscience*, *13*. https://doi.org/10.3389/fnagi.2021.713726

Paz, J. T., Bryant, A. S., Peng, K., Fenno, L. E., Yizhar, O., Frankel, W. N., Deisseroth, K., & Huguenard, J. R. (2011). A new mode of corticothalamic transmission revealed in the Gria4−/− model of absence epilepsy. *Nature Neuroscience*, *14*(9), 1167–1173. https://doi.org/10.1038/nn.2896

Paz, J. T., Davidson, T., Frechette, E., Delord, B., Parada, I., Peng, K., Deisseroth, K., & Huguenard, J. R. (2012). Closed-loop optogenetic control of thalamus as a tool for interrupting seizures after cortical injury. *Nature Neuroscience*, *16*(1), 64–70. https://doi.org/10.1038/nn.3269

Pearce, B. W., & Potter, L. T. (1991). Coupling of ml Muscarinic Receptors to G Protein in Alzheimer Disease. *Alzheimer Disease & Associated Disorders*, *5*(3), 163–172. https://doi.org/10.1097/00002093-199100530-00002

Quintanilla‐Sanchez, C., Schmitt, F., Curdt, N., Westhoff, A. C., Bänfer, I. W. H., Bayer, T. A., & Bouter, Y. (2023). Search strategy analysis of 5xFAD Alzheimer mice in the Morris Water maze reveals sex- and Age-Specific spatial navigation deficits. *Biomedicines*, *11*(2), 599. https://doi.org/10.3390/biomedicines11020599

Ratté, S., Karnup, S. V., & Prescott, S. A. (2018). Nonlinear Relationship Between Spike-Dependent Calcium Influx and TRPC Channel Activation Enables Robust Persistent Spiking in Neurons of the Anterior Cingulate Cortex. *The Journal of Neuroscience*, *38*(7), 1788–1801. https://doi.org/10.1523/jneurosci.0538-17.2018

Rodriguez, G., Sarazin, M., Clemente, A., Holden, S. S., Paz, J. T., & Delord, B. (2018). Conditional Bistability, a Generic Cellular Mnemonic Mechanism for Robust and Flexible Working Memory Computations. *The Journal of Neuroscience*, *38*(22), 5209–5219. https://doi.org/10.1523/jneurosci.1992-17.2017

Romo, R., Brody, C. D., Hernandez, A. V., & Lemus, L. (1999). Neuronal correlates of parametric working memory in the prefrontal cortex. *Nature*, *399*(6735), 470–473. https://doi.org/10.1038/20939

Ruivo, L. M. T., Baker, K. L., Conway, M., Kinsley, P. J., Gilmour, G., Phillips, K. R., Isaac, J., Lowry, J. P., & Mellor, J. R. (2017). Coordinated Acetylcholine Release in Prefrontal Cortex and Hippocampus Is Associated with Arousal and Reward on Distinct Timescales. *Cell Reports*, *18*(4), 905–917. https://doi.org/10.1016/j.celrep.2016.12.085

Rylett, R. J., Ball, M., & Colhoun, E. (1983). Evidence for high affinity choline transport in synaptosomes prepared from hippocampus and neocortex of patients with Alzheimer's disease. *Brain Research*, *289*(1–2), 169–175. https://doi.org/10.1016/0006-8993(83)90017-3

Saunders, N. L., & Summers, M. J. (2009). Attention and working memory deficits in mild cognitive impairment. *Journal of Clinical and Experimental Neuropsychology*, *32*(4), 350–357. https://doi.org/10.1080/13803390903042379

Schwarz, R. D., Bernabei, A. A., Spencer, C., & Pugsley, T. A. (1990). Loss of muscarinic M1 receptors with aging in the cerebral cortex of fisher 344 rats. *Pharmacology, Biochemistry and Behavior*, *35*(3), 589–593. https://doi.org/10.1016/0091-3057(90)90295-s

Shiozaki, K., Iseki, E., Hino, H., & Kosaka, K. (2001). Distribution of m1 muscarinic acetylcholine receptors in the hippocampus of patients with Alzheimer's disease and dementia with Lewy

bodies—an immunohistochemical study. *Journal of the Neurological Sciences*, *193*(1), 23–28. https://doi.org/10.1016/s0022-510x(01)00638-4

Shoji, H., Takao, K., Hattori, S., & Miyakawa, T. (2016). Age-related changes in behavior in C57BL/6J mice from young adulthood to middle age. *Molecular Brain*, *9*(1). https://doi.org/10.1186/s13041-016-0191-9

Smebye, K. L., Kirkevold, M., & Engedal, K. (2015). Ethical dilemmas concerning autonomy when persons with dementia wish to live at home: a qualitative, hermeneutic study. *BMC Health Services Research*, *16*(1). https://doi.org/10.1186/s12913-015-1217-1

Snyder, J. S., Choe, J. S., Clifford, M. A., Jeurling, S. I., Hurley, P., Brown, A., Kamhi, J. F., & Cameron, H. A. (2009). Adult-Born Hippocampal Neurons Are More Numerous, Faster Maturing, and More Involved in Behavior in Rats than in Mice. *The Journal of Neuroscience*, *29*(46), 14484–14495. https://doi.org/10.1523/jneurosci.1768-09.2009

Thuault, S. J., Malleret, G., Constantinople, C. M., Nicholls, R. E., Chen, I. A., Zhu, J. T. T., Panteleyev, A. A., Vronskaya, S., Nolan, M. F., Bruno, R. M., Siegelbaum, S. A., & Kandel, E. R. (2013). Prefrontal Cortex HCN1 Channels Enable Intrinsic Persistent Neural Firing and Executive Memory Function. *The Journal of Neuroscience*, *33*(34), 13583–13599. https://doi.org/10.1523/jneurosci.2427-12.2013

Tsang, S., Lai, M. K., Kirvell, S. L., Francis, P. T., Esiri, M. M., Hope, T., Chen, C., & Wong, P. T. (2006). Impaired coupling of muscarinic M1 receptors to G-proteins in the neocortex is associated with severity of dementia in Alzheimer's disease. *Neurobiology of Aging*, *27*(9), 1216–1223. https://doi.org/10.1016/j.neurobiolaging.2005.07.010

Weiss, C., Shroff, A., & Disterhoft, J. F. (1999). Spatial learning and memory in aging C57BL/6 mice. *Neuroscience Research Communications*, *23*(2), 77–92.

Whishaw, I. Q., Metz, G. a. S., Kolb, B., & Pellis, S. M. (2001). Accelerated nervous system development contributes to behavioral efficiency in the laboratory mouse: A behavioral review and theoretical proposal. *Developmental Psychobiology*, *39*(3), 151–170. https://doi.org/10.1002/dev.1041

Whitehouse, P. J., Price, D. L., Struble, R. G., Clark, A. W., Coyle, J. T., & DeLong, M. R. (1982). Alzheimer's Disease and Senile Dementia: Loss of Neurons in the Basal Forebrain. *Science*, *215*(4537), 1237–1239. https://doi.org/10.1126/science.7058341

Yanai, S., & Endo, S. (2021). Functional Aging in Male C57BL/6J Mice Across the Life-Span: A Systematic Behavioral Analysis of Motor, Emotional, and Memory Function to Define an Aging Phenotype. *Frontiers in Aging Neuroscience*, *13*. https://doi.org/10.3389/fnagi.2021.697621

Yang, W., Zhou, X., & Ma, T. (2019). Memory Decline and Behavioral Inflexibility in Aged Mice Are Correlated With Dysregulation of Protein Synthesis Capacity. *Frontiers in Aging Neuroscience*, *11*. https://doi.org/10.3389/fnagi.2019.00246

Yi, J. H., Whitcomb, D. J., Park, J. B., Martinez-Perez, C., Barbati, S. A., Mitchell, S. G., & Cho, K. (2020). M1 muscarinic acetylcholine receptor dysfunction in moderate Alzheimer's disease pathology. *Brain Communications*, *2*(2). https://doi.org/10.1093/braincomms/fcaa058

Zhang, Z., & Séguéla, P. (2010). Metabotropic Induction of Persistent Activity in Layers II/III of Anterior Cingulate Cortex. *Cerebral Cortex*, *20*(12), 2948–2957. https://doi.org/10.1093/cercor/bhq043

Zhou, Y., Song, W. M., Andhey, P. S., Swain, A., Levy, T., Miller, K. R., Poliani, P. L., Cominelli, M., Grover, S., Gilfillan, S., Cella, M., Ulland, T. K., Zaitsev, K., Miyashita, A., Ikeuchi, T., Sainouchi, M., Kakita, A., Bennett, D. A., Schneider, J. A., . . . Colonna, M. (2020). Human and mouse

single-nucleus transcriptomics reveal TREM2-dependent and TREM2-independent cellular responses in Alzheimer's disease. *Nature Medicine*, *26*(1), 131–142. https://doi.org/10.1038/s41591-019-0695-9

SUPPLEMENTAL TABLE

A **Action potential properties**

Neuronal type	Threshold (mV)	Amplitude (mV)	Half-duration (ms)	Δθ (pA)	# cells
CB	-45.7 ± 1.2	64.8 ± 1.7	2.4 ± 0.2	6.0 ± 2.7	10
M	-44.8 ± 1.2	62.6 ± 2.5	2.4 ± 0.1	-10.6 ± 3.7	16
Statistics	#n.s.	#n.s.	#n.s.	**p=0.0013	

B **Passive electric membrane properties**

Neuronal type	Vm (mV)	Rin (MΩ)	τm (ms)	Sag (%)	Cm (pF)	# cells
CB	-64.2 ± 1.0	342.5 ± 44.7	39.1 ± 6.1	10.1 ± 3.5	272.2 ± 63.6	10
M	-64.4 ± 1.5	381.2 ± 31.2	42.8 ± 5.6	15.2 ± 2.8	235.6 ± 52.4	16
Statistics	#n.s.	#n.s.	*n.s.	#n.s.	*n.s.	

Supplemental table 1. Action potential and passive membrane cell properties from neurons recorded in Fig. 1. A, *Active properties—i.e., action potential threshold, height, and half-duration—and* ***B,*** *passive properties—i.e., resting membrane potential, input resistance, membrane time constant, voltage sag, and membrane capacitance—of layer V mPFC neurons recorded in classical aCSF in the absence of neuromodulation (No NM, n = 26 cells / 4 mice). Note that conditional bistable (CB) and monostable (M) neurons have similar passive and active properties. Statistical comparison was assessed by unpaired t test (#n.s. non significant) and nonparametric Mann-Whitney test (**p<0.01; *n.s non significant).*

II. Traumatic brain injury affects conditional bistability in rats

A. Summary

Traumatic brain injury, which is one of the leading causes of disability worldwide (Dewan et al., 2019), predominantly affects the frontal lobe (Stuss, 2011). One of the cognitive deficits caused by TBI is loss of working memory, and it can start from the TBI of injury and persist for years depending on the location and severity of the injury (Binder, 1986; McAllister et al., 2004). Working memory is the capacity to maintain transient information for seconds to minutes, (Baddeley, 1992). While the effects of TBI on object working memory have been extensively studied (Lindeløv et al., 2017; Jolly et al., 2020; Arciniega et al., 2021), there is no knowledge regarding parametric working memory, which allows memorization of transient quantitative information, such as the amplitude of a sound or the size of an object (Romo et al., 1999; Brody et al., 2003; Nieder and Mieler, 2004; Fassihi et al., 2014). Previous modeling and experimental studies indicate that, *in vivo*, parametric working memory is subserved by graded persistent activity scaling with inputs to be memorized (Major and Tank, 2004), which itself relies on synaptic reverberation activity and the presence of bistable neurons within the prefrontal cortex network. (Koulakov et al., 2002; Goldman, 2003). Conditional bistability, a novel form of bistability, which may contribute to is up-regulated by cholinergic modulation through calcium-activated non-selective cationic conductances (Rodriguez et al., 2018; Leroux et al., manuscript #1 and #2). We wondered whether the working memory loss observed after TBI could be affected by a loss of conditional bistability in the neurons of the prefrontal cortex.

To investigate the impact of traumatic brain injury on conditional bistability, we used a rat model of mild traumatic brain injury in the prefrontal cortex. *In vitro* electrophysiological techniques were used to assess conditional bistability in layer V pyramidal neurons of the prefrontal cortex. We found that conditional bistability is disrupted three weeks following traumatic brain injury through the decrease of the fast calcium-activated non-selective cationic conductance. We suggest that these modifications affect parametric working memory after traumatic frontal injury.

B. Contributions to the project

Research concept development was done by Morgane Leroux, Jeanne Paz, and Bruno Delord. Experimental design was done by Morgane Leroux and Jeanne Paz. Traumatic brain injury surgeries were done by Morgane Leroux and Agnieszka Ciesielska. Electrophysiological recordings were done by Morgane Leroux. Data analysis was done by Morgane Leroux, David Medernach, Jeanne Paz, and Bruno Delord. Writing was done by Morgane Leroux, Bruno Delord, and Jeanne Paz.

C. Introduction

Traumatic brain injury (TBI), a form of acquired brain injury, occurs when a sudden trauma —e.g., falls, assault, traffic incident—causes damage to the brain. TBI is one of the leading causes of disability worldwide, with 69 million people sustaining a TBI each year (Dewan et al., 2018). TBI gives rise to various neurological deficits, resulting in significant disability burdens. These encompass cognitive impairments, motor irregularities, psychiatric disorders, epilepsy, and disturbances in sleep patterns (Ferguson et al., 2009; Jourdan et al., 2018). The nature and severity of clinical outcomes vary depending on various parameters, including the injury location. For example, if the injury is confined to the prefrontal cortex (PFC), disabilities primarily affect executive control, problem solving, processing speed, and working memory (Levin et al., 1990; Mazaux et al., 1997; Salmond et al., 2005; Parente et al., 2011). It is important to note that TBI predominantly affects the frontal lobe (Stuss, 2011), thus working memory (WM) loss is a common feature.

WM is the fundamental ability to retain and manipulate transient information (Fuster and Alexander, 1971). Various studies have characterized TBI-related changes in object WM (Lindeløv et al., 2017; Jolly et al., 2020; Arciniega et al., 2021), but to our knowledge, the effects of TBI on parametric working memory (PWM) are still unknown. PWM retains quantitative information such as numbers, the amplitude of a sound, or the size of an object (Romo et al., 1999; Brody et al., 2003; Nieder and Miller, 2004; Fassihi et al., 2014). Despite its crucial role in daily life, little is still known yet about the neuronal mechanisms underlying PWM.

As we previously mentioned, PWM relies on graded persistent activity (GPA), which is the ability of cortical networks in the PFC to sustain activity levels that scale with the cue parameter to be remembered (Major and Tank, 2004). According to various models (Major and Tank, 2004; Brody et al., 2003), GPA is thought to result from synaptic reverberation within the PFC networks, which contain bistable units (Koulakov et al., 2002; Goldman, 2003). However, these models require precise adjustments of synaptic weights and/or the activation function (F/I curve) of individual neurons, typically around 1%, which is considerably lower than what is commonly observed in the usual plastic and regulatory signaling processes of neurons. Our previous theoretical work showed that GPA can occur in the PFC without the need for such fine-tuning of parameters. Instead, the presence of conditional bistable neurons within the networks could account for the emergence of GPA.

Rodriguez et al. (2018) demonstrated that CB neurons require both a triggering event—i.e., a phasic supra-threshold stimulation—and a tonic pulse—i.e., a sub-threshold depolarizing pulse—to sustain spiking activity. In the case of a PWM task, the triggering event represents the information to be remembered, while the tonic pulse arises from background synaptic inputs resulting from reverberation within the PFC recurrent network. Our recent studies conducted on healthy young adult rats (Leroux et al., manuscript #1) and mice (Leroux et al., manuscript #1) have shown the existence of CB in the PFC layer V, with CB depending on

cholinergic modulation via muscarinic 1 (M1)-type receptors and being mediated by increases of calcium-activated non-selective cationic (CAN) currents through TRPC5/6 channels and producing characteristic after-depolarizations (ADPs). Importantly, we were able to record *in vitro* activity sharing persistence and gradation with *in vivo* GPA in the medial PFC (mPFC) and showed how it depends on the activation of M1 receptors and CAN channels (Leroux et al., manuscript #1), confirming our prediction that CB may take part, together with synaptic reverberation, to the emergence of GPA, the neural correlate of PWM in mPFC networks.

We wondered whether CB, the neuronal correlate of PWM, is impacted by TBI. To explore this question, we performed controlled cortical impact on the PFC of young adult rats, to model mild TBI. Three-weeks after TBI or sham surgeries, *in vitro* recordings were conducted on layer V pyramidal neurons in the PFC to investigate if CB is affected by TBI at chronic time points. We found that TBI affects ADP currents and inhibits CB, which suggests that TBI in the PFC impairs PWM capacities.

D. Methods

Experimental model

We performed all experiments per protocols approved by the Institutional Animal Care and Use Committee at the University of California, San Francisco and Gladstone Institutes. Precautions were taken to minimize stress and the number of animals used in each set of experiments. Male Sprague-Dawley rats were used for these experiments and ages ranged between 8 and 12 weeks.

Controlled cortical impact

We anesthetized two to three month-old rats with 2–5% isoflurane and placed them in a stereotaxic frame. We performed a 3.5 mm craniotomy over the (mPFC centered at +3.0 mm anterior from bregma, ±0 mm lateral from the midline. Traumatic brain injury (TBI) was performed with a controlled cortical impact (CCI; Fig. 35) device (Impact One Stereotaxic Impactor for CCI, Leica Microsystems) equipped with a metal piston using the following parameters: 3 mm tip diameter, 0° angle, depth 1.5 mm from the dura, velocity 5 m/s, and 100 ms dwell time. Sham animals received identical anesthesia and craniotomy, but the injury was not delivered as previously described (Holden et al., 2021; Necula et al., 2022)

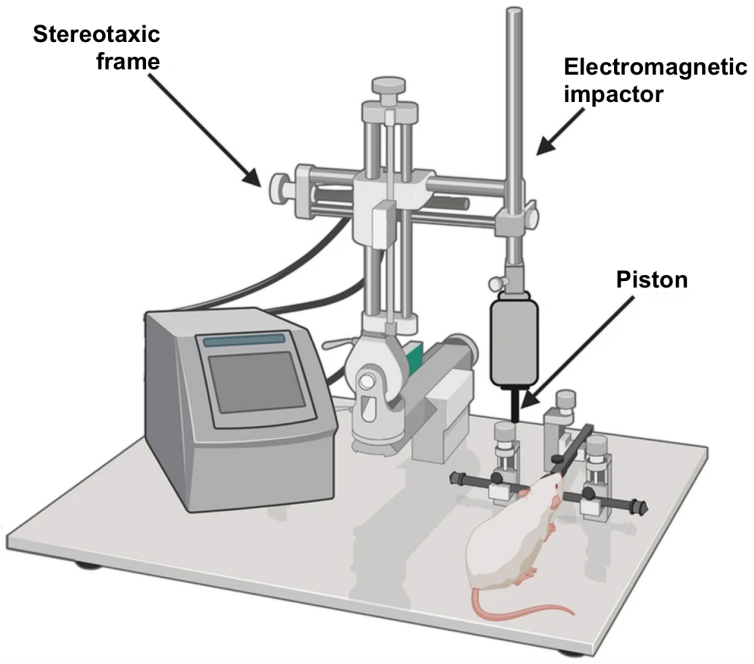

Fig. 35. Rodent model of traumatic brain injury. *Controlled cortical impact set up. Adapted from Fournier et al. (2020).*

Slice Preparation

Three weeks following CCI, rats were euthanized with 4 % isoflurane, perfused with ice-cold cutting solution containing 234 mM sucrose, 11 mM glucose, 2.5 mM KCl, 1.25 mM NaH2PO4, 10 mM MgSO4, 0.5 mM CaCl2 and 26 mM NaHCO3 equilibrated with 95 % O2 and 5 % CO2, pH 7.4, and decapitated. We prepared 250 µm-thick coronal slices containing the mPFC with a Leica VT1200 microtome (Leica Microsystems). We incubated the slices, initially at 32°C for 30 minutes and then at room temperature, in artificial cerebro-spinal fluid (aCSF) containing 126 mM NaCl, 2.5 mM KCl, 1.25 mM NaH2PO4, 1 mM MgSO4, 2 mM CaCl2, 26 mM NaHCO3, and 10 mM glucose, equilibrated with 95 % O2 and 5 % CO2, pH 7.4 as described (Paz et al., 2011, Paz et al., 2013, Clemente-Perez et al., 2017, Holden et al., 2021, Cho et al., 2022).

Patch-clamp electrophysiology

Recordings were performed as previously described (Paz et al., 2011, Paz et al., 2013, Clemente-Perez et al., 2017, Holden et al., 2021, Cho et al., 2022). We visually identified neurons in layer V of the prelimbic (PL, area 32) and infralimbic (IL, area 25) subdivisions of the mPFC by differential contrast optics with an Olympus microscope (60x objective, NA 1.1, WD 1.5 mm; SKU 1-U2M592). Recording electrodes made of borosilicate glass had a resistance of 2.5-4 MΩ when filled with intracellular solution that contained 10 mM HEPES, 11 mM EGTA, 120 mM K-Gluconate, 11 mM KCl, 1 mM MgCl2 and 1 mM CaCl2, pH adjusted to 7.4 with KOH (290

mOsm). Access resistance was monitored in all the recordings, and cells were included only if the access resistance was lower than 30 MOhm and the change of resistance was lower than 20% over the course of the experiment. We corrected offline the potentials for -15 mV liquid junction potential. All intrinsic and firing properties were recorded in the presence of the synaptic blocker kynurenic acid (2 mM, Sigma) diluted in aCSF.

Neuromodulator application

To test the contribution of cholinergic modulation, acetylcholine (ACh) muscarinic 1 receptor agonist carbamylcholine, commonly called carbachol (10µM, Sigma) was diluted in aCSF.

Identification of conditional bistable neurons

We used a *bistability* protocol derived from our previous modeling study (Rodriguez et al., 2018) and experimental study (Leroux et al., manuscript #1) to classify mPFC pyramidal layer V neurons, according to their type of spiking activity and specifically determine whether they were conditional bistable (CB) neurons, or not. The *bistability* stimulation protocol was the same as described in Leroux et al. (manuscript #1 and #2), and the same method was applied to identify CB neurons. Please, refer to the previous papers for Method details.

Quantification of after-polarization potentials

The same method to quantify after-polarization potentials as the one described in Leroux et al. (manuscript #1 and #2) was used. To sum up, we measured a potential difference after spiking which can be interpreted as the following. Positive differences correspond to the presence of currents underlying after-depolarizations (ADP; i.e., depolarizations of the membrane potential following T2) and negative differences to currents underlying after-hyperpolarizations (AHP; i.e., hyperpolarizations of the membrane potential attributable to T2). Please, refer to Leroux et al. (manuscript #1 and #2) for more Method details.

Quantification and Statistical analyses

All numerical values are given as means and error bars are standard error of the mean (SEM) unless stated otherwise. Data analysis was performed with MATLAB (SCR_001622) and GraphPad Prism 7 (SCR_002798). Percentage of CB neurons recorded in different animal groups were compared using Chi 2 test with application of the Bonferroni correction (Q = 10%). Fast, medium, and slow after-polarizations (ADP and AHP) were assessed using Scheirer-Ray-Hare test and Wilcoxon Mann Whitney test for post-hoc analysis.

E. Results

Cholinergic muscarinic 1 receptor-dependent conditional bistability is altered after traumatic brain injury in rats

In our previous experimental study, we demonstrated that conditional bistability (CB) exists in pyramidal neurons of the mPFC in healthy young adult naive rats (Leroux et al., manuscript #1). To determine whether TBI affects CB, we performed whole-cell patch-clamp recordings in coronal mPFC slices obtained from young adult rats three weeks after injury. We applied a *bistability* protocol (Leroux et al., manuscript #1 and #2), derived from our previous modeling study (Rodriguez et al., 2018), to visually identified layer V pyramidal neurons. This electrical stimulation protocol allowed us to identify CB neurons ($\Delta\theta > 0$) from M neurons ($\Delta\theta \leq 0$; refer to the Methods section from Leroux et al., manuscript #1 and #2).

We found that, under ACh modulation, neurons from naive rats and sham rats—which underwent the same surgical conditions as TBI rats but without the injury—presented similar distributions of positive $\Delta\theta$ (Fig. 36A and B, p=0.715) and similar fractions of CB neurons were recorded in both groups: respectively, 97% and 91% (Fig. 36C, p=0.349). However, after TBI and under ACh modulation, neurons presented a significantly smaller average $\Delta\theta$ (Fig. 36B, p=0.0001) than neurons from naive and sham rats. Thus, after TBI, the fraction of neurons exhibiting CB (59%) was significantly lower than in the sham group (Fig. 36C, p=0.003).

These results demonstrate that TBI affects CB, suggesting that the CAN-mediated after-depolarization currents might be reduced after TBI.

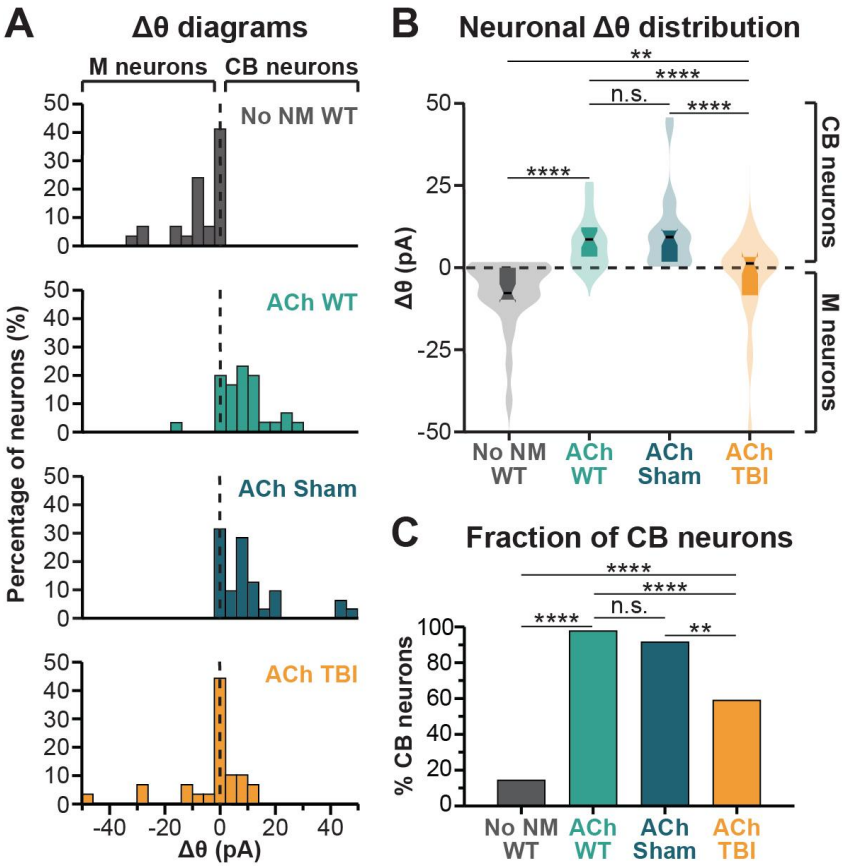

Fig. 36. Acetylcholine-dependent conditional bistability is reduced after traumatic brain injury. A, *Distribution of neuronal Δθ values in naive (WT) rats in absence of neuromodulation (No NM, n=29 cells/3 rats) and under neuromodulation by a cholinergic agonist (carbachol, ACh, n=29 cells/3 rats), in sham rats under ACh modulation (n=34 cells/3 rats), and in TBI rats under ACh modulation (n=32 cells/4 rats).* ***B,*** *Average Δθ values in the different groups. Statistical significance was assessed by Scheirer-Ray-Hare test and Wilcoxon Mann Whitney test for the post hoc analysis (****p<0.0001; ***p<0.001; **p<0.01; *p<0.05; n.s. non significant). Violin plot boxes indicate the 75th, 50th and 25th percentiles (upper border, black line, lower line.* ***C,*** *Fractions of conditional bistable (CB) neurons recorded in the different groups. Statistical significance was assessed by chi 2 test with Bonferroni-Sudak correction (****p<0.0001; **p<0.01; n.s. non significant). Data from naive (WT) rats are also used in Leroux et al. (manuscrit #1).*

Inhibition of conditional bistability after traumatic brain injury is caused by a decrease in after-depolarization potentials

Persistent spiking and bistability in layer V mPFC pyramidal neurons involve fast and slow calcium-activated non-selective cationic (CAN) depolarizing currents characterized by activation time constants of a few tens of milliseconds (I_{fADP}; Haj-Dahmane and Andrade, 1997, 1999) and over a second (I_{sADP}; Andrade, 1991; Haj-Dahmane and Andrade, 1998, 1999; Ratté et al., 2018),

respectively. Following spiking activity, these currents generate depolarizations of the membrane potential called after-depolarizations (ADP). In contrast, medium calcium-activated potassium currents (activation time constant of 100-200 ms; I_{mAHP}; Haj-Dahmane and Andrade, 1998; Satake et al., 2008; Ratté et al., 2018) generate hyperpolarizations of the membrane potential following spiking called after-hyperpolarizations (AHP).

In this study, we examined the potential involvement of I_{fADP}, I_{mADP}, and I_{mADP} in CB and how they are affected after TBI by measuring the after-polarizations following spiking. These measures were achieved following persistent activity during our *bistability* protocol (Fig. 37A; Leroux et al., manuscript #1 and #2) and computed as the relative difference of polarization following persistent spiking minus that observed in its absence (*NS2* - *S1*, see Methods in Leroux et al. (manuscript #1) for more details), to specifically extract CB-related persistent activity currents (Fig. 37B). We specifically focused on three components: the fast (F, 0-50 ms), medium (M, 50-350 ms), and slow (S, 350-500 ms) after-polarizations. These components allowed us to quantify the relative strength of the three currents based on their distinctive kinetics and assess the ADP/AHP balance. Positive values (Fig. 37B) indicated a depolarization of the membrane potential caused by increased activation of CAN currents or decreased activation of AHP currents during CB-related persistent spiking, while negative values (Fig. 37B) indicated decreased CAN and/or increased AHP currents (refer to the Methods section from Leroux et al., manuscript #1 and #2).

Despite a similar fraction of CB neurons recorded in naive and sham groups, under ACh neuromodulation, differences in after-polarization currents were observed. If both groups exhibited statistically similar fast and slow ADP (Fig. 37C, respectively, p=0.077 and p=0.157), neurons from sham rats were characterized by a lower medium ADP than naive neurons (p=0.004). This finding suggests that I_{mAHP} were stronger in the sham group, but this was not sufficient to impact the fraction of CB neurons recorded.

After TBI, fast and medium ADP were significantly lower than in naive rats under cholinergic manipulation (Fig. 37C, respectively, p=0.001 and p=0.0001), suggesting a decrease in fast CAN and an increase in medium AHP conductances. The slow ADP also presented a substantial decrease, although not significant (p=0.053). However, in spite of a significant difference in fraction of CB neurons recorded between sham and TBI groups, medium and slow after-polarization potentials were similar (respectively, p=0.082 and p=0.529). Only fast ADP appeared smaller in neurons from TBI rats than from sham rats (p=0.002). These results suggest that the reduction in fast ADP was sufficient to limit CB in TBI rats.

Altogether, these findings suggest that acetylcholine-dependent CB is mediated through increases of both fast and slow CAN currents, with the fast ADP bringing an essential contribution to the positive feedback responsible for self-sustained spiking in CB neurons.

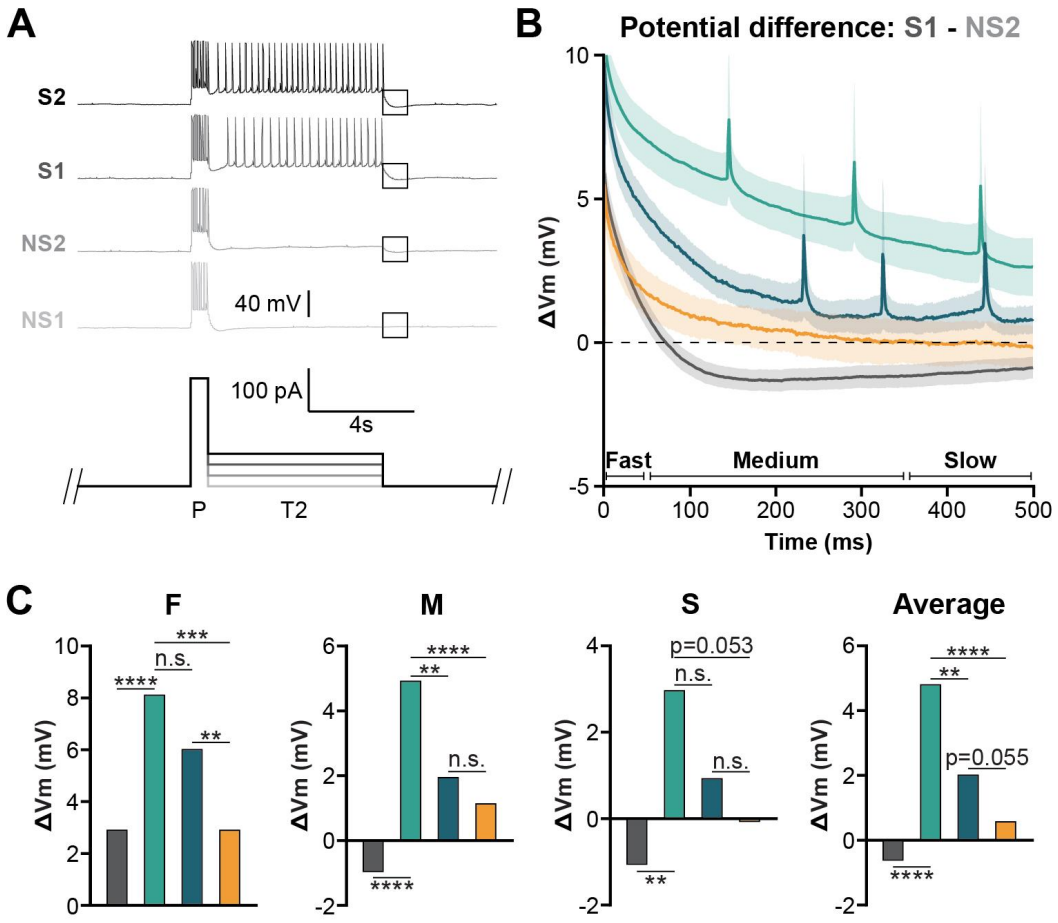

Fig. 37. After traumatic brain injury, fast and slow after-depolarizations (ADP) are reduced, which prevents conditional bistability. A, *Method to identify currents implicated in conditional bistability. Four sweeps of interest were identified in the bistability protocol: NS1 (No Spike 1, first sweep upon which the neuron doesn't fire on T1 and T2); NS2 (No Spike 2, last sweep upon which the neuron doesn't fire on T1 and T2); S1 (Spike 1, first sweep upon which the neuron fires on T1 and T2); and S2 (Spike 2, last sweep upon which the neuron fires on T1 and T2), upon which membrane potentials were extracted during the 500 ms following T2 (black squares).* ***B,*** *Average difference of the membrane potential between sweeps S1 and NS2, after T2 indicates spike-triggered currents activated during CB-related self-sustained persistent activity.* ***C,*** *Average membrane potential difference in the ranges 0-50 ms (fast after-polarization, F), 50-350 ms (medium after-polarization, M), 350-500 ms (slow after-polarization, S) and across the whole window considered (0-500 ms, average after-polarization) after T2. Statistical significance was assessed by Scheirer-Ray-Hare test and Wilcoxon Mann Whitney test for the post hoc analysis (****p<0.0001; ***p<0.001; **p<0.01; *p<0.05; n.s. non significant).*

F. Discussion

Fast after-depolarization potentials are essential to elicit acetylcholine-dependent conditional bistability

In Leroux et al. (manuscript #1), in naive rats, CB depends on the specific activation of M1 receptor which leads to the increase in fast, medium and slow ADP. These increases in the ADP following spiking are caused by the activation of CAN channels by the increase in intracellular Ca^{2+} levels through 1) the Ca_T channels (Haj-Dahmane and Andrade, 1998), and 2) an intracellular signaling pathways involving Protein Gq, inositol triphosphate (IP3), and IP3 R localized on the endoplasmic reticulum (Dasari et al., 2017).

In our previous study (Leroux et al., manuscript #1), flufenamic acid (FFA), a pharmacological blocker of TRPC channels carrying CAN currents, inhibits slow ADP (Haj-Dahmane et Andrade, 1999; Zhang et Seguela, 2010; Ratté et al., 2018), but has little effect on fast ADP (Haj-Dahmane et Andrade, 1999). This observation is accounted for by a strong decrease in slow CAN currents, resulting in a smaller fraction of CB neurons recorded under nodulation of ACh+FFA. However, this fraction of CB neurons recorded is not as small as in the No NM condition, suggesting a potential role of the fast CAN current in CB.

Here, we observed results consistent with the idea that fast CAN currents are important in CB. Under ACh neuromodulation, both naive and sham rats presented a similar high fraction of CB neurons recorded. Both neurons from naive and sham rats presented similar levels of fast ADP currents, but medium and slow components were dominated by AHP currents in neurons from sham rats, compared to those of naive rats. These results suggest that, in a situation where slow CAN currents are largely counter-balanced by AHP current, fast CAN currents are sufficient to elicit CB in mPFC neurons.

Traumatic brain injury down-regulates conditional bistability, through the increase of medium after-hyperpolarizations

After TBI and under ACh neuromodulation, both fast and slow CAN currents significantly decreased, likely through the increase of medium AHP currents. We hypothesize that an over-activation of medium AHP channels caused the fraction of CB neurons recorded to drop in TBI rats. *What could explain an over-activation of AHP channels in TBI?*

Various studies showed that TBI in rodents decreases acetylcholinesterase function (Carver et al., 2021) and increases the affinity of M1 receptor to ACh (Jiang et al., 1994), which resulted in an overactivation of M1 receptor (Delahunty, 1992; Carver et al., 2021) in the first couple of weeks following injury. The consequences are an increased M1/Gq coupling and an overproduction of IP3, which overactivates TRPC channels (Delahunty, 1992; Carver et al., 2021). Here, and in our previous studies (Leroux et al., manuscript #1 and #2), we showed that

M1 activation is crucial for the TRPC channels that mediate CAN currents, and more generally beneficial for parametric mnemonic mechanisms.

However, it has been shown that the over-activation of M1 receptors leads to hyper-excitability in the networks and seizures in the hippocampus and cortex (Carver et al., 2021). Moreover, administration of scopolamine, a M1 receptor blocker, during or soon after a traumatic brain injury procedure reverses working memory impairments caused by the injury in mice (Jiang et al., 1994; Rashid and Ahmed, 2023). From these studies, we can conclude that a balanced level of M1 receptor activation is required for cortical functions, and cholinergic over-activation disrupts mnemonic functions.

Hagenston et al. (2008) showed that AHP conductances are activated at higher concentrations of intracellular Ca^{2+}, compared to CAN conductances. Thus, we can imagine that, in our study, the pathological activation of M1 receptor following TBI drastically increased intracellular Ca^{2+} levels and AHP channels were overactivated compared with sham rats, leading to the increase of medium AHP and the down-regulation of neuronal CB. Our finding about TBI reducing CB three weeks following injury suggest that TBI could cause PWM impairments. This hypothesis should be confirmed by a limited emergence of GPA *in vitro* in PFC networks (Leroux et al., manuscript #1) and by *in vivo* poor performance in a PWM task (Fassihi et al., 2014).

CHAPTER III

Physiological mechanisms and pathological disruption of synaptic excitation in interneurons and network activity in the somatosensory cortex

I. Summary

Mafb and *c-Maf* transcription factors are expressed in medial ganglionic eminence lineages, beginning in progenitors and continuing into mature GABAergic parvalbumin-positive (PV+) and somatostatin-positive (SST+) interneurons, but not in cortical projection neurons (Cobos et al., 2006; Zhao et al., 2008; McKinsey et al., 2013). However, the role of *Mafb* and *c-Maf* in the function of SST+ and PV+ cortical interneurons (CINs) remains unknown. Here, *Mafb* and *c-Maf* were conditionally deleted in either SST+ or PV+ interneurons. We found that *c-Maf* but not *Mafb* deletion specifically in SST+ but not PV+ interneurons resulted in reduced numbers of excitatory synapses onto SST+ neurons, reduced synaptic excitation, and caused epileptic activity. Also, *c-Maf* deletion in SST+ CINs augmented the density of PV+ CINs in superficial layers of the somatosensory cortex, whereas *Mafb* deletion in SST+ CINs reduced the density of SST+ CINs in superficial layers. Deleting *Mafb* or *c-Maf* in PV+ CINs did not affect PV+ neuronal counts in the somatosensory cortex. Thus, *Maf* genes are a key regulator of SST+ CIN function and its loss results in epilepsy.

II. Contributions to the project

Research concept development was done by John Rubenstein and Jeanne Paz. Experimental design was done by Morgane Leroux, Jia Hu, John Rubenstein, and Jeanne Paz. Electrophysiological recordings were done by Morgane Leroux. Histology was done by Jia Hu. Electroencephalographic recordings were done by Irene Lew. Data analysis was done by Morgane Leroux, Jia Hu, John Rubenstein, and Jeanne Paz. Writing was done by Morgane Leroux, Jia Hu, John Rubenstein, and Jeanne Paz.

III. Manuscript #3. *Mafb* and *c-Maf* regulate the function of somatostatin-positive cortical interneurons and epileptic activity

Mafb and *c-Maf* regulate the function of somatostatin-positive cortical interneurons and epileptic activity

Leroux MA*[1,2,3,4], Hu JS*[5], Pai ELL[5,6], Lew I[1], Rubenstein JLR[5,6#], Paz JT[1,2,5,6#]

[1]Gladstone Institute of Neurological Disease, Gladstone Institutes, San Francisco CA 94158, USA

[2]The Kavli Institute for Fundamental Neuroscience, and Neurology Department, University of California San Francisco, San Francisco CA 94158, USA

[3]Institut des Systèmes Intelligents et de Robotique (ISIR), Sorbonne University, 4 Place Jussieu, 75005 Paris, France

[4]Brain-Cognition-Behavior Graduate Program, Sorbonne University, 4 Place Jussieu, 75005 Paris, France, Paris, France

[5]University of California San Francisco, Department of Psychiatry, San Francisco CA 94158, USA

[6]Neuroscience Graduate Program, University of California, San Francisco, San Francisco, CA 94158, USA

*Co-first authors. Contributed equally to the work.

#Correspondence to:

jeanne.paz@gladstone.ucsf.edu

john.rubenstein@ucsf.edu

Keywords: MAF transcription factor; Parvalbumin cortical interneuron; Somatostatin cortical interneuron; Electrophysiology; Cellular and synaptic physiology; Electroencephalography; Epilepsy

Funding: This work was supported by the following research grants: National Institute of Mental Health (NIMH) R01 MH081880 and NIMH R37/R01 MH049428 (to JLRR)

Author contributions: Funding acquisition, JTP and JLRR; Concept Development, JTP and JLRR; Experimental Design, MAL, JSH, JLRR, JTP; Electrophysiological Recordings, MAL; Supervision: JTP supervised electrophysiological recordings, Histology: JSH; JLRR supervised histology stainings. Data Analysis, MAL, JSH, JLRR, JTP. Writing, MAL, JTP. Manuscript editing: all authors.

Competing interests: J.L.R.R. is cofounder, stockholder, and currently on the scientific board of Neurona Therapeutics, a company studying the potential therapeutic use of interneuron transplantation.

Data and materials availability: All data and materials described in the manuscript or supplementary materials will be made available upon request.

Acknowledgements: We thank Francoise Chanut for critical review of the manuscript.

ABSTRACT

Mafb and *c-Maf* transcription factors are expressed in medial ganglionic eminence lineages, beginning in progenitors and continuing into mature GABAergic parvalbumin-positive (PV+) and somatostatin-positive (SST+) interneurons, but not in cortical projection neurons. However, the role of *Mafb* and *c-Maf* in the function of SST+ and PV+ cortical interneurons (CINs) remains unknown. Here, *Mafb* and *c-Maf* were conditionally deleted in either SST+ or PV+ interneurons. We found that *c-Maf* but not *Mafb* deletion specifically in SST+ but not PV+ interneurons resulted in reduced numbers of excitatory synapses onto SST+ neurons, reduced synaptic excitation, and caused epileptic activity. Also, *c-Maf* deletion in SST+ CINs augmented the density of PV+ CINs in superficial layers of the somatosensory cortex, whereas *Mafb* deletion in SST+ CINs reduced the density of SST+ CINs in superficial layers. Deleting *Mafb* or *c-Maf* in PV+ CINs did not affect PV+ neuronal counts in the somatosensory cortex. Thus, *Maf* genes are a key regulator of SST+ CIN function and its loss results in epilepsy.

INTRODUCTION

Some symptoms of neurological and neuropsychiatric disorders—i.e., epilepsy, autism spectrum disorder, and schizophrenia—are believed to be linked to disturbances in the development and maturation of the neocortex. Circuit imbalance in the excitation/inhibition (E/I) ratio could contribute to these symptoms (Rubenstein and Merzenich, 2003; Chao et al., 2010; Yizhar et al., 2011; Han et al., 2012). Cortical Interneurons (CINs) that regulate the GABAergic tone and thus E/I balance in the cortex exhibit diverse morphological, connectivity, molecular, and electrophysiological properties (Huang et al., 2007; Kepecs and Fishell, 2014; Kessaris et al., 2014). These diverse properties of CINs play a crucial role in maintaining the E/I balance in check within the neocortex.

Mature CINs are characterized by the expression of certain molecular markers. Somatostatin-positive (SST+) and parvalbumin-positive (PV+) CINs originate from a subpallial telencephalon region called the medial ganglionic eminences (MGE) and their development is regulated by a combination of transcription factors (TFs) (Wonders and Anderson, 2006; Gelman et al., 2011; Hu et al., 2017; Lim et al., 2018). *Mafb* and *c-Maf* are part of the extensive *Maf* TF family, and either independently or in combination, play crucial roles in controlling neuronal fate and differentiation in brain development. For instance, *Mafb* is involved in regulating the regional patterning of the embryonic hindbrain (Cordes and Barsh, 1994) and plays a role in the formation of auditory ribbon synapses, which are essential for activating inner hair cells (Lu et al., 2011; Yu et al., 2013). On the other hand, *c-Maf* participates in the differentiation of touch receptors in the peripheral nervous system (Wende et al., 2012). In addition, we demonstrated in our previous study that *Mafb* and *c-Maf* affect MGE-derived neuronal maturation, control the timing of when factors specify SST+ and PV+ CIN fate, and impact cellular properties and synaptic excitation (Pai et al., 2019).

Our previous study (Pai et al., 2019) indicated that *Maf* genes in CINs play a crucial role in cortical network excitability. However, how the *Maf* genes regulate the properties of specific cell types—i.e., SST+ and PV+ CINs—remains unknown. Here, we report the individual functions of *Mafb* and *c-Maf* in SST+ and PV+ MGE-derived CINs after conditional deletion in SST+ or PV+ cells.

METHODS

Contact for Reagents and Resource Sharing

Further information and requests for resources and reagents should be directed to and will be fulfilled by the Lead Contacts, Jeanne Paz (jeanne.paz@gladstone.ucsf.edu) and John Rubenstein (john.rubenstein@ucsf.edu).

Experimental model

All protocols were approved by the Institutional Animal Care and Use Committee at the University of California, San Francisco and Gladstone Institutes. Precautions were taken to minimize stress and the number of animals used in each set of experiments. Mice were separately housed after surgical implants.

The following mouse strains have been previously reported: *tdTomato*$^{lox/+}$ (Ai14) Cre-reporter (Madisen et al., 2010), *Maf(c-Maf)*$^{lox/+}$ (Wende et al., 2012), *Mafb*$^{lox/+}$ (Yu et al., 2013), *Somatostatin-IRES-Cre* (Taniguchi et al., 2011), *Parvalbumin-Cre* (Hippenmeyer et al., 2005). All strains were on a mixed C57BL/6 and CD1 background. All animals were housed in a vivarium with a 12 h light/12 h dark cycle. Postnatal animals used for experiments were kept with their littermates. Males and females were both used in all experiments.

The Maf flox allele (in chromosome 8) contains loxP sites 1547 bp upstream (outside of its lone exon) and 411 bp downstream of the open reading frame (within its lone exon) for the *Maf* gene. The *Mafb* flox allele (in chromosome 2) contains loxP sites upstream (outside of its lone exon) and at the end of the exon for the *Mafb* gene. Recombination for *Somatostatin-IRES-Cre* begins around E12.5. Recombination for *Parvalbumin-Cre* begins around P10.

Immunohistochemistry

Mice were anesthetized with intraperitoneal avertin (0.015 ml/g of a 2.5% solution) and perfused transcardially with PBS and then with 4% PFA, followed by brain isolation, 1 hour fixation for synapse immunohistochemistry or overnight fixation for all other immunohistochemistry or *in situ* hybridization, 2 days of cryoprotection and microtome sectioning (coronal, 40 µm).

For all immunohistochemistry on postnatal brains, staining was carried out on free-floating sections as described previously (Stanco et al., 2014). For synapse immunohistochemistry, sections were pre-treated with pepsin for 10 minutes at 37 degree C to enhance the staining as described before (Corteen et al. 2011), and sections were incubated with primary antibodies for two days. We performed all immunohistochemistry on $n \geq 3$ biological replicates for each control and mutant.

In situ hybridization

We performed *in situ* hybridization on a minimum of *n*=3 biological replicates for each control and mutant. In each case, a rostrocaudal series of at least ten sections was examined. *In situ* hybridizations were performed using digoxigenin-labeled riboprobes as described previously (Hoch et al., 2015a,b).

Image acquisition and processing

Fluorescent IHC images in Figure 3 were taken using a Coolsnap camera (Photometrics) mounted on a Nikon Eclipse 80i microscope using NIS Elements acquisition software (Nikon). Brightfield ISH images in Figure 3 were taken using a DP70 camera (Olympus) mounted on an Olympus SZX7 microscope. Brightness and contrast were adjusted, and images merged using ImageJ software. Synapse IHC images from neocortical layers II/III were taken on an OMX-SR confocal microscope with an 60x objective at 1024x1024 pixels of resolution from the Center for Advanced Light Microscopy at UCSF. Synapse IHC images were then aligned and deconvolved before synapse counting.

Cell and synapse counting

For assessing cell densities, 10× images were taken at the somatosensory cortex at postnatal ages from two or three non adjacent sections and from both hemispheres for each replicate. A box of a defined area was drawn over a region of interest. Cells were counted within that box and were divided by the box area. Cell density quantifications were done in a blinded manner. For lamination counts, we used DAPI to subdivide neocortical layers.

For synapse counting, confocal image stacks (0.25 um step size) were processed with ImageJ. Background subtraction was applied and colocalized the channels. We counted the number of synapses that colocalized with vGlut1 and PSD95 in each focal plane. Synapse numbers were then normalized to the length of the dendrite. Length of the dendrite was determined by the segmented line that was drawn over the dendrite where synapses were counted. Synapse density quantifications were done in a blinded manner.

Slice preparation for electrophysiology

Mice were euthanized with 4% isoflurane, perfused with ice-cold sucrose cutting solution containing 234 mM sucrose, 2.5 mM KCl, 1.25 mM NaH2PO4, 10 mM MgSO4, 0.5 mM CaCl2, 26 mM NaHCO3, and 11 mM glucose, equilibrated with 95% O2 and 5% CO2, pH 7.4, and decapitated. We prepared 250 µm-thick horizontal thalamic slices containing Somatosensory Barrel Cortex with a Leica VT1200 microtome (Leica Microsystems). We incubated the slices, initially at 32°C for 1 h and then at 24–26°C, in artificial cerebro-spinal fluid (ACSF) containing 126 mM NaCl, 2.5 mM KCl, 1.25 mM NaH2PO4, 2 mM MgCl2, 2 mM CaCl2, 26 mM NaHCO3, and 10 mM glucose, equilibrated with 95% O2 and 5% CO2, pH 7.4 as described in (Clemente-Perez et al., 2017; Pai et al., 2019; Holden et al., 2021; Cho et al., 2022).

Whole-cell patch-clamp electrophysiology

Recordings were performed as previously described (Clemente-Perez et al., 2017; Pai et al., 2019; Holden et al., 2021; Cho et al., 2022). We visually identified interneurons originating from the MGE based on their expression of tdTomato. Neurons were identified by differential contrast optics with a Zeiss (Oberkochen) Axioskop microscope and an infrared video camera. Recording electrodes made of borosilicate glass had a resistance of 2.5–4 MΩ when filled with intracellular solution. Access resistance was monitored in all the recordings, and cells were included for analysis only if the access resistance was < 25 MΩ. The access resistance was similar in all SST+ and PV+ neurons (WT, *Mafb* cKO, and *c-Maf* cKO; $p > 0.5$), suggesting that differences between genotypes were not due to the quality of the whole-cell patch-clamp recording. Spontaneous excitatory post-synaptic currents (sEPSCs) were recorded in the presence of picrotoxin (50 μM, Tocris). For sEPSCs and current-clamp recordings, the internal solution contained 120 mM potassium gluconate, 11 mM KCl, 1 mM MgCl2, 1 mM CaCl2, 10 mM HEPES, and 1 mM EGTA, pH adjusted to 7.4 with KOH (290 mOsm). The experiments were performed by blinded observers. To test for differences in the sEPSC amplitude, frequency, and decay time constant across groups (comparison between group means), we performed a One Way ANOVA Kruskal-Wallis followed by Dunn's multiple comparisons test. Differences were regarded as significant if $p < 0.05$.

F-I plots were generated using Graphpad Prism. To test for differences in the F-I dataset across genotypes (comparison between group means), we performed a regular two-way ANOVA followed by Tukey's post hoc test for multiple comparisons. Differences were regarded as significant if $p < 0.05$. For statistical analysis, we included only the current pulses that were presented to all genotypes (within cell type). In addition, we only included cells which were recorded at least two of the included current pulses. For both SST+ and PV+ cells, we analyzed responses at current pulses of 20, 40, 60, 80, 100, 120, 140, 160, 180, and 200 pA.

Surgical implantation of devices for electroencephalographic recordings in freely behaving mice

The devices for electrocorticography (ECoG) recordings in freely behaving mice were all custom made in the Paz lab. We designed devices containing multiple screws for acquisition of ECoG signals recorded from tungsten electrode wires. Cortical screws were implanted bilaterally in S1 (−0.5 mm posterior from Bregma, ±3.25 mm lateral), in PFC (+1.78 anterior from Bregma, ±0 mm lateral), and in right V1 (−2.9 mm posterior from Bregma, +3.25 mm lateral).

Mice were allowed to recover for at least 1 week before recording. ECoG signals were recorded using RZ5 (TDT) and sampled at 1221 Hz. A video camera that was synchronized to the signal acquisition was used to monitor the animals during the recordings. Animals were briefly anesthetized with ~2% isoflurane at the start of each recording to connect for recording. Each recording trial lasted 60–180 min. To control for circadian rhythms, we housed our animals using a regular light/dark cycle, and performed recordings between roughly 9:00 AM and 6:00 PM. All the recordings were performed during wakefulness. The location of the optrodes was

validated by histology after euthanasia in mice that did not experience sudden death and whose brains we were able to recover and process.

Quantification and Statistical Analysis

All bar graphs were shown as mean ± SEM. All statistical analyses were performed using Graphpad Prism (version 7) and a p-value of < 0.05 was considered significant. The specific n for each experiment can be found in the Results section, in the Figure legends or in supplementary tables.

For all cell and synapse counts performed for immunohistochemistry and in situ hybridization, we used the cell counter plug-in in FIJI software. All immunohistochemistry and in situ hybridization statistical analyses were carried out on SPSS15 software and Microsoft Excel. Normal distribution was assessed using a Shapiro-Wilk test and equal variance was assessed using a Levene's test. Statistical analysis of the cell density was done using two-tailed Student's t-test or Scheirer-Ray-Hare test and Wilcoxon Mann Whitney test for the post hoc analysis. Statistical analysis of the number of excitatory synapses was done using Scheirer-Ray-Hare test and Wilcoxon Mann Whitney test for the post hoc analysis. All data were collected and processed blindly during the data analysis. No data were randomized.

Analysis of the electrophysiological parameters was performed using Clampfit (version 10.7). All statistical analyses were carried out on GraphPad Prism software (version 9.2.0). Statistical analysis of the spontaneous excitatory post-synaptic currents (sEPSCs) features was done using Kruskal-Wallis test and Dunn's test for the post hoc analysis. Statistical analysis of the cumulative sEPSC interevent intervals was done using Kolmogorov-Smirnov test on cumulative distribution. Statistical analysis of the F-I curves was done using Two-way ANOVA test and Tukey's multiple comparisons test for the post hoc analysis. Statistical analysis of the action potential and passive membrane properties was done using Kruskal-Wallis test and Dunn's multiple comparisons test for the post hoc analysis.

Analysis of the epileptic spikes in ECoG was performed using Spike2 (version 7.20, Cambridge Electronic Design, Cambridge, UK; Holden et al., 2021). Epileptic spikes were defined as sharp events that exceeded the double derivative of 15 V/s/s and larger than 5 x the RMS of the baseline ECoG. All detected events were visually validated by a scientist blinded to the groups. Statistical analysis was carried out on GraphPad Prism software (version 9.2.0) and done using Kruskal-Wallis test and Dunn's multiple comparisons test for the post hoc analysis.

RESULTS

Effect of c-Maf or *Mafb* deletion in SST+ or PV+ interneurons on their synaptic excitation

Mafb or *c-Maf* were conditionally deleted in SST+—at pre-embryonic day 14 (E14)—or PV+—at postnatal day 10 (P10)—CINs in order to generate SST+ *Mafb* cKO, SST+ *c-Maf* cKO, PV+ *Mafb* cKO, and PV+ *c-Maf* mice. To investigate excitatory inputs onto cortical interneurons (CINs) of the primary somatosensory (S1) cortex, we measured the sEPSCs (Fig. 1A, B). The amplitude, decay tau, and charge of sEPSCs of SST+ CINs from SST+ *Mafb* cKO and SST+ *c-Maf* cKO, were similar to SST+ WT mice (Fig. 1C, D). The average sEPSC instantaneous interval of SST+ CINs was longer in SST+ *c-Maf* cKO than in WT and SST+ *Mafb* cKO (Fig. 1E; p=0.0005 and p=0.00002, respectively). In addition, the average sEPSC instantaneous interval of SST+ CINs was smaller in SST+ *Mafb* cKO than in WT (Fig. 1F, G). Spontaneous EPSC instantaneous frequency of SST+ CINs was higher in SST+ *c-Maf* cKO than in SST+ WT and SST+ *Mafb* CINs (Fig. 1G; p=0.0008 and p=0.00009, respectively).

Moreover, we quantified the density of excitatory synapses in SST+ *Mafb* cKO, and in SST+ *c-Maf* cKO CINs, using vGlut1 and PSD95 markers (Fig. 2A). We observed that *c-Maf* deletion in SST+ CINs decreases their number of excitatory synapses (Fig. 2B). Thus, the overall reduction in synaptic excitation in SST+ *c-Maf* cKO CINs might be due, at least in part, toa decreased density of excitatory synapses in SST+ CINs.

In PV+ CINs, the sEPSC amplitude, decay tau, charge (Fig. 1C and D), interval between sEPSCs (Fig. 1E and F), and thus the instantaneous frequency (Fig. 1G) were similar in PV+ *Mafb* cKO, PV+ *c-Maf* cKO mice, and WT littermates. These results show that *Mafb* or *c-Maf* deletions in PV+ CINs do not affect their synaptic excitation.

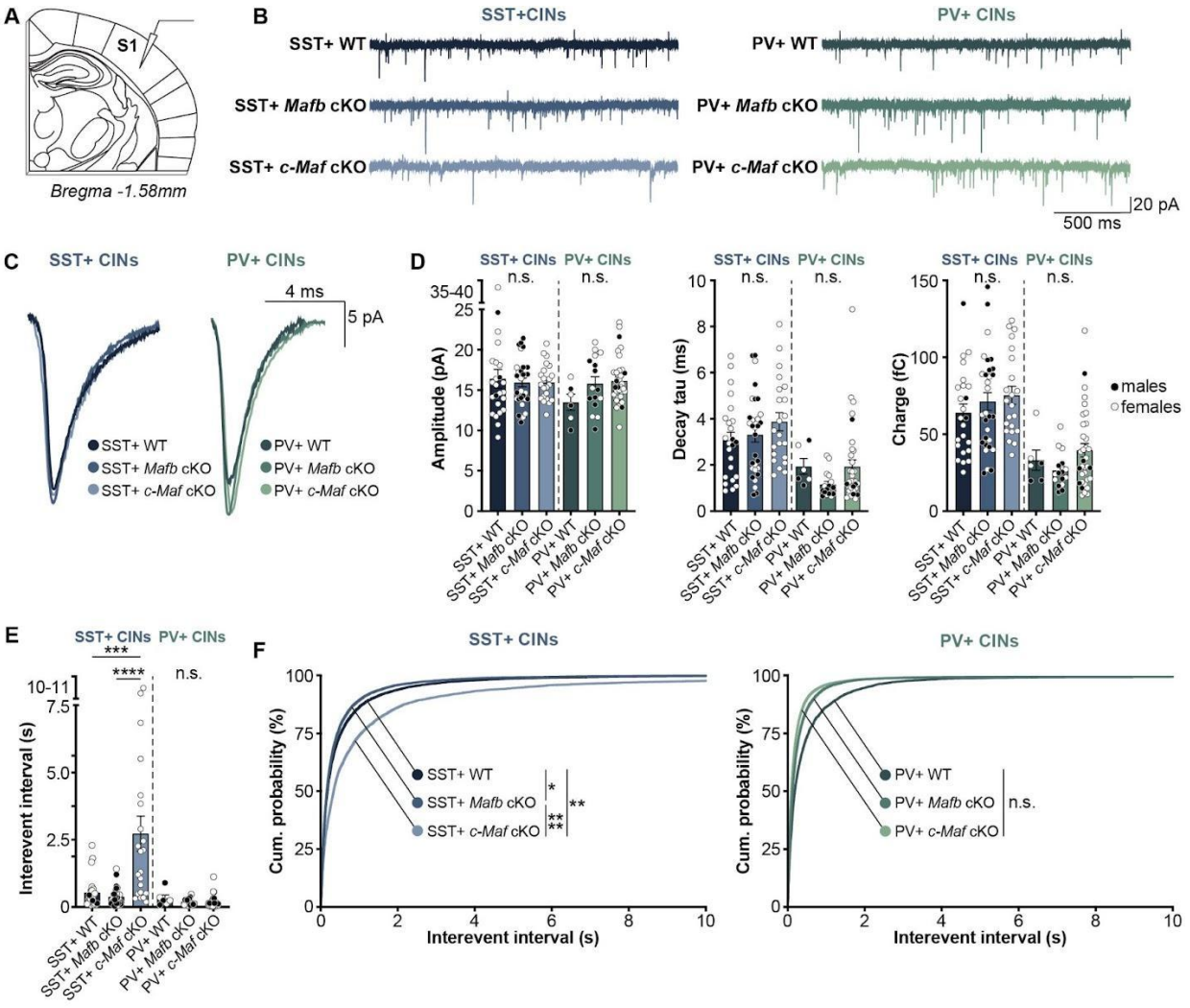

G

Spontaneous EPSCs

Cell type	Genotype	Amplitude (pA)	Decay τ (ms)	Charge (fC)	Inst. Frequency (Hz)	Inter. Interval (ms)	# cells	# mice
SST+	SST+ WT	17.1 ± 1.2	3.07 ± 0.35	64.0 ± 5.7	4.99 ± 0.96	534.4 ± 123.4	26	3
	SST+ *Mafb* cKO	16.6 ± 0.6	3.31 ± 0.32	71.3 ± 5.7	5.47 ± 1.02	383.8 ± 61.6	29	3
	SST+ *c-Maf* cKO	16.6 ± 0.5	3.87 ± 0.39	75.4 ± 5.8	1.38 ± 0.31	2728.0 ± 649.5	22	2
Kruskal-Wallis, Dunn's *post-hoc*		n.s.	n.s.	n.s.	p=0.0008 (WT vs. *c-Maf*) p=0.00009 (*Mafb* vs. *c-Maf*)	p=0.0005 (WT vs. *c-Maf*) p=0.00002 (*Mafb* vs. *c-Maf*)		
PV+	PV+ WT	14.1 ± 1.1	1.94 ± 0.34	33.1 ± 6.6	5.46 ± 1.71	323.7 ± 121.4	6	3
	PV+ *Mafb* cKO	16.4 ± 0.9	1.15 ± 0.14	26.4 ± 2.9	8.09 ± 1.35	196.8 ± 32.9	17	4
	PV+ *c-Maf* cKO	16.8 ± 0.5	1.93 ± 0.29	39.5 ± 4.3	13.36 ± 1.67	169.4 ± 38.3	34	4
Kruskal-Wallis, Dunn's *post-hoc*		n.s.	n.s.	n.s.	n.s.	n.s.		

Figure 1. Effect of Mafb or c-Maf deletion in SST+ or PV+ CINs on their sEPSC properties. A, *Acute brain slice of the somatosensory (S1) cortex prepared for whole-cell recordings of CINs from WT, SST+ Mafb cKO, SST+ c-Maf cKO, PV+ Mafb cKO, and PV+ c-Maf cKO mice.* ***B,*** *Representative traces of spontaneous EPSCs (sEPSCs) from CINs in the S1 layer II/III.* ***C,*** *Overlaid average sEPSCs from the representative cells depicted in (B).* ***D*** *and* ***E,*** *Quantification (means ± SEM) of the amplitude, decay time constant, charge (D), and interevent interval (E) of sEPSCs (Vhold = -70 mV) in CINs. Statistical significance was assessed by Kruskal-Wallis test, Dunn's post-hoc analysis for multiple comparisons*

*(****p<0.0001; ***p<0.001; n.s. non significant). **F,** Cumulative sEPSC interevent intervals. Statistical significance was assessed by Kolmogorov-Smirnov test on cumulative distribution (****p<0.0001; **p<0.01; *p<0.05; n.s. non significant). **G,** Quantification of sEPSCs properties. Data are expressed as the mean ± SEM. Statistical significance was assessed by Kruskal-Wallis test, Dunn's post-hoc analysis for multiple comparisons. All electrophysiological properties were measured in 3-5 month-old mice.*

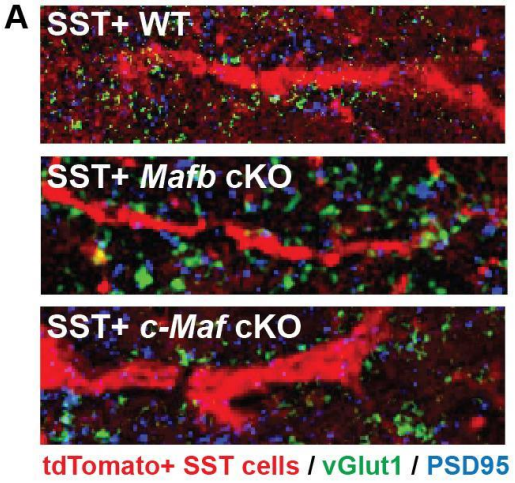

Figure 2. Effect of Mafb or c-Maf deletion in SST+ CINs on their excitatory synapse density on proximal dendrites in adult mice. A, *Immunofluorescent images from somatosensory cortices from WT, SST+ Mafb cKO, and SST+ c-Maf cKO mice. CINs are marked with tdTomato and excitatory synapses are marked with vGlut1 and PSD95.* ***B,*** *Quantification of the number of excitatory synapses/pixel in the somatosensory cortex. Statistical significance was assessed by Scheirer-Ray-Hare test and Wilcoxon Mann Whitney test for the post hoc analysis (*p<0.05). These results were obtained from 8-10 month-old mice, age that matches the age at which the in vivo electroencephalographic activity was recorded.*

Effect of *c-Maf* or *Mafb* deletion in SST+ or PV+ interneurons on their active and passive membrane properties

We measured the mean firing frequency in response to the increasing intensity of intracellular positive current injections in 1) SST+ CINs from SST+ *Mafb* cKO, SST+ *c-Maf* cKO, and SST WT mice, and in 2) PV+ CINs from PV+ *Mafb* cKO, PV+ *c-Maf* mice and PV WT mice (F-I plots, Fig. 3A and B). We found that, in SST+ CINs, the firing frequency (Fig. 3A), as well as the action potential threshold, half-duration, and rheobase (Fig. 3C), were similar in SST+ WT, SST+ *Mafb* cKO, and SST+ *c-Maf* cKO mice. However, the action potential amplitude in SST+ CINs was higher in SST+ *c-Maf* cKO than in WT SST+ CINs (Fig. 3C; p=0.0452).

In the same cells, we also measured the passive electrical membrane properties of CINs in response to intracellular negative current injections. In SST+ CINs, the resting membrane potential, the input resistance, the membrane time constant, and the capacitance were similar between SST+ WT, SST+ *Mafb* cKO, and SST+ *c-Maf* cKO mice.

In PV+ CINs, we found that the firing frequencies reported in the F-I plots were similar between PV+ *Mafb* cKO and PV+ *c-Maf* cKO mice, except for the frequencies recorded in response to 160 and 180 pA for which PV+ *c-Maf* cKO exhibited lower values than WT PV+ CINs (Fig. 3A). This suggests that *c-Maf* deletion in PV+ CINs reduces the ability of PV+ CINs to sustain action potential at high stimulation intensities. We also found that, in PV+ CINs, the action potential threshold, amplitude, and rheobase (Fig. 3C), were similar in WT, PV+ *Mafb* cKO, and PV+ *c-Maf* cKO. However, the action potential half-duration was lower in PV+ CINs from PV+ *Mafb* cKO than WT mice (Fig. 3C; $p=0.0483$). The resting membrane potential, the input resistance, the membrane time constant, and the capacitance of PV+ were similar in WT, PV+ *Mafb* cKO, and PV+ *c-Maf* cKO mice (Fig. 3D).

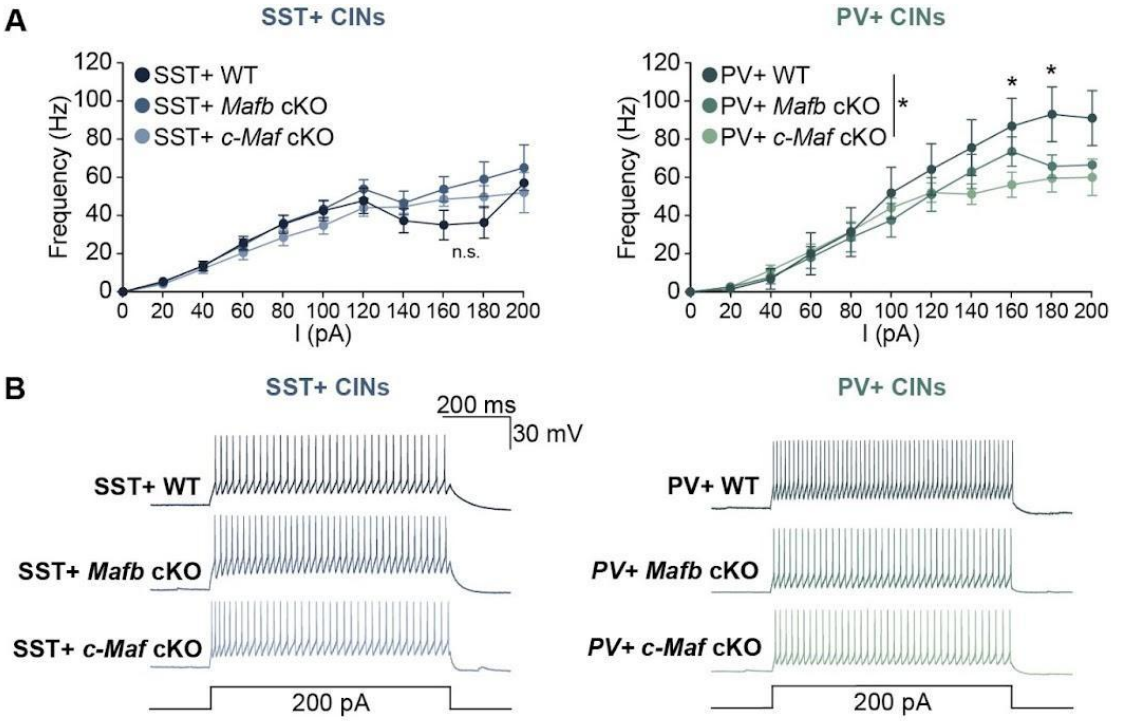

C **Active electric membrane properties**

Cell type	Genotype	Threshold (mV)	Amplitude (mV)	Half-duration (ms)	Rheobase (pA)	# cells	# mice
SST+	SST+ WT	-44.8 ± 0.9	41.9 ± 1.9	1.04 ± 0.06	40.0 ± 5.0	26	3
	SST+ *Mafb* cKO	-45.8 ± 0.8	46.5 ± 1.7	0.95 ± 0.04	38.6 ± 4.9	29	3
	SST+ *c-Maf* cKO	-44.0 ± 1.0	48.5 ± 1.5	1.06 ± 0.05	43.6 ± 6.0	22	2
Kruskal-Wallis, Dunn's *post-hoc*		n.s.	p=0.0452 (WT vs. *c-Maf*)	n.s.	n.s.		
PV+	PV+ WT	-40.0 ± 2.1	32.7 ± 5.7	0.94 ± 0.09	63.3 ± 12.0	6	3
	PV+ *Mafb* cKO	-42.1 ± 1.3	37.5 ± 2.1	0.69 ± 0.03	67.0 ± 8.0	17	4
	PV+ *c-Maf* cKO	-43.0 ± 0.8	39.3 ± 1.2	0.79 ± 0.04	58.8 ± 5.7	34	4
Kruskal-Wallis, Dunn's *post-hoc*		n.s.	n.s.	p=0.0483 (WT vs. *Mafb*)	n.s.		

D **Passive electric membrane properties**

Cell type	Genotype	Vm (mV)	Rin (MΩ)	τm (ms)	Cm (pF)	# cells	# mice
SST+	SST+ WT	-63.6 ± 0.7	592.3 ± 71.8	37.1 ± 4.6	60.2 ± 11.3	26	3
	SST+ *Mafb* cKO	-62.8 ± 0.5	496.6 ± 34.8	38.7 ± 4.0	41.0 ± 5.5	29	3
	SST+ *c-Maf* cKO	-65.3 ± 0.8	542.0 ± 65.4	35.0 ± 3.7	63.3 ± 9.9	22	2
Kruskal-Wallis, Dunn's *post-hoc*		n.s.	n.s.	n.s.	n.s.		
PV+	PV+ WT	-65.8 ± 1.2	404.2 ± 74.3	19.2 ± 3.3	78.3 ± 17.4	6	3
	PV+ *Mafb* cKO	-65.1 ± 1.0	326.5 ± 49.5	13.9 ± 1.5	66.5 ± 10.6	17	4
	PV+ *c-Maf* cKO	-65.0 ± 0.6	339.7 ± 27.1	17.2 ± 1.0	53.1 ± 9.7	34	4
Kruskal-Wallis, Dunn's *post-hoc*		n.s.	n.s.	n.s.	n.s.		

Figure 3 (previous page). Effect of Mafb or c-Maf deletion in SST+ or PV+ CINs on their intrinsic membrane electrical properties. A, *F-I curve for CINs—a plot of the mean action potential firing frequency as a function of current intensity injected in the CINs from WT, SST+ Mafb cKO, SST+ c-Maf cKO, PV+ Mafb cKO, and PV+ c-Maf cKO mice. Statistical significance was assessed by Two-way ANOVA test followed by Tukey's multiple comparisons test for the post hoc analysis (*p<0.05).* ***B,*** *Representative firing traces from CINs for each neuronal type and genotype.* ***C*** *and* ***D,*** *Quantification of active (C) and passive (D) electric membrane properties. Vm: resting membrane potential; Rin: input resistance; τm: membrane time constant; Cm: capacitance. Data are expressed as the mean ± SEM. Statistical significance was assessed by Kruskal-Wallis test, Dunn's post-hoc analysis for multiple comparisons. All electrophysiological properties were measured in 3-5 month-old mice.*

Effect of c-Maf or *Mafb* deletion in SST+ or PV+ interneurons on their density in the somatosensory cortex

Using tdTomato immunofluorescence (Fig. 4A), we found that in SST+ *Mafb* cKO mice, the density of SST+ CINs was reduced (Fig. 4B) in layers II/III and IV compared with WT mice. This result was confirmed using SST+ *in situ* hybridization (Fig. 4C): the number of SST+ CINs was lower in layers II/III and IV of the S1 cortex in SST+ *Mafb* cKO than WT, whereas the SST+ neuronal count in the S1 deep layers—V and VI—was unchanged in both SST+ *Mafb* cKO and SST+ *c-Maf* cKO compared with WT littermate mice. The density of SST+ CINs in the different layers of the S1 cortex was not affected by *Mafb* or *c-Maf* deletion in SST+ CINs at 2 month-old (Suppl. Fig. 1).

Although *c-Maf* deletion in SST+ CINs did not affect SST+ neuronal count at 2 month-old (Suppl. Fig. 1), nor at 8-10 month-old (Fig. 4B-D), it had an effect on PV+ neuronal count: we found that at 8-10 months of age, *c-Maf* deletion in SST+ CINs increases the number of PV+ CINs in the superficial layers of the S1 cortex (Fig. 5), suggesting probable compensatory mechanisms in the cortical inhibition.

In contrast, *Mafb* or *c-Maf* deletion in PV+ CINs did not alter PV+ neuronal counts in the different layers of the S1 cortex at 8-10 month-old (Fig. 6).

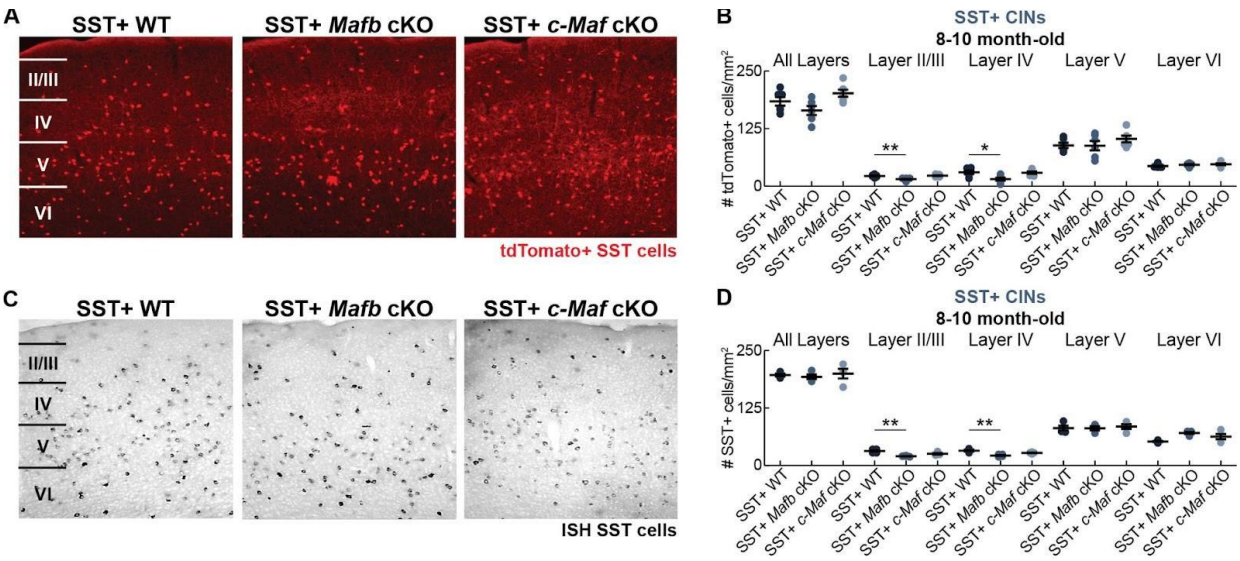

Figure 4. Effect of Mafb or c-Maf deletion in SST+ CINs on their SST+ neuronal count. A, *Immunofluorescent images from the somatosensory cortices from WT, SST+ Mafb cKO, and SST+ c-Maf cKO mice that show CINs marked with tdTomato.* ***B,*** *Quantification of the number of tdTomato+ cells/mm^2 in the somatosensory cortex. Statistical significance was assessed within each layer group, depending on the normality and homoscedasticity, by Student's t-test or Scheirer-Ray-Hare test and Wilcoxon Mann Whitney test for the post hoc analysis (**p<0.01; *p<0.05).* ***C,*** *SST+ in situ hybridization in the somatosensory cortices from WT, Mafb cKO, and c-Maf cKO mice.* ***D,*** *Quantification of SST+ CINs /mm^2 in the somatosensory cortex. Statistical significance was assessed by Statistical significance was assessed within each layer group, depending on the normality and homoscedasticity, by Student's t-test or Scheirer-Ray-Hare test and Wilcoxon Mann Whitney test for the post hoc analysis (**p<0.01). These results were obtained from 8-10 month-old mice, age that matches the age at which the in vivo electroencephalographic activity was recorded.*

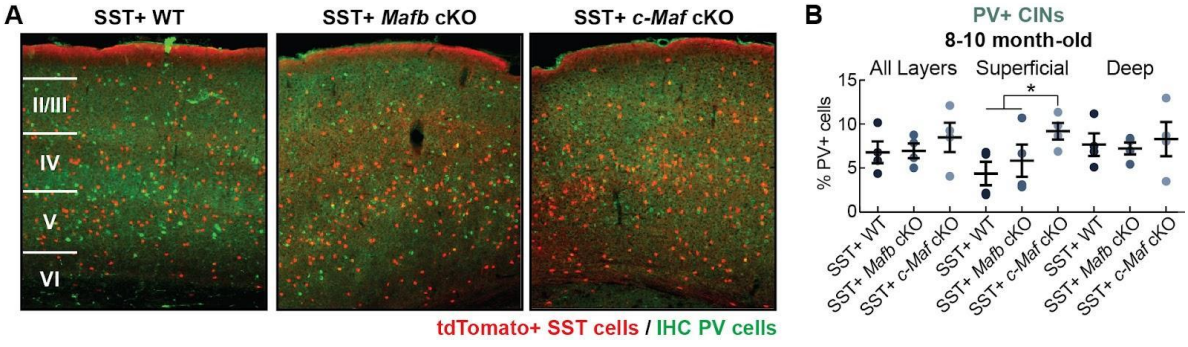

Figure 5. Effect of Mafb or c-Maf deletion in SST+ CINs on the PV+ neuronal count. A, *Immunofluorescent images from the S1 cortex from WT, SST+ Mafb cKO, and SST+ c-Maf cKO mice that show SST+ and PV+ CINs labeled.* ***B,*** *Quantification of the fraction of PV+ CINs in the superficial (II/III and IV) and deep (V and VI) layers of the somatosensory cortex of SST+ Maf mutants. Statistical significance was assessed by Statistical significance was assessed within each layer group, depending on the normality and homoscedasticity, by Student's t-test or Scheirer-Ray-Hare test and Wilcoxon Mann*

*Whitney test for the post hoc analysis (*p<0.05). These results were obtained from 8-10 month-old mice, age that matches the age at which the in vivo electroencephalographic activity was recorded.*

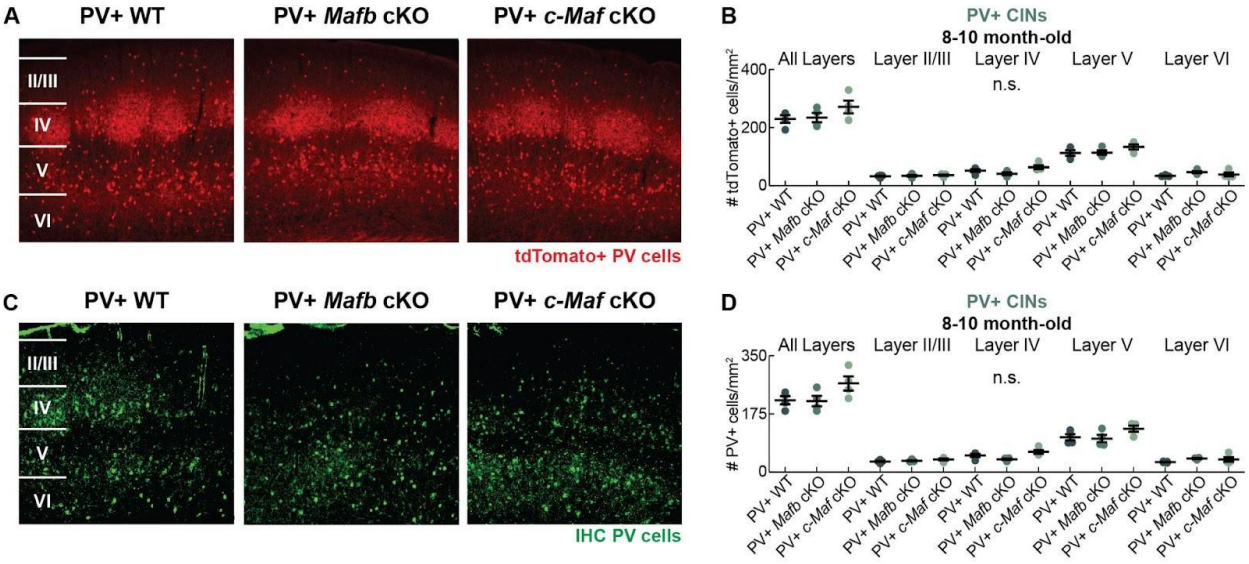

Figure 6. Effect of Mafb or c-Maf deletion in PV+ CINs on their neuronal count. A, *Immunofluorescent images from the somatosensory cortices from WT, PV+ Mafb cKO, and PV+ c-Maf cKO mice that show PV+ CINs marked with tdTomato.* ***B,*** *Quantification of the number of tdTomato+ cells/mm^2 in the somatosensory cortex. Statistical significance was assessed within each layer group, depending on the normality and homoscedasticity, by Student's t-test or Scheirer-Ray-Hare test and Wilcoxon Mann Whitney test for the post hoc analysis (n.s. non significant).* ***C,*** *Immunofluorescent images from the somatosensory cortices that show immunolabeled PV+ CINs in green.* ***D,*** *Quantification of PV+ CINs /mm^2 in the somatosensory cortex. Statistical significance was assessed within each layer group, depending on the normality and homoscedasticity, by Student's t-test or Scheirer-Ray-Hare test and Wilcoxon Mann Whitney test for the post hoc analysis (n.s. non significant). These results were obtained from 8-10 month-old mice, age that matches the age at which the in vivo electroencephalographic activity was recorded.*

Effect of *c-Maf* or *Mafb* deletion in SST+ or PV+ interneurons on epileptic-like activity

Given that our previous results showed that double deletion of both *Mafb* and *c-Maf* in all MGE-derived CINs causes epileptic activities (Pai et al., 2020), we investigated whether specifically deleting *Mafb* or *c-Maf* in either SST+ or PV+ CINs could be sufficient to cause epileptic discharges.

We implanted chronic electrocorticographic (ECoG) devices into the prefrontal cortex (PFC) and the S1 cortex of 1) SST+ *Mafb* cKO, SST+ *c-Maf* cKO, and wild-type littermates (Fig. 7), and 2) PV+ *Mafb* cKO, and PV+ *c-Maf* cKO mice and wild-type littermates (Fig. 8)). We quantified epileptic spikes in ECoG within a 2 to 4-hour window three weeks post-surgery.

We found that *c-Maf*, but not *Mafb*, deletion in SST+ CINs increases the frequency of epileptic spikes in both the PFC (Fig. 7A) and the S1 cortex (Fig. 7B). However, *Mafb* or *c-Maf* deletion in PV+ CINs did not alter the frequency of epileptic spikes in the PFC (Fig. 8A), nor in the S1 cortex (Fig. 8B).

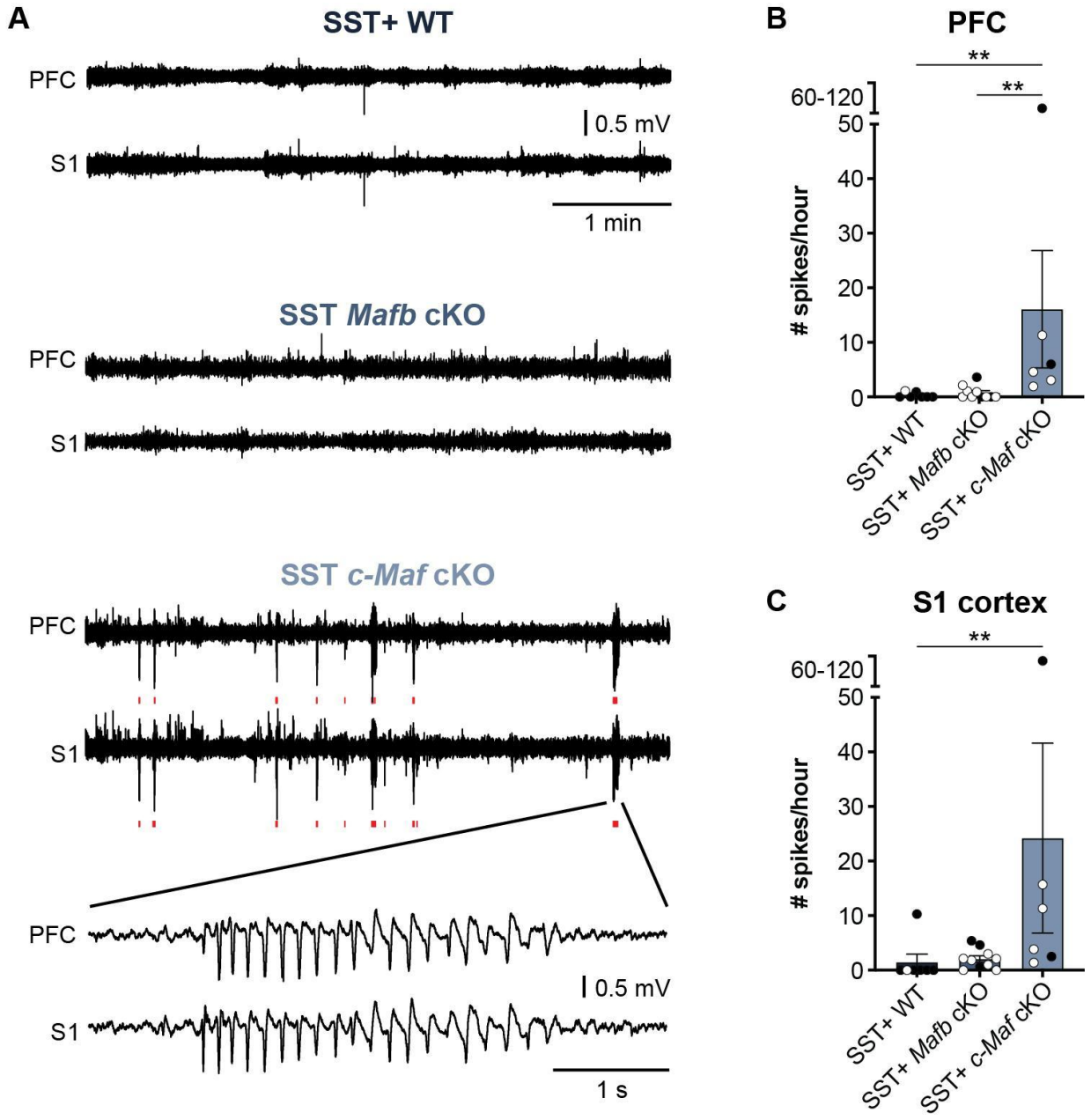

Figure 7. Effect of Mafb or c-Maf deletion in SST+ CINs on epileptic activity in adult mice. A, *ECoG recordings from PFC and S1 cortex from WT, SST+ Mafb cKO, and SST+ c-Maf cKO mice (epileptic spikes are indicated in red)* ***B,*** *Number of epileptic spikes per hour of recordings in the PFC.* ***C,*** *Number of epileptic spikes per hour of recordings in the S1 cortex.. Data are expressed as the mean ± SEM.*

*Statistical significance was assessed by One-way ANOVA Kruskal-Wallis test followed by Dunn's multiple comparisons test for the post hoc analysis (**p<0.01). WT: n=6 males, 1 female; SST+ Mafb cKO: n=3 males, 7 females; SST+ c-Maf cKO: n=2 males, 4 females. Males are represented in black dots and females in white dots. ECoG recordings were performed in 8-9 month-old mice.*

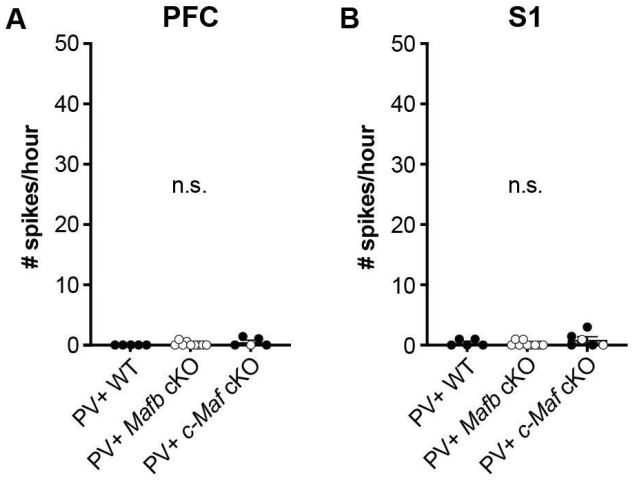

Figure 8. Effect of Mafb or c-Maf deletion in PV+ CINs on epileptic activity in adult mice. ***A,*** *Number of epileptic spikes per hour of ECoG recordings in the PFC from WT, PV+ Mafb cKO, and PV+ c-Maf cKO mice.* ***B,*** *Number of epileptic spikes per hour of ECoG recordings in the S1 cortex from the same mice. Data are expressed as the mean ± SEM. Statistical significance was assessed by One-way ANOVA Kruskal-Wallis test followed by Dunn's multiple comparisons test for the post hoc analysis (n.s. non significant). WT: n=5 males; PV+ Mafb cKO: n=9 females; PV+ c-Maf cKO: n=4 males, 2 females. Males are represented in black dots and females in white dots. ECoG recordings were performed in 8-9 month-old mice.*

DISCUSSION

We used *Somatostatin-IRES-Cre* (Taniguchi et al., 2011) and *Parvalbumin-Cre* (Hippenmeyer et al., 2005) mice to conditionally delete either *Mafb* or *c-Maf* specifically in SST+ or PV+ CINs. We found that *c-Maf* but not *Mafb* deletion in SST+ CINs produced decreased excitatory synapse numbers on the proximal dendrites of SST+ CINs, decreased their excitation, and caused epileptic activity in adult freely behaving mice. In contrast, *Mafb* or *c-Maf* deletion in PV+ CINs did not affect their synaptic excitation and did not cause epileptic activity in adult mice. Below we discuss the significance of these findings.

c-Maf deletion in SST+ or PV+ CINs does not affect their density in the cortex

In our previous study (Pai et al 2019) using *Nkx2.1-Cre* mouse, in which we have shown that deleting *Mafb* or *c-Maf* in all MGE-derived CINs at embryonic day 9.5 (E9.5), the density of PV+ CINs was reduced by ~30% in the cortex of young adult mice (P35). However, our current study shows that when deleting *Mafb* or *c-Maf* in PV+ CINs, we see no change in PV+ neuronal counts in adulthood (8-10 months old mice), which could be explained at least in part by the fact that the deletion of *Maf* genes occurs postnatally in the current study—at postnatal days 10-14 (P10-14).

In our previous study (Pai et al 2019), in which we have shown that deleting *Mafb* or *c-Maf* in all MGE-derived CINs at E9.5, the density of SST+ CINs was reduced by ~12% in *Mafb* cKO and 30% in *c-Maf* cKO in the cortex of young adult mice (one month-old). However, our current study shows that when deleting *Mafb* in SST+ CINs at E12, we see a decreased density of SST+ CINs in the cortex, and no change in SST+ CIN density when deleting *c-Maf* in SST+ CINs. Our results confirm that *Mafb* deletion specifically in SST+ CINs at E12 affects SST+ neuronal counts similar to when it is deleted at E9.5. However, *c-Maf* deletion specifically in SST+ CINs at E12 does not reduce their counts unlike when deleted at E9.5.

Interestingly, when *c-Maf* is deleted in SST+ CINs at E12, the density of PV+ CINs is increased in the cortex of adult mice, which could be due at least in part to compensatory mechanisms in migration of the CINs that remain unknown.

c-Maf has distinct roles in synaptic excitation in SST+ and PV+ CINs in the cortex

Similar to the neuronal counts, deleting *Mafb* or *c-Maf* in PV+ CINs at P10-14 do not have major effects on their synaptic properties measured in the somatosensory cortex of adult mice. Our previous study showed that *c-Maf* deletion in all MGE-derived CINs at E9.5 increased the frequency of sEPSCs in fast-spiking─i.e., PV+─CINs in adult mice (Pai et al., 2019). The differences in sEPSC results between the current and the previous study could be explained at least in part by the fact that deletion of *c-Maf* occurred earlier during development (E9.5) in the previous study in contrast to postnatally in the current study (P10-14). Also, deleting *Mafb* in all MGE-derived CINs at E9.5 did not influence sEPSCs in PV+ CINs of adult mice, which is consistent with the current study in which *Mafb* is deleted from PV+ CINs at P10-14. Altogether, these results show that *c-Maf* deletion at embryonic but not postnatal stage regulates the

mechanism of synaptic excitation of PV+ CINs, in contrast with *Mafb* which does not play a role in synaptic excitation of PV+ CINs in development or adulthood.

Unlike in PV+ CINs, *c-Maf* deletion in SST+ CINs at E12 decreases the density of excitatory synapses and the frequency of spontaneous excitatory post-synaptic currents in SST+ CINs of adult mice. These results suggest that SST+ CINs lacking *c-Maf* are less excited by surrounding neurons.

Altogether, our results suggest that *c-Maf* plays distinct roles in SST+ and PV+ CINs.

Mafb or *c-Maf* deletion in SST+ or PV+ CINs have mild to no effects on intrinsic membrane properties of these cells

We found that *Mafb or c-Maf* deletions in SST+ CINs at E12 do not impact their passive or active membrane properties, such as the firing frequencies caused by intracellular current injections. This result is consistent with our previous finding showing that *Mafb* or *c-Maf* deletions in MGE-derived CINs at E9.5 do not affect the firing frequencies in regular-spiking CINs (Pai et al., 2019). Altogether, these results suggest that Maf genes in SST+ CINs do not influence their intrinsic electrical properties, and regulate their activity by controlling the excitatory synapses on SST+ CINs.

In addition, we found that the recorded frequencies in the F-I curves from PV+ CINS were lower in PV+ *c-Maf* cKO than WT mice. A similar result was observed when *c-Maf* was deleted in all MGE-derived CINs (Pai et al., 2019). This result suggests that *c-Maf* deletion in PV+ CINs at either embryonic or postnatal age reduces the ability of PV+ CINs to sustain action potential at high stimulation intensities, although this effect is much stronger when *c-Maf* is deleted in MGE-derived CINs at E9.5 (versus here *c-Maf* is deleted in PV+ CINs at P10-14. Overall, these results suggest that *c-Maf* in PV+ CINs regulates firing properties but not synaptic excitation of PV+ CINs.

c-Maf deletion in SST+ but not PV+ CINs causes epileptic discharges

One of the most surprising findings in our study was that deleting *c-Maf* in SST+ but not in PV+ CINs was sufficient to cause epileptic discharges in mice. Indeed, it is thought that PV+ CINs contribute more to pyramidal neuron inhibition than do SST+ CINs (Pfeffer et al., 2013) and PV+ CINs are often the usual suspects in epilepsy (Sessolo et al., 2015; Jiang et al., 2016; Godoy et al., 2022). The finding that SST+ *c-Maf* cKO mice have epileptic discharges is consistent with the reduced number of excitatory synapse counts and glutamatergic excitation in SST+ CINs, which is likely to reduce the GABAergic output of SST+ CINs and increase cortical network excitability. The epilepsy phenotype can not be due to loss of CINs unlike in the double *Mafb c-Maf* cKO in all MGE-derived CINs (Pai et al 2020) because in the SST+ *c-Maf* cKO mice with epileptic activity, the number of SST+ and PV+ CINs is not reduced compared with WT littermates. Interestingly, the slight increase in PV+ CINs in SST+ *c-Maf* cKO was insufficient to protect the mice from epileptic activity. Moreover, we can not rule out that potential changes in

CINs in other brain regions—e.g., striatum, hippocampus—do not contribute to the emergence of epileptic activity.

Why *c-Maf* deletions in PV+ CINs do not cause epileptic-like activity whereas deletion in SST+ CINs does? It is possible that the difference in phenotypes is due to the fact that *c-Maf* is deleted postnatally (P10-14) in PV+ CINs but much earlier (E12) in SST+ CINs, due to our experimental design. Another possibility is that *c-Maf* plays distinct roles in PV+ and SST+ CINs. It would be also interesting to investigate whether distinct compensatory mechanisms are in place in PV+ versus SST+ CINs.

The finding that *Mafb* deletion in either SST+ or PV+ CINs did not result in epileptic activity was somewhat unexpected because our previous study in which *Mafb* was deleted in all MGE-derived CINs increased excitability of cortical slices (Pai et al., 2019).

Altogether, our results demonstrate a specific vulnerability of the SST CINs to the loss of *cMaf,* making the brain vulnerable to epilepsy. Future work is warranted to understand the cellular and circuit mechanisms that lead to epileptic discharges in *c-Maf* loss of function in SST+ CINs. Our study points to the SST CINs as potential key players in epileptogenesis and therefore potential targets for treatment.

REFERENCES

Chao, H. T., Chen, H., Samaco, R. C., Xue, M., Chahrour, M., Yoo, J. W., Neul, J. L., Gong, S., Lu, H., Heintz, N., Ekker, M., Rubenstein, J. L., Noebels, J. L., Rosenmund, C., & Zoghbi, H. Y. (2010). Dysfunction in GABA signalling mediates autism-like stereotypies and Rett syndrome phenotypes. Nature, 468(7321), 263–269. https://doi.org/10.1038/nature09582

Cho, F. S., Vainchtein, I. D., Voskobiynyk, Y., Morningstar, A. R., Aparicio, F., Higashikubo, B., Ciesielska, A., Broekaart, D. W. M., Anink, J. J., Van Vliet, E. A., Yu, X., Khakh, B. S., Aronica, E., Molofsky, A. V., & Paz, J. T. (2022). Enhancing GAT-3 in thalamic astrocytes promotes resilience to brain injury in rodents. Science Translational Medicine, 14(652). https://doi.org/10.1126/scitranslmed.abj4310

Clemente-Perez, A., Makinson, S. R., Higashikubo, B., Brovarney, S., Cho, F. S., Urry, A., Holden, S. S., Wimer, M., Dávid, C., Fenno, L. E., Acsády, L., Deisseroth, K., & Paz, J. T. (2017). Distinct thalamic reticular cell types differentially modulate normal and pathological cortical rhythms. Cell Reports, 19(10), 2130–2142. https://doi.org/10.1016/j.celrep.2017.05.044

Cordes, S. P., & Barsh, G. S. (1994). The mouse segmentation gene kr encodes a novel basic domain-leucine zipper transcription factor. Cell, 79(6), 1025–1034. https://doi.org/10.1016/0092-8674(94)90033-7

Corteen, N. L., Cole, T. M., Sarna, A., Sieghart, W., & Swinny, J. D. (2011). Localization of GABA-A receptor alpha subunits on neurochemically distinct cell types in the rat locus coeruleus. European Journal of Neuroscience, 34(2), 250–262. https://doi.org/10.1111/j.1460-9568.2011.07740.x

Gelman, D. M., Griveau, A., Dehorter, N., Teissier, A., Varela, C., Pla, R., Pierani, A., & Marín, O. (2011). A Wide Diversity of Cortical GABAergic Interneurons Derives from the Embryonic Preoptic Area. The Journal of Neuroscience, 31(46), 16570–16580. https://doi.org/10.1523/jneurosci.4068-11.2011

Godoy, L. D., Prizon, T., Rossignoli, M. T., Leite, J. P., & Liberato, J. L. (2022). Parvalbumin Role in Epilepsy and Psychiatric Comorbidities: From Mechanism to intervention. Frontiers in Integrative Neuroscience, 16. https://doi.org/10.3389/fnint.2022.765324

Han, S., Tai, C., Westenbroek, R. E., Yu, F. H., Cheah, C. S., Potter, G. B., Rubenstein, J. L., Scheuer, T., De La Iglesia, H. O., & Catterall, W. A. (2012). Autistic-like behaviour in Scn1a+/− mice and rescue by enhanced GABA-mediated neurotransmission. Nature, 489(7416), 385–390. https://doi.org/10.1038/nature11356

Hippenmeyer, S., Vrieseling, E., Sigrist, M. W., Portmann, T., Laengle, C., Ladle, D. R., & Arber, S. (2005). A developmental switch in the response of DRG neurons to ETS transcription factor signaling. PLOS Biology, 3(5), e159. https://doi.org/10.1371/journal.pbio.0030159

Hoch, R. V., Clarke, J. A., & Rubenstein, J. L. (2015). Fgf signaling controls the telencephalic distribution of Fgf-expressing progenitors generated in the rostral patterning center. Neural Development, 10(1). https://doi.org/10.1186/s13064-015-0037-7

Hoch, R. V., Lindtner, S., Price, J. D., & Rubenstein, J. L. (2015). OTX2 Transcription Factor Controls Regional Patterning within the Medial Ganglionic Eminence and Regional Identity of the Septum. Cell Reports, 12(3), 482–494. https://doi.org/10.1016/j.celrep.2015.06.043

Holden, S. S., Grandi, F. C., Aboubakr, O., Higashikubo, B., Cho, F. S., Chang, A., Osorio-Forero, A., Morningstar, A. R., Mathur, V., Kuhn, L. J., Suri, P., Sankaranarayanan, S., Andrews-Zwilling, Y.,

Tenner, A. J., Lüthi, A., Aronica, E., Corces, M. R., Yednock, T., & Paz, J. T. (2021). Complement factor C1q mediates sleep spindle loss and epileptic spikes after mild brain injury. Science, 373(6560). https://doi.org/10.1126/science.abj2685

Hu, J., Vogt, D., Sandberg, M., & Rubenstein, J. L. (2017). Cortical interneuron development: a tale of time and space. Development, 144(21), 3867–3878. https://doi.org/10.1242/dev.132852

Huang, Z. J., Di Cristo, G., & Ango, F. (2007). Development of GABA innervation in the cerebral and cerebellar cortices. Nature Reviews Neuroscience, 8(9), 673–686. https://doi.org/10.1038/nrn2188

Jiang, X., Lachance, M., & Rossignol, E. (2016). Involvement of cortical fast-spiking parvalbumin-positive basket cells in epilepsy. In Progress in Brain Research (pp. 81–126). https://doi.org/10.1016/bs.pbr.2016.04.012

Kepecs, A., & Fishell, G. (2014). Interneuron cell types are fit to function. Nature, 505(7483), 318–326. https://doi.org/10.1038/nature12983

Kessaris, N., Magno, L., Rubin, A. N., & Oliveira, M. G. (2014). Genetic programs controlling cortical interneuron fate. Current Opinion in Neurobiology, 26, 79–87. https://doi.org/10.1016/j.conb.2013.12.012

Lim, L., Mi, D., Llorca, A., & Marín, O. (2018). Development and functional diversification of cortical interneurons. Neuron, 100(2), 294–313. https://doi.org/10.1016/j.neuron.2018.10.009

Lu, C. C., Appler, J. M., Houseman, E. A., & Goodrich, L. V. (2011). Developmental Profiling of Spiral Ganglion Neurons Reveals Insights into Auditory Circuit Assembly. The Journal of Neuroscience, 31(30), 10903–10918. https://doi.org/10.1523/jneurosci.2358-11.2011

Madisen, L., Zwingman, T., Sunkin, S. M., Oh, S. W., Zariwala, H. A., Gu, H., Ng, L., Palmiter, R. D., Hawrylycz, M., Jones, A. R., Lein, E., & Zeng, H. (2009). A robust and high-throughput Cre reporting and characterization system for the whole mouse brain. Nature Neuroscience, 13(1), 133–140. https://doi.org/10.1038/nn.2467

Pai, E. L., Chen, J., Darbandi, S. F., Cho, F. S., Chen, J., Lindtner, S., Chu, J., Paz, J. T., Vogt, D., Paredes, M. F., & Rubenstein, J. L. (2020). Maf and Mafb control mouse pallial interneuron fate and maturation through neuropsychiatric disease gene regulation. eLife, 9. https://doi.org/10.7554/elife.54903

Pai, E. L. L., Vogt, D., Clemente-Perez, A., McKinsey, G. L., Cho, F. S., Hu, J., Wimer, M., Paul, A., Darbandi, S. F., Pla, R., Nowakowski, T. J., Goodrich, L. V., Paz, J. T., & Rubenstein, J. L. (2019). MAFB and C-MAF have prenatal compensatory and postnatal antagonistic roles in cortical interneuron fate and function. Cell Reports, 26(5), 1157-1173.e5. https://doi.org/10.1016/j.celrep.2019.01.031

Pfeffer, C., Xue, M., He, M., Huang, Z. J., & Scanziani, M. (2013). Inhibition of inhibition in visual cortex: the logic of connections between molecularly distinct interneurons. Nature Neuroscience, 16(8), 1068–1076. https://doi.org/10.1038/nn.3446

Rubenstein, J. L., & Merzenich, M. M. (2003). Model of autism: increased ratio of excitation/inhibition in key neural systems. Genes, Brain and Behavior, 2(5), 255–267. https://doi.org/10.1034/j.1601-183x.2003.00037.x

Sessolo, M., Marcon, I., Bovetti, S., Losi, G., Cammarota, M., Ratto, G. M., Fellin, T., & Carmignoto, G. (2015). Parvalbumin-Positive Inhibitory Interneurons Oppose Propagation But Favor Generation

of Focal Epileptiform Activity. The Journal of Neuroscience, 35(26), 9544–9557. https://doi.org/10.1523/jneurosci.5117-14.2015

Stanco, A., Pla, R., Vogt, D., Chen, Y., Mandal, S., Walker, J. M., Hunt, R., Lindtner, S., Erdman, C. A., Pieper, A. A., Hamilton, S. P., Xu, D., Baraban, S. C., & Rubenstein, J. L. (2014). NPAS1 represses the generation of specific subtypes of cortical interneurons. Neuron, 84(5), 940–953. https://doi.org/10.1016/j.neuron.2014.10.040

Taniguchi, H., He, M., Wu, P., Kim, S. Y., Paik, R., Sugino, K., Kvitsani, D., Fu, Y., Lu, J., Lin, Y., Miyoshi, G., Shima, Y., Fishell, G., Nelson, S. B., & Huang, Z. J. (2011). A resource of CRE driver lines for genetic targeting of GABAergic neurons in cerebral cortex. Neuron, 71(6), 995–1013. https://doi.org/10.1016/j.neuron.2011.07.026

Wende, H., Lechner, S., Cheret, C., Bourane, S., Kolanczyk, M. E., Pattyn, A., Reuter, K., Munier, F. L., Carroll, P., Lewin, G. R., & Birchmeier, C. (2012). The transcription factor C-MAF controls touch receptor development and function. Science, 335(6074), 1373–1376. https://doi.org/10.1126/science.1214314

Wonders, C., & Anderson, S. A. (2006). The origin and specification of cortical interneurons. Nature Reviews Neuroscience, 7(9), 687–696. https://doi.org/10.1038/nrn1954

Yizhar, O., Fenno, L. E., Prigge, M., Schneider, F., Davidson, T. J., O'Shea, D. J., Sohal, V. S., Goshen, I., Finkelstein, J., Paz, J. T., Stehfest, K., Fudim, R., Ramakrishnan, C., Huguenard, J. R., Hegemann, P., & Deisseroth, K. (2011). Neocortical excitation/inhibition balance in information processing and social dysfunction. Nature, 477(7363), 171–178. https://doi.org/10.1038/nature10360

Yu, W., Appler, J. M., Kim, Y., Nishitani, A. M., Holt, J. R., & Goodrich, L. V. (2013). A Gata3–Mafb transcriptional network directs post-synaptic differentiation in synapses specialized for hearing. eLife, 2. https://doi.org/10.7554/elife.01341

SUPPLEMENTAL FIGURE

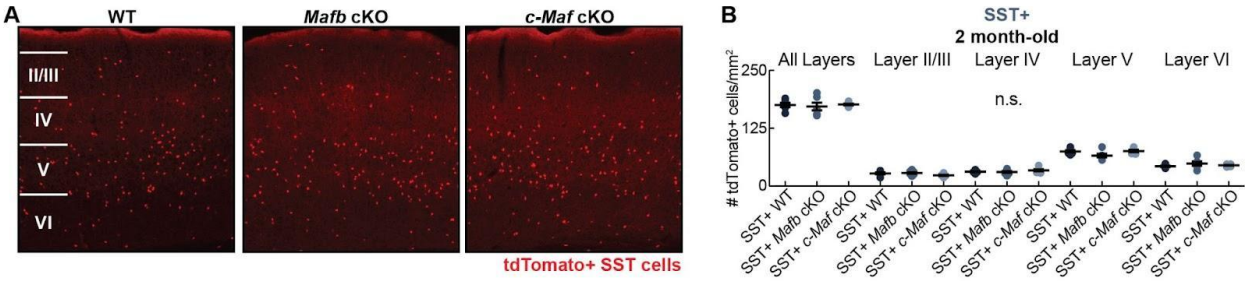

Supplemental figure 1. Effect of Mafb or c-Maf deletion in SST+ CINs on their SST+ neuronal count. A, *Immunofluorescent images from the somatosensory cortices from WT, SST+ Mafb cKO, and SST+ c-Maf cKO mice that show CINs marked with tdTomato.* ***B,*** *Quantification of the number of tdTomato+ cells/mm^2 in the somatosensory cortex. Statistical significance was assessed within each layer group, depending on the normality and homoscedasticity, by Student's t-test or Scheirer-Ray-Hare test and Wilcoxon Mann Whitney test for the post hoc analysis (n.s. non significant). These results were obtained from two month-old mice.*

GENERAL DISCUSSION

I. Conclusions

In **Chapter I**, we investigated the neuronal and network excitability mechanisms underlying parametric working memory (PWM), which is the capacity to maintain and manipulate transient quantitative information. We demonstrated experimentally that conditional bistability (CB), a form of self-sustained spiking triggered by a transient event and dependent of a tonic level of depolarization that may be provided, *in vivo*, by local recurrent synaptic inputs, does exist in the pyramidal neurons of the layer V of the medial prefrontal cortex (mPFC) in rats. We showed that CB is modulated via the activation of calcium-activated non-selective cationic (CAN) channels. We demonstrated that the CAN-mediated CB depends on the activation of the muscarinic 1-like (M1) receptors and is largely insensitive to serotonin, dopamine, and noradrenaline. Moreover, we showed that the neuronal mechanisms underlying CB are required for the emergence of a form of graded persistent activity (GPA) resembling that of underlying PWM in the mPFC. *Our results suggest that CB is crucial for the emergence of GPA emergence and PWM capacities as predicted by coarse-grained neural network models (Koulakov et al., 2002; Goldman et al., 2003) and our biophysical model (Rodriguez et al., 2018).*

In **Chapter II**, we focused on two pathological conditions affecting working memory (WM) capacities. Particularly, we questioned whether CB in the mPFC is affected in rodent models of Alzheimer's disease (AD) and mild traumatic brain injury (TBI). We found that CB is impaired in both AD and TBI, where our results suggested different causal dysregulations. In AD, M1 receptor function and expression seemed to be the main limitation to CB emergence in mouse neurons. However, after TBI, an over-activation of the after-hyperpolarization (AHP) channels that decreases the overall ADP/AHP balance seemed to be the cause of CB disruption in rat neurons. *Our results show that CB deficits are present in two different neurologic disease models and point to new therapeutic targets for treatment.*

In **Chapter III**, we studied the effect of mutations of neurodevelopmental genes, *Mafb* and *c-Maf*, on neuronal excitability. The Maf genes were specifically deleted in somatostatin-positive (SST+) and parvalbumin-positive (PV+) cortical interneurons (CINs) during development, and neuronal and circuit excitability were measured in the somatosensory (S1) cortex of adult mice. On the one hand, we found that *c-Maf* deletion in SST+ CINs decreases excitatory synapses on the dendrites of SST+ CINs, reduces their synaptic excitation, and causes hyper-excitability in form of epileptic spikes in the S1 and mPFC cortices. On the other hand, we found that *Mafb* deletion in SST+ CINs decreases the total number of SST+ CINs in the superficial layers but does not cause changes in network excitability, suggesting a compensatory effect to balance the excitability. *Our results demonstrate a specific vulnerability of the cortex to the loss of cMaf gene in SST+ CINs, making the brain vulnerable to epilepsy, and point to the cMaf and SST CINs as key players in maintaining network excitability in balance.*

II. Open questions & Perspectives

Does graded persistent activity emerge in the medial prefrontal cortex during a parametric working memory task in rodents?

The *in vivo* emergence of GPA in the PFC has experimentally been assessed during a PWM task only using monkeys as animal models (Major and Tank, 2004). The recent development of a PWM task in rats by Fassihi et al. (2014) provides an invaluable and timely opportunity to assess this important type of memory. Their study showed that, like monkeys, rats are capable of performing PWM tasks (Fassihi et al., 2014). However, the emergence of GPA during the delay of the task has not been assessed.

Here, using *in vitro* electrophysiology methods, we demonstrated that not only GPA can emergence in the layer V of the mPFC in rats, but GPA also depends on the CB-mediated mechanisms—i.e., acetylcholine (ACh) modulation, via the activation of M1 receptors, and fast and slow CAN conductances (Leroux et al., manuscript #1). Thus, the next step would be to assess the emergence of GPA in the mPFC *in vivo* in rats performing, for example, the PWM task developed by Fassihi et al. (2014; Fig. 38).

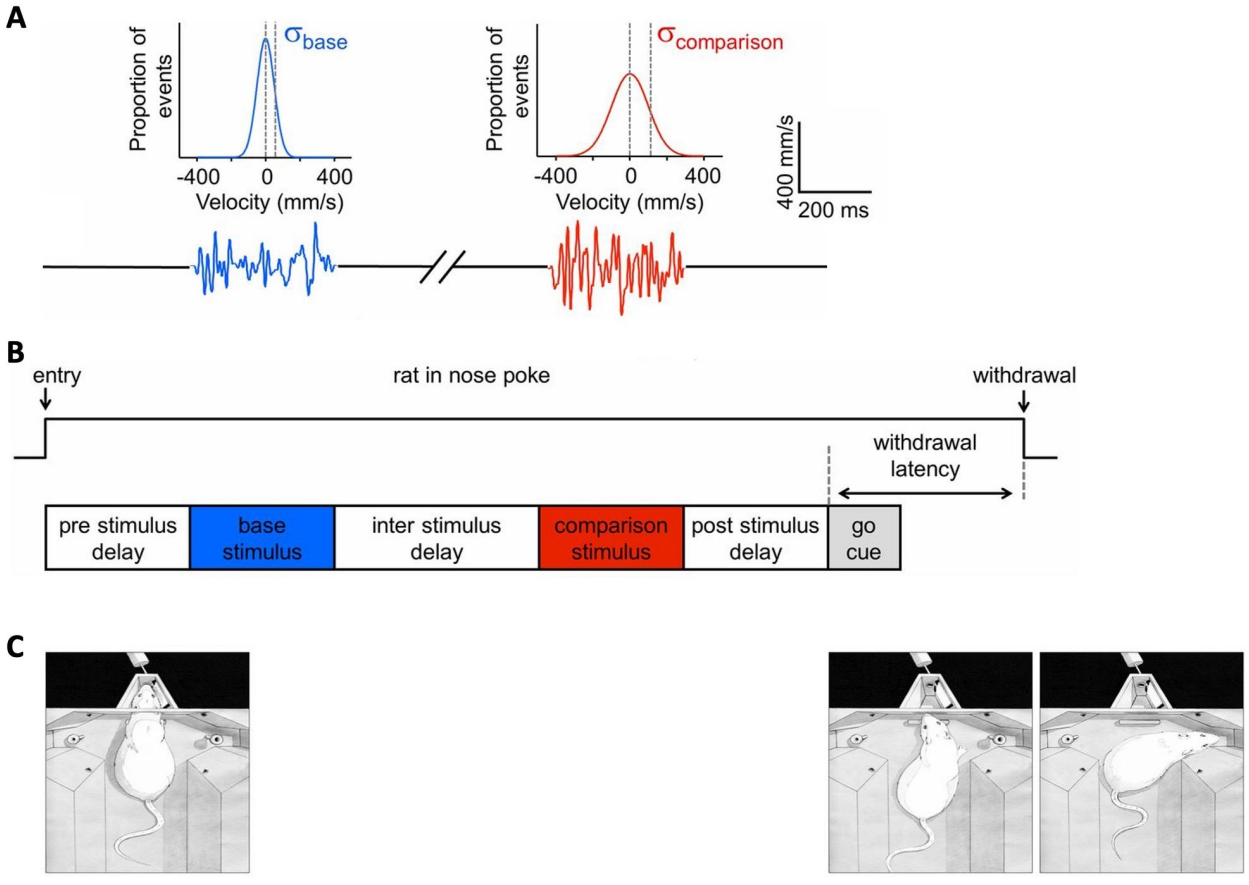

Fig. 38 (previous page). Parametric working memory task in rats. A, *Stimuli are whisker stimulations characterized by vibrations composed of a series of velocity values where the sampling probability of a given velocity value is given by a normal distribution with mean = 0 and SD = σ. Example base and comparison stimuli are illustrated, resulting from the sampling of the distribution shown above each stimulus, with σ = 55 mm/s (blue) and σ = 110 mm/s (red) and duration 400 ms.* ***B,*** *Upper trace indicates at far left the time of entry of the rat in the nose poke and at far right the time of withdrawal. Below, key events of the trial are given. Withdrawal latency is measured as elapsed time between the onset of the go cue and withdrawal from the nose poke.* ***C,*** *Sketches depicting one trial. The rat places its snout in the stimulus delivery port to initiate the trial and receive stimuli. Then, upon hearing the go cue, the rat withdraws. Finally, the rat selects the right reward port. Adapted from Fassihi et al. (2014).*

These ideas could be further investigated in the future by recording unit and multi-unit activity in the mPFC using depth electrodes in healthy young adult (two month-old) rats during the PWM task that consists in presenting two mechanical vibration frequencies applied on the whiskers and separated by a delay of a few seconds. This experimental design would allow us to assess the emergence of GPA in the mPFC, which we anticipate to emerge during the delay of the task, just like in monkeys (Major and Tank, 2004).

In Chapter II, we demonstrated that not only rats, but also mice are endowed with CB neurons in the deep layers of mPFC (Leroux et al., manuscript #2). It would be interesting to study if mice—like rats (Fassihi et al., 2014; Leroux et al., manuscript #1)—are able to display GPA in mPFC brain slices and *in vivo*, while performing PWM tasks. Thus the same *in vivo* experiment as described above for rats would be used for mice. Because mice are capable of learning object and spatial WM tasks (D'Isa et al., 2021; Keller et al., 2022), and are endowed with CB neurons in the mPFC (Leroux et al., manuscript #2), we anticipate that mice will be able to perform PWM tasks as well.

Can we demonstrate a direct causal link between conditional bistability mechanisms and parametric working memory performance?

In this study, we were able to demonstrate a direct causal link between the mechanisms underlying CB—i.e., cholinergic modulation through the activation of M1 receptors and the CAN current-mediated after-depolarizations—and the emergence of GPA in the mPFC network in rats brain slices (Leroux et al., manuscript #1). However, we have not yet established a direct causal link between CB mechanisms and PWM. Thus, after demonstrating that GPA emerges in the mPFC during a PWM task in healthy rats, the next step would be to test whether inhibiting CB mechanisms reduces the emergence of GPA and behavioral performance in PWM tasks.

Our studies suggest that passive electrical membrane properties do not play a role in CB, however we identified the M1 receptors and the CAN-mediated after-depolarizations (ADPs) as key in CB emergence in mPFC layer V pyramidal neurons (Leroux et al., manuscript #1). It is

known that the intracellular cascade activated by the binding of ACh on the M1 receptors includes inositol trisphosphate and its receptor located on the endoplasmic reticulum (ER). Therefore, we propose this pathway might be involved in CB.

Do *in vivo* GPA emergence in the mPFC and PWM performance depend on M1 receptor activation in the mPFC? If inhibiting M1 receptors in mPFC during the PWM task disrupts GPA emergence in mPFC and PWM performance, it would suggest that M1 receptor activation plays a role in GPA/PWM. Pharmacological tools to inhibit M1 receptors have been widely used in cognitive studies: for instance, administration of scopolamine (Newman et al., 2015) and VU0255035 (Rahman et al., 2020) subcutaneously or intraperitoneally in rodents has been used to study the role of M1 receptors in cognitive behavior. However, such systemic administration of drugs would disrupt M1 receptors globally (Felder et al., 2000; Xiang et al., 2012) rather than locally in mPFC and are likely to have effects unrelated to mPFC-dependent PWM.

To test the specific role of M1 receptors in mPFC, local injections of drugs would be more desirable. We propose to perform stereotaxic surgeries on the rodents and implant bilateral stainless steel guide shafts right above the right and left mPFC to serve as guides for pump-controlled drug injectors. Then, after recovery from the surgery, the rats could be trained to perform the PWM task and M1 receptor blockers could be injected directly in the mPFC at specific times of the PWM tasks. As GPA emerges in the mPFC during the delay of the task, we suspect that blocking M1 receptor function right at the beginning or at the end of the first cue presentation (before the delay period) would disrupt GPA in the network and PWM performances. The different drugs that could be considered for this experiment are pirenzepine hydrochloride—a M1 antagonist—, scopolamine hydrobromide—a mixed M1/M2 antagonist—, and oxotremorine—a non-specific muscarinic agonist (Chau et al., 2001; all currently available to purchase). These pharmacological experiments would establish the link between M1 receptors in mPFC and GPA emergence and PWM performance.

Do *in vivo* GPA emergence in the mPFC and PWM performance depend on TRPC-mediated CAN currents in the mPFC? We could perturb the CAN-mediated ADPs using pharmacological agents. In our *in vitro* experiment, we used flufenamic acid (FFA), which is a non-specific blocker of the slow CAN channels, to demonstrate that CB depends on the slow CAN conductances (Leroux et al., manuscript #1). The slow CAN currents are known to be mediated by TRPC5 and TRPC6 channels (Haj-Dahmane and Andrade, 1998; Strübing et al., 2001; Yan et al., 2009), so ideally we would like to target only these channels to address our question. However, the lack of specificity of available CAN channel blockers is a major issue, and makes it difficult to conduct proper *in vivo* experiments to address our question. Subcutaneous, intraperitoneal, or intravenous injections of FFA would not be desirable as TRPC channels are expressed in the whole animal body, including the heart (Guinamard et al., 2013) and the respiratory system

(Achanta and Jordt, 2020). Although FFA has been known since the 1960s (Winder et al., 1963), to our knowledge, local FFA injections into the brains of living rodents have not yet been performed. Other drugs, such as SKF-96365 (Kurowski et al., 2015; Ratte et al., 2018), have also been used to inhibit TRPC-mediated CAN currents and investigate self-sustained spiking activity, but they present the same lack of specificity (Kurowski et al., 2015).

In this thesis, we also demonstrated the role of fast CAN conductances in CB emergence (Leroux et al., manuscript #1). In a couple of *in vitro* studies, amiloride (Zufall et al., 1991; McQuiston and Madison, 1999) has been identified as a pharmacological blockers of the fast ADPs. Amiloride can be administered *in vivo* intraperitoneally into mice and cross the blood-brain barrier—amiloride has notably been proven beneficial in the treatment of several neuropathological conditions such as seizures (Ali et al., 2004, 2005; N'Gouemo, 2008). However, to disrupt the fast CAN conductances specifically in mPFC we would need to proceed with local intra-mPFC injections during the PWM task as described above.

An alternative option to delete CAN conductances, at least the slow ones, in excitatory pyramidal neurons of the mPFC would be to generate a transgenic mouse line enabling the tamoxifen-induced, conditional deletion of loxP-flanked *Trpc5* and/or *Trpc6* genes in layer V glutamatergic neurons. First, a mouse line expressing *Cre recombinase* into glutamatergic pyramidal neurons—e.g., *Vglut2-IRES-Cre* (Jax Laboratory, strain #028863)—would have to be crossed with mice harboring *Trpc5* gene flanked by loxP site—e.g., $Trpc5^{fx/fx}$ (Jax Laboratory, strain #030803). Then, tamoxifen would be stereotaxically injected into the mPFC at the age of our choice to delete *Trpc5* gene expression, and thus slow CAN channel expression. This genetic manipulation of the CAN channels in a specific type of neurons in the mPFC would allow us to establish a causal link between the slow CAN channels, required for CB, and *in vivo* GPA emergence in the mPFC and PWM capacities.

Do *in vivo* GPA emergence in the mPFC and PWM performance depend on intracellular Ca^{2+} levels in the mPFC? An increase in intracellular Ca^{2+} levels consecutive to the binding of ACh to the M1 receptors leads to the increase in CAN-mediated ADPs (Haj-Dahmane and Andrade, 1996, 1998; Gulledge et al., 2007; Gulledge et al., 2009; Zhang and Séguéla, 2010; Kurowski et al., 2015). It has been shown that the Ca^{2+} necessary to activate the CAN channels can enter into the intracellular space through Ca_T channels (Haj-Dahmane and Andrade, 1998), but a complementary mechanism could be the activation of the IP3 receptors located at the membrane of the ER. Thus, we could perturb the activation of the CAN channels by blocking the ER Ca^{2+} release.

One option could be to inhibit the inositol trisphosphate receptor (IP3R) to prevent Ca^{2+} inflow into the cell. 2-APB (200 µM) has been used to inhibit IP3-Ca^{2+} release in mPFC neurons *in vitro* in rats: studies have shown that the 2-APB-mediated IP3 R inhibition decreases both fast (Hagenston et al., 2009) and slow (Dasari et al., 2013) TRPC-mediated ADP. In addition, some

studies show that *in vivo* 2-APB administration is feasible, but here again the drug is injected intraperitoneally (Fernández-Serra et al., 2022), which would not specifically affect mPFC.

Another option could be to use IP3R knockout (IP3R KO) mice. Constitutive IP3R KO mice do exist already (Matsumoto and Nagata, 1999; Higo et al., 2010). However, in our experiment, we would not want to affect pre- and postnatal development, nor to impact other brain regions than the mPFC and other neuronal types than the excitatory pyramidal neurons. In contrast, conditional IP3R KO mice could be a more suitable tool, as we could locally inject a *Cre recombinase* to delete genes coding for IP3R at the time we decide. Multiple *Cre;Itpr1*$^{flox/flox}$ lines already do exist but the *Cre recombinase* is under other promoters (Sugawara et al., 2013; Wang et al., 2018; Lo et al., 2020) than the ones commonly used for targeting excitatory neurons—i.e., *Thy* and *Syn*. Thus developing conditional IP3R KO mice with *Cre* expressed in excitatory neurons (CamKII-, *Thy*-, or *Syn-Cre;Itpr1*$^{flox/flox}$) would offer the tool we are lacking to test the causal link between ER-released Ca^{2+} and PWM mechanisms and capacities.

In sum, the experimental ideas proposed in this section would be beneficial to address causal links of M1 receptors, or CAN conductances, or intracellular Ca^{2+} with the emergence of GPA in the mPFC and PWM performance. The development of more specific pharmacological agents or genetic manipulations would offer better tools to investigate the role of these actors in the mPFC during a PWM task.

Are parametric working memory mechanisms sex-dependent?

Studies have suggested sex-differences in WM tasks: for instance, women perform better in WM tasks involving verbal and writing skills, and men perform better in mathematical, spatial, and object WM (Hill et al., 2014). In addition, previous experiments provided evidence for gender-specific WM networks; for example, in women, limbic—e.g., amygdala and hippocampus—and prefrontal structures are more activated than in men, and parietal regions are more activated in men than in women (Hill et al., 2014). We can note that despite a presumably greater activity in the PFC regions in women, men seem to perform better parametric-related WM tasks. This observation questions the crucial role of other brain structures in PWM mechanisms, such as the parietal cortex crucial for WM processes (Murray et al., 2017), but also raises the question whether there are sex-differences in the neuronal mechanisms underlying PWM.

In the literature, *in vivo* studies investigating PWM capacities in animals either didn't specify the sex when they were done using monkeys (Brody, 2003; Barak et al., 2010), or only used males when done with rats (Fassihi et al., 2014), thus all the *in vitro* experiments about CB and GPA were conducted in male rodents (Leroux et al., manuscript #1 and #2). However, in the future, it would be interesting to conduct the same *in vitro* analysis in females.

Little (if none) work has been done in rodent females about the mechanisms underlying the emergence of self-sustained spiking in cortical neurons. Stephens et al. (2018) is the only team who conducted experiments on both males and females. Their study was about the effect of serotonin phasic exposure on persistent spiking, and they didn't observe any difference between males and females in neuronal intrinsic properties, nor spiking.

However, differences exist in synaptic properties between males and females. For example, female mice exhibit higher levels of synaptosomal glutamate, and higher spontaneous excitatory post-synaptic current (sEPSC) frequency and amplitude in the mPFC than males (Knouse et al., 2022). In contrast, dopamine levels in mPFC are similar across sexes, but NMDA receptor inhibition (with APV) decreases dopamine levels in females only, suggesting different regulation mechanisms between males and females (Locklear et al., 2014). Also, excitability of PV+ interneurons, but not SST+ interneurons, in the mPFC is higher—i.e., higher frequency of spiking in F/I curves and higher frequency of sEPCS—in females than in males, suggesting a stronger inhibition in cortical circuits in females (Jones and Sheets, 2020). These examples demonstrate that differences in neuronal excitability modulation exist between males and females, and provide evidence to continue to investigate neuronal, and thus circuit, mechanisms in both sexes.

In addition to differences in neuronal excitability, differences between male and female rodents have been observed *in vivo* in cognitive behavioral tasks. For example, it was shown that female mice spend less time in the open arms of an O-maze, which translates a higher anxiety levels in females (Cardenas et al., 2021), but perform better than males in a spatial WM task (Y-maze alternation test), suggesting again differences between both sexes.

Altogether, the experiments performed in rodents cited above suggest that differences in PWM mechanisms and performance between male and female rodents could exist. However, if CB and GPA were proven to be not sex-dependent in rodents, it could suggest that the mechanisms underlying PWM are the same in men and women. In that situation, an alternative explanation to the differences observed in mathematical, spatial, and object WM between men and women (Hill et al., 2014) could be social.

It has been shown that education of girls and boys vary in many ways, which ultimately fuel gender stereotypes. Generally, girls are encouraged to endorse self-transcendence values—e.g., being calm and helping people—, whereas boys are encouraged to endorse self-enhancement values—e.g., competing and wanting to be in charge (Aelenei et al., 2016). More specifically, a study conducted by Dersch et al. revealed that, math-gender-streotypes—i.e., stereotypes of girls having weaker mathematical abilities than boys—still persist (Dersch et al., 2022). Such educational differences between genders result in major disparities between representation of men and women studying mathematics, physics, and engineering in Colleges and Universities (Charlesworth and Banaji, 2019). To a certain

extent, we could imagine that girls and women are not encouraged to develop their parametric-related mnemonic capacities, which could result in PWM differences between men and women.

What pathological mechanisms are likely to disrupt parametric working memory?

We demonstrated that CB is altered in male rodents modeling Alzheimer's disease (AD) and later in normal aging (Leroux et al., manuscript #2), as well as after mild traumatic brain injury (TBI; second section of Chapter II).

We showed that CB is reduced in 6 month-old 5xFAD mice, an AD model, and 12 month-old control mice (Leroux et al., manuscript #2). To further investigate the pathological consequences at the network level, we could first perform extracellular recordings in slice using multi-unit arrays to assess the presence or the absence of GPA emergence in the mPFC from control and 5xFAD mice. Then, we could perform the same *in vivo* PWM paradigm as described above. According to the CB decrease at 6 month-old and the decline in spatial WM capacities at 4 month-old in 5xFAD mice (Oakley et al., 2006), we hypothesize that 5xFAD mice would exhibit GPA disruption and PWM impairments starting 4-6 month-old.

We also demonstrated that CB is reduced three weeks following TBI in two month-old rats. Similar to AD and aging animals, the next steps would be to record *in vitro* and *in vivo* the emergence of GPA in the mPFC, and to measure PWM performance following TBI in young adult rats. Previous studies showed that 10 days and 4 weeks post-injury, male mice with mild and severe TBI presented reduced spatial working memory capacities (Tucker et al., 2016; Wang et al., 2018). From these findings, we anticipate that three weeks post-TBI, male young adult rats would have PWM mechanisms and capacity impairments.

More than pursuing those experiments to cover the PWM multi-scale disruptions that likely arise in AD and after TBI, it would be particularly important to investigate the cellular and circuit mechanisms of PWM.

Litterature (Satake et al., 2008; Cannady et al., 2017), as well as our results, indicate that the medium AHP mediated by SK channels is a limiting element in the emergence of CB, especially in pathological conditions such as AD and TBI (Chapter II). Apamin has been extensively used *in vitro* to block SK channel-mediated AHP currents (Satake et al., 2008; Faber, 2010; Cannady et al., 2017; Joffe et al., 2019). Gui et al. (2012) showed that apamin injection in a specific brain region is feasible. After placing rats in a stereotaxic frame, researchers injected apamin (0.125-25 pM) in the hypothalamic paraventricular nucleus using glass microinjector pipettes. Thus, injecting apamin in the mPFC in rodents to block SK channels might present a feasible experimental approach to block predominant AHP currents in rodent models of diseases.

In Chapter II, we used the single-nuclear RNA sequencing (snRNA-Seq) data set generated from the cortex of seven month-old 5xFAD mice and AD post-mortem brains by Zhou et al. (2020) to investigate the expression of genes coding for M1 receptors, TRPC channels, G proteins, and IP3 (Fig. 39). On the one hand, our analysis showed that M1 receptor expression is reduced in the cortex of AD post-mortem brains (Fig. 39A) and starting seven months of age in 5xFAD mice (Fig. 39B). Moreover, it has been shown that M1 receptor function is affected in 5xFAD mice starting two month-old (Yi et al., 2020). On the other hand, *Trpc5* gene has been shown to be reduced in the cortex of AD post-mortem brains (Fig. 39A), but not in seven month-old in 5xFAD mice (Fig. 39B). Thus, instead of acting on M1 receptors *in vivo* to improve the mechanisms underlying PWM, and presumably PWM capacities (as discussed in manuscript #2), we propose to enhance the expression of CAN channels. Specifically, we propose to enhance *TRPC5* channel expression in six month-old mice, that seems to be the critical age at which CB significantly decreases (Leroux et la., manuscript #2), by stereotaxically injecting in the mPFC a virus that upregulates the expression of *Trpc5* gene in excitatory neurons—e.g., *AAV9-CaMKIIα-TRPC5* (Vigene Biosciences, Inc., China).

We would recommend that all the experiments cited above were performed in both sexes, as pathologies don't affect men and women in the same way.

On the one hand, men are approximately 40% more likely to suffer a TBI compared with women in the general adult population (Gupte et al., 2019). However, women victims of domestic violence represent one of the largest population groups susceptible to suffering from a TBI, as one in four married women are struck by their spouse at some time during their marriage (Strauss et al., 2006).

On the other hand, in countries with established socio-economic order women live on the average 4-7 years longer than men (Ginter and Simko, 2013). Also, women represent almost ⅔ of the 6 million Americans living with AD (Alzheimer's Association, USA).

These epidemiological data demonstrate the crucial need to understand the pathological impacts on neuronal and cortical excitability mechanisms. In this direction, the National Institutes of Health (United States) require researchers to provide "*strong justification from the scientific literature, preliminary data, or other relevant considerations [...] for applications proposing to study only one sex*" (Landis et al., 2012).

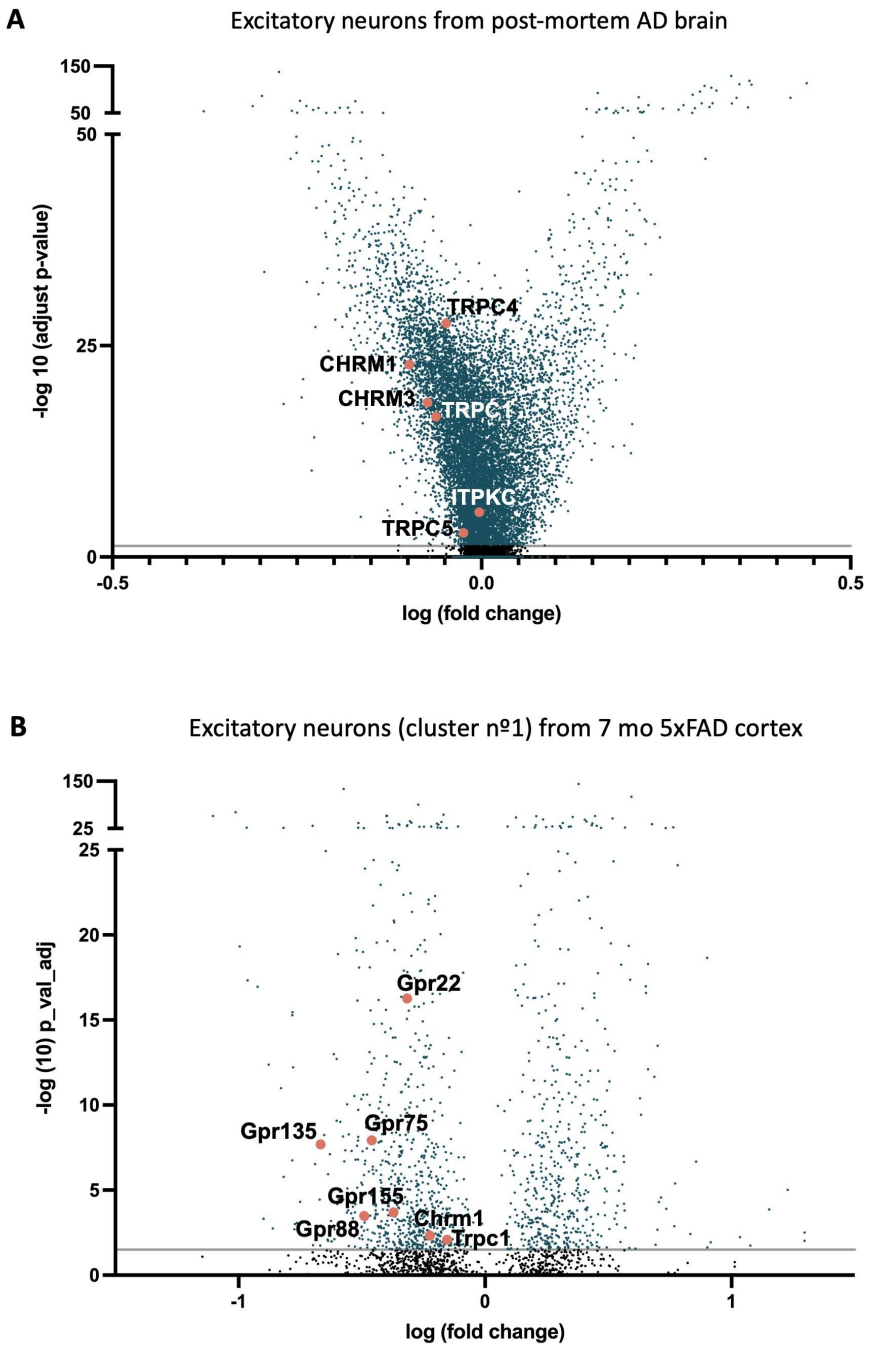

Fig. 39. Single nucleus RNA-seq analysis from human AD post-mortem cortex and 7 month-old 5xFAD mouse cortex reveals downregulation of genes involved in CB mechanisms. *Volcano plot of differences in gene expression levels with log-twofold change (x-axis) against adjusted p-value (FDR, y-axis, exact test) between cortical neurons from* ***A,*** *AD post-mortem brains and non-AD post-mortem brains, and* ***B,*** *seven month-old 5xFAD mice and littermate controls. Human genes: CHRM1/3, muscarinic 1/3 receptors; TRPC1/4/5, TRPC1/4/5 channels; ITPKC, inositol trisphosphate kinase. Mouse genes: Chrm1, muscarinic 1 receptor; Trpc1, TRCP1 channel; Gpr, G proteins. Data sets from Zhou et al. (2020).*

Are parametric working memory mechanisms affected in neurodevelopmental disorders?

In humans, WM capacities have been proven to dramatically increase during the first months of life, and by 6 month-old babies respond well on WM procedures with only a single item to be remembered. Between 8 months-old and one year-old, infants appear to have a WM capacity of about 3 items (Cowan, 2016). Another study conducted with children aged from four to fifteen years-old showed that during these years, WM capacities linearly increase (Gathercole et al., 2004), until peaking at adulthood and declining in aging (Matysiak et al., 2019). PWM capacities were not assessed—neither CAN currents—, to our knowledge, during development in humans, monkeys, or rodents; it is possible that PWM capacities follow the same linear development as other types, such as object and spatial WM.

In Chapter III, we discussed disruptions in neuronal and network excitability caused by mutations in neurodevelopmental genes—*Mafb* and *c-Maf*—in cortical interneurons (CINs; Leroux et al., manuscript #3). It is well established that circuit imbalance in the excitation/inhibition ratio contributes to symptoms in many neurodevelopmental disorders (Chao et al., 2010; Han et al., 2012; Rubenstein and Merzenich, 2003; Yizhar et al., 2011). In our study, we showed that *Mafb* and *c-Maf* in SST+ CINs don't act on the same postnatal mechanisms (Leroux et al., manuscript #3). In fact, we demonstrated that *c-Maf* in SST+ CINs is crucial for their synaptic excitation, and mutation in this gene resulted in hyper-excitability—i.e., epileptic-like activity—of the cortex, including the mPFC, in adult mice (Leroux et al., manuscript #3). We also showed that *Mafb* deletion in SST+ CINs decreased their density in the cortical superficial layers, but no change in cortical excitability (Leroux et al., manuscript #3).

One of the many symptoms of neurodevelopmental disorders—such as autism spectrum disorder, attention deficit hyperactivity disorder, and the FOXG1 syndrome—is epilepsy (Dunn et al., 2003; Florian et al., 2012; Keller et al., 2017; Wong et al., 2019). Epilepsy comprises a broad category of diseases united by a common tendency toward unprovoked seizures (Fisher et al., 2017). There exist focal and generalized epilepsy that, respectively, remains localized to specific parts of the brain or involves the whole brain (Lindquist et al., 2023). If we take the example of the *c-Maf* mutation in SST+ CINs, which increases epileptic-like activity in at least two cortical regions—S1 and mPFC—, we can therefore wonder what are some of the cognitive behavioral consequences.

It is well established that epilepsy disrupts WM capacities (Motamedi and Meador, 2003; Holmes, 2013; Nickels et al., 2016), which significatively diminishes quality of life (Danguecan and Smith, 2017). In the study presented in Chapter III, we didn't conduct WM assessment with the *Maf* mutant mice. Moreover, in our 2-hour-long *in vivo* recordings, we didn't capture absent or convulsive seizures, 'only' epileptic-like spikes. Thus, we can hypothesize that, depending on the severity of the hyper-excitability generated in the cortex, PWM mechanisms and performance would be or not be affected in SST+ *c-Maf* cKO mice. In addition, to this date, M1 receptor and CAN channel mechanisms have not been investigated in *Maf* mutants. Thus,

longer *in vivo* ECoG recordings, as well as the intensive study of PWM mechanisms and performance as described above, would be required to investigate whether *Maf*-mediated epileptic-like activity disrupts PWM neuronal and circuit mechanisms.

Altogether, in this thesis, we highlighted multiple components of the neuronal and circuit excitability in the cortex. We discussed the intrinsic properties responsible for CB-related self-sustained spiking in excitatory neurons in the context of parametric working memory. We showed how neuromodulators affect this neuronal property and we demonstrated how graded persistent activity can emerge in the prefrontal cortex. We also discussed the synaptic excitation in inhibitory interneurons of the primary somatosensory cortex and the excitatory/inhibitory ratio in the cortex. We observed these components in physiological and pathological contexts. We showed that cellular memorization, mediated through self-sustained spiking, is affected in Alzheimer's disease and traumatic brain injury, and cortical epileptic-like activity emerges in the case of neurodevelopmental-like disorders.

With these different project, we demonstrated that neuronal excitability and circuit excitatory/inhibitory balance in the cortex are crucial for cognitive functions, and dysregulations at any of the levels—synapse, post-synaptic neuron, circuit, brain region—can lead to dramatic impairments.

SUMMARY OF ACHIEVEMENTS

FUNDING

2016 - 2020	Agence Nationale de la Recherche, France (PARABIST – Delord, PI)
2016 - 2020	National Science Foundation, U.S.A. (1608236 – Paz, PI)
2022 - 2023	FOXG1 Foundation, Fellowship Research Grant, U.S.A. (Leroux, PI)

AWARDS

2021	Robert and Linda Mahley Career Advancement Award, Gladstone Institutes, San Francisco, U.S.A.
2022	Research Support for Female Learners Impacted by COVID-19 Award, Weill Institute, San Francisco, U.S.A.
2023	'Commit to Teamwork' Core Value Award, Gladstone Institutes, San Francisco, U.S.A.

LIST OF PUBLICATIONS

Leroux MA, Medernach D, Ford JB, Necula D, Cho FS, Holden SS, Clemente-Perez A, Paz JT, Delord B. *In Preparation*. **Identification and characterization of intrinsic conditional bistability and network graded persistent activity in the prefrontal cortex of rats.**

Leroux MA, DeNittis V, Ford JB, Medernach D, Necula D, Delord B, Paz JT. *In Preparation*. **Neuronal conditional bistability is impaired in a mouse model of Alzheimer's disease and in normal aging.**

Leroux MA, Hu JS, Pai ELL, Lew I, Rubenstein JLR, Paz JT. *In Preparation*. ***Mafb*** **and** ***c-Maf*** **regulate the function of somatostatin-positive cortical interneurons and epileptic activity.**

SCIENTIFIC COMMUNICATIONS

Posters

May 2022	Scientific Advisory Board, Gladstone Institutes, San Francisco, U.S.A.
July 2022	European Neuroscience Conference by Doctorale Students (ENCODS), Paris, France

July 2022 Federation of European Neuroscience Societies (FENS) Forum, Paris, France

Nov. 2022 Society for Neuroscience (SfN) Annual Meeting, San Diego, U.S.A.

Oral presentations

April 2023 Research in Progress Seminar, Gladstone Institutes, San Francisco, U.S.A.

May 2023 European Neuroscience Conference by Doctorale Students (ENCODS), Faro, Portugal

SCIENTIFIC MEDIATION

2021 - 2023 **Scientist Volunteer for Inclusion and Diversity**
Internship program: Promoting Underrepresented Minorities Advancing in the Sciences (PUMAS) – *Review of applications and interviews*

2022 - 2023 **ENCODS 2023 Committee Organizer**
European Neuroscience Conference by Doctorale Students
FENS satellite event, 01-02 May 2023 (136 attendees)
Fundraising, marketing/communication, workshops and social event planning

May 2023 **Scientist Volunteer for Pint of Science**
Science popularization festival, 22-24 May 2023 (~30 attendees/day)
Event organization, invited speaker coordination, quiz animation

TRAININGS & WORKSHOPS

Title	Format	Host	Duration	Year
Scientific ethics and integrity				
Ethics and compliance briefing for researchers	Online course	University of California	$2^{H}00$	Once a year
Scientific Integrity with Kevin Mullane	Workshop	Gladstone Institutes	$1^{H}30$	2020
Responsible conduct of research: protect your research and reputation with Kevin Mullane	Workshop	Gladstone Institutes	$1^{H}30$	2022

The lab: avoiding research misconduct with Sudha Krishnamurthy	Interactive movie	Gladstone Institutes	2H00	2022

Laboratory practice

Laboratory safety for researchers	Online course	University of California	2H00	Once a year
Biosafety	Online course	University of California	2H00	Once a year
Controlled substance use	Online course	University of California	4H00	Once a year
Laser awareness	Online course	University of California	2H00	Once a year
Cage density and policy	Online course	University of California	2H00	Once a year
Safe shipper – Biohazards	Online course	University of California	2H00	Once a year
Carcinogen training	Online course	University of California	2H00	Once a year
Bloodborne pathogen training	Online course	University of California	2H00	Once a year
Security awareness	Online course	Gladstone Institutes	1H30	2020

Animal experimentation

Work with animals	Online course	UC IACUC	2H00	2019
Anesthesia, surgery and post surgery role	Online course	UC IACUC	2H00	2019
Mouse: introduction and basics	In person training	UC IACUC	4H00	2019
Mouse: euthanasia training	In person training	UC IACUC	4H00	2019
Rat: introduction and basics	In person training	UC IACUC	4H00	2019

Rat: euthanasia training	In person training	UC IACUC	4^{H}00	2019
Rodent surgery	In person training	UC IACUC	4^{H}00	2019

IACUC: Institutional Animal Care and Use Program

Scientific expertise and methods

Introduction à la modélisation en biologie with Pr. Bruno Delord	Lecture and workshop	Sorbonne University	16^{H}00	2019
Modèles biochimiques des processus cellulaires with Pr. Bruno Delord	Lecture and workshop	Sorbonne University	8^{H}00	2019
Cerveau et comportement with Pr. Bruno Delord	Lecture and workshop	Sorbonne University	2^{H}00	2019
qPCR: from basics to instrument operation with ThermoFisher representative	Lecture	Gladstone Institutes	2^{H}00	2023

Communication

The art of lecturing with Dr. Robert Mahley	Workshop	Gladstone Institutes	2^{H}30	2020
Nuts & Bolts of Manuscript Writing Course With Françoise Chanut	Workshop	Gladstone Institutes	10^{H}	2023

Diversity, equity and inclusion

Foundations of diversity, equity and inclusion	Online training	University of California	1^{H}00	2020
Harassment prevention training: a commonsense approach	Online training	University of California	2^{H}00	2020
Precise language with Mercedes Jenkins	Workshop	Gladstone Institutes	2^{H}00	2020

Professional perspectives

Interviewing and negotiating for an academic position with Dr. Casey Gifford and Dr. Elphège Nora	Workshop	Gladstone Institutes	1H30	2020
Informational interview: a key networking tool with Alicia Roy	Workshop	Gladstone Institutes	2H00	2023

MENTORSHIP

2019	**Francisco Aparicio** – Neuroscience Rotation Student, Gladstone Institutes
2020	**Yanilka Soto** – Neuroscience Rotation Student, Gladstone Institutes
2022	**Olive Tambou** – Neuroscience Rotation Student, Gladstone Institutes
2022 - 2023	**Vivianna DeNittis** – Research Associate, Gladstone Institutes

OTHER SCIENTIFIC PROJECTS

<u>Project 1:</u> Identification of seizure phenotypes and brain regions involved in seizure expression in mouse models of FOXG1 syndrome

Under the supervision of Jeanne Paz (Gladstone Institutes, UCSF, U.S.A.) and in collaboration with Soo-Kyung Lee (University at Buffalo, U.S.A.), after receiving a fellowship research grant from the FOXG1 Foundation (U.S.A.)

FOXG1 syndrome is a rare neuro-developmental disorder caused by mutations in the *FoxG1* gene, which is involved in brain development. This syndrome affects children and is characterized by microcephaly, low muscle tone, limited social interactions, sleep disruption and epileptic seizures. The seizures occur in early childhood (before the age of 3 years), and can be life-threatening. Despite previous work, it remains unknown which brain regions are responsible for the seizures in the FOXG1 syndrome, and to what extent the seizures contribute to sleep disruption and cognitive deficits.

In this study, the goal is to identify the seizure phenotypes and the brain regions in seizure expression. To do so, in young adults of three different mouse models of the FOXG1 syndrome, chronic devices with electro-corticographic (ECoG) electrodes were implanted in various cortical regions including the motor cortex, the somatosensory cortex, the visual cortex and the prefrontal cortex. One week after the mice recovered from surgery, recordings of brain activity in freely behaving mice were performed. *Experiments are currently in progress.*

<u>Project 2:</u> Transient developmental exposure to patient-derived anti-NMDA receptor autoantibodies causes long-term axonal and behavioral defects

Under the supervision of Jeanne Paz (Gladstone Institutes, UCSF, U.S.A.) and in collaboration with Samuel Pleasure and Jing Zhou (Weill Institute for Neurosciences, UCSF, U.S.A.)

NMDA receptor antibody encephalitis (NMDAR-AE) is characterized by cerebrospinal fluid (CSF)-resident anti-NMDA receptor autoantibodies that cause a wide range of neurological manifestations. Although many symptoms are responsive to immunotherapy, behavioral deficits persist especially in young patients and the underlying mechanisms of these long-lasting impairments are unknown.

In this project, patient-derived GluN1-specific monoclonal antibodies (mAb) were used to interrogate the underlying mechanisms of long-lasting sensory-motor impairments in mice. Transient exposure to this mAb led to excess callosal projections in the primary somatosensory cortex (S1) and resulted in permanent callosal axon alterations in mice. Importantly, these mice displayed persistent fine movement impairments which were similar to those in NMDAR-AE patients. Notably, the severity of these behavioral deficits was tightly correlated with the severity of callosal axon alterations.

However, whether and how the morphology alteration of callosal neurons led to S1 excitability imbalance and the persistent fine movement change needed to be further examined. To address this gap, extracellular local field potentials and multi-unit activity recordings in acute S1 mouse slices were performed. *Analysis is currently in progress.*

REFERENCES

Achanta, S., & Jordt, S. (2020). Transient receptor potential channels in pulmonary chemical injuries and as countermeasure targets. Annals of the New York Academy of Sciences, 1480(1), 73–103. https://doi.org/10.1111/nyas.14472

Ackerman, S. (1992). Major structures and functions of the brain. Discovering the Brain - NCBI Bookshelf. https://www.ncbi.nlm.nih.gov/books/NBK234157/

Aelenei, C., Darnon, C., & Martinot, D. (2016). Boys, girls, and the school cultural environment: Teachers' judgment and students' values. Journal of Social Psychology, 157(5), 556–570. https://doi.org/10.1080/00224545.2016.1243514

Akirav, I., & Maroun, M. (2005). Ventromedial prefrontal cortex is obligatory for consolidation and reconsolidation of object recognition memory. Cerebral Cortex, 16(12), 1759–1765. https://doi.org/10.1093/cercor/bhj114

Ali, A., Ahmad, F., Pillai, K. K., & Vohora, D. (2004). Evidence of the antiepileptic potential of amiloride with neuropharmacological benefits in rodent models of epilepsy and behavior. Epilepsy & Behavior, 5(3), 322–328. https://doi.org/10.1016/j.yebeh.2004.01.005

Ali, A., Ahmad, F., Pillai, K. K., & Vohora, D. (2005). Amiloride protects against pentylenetetrazole-induced kindling in mice. British Journal of Pharmacology, 145(7), 880–884. https://doi.org/10.1038/sj.bjp.0706291

Alves, F. M., Kallinowski, P., & Ayton, S. (2023). Accelerated brain volume loss caused by Anti–B-Amyloid drugs. Neurology, 100(20), e2114–e2124. https://doi.org/10.1212/wnl.0000000000207156

Alzheimer, A. (1907). Über eine eigenartige Erkrankung der Hirnrinde. Allgemeine Zeitschrift Fur Psychiatrie Und Psychisch-gerichtliche Medizin.

Andrade, R. (1991). Cell excitation enhances muscarinic cholinergic responses in rat association cortex. Brain Research, 548(1–2), 81–93. https://doi.org/10.1016/0006-8993(91)91109-e

Antoine, M. W. (2022). Paradoxical hyperexcitability in disorders of neurodevelopment. Frontiers in Molecular Neuroscience, 15. https://doi.org/10.3389/fnmol.2022.826679

Araneda, R. C., & Andrade, R. (1991). 5-Hydroxytryptamine2 and 5-hydroxytryptamine1A receptors mediate opposing responses on membrane excitability in rat association cortex. Neuroscience, 40(2), 399–412. https://doi.org/10.1016/0306-4522(91)90128-b

Arciniega, H., Shires, J., Furlong, S., Kilgore-Gomez, A., Cerreta, A., Murray, N. G., & Berryhill, M. E. (2021). Impaired visual working memory and reduced connectivity in undergraduates with a history of mild traumatic brain injury. Scientific Reports, 11(1). https://doi.org/10.1038/s41598-021-80995-1

Baddeley, A. (1992). Working memory. Science, 255(5044), 556–559. https://doi.org/10.1126/science.1736359

Baddeley, A., Bressi, S., Della Sala, S., Logie, R. H., & Spinnler, H. (1991). THE DECLINE OF WORKING MEMORY IN ALZHEIMER'S DISEASE. Brain, 114(6), 2521–2542. https://doi.org/10.1093/brain/114.6.2521

Baeg, E. H., Kim, Y. B., Jang, J., Kim, H. T., Mook-Jung, I., & Jung, M. W. (2001). Fast spiking and regular spiking neural correlates of fear conditioning in the medial prefrontal cortex of the rat. Cerebral Cortex, 11(5), 441–451. https://doi.org/10.1093/cercor/11.5.441

Baillarger, J. G. F. (1840). Recherches sur la structure de la couche corticale des circonvolutions du cerveau. Mem. Acad. Med.

Barak, O., Tsodyks, M., & Romo, R. (2010). Neuronal population coding of parametric working memory. The Journal of Neuroscience, 30(28), 9424–9430. https://doi.org/10.1523/jneurosci.1875-10.2010

Barbieri, F., & Brunel, N. (2008). Can attractor network models account for the statistics of firing during persistent activity in prefrontal cortex? Frontiers in Neuroscience, 2(1), 114–122. https://doi.org/10.3389/neuro.01.003.2008

Barkai, E., & Hasselmo, M. E. (1994). Modulation of the input/output function of rat piriform cortex pyramidal cells. Journal of Neurophysiology, 72(2), 644–658. https://doi.org/10.1152/jn.1994.72.2.644

Barnes, N. M., & Sharp, T. (1999). A review of central 5-HT receptors and their function. Neuropharmacology, 38(8), 1083–1152. https://doi.org/10.1016/s0028-3908(99)00010-6

Başar, E., Basar-Eroglu, C., Karakaş, S., & Schürmann, M. (2001). Gamma, alpha, delta, and theta oscillations govern cognitive processes. International Journal of Psychophysiology, 39(2–3), 241–248. https://doi.org/10.1016/s0167-8760(00)00145-8

Bastos, A. M., Usrey, W. M., Adams, R. A., Mangun, G. R., Fries, P., & Friston, K. J. (2012). Canonical microcircuits for predictive coding. Neuron, 76(4), 695–711. https://doi.org/10.1016/j.neuron.2012.10.038

Batuev, A. S., Kursina, N. P., & Shutov, A. P. (1990). Unit activity of the medial wall of the frontal cortex during delayed performance in rats. Behavioural Brain Research, 41(2), 95–102. https://doi.org/10.1016/0166-4328(90)90145-5

Bhattacherjee, A., Djekidel, M. N., Chen, R., Chen, W., Tuesta, L. M., & Zhang, Y. (2019). Cell type-specific transcriptional programs in mouse prefrontal cortex during adolescence and addiction. Nature Communications, 10(1). https://doi.org/10.1038/s41467-019-12054-3

Binder, L. M. (1986). Persisting symptoms after mild head injury: A review of the postconcussive syndrome. Journal of Clinical and Experimental Neuropsychology, 8(4), 323–346. https://doi.org/10.1080/01688638608401325

Bittar, T., & Labonté, B. (2021). Functional contribution of the medial prefrontal circuitry in major depressive disorder and Stress-Induced Depressive-Like behaviors. Frontiers in Behavioral Neuroscience, 15. https://doi.org/10.3389/fnbeh.2021.699592

Bizon, J. L., Foster, T. C., Alexander, G. E., & Glisky, E. L. (2012). Characterizing cognitive aging of working memory and executive function in animal models. Frontiers in Aging Neuroscience, 4. https://doi.org/10.3389/fnagi.2012.00019

Bontempi, B., Laurent-Demir, C., Destrade, C., & Jaffard, R. (1999). Time-dependent reorganization of brain circuitry underlying long-term memory storage. Nature, 400(6745), 671–675. https://doi.org/10.1038/23270

Brion, J. P. (1998). Neurofibrillary tangles and Alzheimer's disease. European Neurology, 40(3), 130–140. https://doi.org/10.1159/000007969

Brodmann, K. (1909). Vergleichende Lokalisationslehre der Grosshirnrinde: in ihren Prinzipien dargestellt auf Grund des Zellenbaues. Barth, Leipzig.

Brody, C. D. (2003). Timing and neural encoding of somatosensory parametric working memory in macaque prefrontal cortex. Cerebral Cortex, 13(11), 1196–1207. https://doi.org/10.1093/cercor/bhg100

Burke, S. N., & Barnes, C. A. (2006). Neural plasticity in the ageing brain. Nature Reviews Neuroscience, 7(1), 30–40. https://doi.org/10.1038/nrn1809

Burton, B. G., Hok, V., Save, E., & Poucet, B. (2009). Lesion of the ventral and intermediate hippocampus abolishes anticipatory activity in the medial prefrontal cortex of the rat. Behavioural Brain Research, 199(2), 222–234. https://doi.org/10.1016/j.bbr.2008.11.045

Cain, S. M., & Snutch, T. P. (2010). Contributions of T-type calcium channel isoforms to neuronal firing. Channels, 4(6), 475–482. https://doi.org/10.4161/chan.4.6.14106

Cannady, R., McGonigal, J. T., Newsom, R. J., Woodward, J. J., Mulholland, P. J., & Gass, J. T. (2017). Prefrontal Cortex KCa2 Channels Regulate mGlu5-Dependent Plasticity and Extinction of Alcohol-Seeking Behavior. The Journal of Neuroscience, 37(16), 4359–4369. https://doi.org/10.1523/jneurosci.2873-16.2017

Canter, R. G., Huang, W., Choi, H., Wang, J., Watson, L. A., Yao, C. G., Abdurrob, F., Bousleiman, S. M., Young, J. Z., Bennett, D. A., Delalle, I., Chung, K., & Tsai, L. H. (2019). 3D mapping reveals network-specific amyloid progression and subcortical susceptibility in mice. Communications Biology, 2(1). https://doi.org/10.1038/s42003-019-0599-8

Carballo-Márquez, A., Vale-Martínez, A., Guillazo-Blanch, G., & Martí-Nicolovius, M. (2009). Muscarinic receptor blockade in ventral hippocampus and prelimbic cortex impairs memory for socially transmitted food preference. Hippocampus, 19(5), 446–455. https://doi.org/10.1002/hipo.20530

Carballo-Márquez, A., Vale-Martínez, A., Guillazo-Blanch, G., Torras-Garcia, M., Boix-Trelis, N., & Martí-Nicolovius, M. (2007). Differential effects of muscarinic receptor blockade in prelimbic cortex on acquisition and memory formation of an odor-reward task. Learn Mem, 14(9), 616–624. https://doi.org/10.1101/lm.597507

Cardenas, A., Papadogiannis, A., & Dimitrov, E. (2021). The role of medial prefrontal cortex projections to locus ceruleus in mediating the sex differences in behavior in mice with inflammatory pain. The FASEB Journal, 35(7). https://doi.org/10.1096/fj.202100319rr

Carvell, G. E., & Simons, D. J. (1987). Thalamic and corticocortical connections of the second somatic sensory area of the mouse. Journal of Comparative Neurology, 265(3), 409–427. https://doi.org/10.1002/cne.902650309

Carver, C. M., Dewitt, H., Stoja, A., & Shapiro, M. S. (2021). Blockade of TRPC channels limits Cholinergic-Driven hyperexcitability and seizure susceptibility after traumatic brain injury. Frontiers in Neuroscience, 15. https://doi.org/10.3389/fnins.2021.681144

Casale, A. E., Foust, A. J., Bal, T., & McCormick, D. A. (2015). Cortical interneuron subtypes vary in their axonal action potential properties. The Journal of Neuroscience, 35(47), 15555–15567. https://doi.org/10.1523/jneurosci.1467-13.2015

Casem, M. L. (2016). Membranes and Membrane Transport. In Case Studies in Cell Biology (pp. 105–125). https://doi.org/10.1016/b978-0-12-801394-6.00005-1

Catterall, W. A. (2011). Voltage-Gated calcium channels. Cold Spring Harbor Perspectives in Biology, 3(8), a003947. https://doi.org/10.1101/cshperspect.a003947

Chang, C., Evans, M. D., Yu, X., Yu, G., & Mucke, L. (2021). Tau reduction affects excitatory and inhibitory neurons differently, reduces excitation/inhibition ratios, and counteracts network hypersynchrony. Cell Reports, 37(3), 109855. https://doi.org/10.1016/j.celrep.2021.109855

Chang, C., Shao, Q., & Mucke, L. (2021). Tau: Enabler of diverse brain disorders and target of rapidly evolving therapeutic strategies. Science, 371(6532). https://doi.org/10.1126/science.abb8255

Chao, H. T., Chen, H., Samaco, R. C., Xue, M., Chahrour, M., Yoo, J. W., Neul, J. L., Gong, S., Lu, H., Heintz, N., Ekker, M., Rubenstein, J. L., Noebels, J. L., Rosenmund, C., & Zoghbi, H. Y. (2010). Dysfunction in GABA signalling mediates autism-like stereotypies and Rett syndrome phenotypes. Nature, 468(7321), 263–269. https://doi.org/10.1038/nature09582

Charlesworth, T. E. S., & Banaji, M. R. (2019). Gender in Science, Technology, Engineering, and Mathematics: Issues, Causes, Solutions. The Journal of Neuroscience, 39(37), 7228–7243. https://doi.org/10.1523/jneurosci.0475-18.2019

Chau, D. T., Rada, P., Kosloff, R. A., Taylor, J. L., & Hoebel, B. G. (2001). Nucleus accumbens muscarinic receptors in the control of behavioral depression: antidepressant-like effects of local M1 antagonist in the Porsolt swim test. Neuroscience, 104(3), 791–798. https://doi.org/10.1016/s0306-4522(01)00133-6

Chen, L., Bohanick, J. D., Nishihara, M., Seamans, J. K., & Yang, C. R. (2007). Dopamine D1/5 Receptor-Mediated Long-Term Potentiation of Intrinsic Excitability in Rat Prefrontal Cortical Neurons: Ca2+-Dependent Intracellular Signaling. Journal of Neurophysiology, 97(3), 2448–2464. https://doi.org/10.1152/jn.00317.2006

Chmielowska, J., Carvell, G. E., & Simons, D. J. (1989). Spatial organization of thalamocortical and corticothalamic projection systems in the rat SmI barrel cortex. Journal of Comparative Neurology, 285(3), 325–338. https://doi.org/10.1002/cne.902850304

Cho, F. S., Vainchtein, I. D., Voskobiynyk, Y., Morningstar, A. R., Aparicio, F., Higashikubo, B., Ciesielska, A., Broekaart, D. W. M., Anink, J. J., Van Vliet, E. A., Yu, X., Khakh, B. S., Aronica, E., Molofsky, A. V., & Paz, J. T. (2022). Enhancing GAT-3 in thalamic astrocytes promotes resilience to brain injury in rodents. Science Translational Medicine, 14(652). https://doi.org/10.1126/scitranslmed.abj4310

Choe, Y. (2003). Processing of analogy in the thalamocortical circuit. IEEE Conference Publication | IEEE Xplore. https://ieeexplore.ieee.org/document/1223916/authors

Christova, M., Pondev, N., Christova, L., Wolf, W., Dengler, R., & Kossev, A. (2006). Motor cortex excitability during unilateral muscle activity. Journal of Electromyography and Kinesiology, 16(5), 477–484. https://doi.org/10.1016/j.jelekin.2005.09.002

Chudasama, Y. (2011). Animal models of prefrontal-executive function. Behavioral Neuroscience, 125(3), 327–343. https://doi.org/10.1037/a0023766

Clemente-Perez, A., Makinson, S. R., Higashikubo, B., Brovarney, S., Cho, F. S., Urry, A., Holden, S. S., Wimer, M., Dávid, C., Fenno, L. E., Acsády, L., Deisseroth, K., & Paz, J. T. (2017). Distinct thalamic reticular cell types differentially modulate normal and pathological cortical rhythms. Cell Reports, 19(10), 2130–2142. https://doi.org/10.1016/j.celrep.2017.05.044

Cobos, I., Long, J. E., Thwin, M. T., & Rubenstein, J. L. (2006). Cellular patterns of transcription factor expression in developing cortical interneurons. Cerebral Cortex, 16(suppl_1), i82–i88. https://doi.org/10.1093/cercor/bhk003

Compte, A. (2006). Computational and in vitro studies of persistent activity: Edging towards cellular and synaptic mechanisms of working memory. Neuroscience, 139(1), 135–151. https://doi.org/10.1016/j.neuroscience.2005.06.011

Compte, A., Constantinidis, C., Tegnér, J., Raghavachari, S., Chafee, M. V., Goldman-Rakic, P. S., & Wang, X. J. (2003). Temporally irregular mnemonic persistent activity in prefrontal neurons of monkeys during a delayed response task. Journal of Neurophysiology, 90(5), 3441–3454. https://doi.org/10.1152/jn.00949.2002

Corcoran, K. A., & Quirk, G. J. (2007). Activity in Prelimbic Cortex Is Necessary for the Expression of Learned, But Not Innate, Fears. The Journal of Neuroscience, 27(4), 840–844. https://doi.org/10.1523/jneurosci.5327-06.2007

Cordes, S. P., & Barsh, G. S. (1994). The mouse segmentation gene kr encodes a novel basic domain-leucine zipper transcription factor. Cell, 79(6), 1025–1034. https://doi.org/10.1016/0092-8674(94)90033-7

Courtney, S., Petit, L., Maisog, J. M., Ungerleider, L. G., & Haxby, J. V. (1998). An area specialized for spatial working memory in human frontal cortex. Science, 279(5355), 1347–1351. https://doi.org/10.1126/science.279.5355.1347

Cowan, N. (2016). Working memory maturation. Perspectives on Psychological Science, 11(2), 239–264. https://doi.org/10.1177/1745691615621279

Creighton, S. D., Mendell, A. L., Palmer, D. D., Kalisch, B. E., MacLusky, N. J., Prado, V. F., Prado, M. a. M., & Winters, B. D. (2019). Dissociable cognitive impairments in two strains of transgenic Alzheimer's disease mice revealed by a battery of object-based tests. Scientific Reports, 9(1). https://doi.org/10.1038/s41598-018-37312-0

Dai, M., Zheng, H., Zeng, L., & Zhang, Y. (2017). The genes associated with early-onset Alzheimer's disease. Oncotarget, 9(19), 15132–15143. https://doi.org/10.18632/oncotarget.23738

Danguecan, A., & Smith, M. L. (2017). Academic Outcomes in Individuals with Childhood-Onset Epilepsy: Mediating Effects of working Memory. Journal of the International Neuropsychological Society, 23(7), 594–604. https://doi.org/10.1017/s135561771700008x

Dasari, S., Abramowitz, J., Birnbaumer, L., & Gulledge, A. T. (2013). Do canonical transient receptor potential channels mediate cholinergic excitation of cortical pyramidal neurons? Neuroreport, 24(10), 550–554. https://doi.org/10.1097/wnr.0b013e3283621344

Dasari, S., Hill, C., & Gulledge, A. T. (2016). A unifying hypothesis for M1 muscarinic receptor signalling in pyramidal neurons. The Journal of Physiology, 595(5), 1711–1723. https://doi.org/10.1113/jp273627

Davies, M. F., Tsui, J. Y., Flannery, J. A., Li, X., DeLorey, T. M., & Hoffman, B. B. (2003). Activation of α2 Adrenergic Receptors Suppresses Fear Conditioning: Expression of c-Fos and Phosphorylated CREB in Mouse Amygdala. Neuropsychopharmacology, 29(2), 229–239. https://doi.org/10.1038/sj.npp.1300324

Deen, M., Christensen, C. E., Hougaard, A., Hansen, H. D., Knudsen, G. M., & Ashina, M. (2016). Serotonergic mechanisms in the migraine brain – a systematic review. Cephalalgia, 37(3), 251–264. https://doi.org/10.1177/0333102416640501

Delahunty, T. M. (1992). Mild traumatic brain injury enhances muscarinic receptor-linked inositol phosphate production in rat hippocampus. Brain Research, 594(2), 307–310. https://doi.org/10.1016/0006-8993(92)91140-a

Dersch, A., Heyder, A., & Eitel, A. (2022). Exploring the nature of teachers' Math-Gender stereotypes: The Math-Gender Misconception Questionnaire. Frontiers in Psychology, 13. https://doi.org/10.3389/fpsyg.2022.820254

D'Esposito, M., Cooney, J. W., Gazzaley, A., Gibbs, S. E. B., & Postle, B. R. (2006). Is the Prefrontal Cortex Necessary for Delay Task Performance? Evidence from Lesion and fMRI Data. Journal of the International Neuropsychological Society, 12(2), 248–260. https://doi.org/10.1017/s1355617706060322

Dewan, M. C., Rattani, A., Gupta, S., Baticulon, R. E., Hung, Y., Punchak, M., Agrawal, A., Adeleye, A. O., Shrime, M. G., Rubiano, A. M., Rosenfeld, J. V., & Park, K. B. (2019). Estimating the global

incidence of traumatic brain injury. Journal of Neurosurgery, 130(4), 1080–1097. https://doi.org/10.3171/2017.10.jns17352

Diehl, G. W., & Redish, A. D. (2023). Differential processing of decision information in subregions of rodent medial prefrontal cortex. eLife, 12. https://doi.org/10.7554/elife.82833

Ding, H. K., Teixeira, C. M., & Frankland, P. W. (2008). Inactivation of the anterior cingulate cortex blocks expression of remote, but not recent, conditioned taste aversion memory. Learning & Memory, 15(5), 290–293. https://doi.org/10.1101/lm.905008

D'Isa, R., Comi, G., & Leocani, L. (2021). Apparatus design and behavioural testing protocol for the evaluation of spatial working memory in mice through the spontaneous alternation T-maze. Scientific Reports, 11(1). https://doi.org/10.1038/s41598-021-00402-7

Douglas, R. J., & Martin, K. A. (2004). Neuronal Circuits of the Neocortex. Annual Review of Neuroscience, 27(1), 419–451. https://doi.org/10.1146/annurev.neuro.27.070203.144152

Douglas, R. J., & Martin, K. A. (2007). Recurrent neuronal circuits in the neocortex. Current Biology, 17(13), R496–R500. https://doi.org/10.1016/j.cub.2007.04.024

Dronkers, N. F., Ivanova, M. V., & Baldo, J. V. (2017). What Do Language Disorders Reveal about Brain–Language Relationships? From Classic Models to Network Approaches. Journal of the International Neuropsychological Society, 23(9–10), 741–754. https://doi.org/10.1017/s1355617717001126

Dudchenko, P. A. (2004). An overview of the tasks used to test working memory in rodents. Neuroscience & Biobehavioral Reviews, 28(7), 699–709. https://doi.org/10.1016/j.neubiorev.2004.09.002

Dunn, D. W., Austin, J. K., Harezlak, J., & Ambrosius, W. T. (2003). ADHD and epilepsy in childhood. Dev Med Child Neurol, 45(1), 50–54. https://pubmed.ncbi.nlm.nih.gov/12549755/

Egorov, A. V., Hamam, B., Fransen, E., Hasselmo, M. E., & Alonso, A. (2002). Graded persistent activity in entorhinal cortex neurons. Nature, 420(6912), 173–178. https://doi.org/10.1038/nature01171

Eijkelkamp, N., Linley, J. E., Baker, M. D., Minett, M. S., Cregg, R., Werdehausen, R., Rugiero, F., & Wood, J. N. (2012). Neurological perspectives on voltage-gated sodium channels. Brain, 135(9), 2585–2612. https://doi.org/10.1093/brain/aws225

Engel, M., Smidt, M. P., & Van Hooft, J. A. (2013). The serotonin 5-HT3 receptor: a novel neurodevelopmental target. Frontiers in Cellular Neuroscience, 7. https://doi.org/10.3389/fncel.2013.00076

Ennaceur, A., & Delacour, J. (1988). A new one-trial test for neurobiological studies of memory in rats. 1: Behavioral data. Behavioural Brain Research, 31(1), 47–59. https://doi.org/10.1016/0166-4328(88)90157-x

Erisir, A., Lau, D., Rudy, B., & Leonard, C. (1999). Function of Specific K+ Channels in Sustained High-Frequency Firing of Fast-Spiking Neocortical Interneurons. Journal of Neurophysiology, 82(5), 2476–2489. https://doi.org/10.1152/jn.1999.82.5.2476

Eryilmaz, H., Tanner, A., Ho, N. F., Nitenson, A. Z., Silverstein, N. J., Petruzzi, L., Goff, D. C., Manoach, D. S., & Roffman, J. L. (2016). Disrupted Working Memory Circuitry in Schizophrenia: Disentangling fMRI Markers of Core Pathology vs Other Aspects of Impaired Performance. Neuropsychopharmacology, 41(9), 2411–2420. https://doi.org/10.1038/npp.2016.55

Euston, D. R., Gruber, A. J., & McNaughton, B. L. (2012). The role of medial prefrontal cortex in memory and decision making. Neuron, 76(6), 1057–1070. https://doi.org/10.1016/j.neuron.2012.12.002

Faber, E. S. L. (2010). Functional interplay between NMDA receptors, SK channels and voltage-gated Ca2+channels regulates synaptic excitability in the medial prefrontal cortex. The Journal of Physiology, 588(8), 1281–1292. https://doi.org/10.1113/jphysiol.2009.185645

Faber, E. S. L., & Sah, P. (2007). Functions of SK channels in central neurons. Clinical and Experimental Pharmacology and Physiology, 34(10), 1077–1083. https://doi.org/10.1111/j.1440-1681.2007.04725.x

Fassihi, A., Akrami, A., Esmaeili, V., & Diamond, M. E. (2014). Tactile perception and working memory in rats and humans. Proceedings of the National Academy of Sciences of the United States of America, 111(6), 2331–2336. https://doi.org/10.1073/pnas.1315171111

Felder, C. C., Bymaster, F. P., Ward, J. S., & DeLapp, N. W. (2000). Therapeutic opportunities for muscarinic receptors in the central nervous system. Journal of Medicinal Chemistry, 43(23), 4333–4353. https://doi.org/10.1021/jm990607u

Ferguson, B. R., Glick, C., & Huguenard, J. R. (2023). Prefrontal PV interneurons facilitate attention and are linked to attentional dysfunction in a mouse model of absence epilepsy. eLife, 12. https://doi.org/10.7554/elife.78349

Ferguson, P. L., Smith, G., Wannamaker, B. B., Thurman, D. J., Pickelsimer, E., & Selassie, A. W. (2009). A population-based study of risk of epilepsy after hospitalization for traumatic brain injury. Epilepsia, 51(5), 891–898. https://doi.org/10.1111/j.1528-1167.2009.02384.x

Fernández-Serra, R., Martínez-Alonso, E., Alcázar, A., Chioua, M., Marco-Contelles, J., Martínez-Murillo, R., Ramos, M., Guinea, G. V., & González-Nieto, D. (2022). Postischemic neuroprotection of aminoethoxydiphenyl borate associates shortening of Peri-Infarct depolarizations. International Journal of Molecular Sciences, 23(13), 7449. https://doi.org/10.3390/ijms23137449

Fisher, R. S., Cross, J. H., French, J., Higurashi, N., Hirsch, E., Jansen, F. E., Lagae, L., Moshé, S. L., Peltola, J., Perez, E. R., Scheffer, I. E., & Zuberi, S. M. (2017). Operational classification of seizure types by the International League Against Epilepsy: Position Paper of the ILAE Commission for Classification and Terminology. Epilepsia, 58(4), 522–530. https://doi.org/10.1111/epi.13670

Flanigan, T. J., Xue, Y., Rao, S. K., Dhanushkodi, A., & McDonald, M. P. (2014). Abnormal vibrissa-related behavior and loss of barrel field inhibitory neurons in 5xFAD transgenics. Genes, Brain and Behavior, 13(5), 488–500. https://doi.org/10.1111/gbb.12133

Florian, C., Bahi-Buisson, N., & Bienvenu, T. (2011). FOXG1-Related Disorders: From Clinical Description to Molecular Genetics. Molecular Syndromology, 2(3–5), 153–163. https://doi.org/10.1159/000327329

Fournier, M., Clément, T., Aussudre, J., Plesnila, N., Obenaus, A., & Badaut, J. (2020). Contusion rodent model of traumatic brain injury: Controlled cortical impact. In Methods in molecular biology (pp. 49–65). https://doi.org/10.1007/978-1-0716-0845-6_6

Frankland, P. W., Bontempi, B., Talton, L. E., Kaczmarek, L., & Silva, A. J. (2004). The involvement of the anterior cingulate cortex in remote contextual fear memory. Science, 304(5672), 881–883. https://doi.org/10.1126/science.1094804

Frenda, S. J., & Fenn, K. M. (2016). Sleep less, think worse: The effect of sleep deprivation on working memory. Journal of Applied Research in Memory and Cognition, 5(4), 463–469. https://doi.org/10.1016/j.jarmac.2016.10.001

Funahashi, S., Bruce, C. J., & Goldman-Rakic, P. S. (1989). Mnemonic coding of visual space in the monkey's dorsolateral prefrontal cortex. Journal of Neurophysiology, 61(2), 331–349. https://doi.org/10.1152/jn.1989.61.2.331

Fuster, J. M. (1973). Unit activity in prefrontal cortex during delayed-response performance: neuronal correlates of transient memory. Journal of Neurophysiology, 36(1), 61–78. https://doi.org/10.1152/jn.1973.36.1.61

Fuster, J. M. (2002). Frontal lobe and cognitive development. Journal of Neurocytology, 31(3/5), 373–385. https://doi.org/10.1023/a:1024190429920

Fuster, J. M., & Alexander, G. E. (1971). Neuron Activity Related to Short-Term Memory. Science, 173(3997), 652–654. https://doi.org/10.1126/science.173.3997.652

Gabbott, P., Warner, T., Jays, P. R., Salway, P., & Busby, S. (2005). Prefrontal cortex in the rat: Projections to subcortical autonomic, motor, and limbic centers. Journal of Comparative Neurology, 492(2), 145–177. https://doi.org/10.1002/cne.20738

Garavan, H., Ross, T. J., Murphy, K., Roche, R., & Stein, E. A. (2002). Dissociable executive functions in the dynamic control of behavior: inhibition, error detection, and correction. NeuroImage, 17(4), 1820–1829. https://doi.org/10.1006/nimg.2002.1326

Gathercole, S. E., Pickering, S. J., Ambridge, B., & Wearing, H. (2004). The structure of working memory from 4 to 15 years of age. Developmental Psychology, 40(2), 177–190. https://doi.org/10.1037/0012-1649.40.2.177

Gee, S. M., Ellwood, I. T., Patel, T., Luongo, F., Deisseroth, K., & Sohal, V. S. (2012). Synaptic Activity Unmasks Dopamine D2 Receptor Modulation of a Specific Class of Layer V Pyramidal Neurons in Prefrontal Cortex. The Journal of Neuroscience, 32(14), 4959–4971. https://doi.org/10.1523/jneurosci.5835-11.2012

Gil, Z., Connors, B. W., & Amitai, Y. (1997). Differential regulation of neocortical synapses by neuromodulators and activity. Neuron, 19(3), 679–686. https://doi.org/10.1016/s0896-6273(00)80380-3

Gilissen, C., Hehir-Kwa, J. Y., Thung, D. T., Van De Vorst, M., Van Bon, B. W., Willemsen, M. H., Kwint, M., Janssen, I. M., Hoischen, A., Schenck, A., Leach, R. A., Klein, R. J., Tearle, R., Tan, B., Pfundt, R., Yntema, H. G., De Vries, B. B., Kleefstra, T., Brunner, H. G., . . . Veltman, J. A. (2014). Genome sequencing identifies major causes of severe intellectual disability. Nature, 511(7509), 344–347. https://doi.org/10.1038/nature13394

Ginter, E., & Simko. (2013). Women live longer than men. Bratislavské LekáRske Listy, 114(02), 45–49. https://doi.org/10.4149/bll_2013_011

Glenner, G. G., & Wong, C. W. (1984). Alzheimer's disease: Initial report of the purification and characterization of a novel cerebrovascular amyloid protein. Biochemical and Biophysical Research Communications, 120(3), 885–890. https://doi.org/10.1016/s0006-291x(84)80190-4

Goldman, M. S. (2003). Robust Persistent Neural Activity in a Model Integrator with Multiple Hysteretic Dendrites per Neuron. Cerebral Cortex, 13(11), 1185–1195. https://doi.org/10.1093/cercor/bhg095

Goldman-Rakic, P. S. (1995). Cellular basis of working memory. Neuron, 14(3), 477–485. https://doi.org/10.1016/0896-6273(95)90304-6

Gonzalez-Burgos, G. (2000). Horizontal Synaptic Connections in Monkey Prefrontal Cortex: An In Vitro Electrophysiological Study. Cerebral Cortex, 10(1), 82–92. https://doi.org/10.1093/cercor/10.1.82

Gould, T. J. (n.d.). Addiction and Cognition. In Addict Sci Clin Pract (Vol. 5, Issue 2, pp. 4–14). https://www.ncbi.nlm.nih.gov/pmc/articles/PMC3120118/

Graner, J. L., Oakes, T. R., French, L. M., & Riedy, G. (2013). Functional MRI in the investigation of Blast-Related Traumatic Brain Injury. Frontiers in Neurology, 4. https://doi.org/10.3389/fneur.2013.00016

Greene, C. C., Schwindt, P. C., & Crill, W. E. (1994). Properties and ionic mechanisms of a metabotropic glutamate receptor-mediated slow afterdepolarization in neocortical neurons. Journal of Neurophysiology, 72(2), 693–704. https://doi.org/10.1152/jn.1994.72.2.693

Greenman, D. L., La, M., Shah, S. S., Chen, Q., Berman, K. F., Weinberger, D. R., & Tan, H. H. (2020). Parietal-Prefrontal feedforward connectivity in association with schizophrenia genetic risk and delusions. American Journal of Psychiatry, 177(12), 1151–1158. https://doi.org/10.1176/appi.ajp.2020.19111176

Gruber, A. J., Calhoon, G. G., Shusterman, I., Schoenbaum, G., Roesch, M. R., & O'Donnell, P. (2010). More is less: A disinhibited prefrontal cortex impairs cognitive flexibility. The Journal of Neuroscience, 30(50), 17102–17110. https://doi.org/10.1523/jneurosci.4623-10.2010

Gui, L., LaGrange, L. P., Larson, R. A., Gu, M., Zhu, J., & Chen, Q. (2012). Role of small conductance calcium-activated potassium channels expressed in PVN in regulating sympathetic nerve activity and arterial blood pressure in rats. American Journal of Physiology-regulatory Integrative and Comparative Physiology, 303(3), R301–R310. https://doi.org/10.1152/ajpregu.00114.2012

Guinamard, R., Simard, C., & Del Negro, C. (2013). Flufenamic acid as an ion channel modulator. Pharmacology & Therapeutics, 138(2), 272–284. https://doi.org/10.1016/j.pharmthera.2013.01.012

Gulledge, A. T., Bucci, D. J., Zhang, S. S., Matsui, M., & Yeh, H. H. (2009). M1 Receptors Mediate Cholinergic Modulation of Excitability in Neocortical Pyramidal Neurons. The Journal of Neuroscience, 29(31), 9888–9902. https://doi.org/10.1523/jneurosci.1366-09.2009

Gulledge, A. T., Park, S., Kawaguchi, Y., & Stuart, G. J. (2007). Heterogeneity of phasic cholinergic signaling in neocortical neurons. Journal of Neurophysiology, 97(3), 2215–2229. https://doi.org/10.1152/jn.00493.2006

Guo, J., Ragland, J. D., & Carter, C. S. (2018). Memory and cognition in schizophrenia. Molecular Psychiatry, 24(5), 633–642. https://doi.org/10.1038/s41380-018-0231-1

Gupte, R., Brooks, W. M., Vukas, R., Pierce, J. D., & Harris, J. I. (2019). Sex differences in Traumatic Brain Injury: What we know and what we should know. Journal of Neurotrauma, 36(22), 3063–3091. https://doi.org/10.1089/neu.2018.6171

Ha, G. E., & Cheong, E. (2017). Spike frequency adaptation in neurons of the central nervous system. Experimental Neurobiology, 26(4), 179–185. https://doi.org/10.5607/en.2017.26.4.179

Hadjikoutis, S., & Sawhney, I. M. (2003). Occipital seizures presenting with bilateral visual loss. Neurol India. https://pubmed.ncbi.nlm.nih.gov/12865542/

Hagenston, A. M., Fitzpatrick, J. S., & Yeckel, M. F. (2007). MGluR-Mediated Calcium Waves that Invade the Soma Regulate Firing in Layer V Medial Prefrontal Cortical Pyramidal Neurons. Cerebral Cortex, 18(2), 407–423. https://doi.org/10.1093/cercor/bhm075

Hagenston, A. M., Rudnick, N. D., Boone, C., & Yeckel, M. F. (2009). 2-Aminoethoxydiphenyl-borate (2-APB) increases excitability in pyramidal neurons. Cell Calcium, 45(3), 310–317. https://doi.org/10.1016/j.ceca.2008.11.003

Haj-Dahmane, S., & Andrade, R. (1996). Muscarinic activation of a Voltage-Dependent cation nonselective current in Rat association cortex. The Journal of Neuroscience, 16(12), 3848–3861. https://doi.org/10.1523/jneurosci.16-12-03848.1996

Haj-Dahmane, S., & Andrade, R. (1997). Calcium-Activated Cation nonselective current contributes to the fast afterdepolarization in rat prefrontal cortex neurons. Journal of Neurophysiology, 78(4), 1983–1989. https://doi.org/10.1152/jn.1997.78.4.1983

Haj-Dahmane, S., & Andrade, R. (1998). Ionic mechanism of the slow afterdepolarization induced by muscarinic receptor activation in rat prefrontal cortex. Journal of Neurophysiology, 80(3), 1197–1210. https://doi.org/10.1152/jn.1998.80.3.1197

Haj-Dahmane, S., & Andrade, R. (1999). Muscarinic receptors regulate two different calcium-dependent non-selective cation currents in rat prefrontal cortex. European Journal of Neuroscience, 11(6), 1973–1980. https://doi.org/10.1046/j.1460-9568.1999.00612.x

Hall, J. E., & Guyton, A. C. (2010). Textbook of Medical Physiology (12th ed.). Saunders.

Hammelrath, L., Škokić, S., Khmelinskii, A., Hess, A., Van Der Knaap, N., Staring, M., Lelieveldt, B. P. F., Wiedermann, D., & Hoehn, M. (2016). Morphological maturation of the mouse brain: An in vivo MRI and histology investigation. NeuroImage, 125, 144–152. https://doi.org/10.1016/j.neuroimage.2015.10.009

Han, S., Tai, C., Westenbroek, R. E., Yu, F. H., Cheah, C. S., Potter, G. B., Rubenstein, J. L., Scheuer, T., De La Iglesia, H. O., & Catterall, W. A. (2012). Autistic-like behaviour in Scn1a+/− mice and rescue by enhanced GABA-mediated neurotransmission. Nature, 489(7416), 385–390. https://doi.org/10.1038/nature11356

Hardy, J., Duff, K., Hardy, K. G., Perez-Tur, J., & Hutton, M. (1998). Genetic dissection of Alzheimer's disease and related dementias: amyloid and its relationship to tau. Nature Neuroscience, 1(5), 355–358. https://doi.org/10.1038/1565

Hasselmo, M. E., & McGaughy, J. (2004). High acetylcholine levels set circuit dynamics for attention and encoding and low acetylcholine levels set dynamics for consolidation. In Elsevier eBooks (pp. 207–231). https://doi.org/10.1016/s0079-6123(03)45015-2

Hebert, L. E., Weuve, J., Scherr, P. A., & Evans, D. A. (2013). Alzheimer disease in the United States (2010-2050) estimated using the 2010 census. Neurology, 80(19), 1778–1783. https://doi.org/10.1212/wnl.0b013e31828726f5

Heidbreder, C., & Groenewegen, H. J. (2003). The medial prefrontal cortex in the rat: evidence for a dorso-ventral distinction based upon functional and anatomical characteristics. Neuroscience & Biobehavioral Reviews, 27(6), 555–579. https://doi.org/10.1016/j.neubiorev.2003.09.003

Hempel, C. M., Hartman, K. H., Wang, X., Turrigiano, G. G., & Nelson, S. B. (2000). Multiple forms of Short-Term plasticity at excitatory synapses in rat medial prefrontal cortex. Journal of Neurophysiology, 83(5), 3031–3041. https://doi.org/10.1152/jn.2000.83.5.3031

Higo, T., Hamada, K., Hisatsune, C., Nukina, N., Hashikawa, T., Hattori, M., Nakamura, T., & Mikoshiba, K. (2010). Mechanism of ER Stress-Induced Brain damage by IP3 receptor. Neuron, 68(5), 865–878. https://doi.org/10.1016/j.neuron.2010.11.010

Hikosaka, O. (2010). The habenula: from stress evasion to value-based decision-making. Nature Reviews Neuroscience, 11(7), 503–513. https://doi.org/10.1038/nrn2866

Hikosaka, O., Sakamoto, M., & Usui, S. (1989). Functional properties of monkey caudate neurons. I. Activities related to saccadic eye movements. Journal of Neurophysiology, 61(4), 780–798. https://doi.org/10.1152/jn.1989.61.4.780

Hill, A. C., Laird, A. R., & Robinson, J. L. (2014). Gender differences in working memory networks: A BrainMap meta-analysis. Biological Psychology, 102, 18–29. https://doi.org/10.1016/j.biopsycho.2014.06.008

Hillman, K. L., & Bilkey, D. K. (2012). Neural encoding of competitive effort in the anterior cingulate cortex. Nature Neuroscience, 15(9), 1290–1297. https://doi.org/10.1038/nn.3187

Hirsch, J. F., & Crepel, F. (1990). Use-dependent changes in synaptic efficacy in rat prefrontal neurons in vitro. The Journal of Physiology, 427(1), 31–49. https://doi.org/10.1113/jphysiol.1990.sp018159

Hodgkin, A. L. (1964). The ionic basis of nervous conduction. Science, 145(3637), 1148–1154. https://doi.org/10.1126/science.145.3637.1148

Hodgkin, A. L., & Huxley, A. (1952). A quantitative description of membrane current and its application to conduction and excitation in nerve. The Journal of Physiology, 117(4), 500–544. https://doi.org/10.1113/jphysiol.1952.sp004764

Hoffmann, M. (2013). The Human Frontal Lobes and Frontal Network Systems: An Evolutionary, Clinical, and Treatment Perspective. ISRN Neurology, 2013, 1–34. https://doi.org/10.1155/2013/892459

Holahan, M. R., & Routtenberg, A. (2007). Post-translational synaptic protein modification as substrate for long-lasting, remote memory: An initial test. Hippocampus, 17(2), 93–97. https://doi.org/10.1002/hipo.20245

Holden, S. S., Grandi, F. C., Aboubakr, O., Higashikubo, B., Cho, F. S., Chang, A., Osorio-Forero, A., Morningstar, A. R., Mathur, V., Kuhn, L. J., Suri, P., Sankaranarayanan, S., Andrews-Zwilling, Y., Tenner, A. J., Lüthi, A., Aronica, E., Corces, M. R., Yednock, T., & Paz, J. T. (2021). Complement factor C1q mediates sleep spindle loss and epileptic spikes after mild brain injury. Science, 373(6560). https://doi.org/10.1126/science.abj2685

Holmes, G. L. (2013). EEG abnormalities as a biomarker for cognitive comorbidities in pharmacoresistant epilepsy. Epilepsia, 54, 60–62. https://doi.org/10.1111/epi.12186

Holtzman, D. M., Morris, J. C., & Goate, A. M. (2011). Alzheimer's Disease: the challenge of the second century. Science Translational Medicine, 3(77). https://doi.org/10.1126/scitranslmed.3002369

Hoover, W. B., & Vertes, R. P. (2007). Anatomical analysis of afferent projections to the medial prefrontal cortex in the rat. Brain Struct Funct, 212(2), 149–179. https://doi.org/10.1007/s00429-007-0150-4

Houck, J. M., & Ewing, S. W. F. (2017). Working memory capacity and addiction treatment outcomes in adolescents. American Journal of Drug and Alcohol Abuse, 44(2), 185–192. https://doi.org/10.1080/00952990.2017.1344680

Huang, Y., Weisgraber, K. H., Mucke, L., & Mahley, R. W. (2004). Apolipoprotein E: Diversity of cellular origins, structural and biophysical properties, and effects in Alzheimer's disease. Journal of Molecular Neuroscience, 23(3), 189–204. https://doi.org/10.1385/jmn:23:3:189

Huecker, M. R. (2023). Domestic Violence. In StatPearls - NCBI Bookshelf.

Huxley, A. (1964). Excitation and conduction in nerve: Quantitative analysis. Science, 145(3637), 1154–1159. https://doi.org/10.1126/science.145.3637.1154

Inan, M., Welagen, J., & Anderson, S. A. (2011). Spatial and temporal bias in the mitotic origins of somatostatin- and Parvalbumin-Expressing interneuron subgroups and the chandelier subtype in the medial ganglionic eminence. Cerebral Cortex, 22(4), 820–827. https://doi.org/10.1093/cercor/bhr148

Isik, A. T. (2010). Late onset Alzheimer’s disease in older people. Clinical Interventions in Aging, 307. https://doi.org/10.2147/cia.s11718

Itoi, K., & Sugimoto, N. (2010). The Brainstem Noradrenergic Systems in Stress, Anxiety and Depression. Journal of Neuroendocrinology, 22(5), 355–361. https://doi.org/10.1111/j.1365-2826.2010.01988.x

Izaki, Y., Hori, K., & Nomura, M. (2000). Disturbance of rat lever-press learning by hippocampo-prefrontal disconnection. Brain Research, 860(1–2), 199–202. https://doi.org/10.1016/s0006-8993(00)02039-4

Jackson, H., Philp, E., Nuttall, R. L., & Diller, L. (2002). Traumatic brain injury: A hidden consequence for battered women. Professional Psychology: Research and Practice, 33(1), 39–45. https://psycnet.apa.org/record/2002-10109-006

Jankowsky, J. L., & Zheng, H. (2017). Practical considerations for choosing a mouse model of Alzheimer's disease. Molecular Neurodegeneration, 12(1). https://doi.org/10.1186/s13024-017-0231-7

Jasmin, L., Granato, A., & Ohara, P. T. (2003). Rostral agranular insular cortex and pain areas of the central nervous system: A tract-tracing study in the rat. Journal of Comparative Neurology, 468(3), 425–440. https://doi.org/10.1002/cne.10978

Jiang, J. Y., Lyeth, B. G., Delahunty, T. M., Phillips, L. R., & Hamm, R. J. (1994). Muscarinic cholinergic receptor binding in rat brain at 15 days following traumatic brain injury. Brain Research. https://doi.org/10.1016/0006-8993(94)90687-4

Joe, E., & Ringman, J. M. (2019). Cognitive symptoms of Alzheimer's disease: clinical management and prevention. BMJ, l6217. https://doi.org/10.1136/bmj.l6217

Joffe, M. E., Santiago, C. I., Stansley, B. J., Maksymetz, J., Gogliotti, R. G., Engers, J. L., Nicoletti, F., Lindsley, C. W., & Conn, P. J. (2019). Mechanisms underlying prelimbic prefrontal cortex mGlu3/mGlu5-dependent plasticity and reversal learning deficits following acute stress. Neuropharmacology, 144, 19–28. https://doi.org/10.1016/j.neuropharm.2018.10.013

Jolly, A., Scott, G., Sharp, D. J., & Hampshire, A. (2020). Distinct patterns of structural damage underlie working memory and reasoning deficits after traumatic brain injury. Brain, 143(4), 1158–1176. https://doi.org/10.1093/brain/awaa067

Jones, A. F., & Sheets, P. L. (2020). Sex-Specific disruption of distinct MPFC inhibitory neurons in Spared-Nerve injury model of neuropathic pain. Cell Reports, 31(10), 107729. https://doi.org/10.1016/j.celrep.2020.107729

Jourdan, C., Azouvi, P., Genet, F., Selly, N., Josseran, L., & Schnitzler, A. (2018). Disability and health consequences of traumatic brain injury. American Journal of Physical Medicine & Rehabilitation, 97(5), 323–331. https://doi.org/10.1097/phm.0000000000000848

Kadowaki, H., Nishitoh, H., Urano, F., Sadamitsu, C., Matsuzawa, A., Takeda, K., Masutani, H., Yodoi, J., Urano, Y., Nagano, T., & Ichijo, H. (2004). Amyloid β induces neuronal cell death through ROS-mediated ASK1 activation. Cell Death & Differentiation, 12(1), 19–24. https://doi.org/10.1038/sj.cdd.4401528

Kasper, L. J., Alderson, R. M., & Hudec, K. L. (2012). Moderators of working memory deficits in children with attention-deficit/hyperactivity disorder (ADHD): A meta-analytic review. Clinical Psychology Review, 32(7), 605–617. https://doi.org/10.1016/j.cpr.2012.07.001

Kazim, S. F., Seo, J. S., Bianchi, R. M., Larson, C. S., Sharma, A., Wong, R. K. S., Gorbachev, K., & Pereira, A. C. (2021). Neuronal Network Excitability in Alzheimer's Disease: The Puzzle of Similar versus Divergent Roles of Amyloid β and Tau. eNeuro, 8(2), ENEURO.0418-20.2020. https://doi.org/10.1523/eneuro.0418-20.2020

Keller, C., Rading, S., Bindila, L., & Karsak, M. (2022). Behavioral Studies of p62 KO Animals with Implications of a Modulated Function of the Endocannabinoid System. Cells, 11(9), 1517. https://doi.org/10.3390/cells11091517

Keller, R., Basta, R., Salerno, L., & Elia, M. (2017). Autism, epilepsy, and synaptopathies: a not rare association. Neurological Sciences, 38(8), 1353–1361. https://doi.org/10.1007/s10072-017-2974-x

Kessels, R. P. C., Meulenbroek, O., Fernández, G., & Rikkert, M. O. (2010). Spatial working memory in aging and mild cognitive impairment: effects of task load and contextual cueing. Aging Neuropsychology and Cognition, 17(5), 556–574. https://doi.org/10.1080/13825585.2010.481354

Klencklen, G., Després, O., & Dufour, A. (2012). What do we know about aging and spatial cognition? Reviews and perspectives. Ageing Research Reviews, 11(1), 123–135. https://doi.org/10.1016/j.arr.2011.10.001

Klencklen, G., Lavenex, P. B., Brandner, C., & Lavenex, P. (2017). Working memory decline in normal aging: Is it really worse in space than in color? Learning and Motivation, 57, 48–60. https://doi.org/10.1016/j.lmot.2017.01.007

Knouse, M. C., McGrath, A. G., Deutschmann, A. U., Rich, M. T., Zallar, L. J., Rajadhyaksha, A. M., & Briand, L. A. (2022). Sex differences in the medial prefrontal cortical glutamate system. Biology of Sex Differences, 13(1). https://doi.org/10.1186/s13293-022-00468-6

Kong, L., Zhang, R., Hu, S., & Lai, J. (2022). Military traumatic brain injury: a challenge straddling neurology and psychiatry. Military Medical Research, 9(1). https://doi.org/10.1186/s40779-021-00363-y

Kortüm, F., Das, S., Flindt, M., Morris-Rosendahl, D. J., Stefanova, I., Goldstein, A., Horn, D., Klopocki, E., Kluger, G., Martin, P., Rauch, A., Roumer, A., Saitta, S. C., Walsh, L. E., Wieczorek, D., Uyanik, G., Kutsche, K., & Dobyns, W. B. (2011). The core FOXG1 syndrome phenotype consists of postnatal microcephaly, severe mental retardation, absent language, dyskinesia, and corpus callosum hypogenesis. Journal of Medical Genetics, 48(6), 396–406. https://doi.org/10.1136/jmg.2010.087528

Koulakov, A. A., Raghavachari, S., Kepecs, A., & Lisman, J. (2002). Model for a robust neural integrator. Nature Neuroscience, 5(8), 775–782. https://doi.org/10.1038/nn893

Kranz, G. S., Kasper, S., & Lanzenberger, R. (2010). Reward and the serotonergic system. Neuroscience, 166(4), 1023–1035. https://doi.org/10.1016/j.neuroscience.2010.01.036

Kritzer, M. F., & Goldman-Rakic, P. S. (1995). Intrinsic circuit organization of the major layers and sublayers of the dorsolateral prefrontal cortex in the rhesus monkey. Journal of Comparative Neurology, 359(1), 131–143. https://doi.org/10.1002/cne.903590109

Kronovsek, T., Hermand, E., Berthoz, A., Castilla, A., Gallou-Guyot, M., Daviet, J., & Perrochon, A. (2021). Age-related decline in visuo-spatial working memory is reflected by dorsolateral prefrontal activation and cognitive capabilities. Behavioural Brain Research, 398, 112981. https://doi.org/10.1016/j.bbr.2020.112981

Krueger, C. E., Laluz, V., Rosen, H. J., Neuhaus, J., Miller, B. L., & Kramer, J. H. (2011). Double dissociation in the anatomy of socioemotional disinhibition and executive functioning in dementia. Neuropsychology (Journal), 25(2), 249–259. https://doi.org/10.1037/a0021681

Kurowski, P., Gawlak, M., & Szulczyk, P. (2015). Muscarinic receptor control of pyramidal neuron membrane potential in the medial prefrontal cortex (mPFC) in rats. Neuroscience, 303, 474–488. https://doi.org/10.1016/j.neuroscience.2015.07.023

Kurtz, M. M., & Gerraty, R. T. (2009). A meta-analytic investigation of neurocognitive deficits in bipolar illness: Profile and effects of clinical state. Neuropsychology (Journal), 23(5), 551–562. https://doi.org/10.1037/a0016277

LaLumiere, R. T., Niehoff, K. E., & Kalivas, P. W. (2010). The infralimbic cortex regulates the consolidation of extinction after cocaine self-administration. Learn Mem, 17(4), 168–175. https://doi.org/10.1101/lm.1576810

Landis, S. C., Amara, S. G., Asadullah, K., Austin, C., Blumenstein, R., Bradley, E. C., Crystal, R. G., Darnell, R. B., Ferrante, R. J., Fillit, H., Finkelstein, R., Fisher, M., Gendelman, H. E., Golub, R. M., Goudreau, J. L., Gross, R. A., Gubitz, A. K., Hesterlee, S., Howells, D. W., . . . Silberberg, S. D. (2012). A call for transparent reporting to optimize the predictive value of preclinical research. Nature, 490(7419), 187–191. https://doi.org/10.1038/nature11556

Lapish, C. C., Durstewitz, D., Chandler, L. J., & Seamans, J. K. (2008). Successful choice behavior is associated with distinct and coherent network states in anterior cingulate cortex. Proceedings of the National Academy of Sciences of the United States of America, 105(33), 11963–11968. https://doi.org/10.1073/pnas.0804045105

Lechner, H. A., Squire, L. R., & Byrne, J. H. (1999, April 1). 100 years of consolidation--remembering Müller and Pilzecker. PubMed. https://pubmed.ncbi.nlm.nih.gov/10327233/

Lechner, W. V., Day, A. M., Metrik, J., Leventhal, A. M., & Kahler, C. W. (2015). Effects of alcohol-induced working memory decline on alcohol consumption and adverse consequences of use. Psychopharmacology, 233(1), 83–88. https://doi.org/10.1007/s00213-015-4090-z

Leon, W., Bruno, M. A., Allard, S., Nader, K., & Cuello, A. C. (2010). Engagement of the PFC in consolidation and recall of recent spatial memory. Learning & Memory, 17(6), 297–305. https://doi.org/10.1101/lm.1804410

Levin, H. S., Amparo, E. G., Eisenberg, H. M., Williams, D. H., High, W. M., McArdle, C. B., & Weiner, R. L. (1987). Magnetic resonance imaging and computerized tomography in relation to the neurobehavioral sequelae of mild and moderate head injuries. Journal of Neurosurgery, 66(5), 706–713. https://doi.org/10.3171/jns.1987.66.5.0706

Levin, H. S., Gary, H. E., Eisenberg, H. M., Ruff, R. M., Barth, J. T., Kreutzer, J. S., High, W. M., Portman, S. M., Foulkes, M. A., Jane, J. A., Marmarou, A., & Marshall, L. F. (1990). Neurobehavioral outcome 1 year after severe head injury. Journal of Neurosurgery, 73(5), 699–709. https://doi.org/10.3171/jns.1990.73.5.0699

Levin, H. S., & Kraus, M. F. (1994). The frontal lobes and traumatic brain injury. J Neuropsychiatry Clin Neurosci, 6(4), 443–454. https://doi.org/10.1176/jnp.6.4.443

Levitt, J. B., Lewis, D. A., Yoshioka, T., & Lund, J. S. (1993). Topography of pyramidal neuron intrinsic connections in macaque monkey prefrontal cortex (areas 9 and 46). Journal of Comparative Neurology, 338(3), 360–376. https://doi.org/10.1002/cne.903380304

Li, B., Piriz, J., Mirrione, M. M., Chung, C., Proulx, C. D., Schulz, D., Henn, F. A., & Malinow, R. (2011). Synaptic potentiation onto habenula neurons in the learned helplessness model of depression. Nature, 470(7335), 535–539. https://doi.org/10.1038/nature09742

Lien, C. C., & Jonas, P. (2003). Kv3 Potassium Conductance is Necessary and Kinetically Optimized for High-Frequency Action Potential Generation in Hippocampal Interneurons. The Journal of Neuroscience, 23(6), 2058–2068. https://doi.org/10.1523/jneurosci.23-06-02058.2003

Lim, L., Pakan, J. M., Selten, M., Marques-Smith, A., Llorca, A., Bae, S. E., Rochefort, N. L., & Marín, O. (2018). Optimization of interneuron function by direct coupling of cell migration and axonal targeting. Nature Neuroscience, 21(7), 920–931. https://doi.org/10.1038/s41593-018-0162-9

Lindeløv, J. K., Overgaard, R., & Overgaard, M. (2017). Improving working memory performance in brain-injured patients using hypnotic suggestion. Brain, 140(4), 1100–1106. https://doi.org/10.1093/brain/awx001

Lindquist, B. E., Timbie, C., Voskobiynyk, Y., & Paz, J. T. (2023). Thalamocortical circuits in generalized epilepsy: Pathophysiologic mechanisms and therapeutic targets. Neurobiol Dis, 181. https://www.ncbi.nlm.nih.gov/pmc/articles/PMC10192143/

Lipscombe, D. (2002). L-Type calcium channels. Circulation Research, 90(9), 933–935. https://doi.org/10.1161/01.res.0000019740.52306.92

Liu, Y., Ouyang, P., Zheng, Y., Mi, L., Zhao, J., Ning, Y., & Guo, W. (2021). A selective review of the Excitatory-Inhibitory Imbalance in Schizophrenia: underlying biology, genetics, microcircuits, and symptoms. Frontiers in Cell and Developmental Biology, 9. https://doi.org/10.3389/fcell.2021.664535

Lo Yang, F., Huang, L., Tso, A., Wang, H., Cui, L., Lin, L., Wang, X., Ren, M., Fang, X., Liu, J., Han, Z., Chen, J., & Ouyang, K. (2020). Inositol 1,4,5-trisphosphate receptors are essential for fetal-maternal connection and embryo viability. PLOS Genetics, 16(4), e1008739. https://doi.org/10.1371/journal.pgen.1008739

Locklear, M. N., Cohen, A., Jone, A., & Kritzer, M. F. (2014). Sex differences distinguish intracortical glutamate Receptor-Mediated regulation of extracellular dopamine levels in the prefrontal cortex of adult rats. Cerebral Cortex, bhu222. https://doi.org/10.1093/cercor/bhu222

Lu, C. C., Appler, J. M., Houseman, E. A., & Goodrich, L. V. (2011). Developmental Profiling of Spiral Ganglion Neurons Reveals Insights into Auditory Circuit Assembly. The Journal of Neuroscience, 31(30), 10903–10918. https://doi.org/10.1523/jneurosci.2358-11.2011

Luethi, M. (2008). Stress effects on working memory, explicit memory, and implicit memory for neutral and emotional stimuli in healthy men. Frontiers in Behavioral Neuroscience, 2. https://doi.org/10.3389/neuro.08.005.2008

Lugtmeijer, S., Lammers, N. A., De Haan, E., De Leeuw, F., & Kessels, R. P. C. (2020). Post-Stroke Working Memory Dysfunction: A Meta-Analysis and Systematic Review. Neuropsychology Review, 31(1), 202–219. https://doi.org/10.1007/s11065-020-09462-4

Luo, H., Hasegawa, K., Liu, M., & Song, W. J. (2017). Comparison of the Upper Marginal Neurons of Cortical Layer 2 with Layer 2/3 Pyramidal Neurons in Mouse Temporal Cortex. Frontiers in Neuroanatomy, 11. https://doi.org/10.3389/fnana.2017.00115

M.A. Rahman, Tanaka, N., Nuruzzaman, DebNath, S., & Kawahara, S. (2020). Blockade of the M1 muscarinic acetylcholine receptors impairs eyeblink serial feature-positive discrimination learning in mice. PLOS ONE, 15(8), e0237451. https://doi.org/10.1371/journal.pone.0237451

MacDonald, A. W., Cohen, J. D., Stenger, V. A., & Carter, C. S. (2000). Dissociating the role of the dorsolateral prefrontal and anterior cingulate cortex in cognitive control. Science, 288(5472), 1835–1838. https://doi.org/10.1126/science.288.5472.1835

Machens, C. K., & Brody, C. D. (2008). Design of Continuous Attractor Networks with Monotonic Tuning Using a Symmetry Principle. Neural Computation, 20(2), 452–485. https://doi.org/10.1162/neco.2007.07-06-297

Machens, C. K., Romo, R., & Brody, C. D. (2005). Flexible control of mutual inhibition: a neural model of Two-Interval discrimination. Science, 307(5712), 1121–1124. https://doi.org/10.1126/science.1104171

Madison, D. V., & Nicoll, R. (1984). Control of the repetitive discharge of rat CA 1 pyramidal neurones in vitro. The Journal of Physiology, 354(1), 319–331. https://doi.org/10.1113/jphysiol.1984.sp015378

Mahley, R. W., Weisgraber, K. H., & Huang, Y. (2006). Apolipoprotein E4: A causative factor and therapeutic target in neuropathology, including Alzheimer's disease. Proceedings of the National Academy of Sciences of the United States of America, 103(15), 5644–5651. https://doi.org/10.1073/pnas.0600549103

Maier, S. F., & Watkins, L. R. (2005). Stressor controllability and learned helplessness: The roles of the dorsal raphe nucleus, serotonin, and corticotropin-releasing factor. Neuroscience & Biobehavioral Reviews, 29(4–5), 829–841. https://doi.org/10.1016/j.neubiorev.2005.03.021

Major, G., & Tank, D. W. (2004). Persistent neural activity: prevalence and mechanisms. Current Opinion in Neurobiology, 14(6), 675–684. https://doi.org/10.1016/j.conb.2004.10.017

Maldonado, K. A. (2023, March 17). Physiology, brain. StatPearls - NCBI Bookshelf. https://www.ncbi.nlm.nih.gov/books/NBK551718/

Manktelow, A., Menon, D., Sahakian, B. J., & Stamatakis, E. A. (2017). Working Memory after Traumatic Brain Injury: The Neural Basis of Improved Performance with Methylphenidate. Frontiers in Behavioral Neuroscience, 11. https://doi.org/10.3389/fnbeh.2017.00058

Marsh, J., & Alifragis, P. (2018). Synaptic dysfunction in Alzheimer's disease: the effects of amyloid beta on synaptic vesicle dynamics as a novel target for therapeutic intervention. Neural Regeneration Research, 13(4), 616. https://doi.org/10.4103/1673-5374.230276

Matsumoto, M., & Nagata, E. (1999). Type 1 inositol 1,4,5-trisphosphate receptor knock-out mice: their phenotypes and their meaning in neuroscience and clinical practice. Journal of Molecular Medicine, 77(5), 406–411. https://doi.org/10.1007/s001090050370

Matysiak, O., Kroemeke, A., & Brzezicka, A. (2019). Working memory capacity as a predictor of cognitive training efficacy in the elderly population. Frontiers in Aging Neuroscience, 11. https://doi.org/10.3389/fnagi.2019.00126

Maviel, T., Durkin, T., Menzaghi, F., & Bontempi, B. (2004). Sites of neocortical reorganization critical for remote spatial memory. Science, 305(5680), 96–99. https://doi.org/10.1126/science.1098180

Mayeux, R., & Stern, Y. (2012). Epidemiology of Alzheimer Disease. Cold Spring Harbor Perspectives in Medicine, 2(8), a006239. https://doi.org/10.1101/cshperspect.a006239

Mazaux, J., Masson, F., Levin, H. S., Alaoui, P., Maurette, P., & Barat, M. (1997). Long-term neuropsychological outcome and loss of social autonomy after traumatic brain injury. Archives of Physical Medicine and Rehabilitation, 78(12), 1316–1320. https://doi.org/10.1016/s0003-9993(97)90303-8

McAllister, T. W., Flashman, L. A., Sparling, M. B., & Saykin, A. J. (2004). Working memory deficits after traumatic brain injury: catecholaminergic mechanisms and prospects for treatment — a review. Brain Injury, 18(4), 331–350. https://doi.org/10.1080/02699050310001617370

McKinsey, G. L., Lindtner, S., Trzcinski, B., Visel, A., Pennacchio, L. A., Huylebroeck, D., Higashi, Y., & Rubenstein, J. L. (2013). Dlx1&2-Dependent Expression of Zfhx1b (Sip1, Zeb2) Regulates the Fate Switch between Cortical and Striatal Interneurons. Neuron, 77(1), 83–98. https://doi.org/10.1016/j.neuron.2012.11.035

McQuiston, A. R., & Madison, D. V. (1999). Muscarinic receptor activity induces an afterdepolarization in a subpopulation of hippocampal CA1 interneurons. The Journal of Neuroscience, 19(14), 5703–5710. https://doi.org/10.1523/jneurosci.19-14-05703.1999

Meynert, T. (1868). Der Bau der Großhirnrinde und seiner örtlichen Verschiedenheiten, nebst einem pathologisch-anatomischen Collarium. J.H. Heuser, Neuwied.

Mez, J., Daneshvar, D. H., Kiernan, P. T., Abdolmohammadi, B., Alvarez, V. E., Huber, B. R., Alosco, M. L., Solomon, T. M., Nowinski, C. J., McHale, L., Cormier, K., Kubilus, C. A., Martin, B., Murphy, L., Baugh, C. M., Montenigro, P. H., Chaisson, C. E., Tripodis, Y., Kowall, N. W., . . . McKee, A. C. (2017). Clinicopathological evaluation of chronic traumatic encephalopathy in players of American football. JAMA, 318(4), 360. https://doi.org/10.1001/jama.2017.8334

Mi, D., Li, Z., Lim, L., Li, M., Moissidis, M., Yang, Y., Gao, T., Hu, X., Pratt, T., Price, D. J., Sestan, N., & Marín, O. (2018). Early emergence of cortical interneuron diversity in the mouse embryo. Science, 360(6384), 81–85. https://doi.org/10.1126/science.aar6821

Michel, M., & Morales, J. (2019). Minority reports: Consciousness and the prefrontal cortex. Mind & Language, 35(4), 493–513. https://doi.org/10.1111/mila.12264

Michelucci, R. (2019, January 10). Autosomal Dominant Epilepsy with Auditory Features. GeneReviews® - NCBI Bookshelf. https://www.ncbi.nlm.nih.gov/books/NBK1537/

Miller, E. K., Erickson, C. A., & Desimone, R. (1996). Neural mechanisms of visual working memory in prefrontal cortex of the macaque. The Journal of Neuroscience, 16(16), 5154–5167. https://doi.org/10.1523/jneurosci.16-16-05154.1996

Miller, E. K., Nieder, A., Freedman, D. J., & Wallis, J. D. (2003). Neural correlates of categories and concepts. Current Opinion in Neurobiology, 13(2), 198–203. https://doi.org/10.1016/s0959-4388(03)00037-0

Miyoshi, G., Butt, S. J. B., Takebayashi, H., & Fishell, G. (2007). Physiologically Distinct Temporal Cohorts of Cortical Interneurons Arise from Telencephalic Olig2-Expressing Precursors. The Journal of Neuroscience, 27(29), 7786–7798. https://doi.org/10.1523/jneurosci.1807-07.2007

Moberg, S., & Takahashi, N. (2022). Neocortical layer 5 subclasses: From cellular properties to roles in behavior. Frontiers in Synaptic Neuroscience, 14. https://doi.org/10.3389/fnsyn.2022.1006773

Moechars, D. (1996, March 3). Expression in brain of amyloid precursor protein mutated in the alpha-secretase site causes disturbed behavior, neuronal degeneration and premature death in transgenic mice. PubMed Central (PMC). https://www.ncbi.nlm.nih.gov/pmc/articles/PMC450029/

Moloney, C. M., Lowe, V. J., & Murray, M. E. (2021). Visualization of neurofibrillary tangle maturity in Alzheimer's disease: A clinicopathologic perspective for biomarker research. Alzheimers & Dementia, 17(9), 1554–1574. https://doi.org/10.1002/alz.12321

Morisset, V., & Nagy, F. (1999). Ionic basis for plateau potentials in deep dorsal horn neurons of the rat spinal cord. The Journal of Neuroscience, 19(17), 7309–7316. https://doi.org/10.1523/jneurosci.19-17-07309.1999

Motamedi, G. K., & Meador, K. J. (2003). Epilepsy and cognition. Epilepsy & Behavior, 4, 25–38. https://doi.org/10.1016/j.yebeh.2003.07.004

Mu ̈Ller, G. E., & Pilzecker, A. (1900). Experimentelle Beitra ̈ge zur Lehre vom Geda ̈chtniss. J.A. Barth, Leipzig.

Murman, D. L. (2015). The impact of age on cognition. Seminars in Hearing, 36(03), 111–121. https://doi.org/10.1055/s-0035-1555115

Murray, J. D., Jaramillo, J., & Wang, X. J. (2017). Working memory and Decision-Making in a frontoparietal circuit model. The Journal of Neuroscience, 37(50), 12167–12186. https://doi.org/10.1523/jneurosci.0343-17.2017

Narahashi, T., Deguchi, T., Urakawa, N., & Ohkubo, Y. (1960). Stabilization and rectification of muscle fiber membrane by tetrodotoxin. American Journal of Physiology, 198(5), 934–938. https://doi.org/10.1152/ajplegacy.1960.198.5.934

Narahashi, T., Moore, J. W., & Scott, W. R. (1964). Tetrodotoxin Blockage of Sodium Conductance Increase in Lobster Giant Axons. J Gen Physiol, 47(5), 965–974. https://doi.org/10.1085/jgp.47.5.965

Narayanan, N. S., Horst, N. K., & Laubach, M. (2006). Reversible inactivations of rat medial prefrontal cortex impair the ability to wait for a stimulus. Neuroscience, 139(3), 865–876. https://doi.org/10.1016/j.neuroscience.2005.11.072

Narayanan, N. S., & Laubach, M. (2009). Delay activity in rodent frontal cortex during a simple reaction time task. Journal of Neurophysiology, 101(6), 2859–2871. https://doi.org/10.1152/jn.90615.2008

National Academies of Sciences, Engineering, and Medicine; Health and Medicine Division; Board on Health Care Services; Committee on the Review of the Department of Veterans Affairs Examinations for Traumatic Brain Injury. (2019). Evaluation of the disability determination process for traumatic brain injury in veterans. National Academies Press eBooks. https://doi.org/10.17226/25317

Necula, D., Cho, F. S., He, A., & Paz, J. T. (2021). Secondary thalamic neuroinflammation after focal cortical stroke and traumatic injury mirrors corticothalamic functional connectivity. Journal of Comparative Neurology, 530(7), 998–1019. https://doi.org/10.1002/cne.25259

Netter, F. H. (2010). Atlas of Human Anatomy, Professional Edition (5th ed.). Saunders.

Newman, L. A., & Gold, P. E. (2015). Attenuation in rats of impairments of memory by scopolamine, a muscarinic receptor antagonist, by mecamylamine, a nicotinic receptor antagonist. Psychopharmacology, 233(5), 925–932. https://doi.org/10.1007/s00213-015-4174-9

N'Gouemo, P. (2008). Amiloride delays the onset of pilocarpine-induced seizures in rats. Brain Research, 1222, 230–232. https://doi.org/10.1016/j.brainres.2008.05.010

Nickels, K. C., Zaccariello, M. J., Hamiwka, L., & Wirrell, E. (2016). Cognitive and neurodevelopmental comorbidities in paediatric epilepsy. Nature Reviews Neurology, 12(8), 465–476. https://doi.org/10.1038/nrneurol.2016.98

Nieder, A., & Miller, E. K. (2004). A parieto-frontal network for visual numerical information in the monkey. Proceedings of the National Academy of Sciences of the United States of America, 101(19), 7457–7462. https://doi.org/10.1073/pnas.0402239101

Niemi, M., Martin, H. C., Dl, R., Gallone, G., Gordon, S., Kelemen, M., McAloney, K., McRae, J. F., Radford, E. J., Yu, S., Gécz, J., Martin, N. G., Wright, C. F., FitzPatrick, D. R., Firth, H. V., Hurles, M. E., & Barrett, J. C. (2018). Common genetic variants contribute to risk of rare severe neurodevelopmental disorders. Nature, 562(7726), 268–271. https://doi.org/10.1038/s41586-018-0566-4

Nyberg, L. (2002). Levels of processing: A view from functional brain imaging. Memory, 10(5–6), 345–348. https://doi.org/10.1080/09658210244000171

Oakley, H. D., Cole, S. L., Logan, S., Maus, E., Shao, P., Craft, J., Guillozet-Bongaarts, A. L., Ohno, M., Disterhoft, J. F., Van Eldik, L., Berry, R. W., & Vassar, R. (2006). Intraneuronal β-Amyloid Aggregates, Neurodegeneration, and Neuron Loss in Transgenic Mice with Five Familial Alzheimer's Disease Mutations: Potential Factors in Amyloid Plaque Formation. The Journal of Neuroscience, 26(40), 10129–10140. https://doi.org/10.1523/jneurosci.1202-06.2006

Oblak, A. L., Lin, P. B., Kotredes, K. P., Pandey, R. S., Garceau, D., Williams, H., Uyar, A., O'Rourke, R., O'Rourke, S., Ingraham, C. M., Bednarczyk, D., Belanger, M., Cope, Z. A., Little, G., Williams, S. G., Ash, C., Bleckert, A., Ragan, T., Logsdon, B. A., . . . Lamb, B. T. (2021). Comprehensive Evaluation of the 5XFAD mouse model for preclinical testing applications: A MODEL-AD study. Frontiers in Aging Neuroscience, 13. https://doi.org/10.3389/fnagi.2021.713726

O'Connor, D. H., Krubitzer, L., & Bensmaia, S. J. (2021). Of mice and monkeys: Somatosensory processing in two prominent animal models. Progress in Neurobiology, 201, 102008. https://doi.org/10.1016/j.pneurobio.2021.102008

O'Donnell, J., Zeppenfeld, D., McConnell, E., Pena, S., & Nedergaard, M. (2012). Norepinephrine: a neuromodulator that boosts the function of multiple cell types to optimize CNS performance. Neurochemical Research, 37(11), 2496–2512. https://doi.org/10.1007/s11064-012-0818-x

Ortega, R., López, V., Carrasco, X., Escobar, M. J., García, A. M., Parra, M. A., & Aboitiz, F. (2020). Neurocognitive mechanisms underlying working memory encoding and retrieval in Attention-Deficit/Hyperactivity Disorder. Scientific Reports, 10(1). https://doi.org/10.1038/s41598-020-64678-x

Padberg, J., Cerkevich, C. M., Engle, J. R., Rajan, A. T., Recanzone, G. H., Kaas, J. H., & Krubitzer, L. (2009). Thalamocortical Connections of Parietal Somatosensory Cortical Fields in Macaque Monkeys are Highly Divergent and Convergent. Cerebral Cortex, 19(9), 2038–2064. https://doi.org/10.1093/cercor/bhn229

Pai, E. L. L., Vogt, D., Clemente-Perez, A., McKinsey, G. L., Cho, F. S., Hu, J., Wimer, M., Paul, A., Darbandi, S. F., Pla, R., Nowakowski, T. J., Goodrich, L. V., Paz, J. T., & Rubenstein, J. L. (2019). Mafb and c-Maf Have Prenatal Compensatory and Postnatal Antagonistic Roles in Cortical Interneuron Fate and Function. Cell Reports, 26(5), 1157-1173.e5. https://doi.org/10.1016/j.celrep.2019.01.031

Palop, J. J., & Mucke, L. (2016). Network abnormalities and interneuron dysfunction in Alzheimer disease. Nature Reviews Neuroscience, 17(12), 777–792. https://doi.org/10.1038/nrn.2016.141

Panegyres, P. K. (2013). Differences between early and late onset Alzheimer's disease. PubMed Central (PMC). https://www.ncbi.nlm.nih.gov/pmc/articles/PMC3852569/

Parente, R., DeMott, E., Johnson, C. M., Jennings, P., & Silver, R. (2011). Measuring and manipulating subjective organization after traumatic brain injury. NeuroRehabilitation, 29(2), 117–124. https://doi.org/10.3233/nre-2011-0685

Park, D. C., Lautenschlager, G., Hedden, T., Davidson, N. S., Smith, A. D., & Smith, P. K. (2002, June 1). Models of visuospatial and verbal memory across the adult life span. Psychol. Aging. https://pubmed.ncbi.nlm.nih.gov/12061414/

Patil, M., & Hasselmo, M. E. (1999). Modulation of inhibitory synaptic potentials in the piriform cortex. Journal of Neurophysiology, 81(5), 2103–2118. https://doi.org/10.1152/jn.1999.81.5.2103

Paxinos, G., & Mai, J. K. (2003). The Human Nervous System (2nd ed.). ELSEVIER.

Paxinos, G., & Watson, C. (2007). The Rat Brain in Stereotaxic Coordinates (6th ed.). ELSEVIER.

Paz, J. T., Bryant, A. S., Peng, K., Fenno, L. E., Yizhar, O., Frankel, W. N., Deisseroth, K., & Huguenard, J. R. (2011). A new mode of corticothalamic transmission revealed in the Gria4−/− model of absence epilepsy. Nature Neuroscience, 14(9), 1167–1173. https://doi.org/10.1038/nn.2896

Paz, J. T., Davidson, T. J., Frechette, E., Delord, B., Parada, I., Peng, K., Deisseroth, K., & Huguenard, J. R. (2013). Closed-loop optogenetic control of thalamus as a tool for interrupting seizures after cortical injury. Nature Neuroscience, 16(1), 64–70. https://doi.org/10.1038/nn.3269

Peng, Z., Dai, C., Ba, Y., Zhang, L., Shao, Y., & Tian, J. (2020). Effect of sleep deprivation on the working Memory-Related N2-P3 components of the Event-Related Potential waveform. Frontiers in Neuroscience, 14. https://doi.org/10.3389/fnins.2020.00469

Perez-Reyes, E. (2003). Molecular Physiology of Low-Voltage-Activated T-type calcium channels. Physiological Reviews, 83(1), 117–161. https://doi.org/10.1152/physrev.00018.2002

Phillis, J. W. (2005). Acetylcholine Release from the Central Nervous System: A 50-Year Retrospective. Critical Reviews in Neurobiology, 17(3–4), 161–217. https://doi.org/10.1615/critrevneurobiol.v17.i3-4.30

Pirau, L. (2022, December 22). Frontal Lobe Syndrome. StatPearls - NCBI Bookshelf. https://www.ncbi.nlm.nih.gov/books/NBK532981/

Pithadia, A. B. (2009). 5-Hydroxytryptamine Receptor Subtypes and their Modulators with Therapeutic Potentials. Pithadia | Journal of Clinical Medicine Research. https://doi.org/10.4021/jocmr.v0i2.61

Porter, L., & White, E. L. (1983). Afferent and efferent pathways of the vibrissal region of primary motor cortex in the mouse. Journal of Comparative Neurology, 214(3), 279–289. https://doi.org/10.1002/cne.902140306

Pratt, W. E., & Mizumori, S. J. Y. (2001). Neurons in rat medial prefrontal cortex show anticipatory rate changes to predictable differential rewards in a spatial memory task. Behavioural Brain Research, 123(2), 165–183. https://doi.org/10.1016/s0166-4328(01)00204-2

Purves, D. (2001). The Somatic Sensory Cortex. Neuroscience - NCBI Bookshelf. https://www.ncbi.nlm.nih.gov/books/NBK11153/#:~:text=The%20somatic%20sensory%20cortex%20in,3b%2C%201%2C%20and%202

Purves, D. (2021). The Somatic Sensory Cortex. In Neuroscience - NCBI Bookshelf. https://www.ncbi.nlm.nih.gov/books/NBK11153/#:~:text=The%20somatic%20sensory%20cortex%20in,3b%2C%201%2C%20and%202

Quentin, R., J, K., Sallard, E., Fishman, N., Thompson, R., Buch, E. R., & Cohen, L. G. (2019). Differential Brain Mechanisms of Selection and Maintenance of Information during Working Memory. The Journal of Neuroscience, 39(19), 3728–3740. https://doi.org/10.1523/jneurosci.2764-18.2019

Quintanilla-Sanchez, C., Schmitt, F., Curdt, N., Westhoff, A. C., Bänfer, I. W. H., Bayer, T. A., & Bouter, Y. (2023). Search strategy analysis of 5xFAD Alzheimer mice in the Morris Water maze reveals sex- and Age-Specific spatial navigation deficits. Biomedicines, 11(2), 599. https://doi.org/10.3390/biomedicines11020599

Radnikow, G., & Feldmeyer, D. (2018). Layer- and Cell Type-Specific modulation of excitatory neuronal activity in the neocortex. Frontiers in Neuroanatomy, 12. https://doi.org/10.3389/fnana.2018.00001

Raju, H. (2022). Neuroanatomy, Somatosensory Cortex. In StatPearls - NCBI Bookshelf. https://www.ncbi.nlm.nih.gov/books/NBK555915/

Ramón Y Cajal, S. (1899). Comparative study of the sensory areas of the human cortex. Clark University.

Rao, Y. L., Ganaraja, B., Nayak, V. S., Joy, T., Krishnamurthy, A., & Agrawal, A. (2022). Hippocampus and its involvement in Alzheimer's disease: a review. 3 Biotech, 12(2). https://doi.org/10.1007/s13205-022-03123-4

Rashid, H., & Ahmed, T. (2023). Influence of sex and muscarinic activity on memory retrieval in mouse model of traumatic brain injury. Brain Sciences, 13(1), 108. https://doi.org/10.3390/brainsci13010108

Ratté, S., Karnup, S., & Prescott, S. A. (2018). Nonlinear relationship between Spike-Dependent calcium influx and TRPC channel activation enables robust persistent spiking in neurons of the anterior cingulate cortex. The Journal of Neuroscience, 38(7), 1788–1801. https://doi.org/10.1523/jneurosci.0538-17.2018

Reboreda, A., Jiménez-Díaz, L., & Navarro-López, J. D. (2010). TRP channels and neural persistent activity. In Advances in Experimental Medicine and Biology (pp. 595–613). https://doi.org/10.1007/978-94-007-0265-3_32

Rehman, A. (2022, July 25). Neuroanatomy, occipital lobe. StatPearls - NCBI Bookshelf. https://www.ncbi.nlm.nih.gov/books/NBK544320/

Restivo, L., Vetere, G., Bontempi, B., & Ammassari-Teule, M. (2009). The Formation of Recent and Remote Memory Is Associated with Time-Dependent Formation of Dendritic Spines in the Hippocampus and Anterior Cingulate Cortex. The Journal of Neuroscience, 29(25), 8206–8214. https://doi.org/10.1523/jneurosci.0966-09.2009

Rho, H., Kim, J., & Lee, S. (2018). Function of selective neuromodulatory projections in the mammalian cerebral cortex: comparison between cholinergic and noradrenergic systems. Frontiers in Neural Circuits, 12. https://doi.org/10.3389/fncir.2018.00047

Rich, E. L., & Shapiro, M. L. (2009). RAT prefrontal cortical neurons selectively code strategy switches. The Journal of Neuroscience, 29(22), 7208–7219. https://doi.org/10.1523/jneurosci.6068-08.2009

Riedemann, T. (2019). Diversity and function of Somatostatin-Expressing interneurons in the cerebral cortex. International Journal of Molecular Sciences, 20(12), 2952. https://doi.org/10.3390/ijms20122952

Robinson, L., Thompson, J., Gallagher, P., Goswami, U., Young, A. H., Ferrier, I. N., & Moore, P. A. (2006). A meta-analysis of cognitive deficits in euthymic patients with bipolar disorder. Journal of Affective Disorders, 93(1–3), 105–115. https://doi.org/10.1016/j.jad.2006.02.016

Rodriguez, A. M., & Festini, S. B. (2022). Working Memory Defcits in Alzheimer's Disease. Psychology, 6(1), 19–22.

Rodriguez, G., Sarazin, M., Clemente, A., Holden, S. S., Paz, J. T., & Delord, B. (2018). Conditional bistability, a generic cellular mnemonic mechanism for robust and flexible working memory computations. The Journal of Neuroscience, 38(22), 5209–5219. https://doi.org/10.1523/jneurosci.1992-17.2017

Romo, R., Brody, C. D., Hernandez, A., & Lemus, L. (1999). Neuronal correlates of parametric working memory in the prefrontal cortex. Nature, 399(6735), 470–473. https://doi.org/10.1038/20939

Roth, T., Roehrs, T., Wittig, R. M., & Zorick, F. (1984). Benzodiazepines and memory. British Journal of Clinical Pharmacology, 18(S1), 45S-49S. https://doi.org/10.1111/j.1365-2125.1984.tb02581.x

Rubenstein, J. L., & Merzenich, M. M. (2003). Model of autism: increased ratio of excitation/inhibition in key neural systems. Genes, Brain and Behavior, 2(5), 255–267. https://doi.org/10.1034/j.1601-183x.2003.00037.x

Rudy, B., Fishell, G., Lee, S. H., & Hjerling-Leffler, J. (2010). Three groups of interneurons account for nearly 100% of neocortical GABAergic neurons. Developmental Neurobiology, 71(1), 45–61. https://doi.org/10.1002/dneu.20853

Rudy, B., & McBain, C. J. (2001). Kv3 channels: voltage-gated K+ channels designed for high-frequency repetitive firing. Trends in Neurosciences, 24(9), 517–526. https://doi.org/10.1016/s0166-2236(00)01892-0

Runyan, J. D., Moore, A. N., & Dash, P. K. (2004). A role for prefrontal cortex in memory storage for trace fear conditioning. The Journal of Neuroscience, 24(6), 1288–1295. https://doi.org/10.1523/jneurosci.4880-03.2004

Sakmann, B., & Neher, E. (1995). Single-Channel recording. In Springer eBooks. https://doi.org/10.1007/978-1-4419-1229-9

Salmond, C. H., Chatfield, D. A., Menon, D. K., Pickard, J. D., & Sahakian, B. J. (2005). Cognitive sequelae of head injury: involvement of basal forebrain and associated structures. Brain, 128(1), 189–200. https://pubmed.ncbi.nlm.nih.gov/15548553/

Salmond, C. H., & Sahakian, B. J. (2005). Cognitive outcome in traumatic brain injury survivors. Current Opinion in Critical Care, 11(2), 111–116. https://doi.org/10.1097/01.ccx.0000155358.31983.37

Satake, T., Mitani, H., Nakagome, K., & Kaneko, K. (2008). Individual and additive effects of neuromodulators on the slow components of afterhyperpolarization currents in layer V pyramidal cells of the rat medial prefrontal cortex. Brain Research, 1229, 47–60. https://doi.org/10.1016/j.brainres.2008.06.098

Saunders, N. L., & Summers, M. J. (2009). Attention and working memory deficits in mild cognitive impairment. Journal of Clinical and Experimental Neuropsychology, 32(4), 350–357. https://doi.org/10.1080/13803390903042379

Schultz, W. (2001). Book review: Reward Signaling by Dopamine Neurons. The Neuroscientist, 7(4), 293–302. https://doi.org/10.1177/107385840100700406

Seamans, J. K., Floresco, S., & Phillips, A. G. (1995). Functional differences between the prelimbic and anterior cingulate regions of the rat prefrontal cortex. Behavioral Neuroscience, 109(6), 1063–1073. https://doi.org/10.1037/0735-7044.109.6.1063

Seamans, J. K., Gorelova, N., & Yang, C. R. (1997). Contributions of Voltage-Gated Ca2+Channels in the Proximal versus Distal Dendrites to Synaptic Integration in Prefrontal Cortical Neurons. The Journal of Neuroscience, 17(15), 5936–5948. https://doi.org/10.1523/jneurosci.17-15-05936.1997

Seamans, J. K., Lapish, C. C., & Durstewitz, D. (2008). Comparing the prefrontal cortex of rats and primates: Insights from electrophysiology. Neurotoxicity Research, 14(2–3), 249–262. https://doi.org/10.1007/bf03033814

Seidemann, E., Meilijson, I., Abeles, M., Bergman, H., & Vaadia, E. (1996). Simultaneously recorded single units in the frontal cortex go through sequences of discrete and stable states in monkeys

performing a delayed localization task. The Journal of Neuroscience, 16(2), 752–768. https://doi.org/10.1523/jneurosci.16-02-00752.1996

Selkoe, D. J. (2002). Alzheimer's disease is a synaptic failure. Science, 298(5594), 789–791. https://doi.org/10.1126/science.1074069

Semple, B. D., Blomgren, K., Gimlin, K., Ferriero, D. M., & Noble-Haeusslein, L. J. (2013). Brain development in rodents and humans: Identifying benchmarks of maturation and vulnerability to injury across species. Progress in Neurobiology, 106–107, 1–16. https://doi.org/10.1016/j.pneurobio.2013.04.001

Serra, L., Perri, R., Cercignani, M., Spanò, B., Fadda, L., Marra, C., Carlesimo, G. A., Caltagirone, C., & Bozzali, M. (2010). Are the Behavioral Symptoms of Alzheimer's Disease Directly Associated with Neurodegeneration? Journal of Alzheimer's Disease, 21(2), 627–639. https://doi.org/10.3233/jad-2010-100048

Seung, H. S., Lee, D. D., Reis, B. Y., & Tank, D. W. (2000). Journal of Computational Neuroscience. Journal of Computational Neuroscience, 9(2), 171–185. https://doi.org/10.1023/a:1008971908649

Shafi, M. M., Zhou, Y., Quintana, J., Chow, C. C., Fuster, J. M., & Bodner, M. (2007). Variability in neuronal activity in primate cortex during working memory tasks. Neuroscience, 146(3), 1082–1108. https://doi.org/10.1016/j.neuroscience.2006.12.072

Shah, V. N., Chagot, B., & Chazin, W. J. (2006). Calcium-Dependent regulation of ion channels. HAL (Le Centre Pour La Communication Scientifique Directe), 1(4), 203–212. https://hal.archives-ouvertes.fr/hal-01652606

Shao, J., Yh, L., Gao, D., Tu, J., & Yang, F. (2021). Neural burst firing and its roles in mental and neurological disorders. Frontiers in Cellular Neuroscience, 15. https://doi.org/10.3389/fncel.2021.741292

Sidiropoulou, K., Lu, F., Fowler, M., Xiao, R., Phillips, C., Ozkan, E. D., Zhu, M. X., White, F. J., & Cooper, D. (2009). Dopamine modulates an mGluR5-mediated depolarization underlying prefrontal persistent activity. Nature Neuroscience, 12(2), 190–199. https://doi.org/10.1038/nn.2245

Sieber, A. R., Min, R., & Nevian, T. (2013). Non-Hebbian Long-Term potentiation of inhibitory synapses in the thalamus. The Journal of Neuroscience, 33(40), 15675–15685. https://doi.org/10.1523/jneurosci.0247-13.2013

Sisodia, S. S. (1999). Series Introduction: Alzheimer's disease: perspectives for the new millennium. Journal of Clinical Investigation, 104(9), 1169–1170. https://doi.org/10.1172/jci8508

Smith, C. J., Xiong, G., Elkind, J. A., Putnam, B., & Cohen, A. S. (2015). Brain injury impairs working memory and prefrontal circuit function. Frontiers in Neurology, 6. https://doi.org/10.3389/fneur.2015.00240

Smith, J. B., & Alloway, K. D. (2013). Rat whisker motor cortex is subdivided into sensory-input and motor-output areas. Frontiers in Neural Circuits, 7. https://doi.org/10.3389/fncir.2013.00004

Sohal, V. S., Huntsman, M. M., & Huguenard, J. R. (2000). Reciprocal inhibitory connections regulate the spatiotemporal properties of intrathalamic oscillations. The Journal of Neuroscience, 20(5), 1735–1745. https://doi.org/10.1523/jneurosci.20-05-01735.2000

Sohal, V. S., & Rubenstein, J. L. (2019). Excitation-inhibition balance as a framework for investigating mechanisms in neuropsychiatric disorders. Molecular Psychiatry, 24(9), 1248–1257. https://doi.org/10.1038/s41380-019-0426-0

Soraggi-Frez, C., Santos, F. H. D., Albuquerque, P. B., & Malloy-Diniz, L. F. (2017). Disentangling working Memory Functioning in Mood States of Bipolar Disorder: A Systematic review. Frontiers in Psychology, 8. https://doi.org/10.3389/fpsyg.2017.00574

Stephens, E. K., Baker, A. L., & Gulledge, A. T. (2018). Mechanisms underlying serotonergic excitation of callosal projection neurons in the mouse medial prefrontal cortex. Frontiers in Neural Circuits, 12. https://doi.org/10.3389/fncir.2018.00002

Straus, M. A., Gelles, R. J., & Steinmetz, S. K. (2006). Behind Closed Doors - Violence in the American Family. Transaction Publishers.

Strübing, C., Krapivinsky, G., Krapivinsky, L., & Clapham, D. E. (2001). TRPC1 and TRPC5 form a novel cation channel in mammalian brain. Neuron, 29(3), 645–655. https://doi.org/10.1016/s0896-6273(01)00240-9

Stuss, D. T. (2011). Functions of the frontal lobes: relation to executive functions. Journal of the International Neuropsychological Society, 17(05), 759–765. https://doi.org/10.1017/s1355617711000695

Subkhankulova. (2010). Grouping and classifying electrophysiologically-defined classes of neocortical neurons by single cell, whole-genome expression profiling. Frontiers in Molecular Neuroscience. https://doi.org/10.3389/fnmol.2010.00010

Sugawara, T., Hisatsune, C., Le, T. D., Hashikawa, T., Hirono, M., Hattori, M., Nagao, S., & Mikoshiba, K. (2013). Type 1 inositol trisphosphate receptor regulates cerebellar circuits by maintaining the spine morphology of purkinje cells in adult mice. The Journal of Neuroscience, 33(30), 12186–12196. https://doi.org/10.1523/jneurosci.0545-13.2013

Sumi, T., & Harada, K. (2020). Mechanism underlying hippocampal long-term potentiation and depression based on competition between endocytosis and exocytosis of AMPA receptors. Scientific Reports, 10(1). https://doi.org/10.1038/s41598-020-71528-3

Surmeier, D. J., Ding, J., Day, M., Wang, Z., & Shen, W. (2007). D1 and D2 dopamine-receptor modulation of striatal glutamatergic signaling in striatal medium spiny neurons. Trends in Neurosciences, 30(5), 228–235. https://doi.org/10.1016/j.tins.2007.03.008

Tahvildari, B., Alonso, A., & Bourque, C. W. (2008). Ionic Basis of on and off Persistent Activity in Layer III Lateral Entorhinal Cortical Principal Neurons. Journal of Neurophysiology, 99(4), 2006–2011. https://doi.org/10.1152/jn.00911.2007

Takashima, A., Petersson, K. M., Rutters, F., Tendolkar, I., Jensen, O., Zwarts, M., McNaughton, B. L., & Fernández, G. (2006). Declarative memory consolidation in humans: A prospective functional magnetic resonance imaging study. Proceedings of the National Academy of Sciences of the United States of America, 103(3), 756–761. https://doi.org/10.1073/pnas.0507774103

Takehara-Nishiuchi, K., Kawahara, S., & Kirino, Y. (2005). NMDA receptor-dependent processes in the medial prefrontal cortex are important for acquisition and the early stage of consolidation during trace, but not delay eyeblink conditioning. Learning & Memory, 12(6), 606–614. https://doi.org/10.1101/lm.5905

Tarlungeanu, D., & Novarino, G. (2018). Genomics in neurodevelopmental disorders: an avenue to personalized medicine. Experimental and Molecular Medicine, 50(8), 1–7. https://doi.org/10.1038/s12276-018-0129-7

Teixeira, C. M., Pomedli, S. R., Maei, H. R., Kee, N., & Frankland, P. W. (2006). Involvement of the Anterior Cingulate Cortex in the Expression of Remote Spatial Memory. The Journal of Neuroscience, 26(29), 7555–7564. https://doi.org/10.1523/jneurosci.1068-06.2006

Telias, M., & Segal, M. (2022). Editorial: Pathological hyperactivity and hyperexcitability in the central nervous system. Frontiers in Molecular Neuroscience, 15. https://doi.org/10.3389/fnmol.2022.955542

Thuault, S., Malleret, G., Constantinople, C. M., Nicholls, R. E., Chen, I., Zhu, J., Panteleyev, A. A., Vronskaya, S., Nolan, M. F., Bruno, R. M., Siegelbaum, S. A., & Kandel, E. R. (2013). Prefrontal cortex HCN1 channels enable intrinsic persistent neural firing and executive memory function. The Journal of Neuroscience, 33(34), 13583–13599. https://doi.org/10.1523/jneurosci.2427-12.2013

Trobe, J. D. (2010). The Human Brain. An Introduction to Its Functional Anatomy, 6th edition. Journal of Neuro-ophthalmology, 30(1), 107. https://doi.org/10.1097/01.wno.0000369168.32606.54

Tronel, S., Feenstra, M. G., & Sara, S. J. (2004). Noradrenergic action in prefrontal cortex in the late stage of memory consolidation. Learning & Memory, 11(4), 453–458. https://doi.org/10.1101/lm.74504

Tronel, S., & Sara, S. J. (2003). Blockade of NMDA receptors in prelimbic cortex induces an enduring amnesia for Odor–Reward associative learning. The Journal of Neuroscience, 23(13), 5472–5476. https://doi.org/10.1523/jneurosci.23-13-05472.2003

Tseng, G., & Haberly, L. B. (1989). Deep neurons in piriform cortex. II. Membrane properties that underlie unusual synaptic responses. Journal of Neurophysiology, 62(2), 386–400. https://doi.org/10.1152/jn.1989.62.2.386

Tucker, L. B., Fu, A. H., & McCabe, J. T. (2016). Performance of male and female C57BL/6J mice on motor and cognitive tasks commonly used in Pre-Clinical Traumatic Brain Injury research. Journal of Neurotrauma, 33(9), 880–894. https://doi.org/10.1089/neu.2015.3977

Utermohlen, W. J. (2008). Portraits from the Mind: The Works of William Utermohlen—1955 to 2000: A Retrospective of the Artist's Work Before and After his Diagnosis. Alzheimer's Association ; Myriad Pharmaceuticals, Inc., Chicago, IL, Salt Lake City, UT. https://www.worldcat.org/title/portraits-from-the-mind-the-works-of-william-utermohlen-1955-to-2000-a-retrospective-of-the-artists-work-before-and-after-his-diagnosis-with-alzheimers-disease/oclc/239423099

Vergara, C., Latorre, R., Marrion, N. V., & Adelman, J. P. (1998). Calcium-activated potassium channels. Current Opinion in Neurobiology, 8(3), 321–329. https://doi.org/10.1016/s0959-4388(98)80056-1

Veselis, R. A., Reinsel, R. A., Feshchenko, V. A., & Johnson, R. (2004). Information Loss over Time Defines the Memory Defect of Propofol. Anesthesiology, 101(4), 831–841. https://doi.org/10.1097/00000542-200410000-00006

Vo, H. T., Schacht, R. L., Mintzer, M. Z., & Fishman, M. (2014). Working memory impairment in cannabis- and Opioid-Dependent adolescents. Substance Abuse, 35(4), 387–390. https://doi.org/10.1080/08897077.2014.954027

Vogt, B. A., & Gabriel, M. (1993). Neurobiology of cingulate cortex and limbic thalamus : a comprehensive handbook. Birkhäuser.

Vogt, O. (1906). Ueber strukturelle Hirncentra mit besonderer Berücksichtigung der strukturellen Felder des Cortex pallii (Mit 66 Abbildungen). Anat. Anz.

Voskobiynyk, Y., Roth, J. R., Cochran, J. N., Rush, T., Carullo, N. V., Mesina, J. S., Waqas, M., Vollmer, R. M., Day, J. J., McMahon, L. L., & Roberson, E. D. (2020). Alzheimer's disease risk gene BIN1 induces Tau-dependent network hyperexcitability. eLife, 9. https://doi.org/10.7554/elife.57354

Walker, D. S., & De Waard, M. (1998). Subunit interaction sites in voltage-dependent Ca2+ channels: role in channel function. Trends in Neurosciences, 21(4), 148–154. https://doi.org/10.1016/s0166-2236(97)01200-9

Wang, H., Jing, R., Trexler, C., Li, Y., Tang, H., Pan, Z., Zhu, S., Zhao, B., Fang, X., Liu, J., Chen, J., & Ouyang, K. (2018). Deletion of IP3R1 by Pdgfrb-Cre in mice results in intestinal pseudo-obstruction and lethality. Journal of Gastroenterology, 54(5), 407–418. https://doi.org/10.1007/s00535-018-1522-7

Wang, J., Ou, S., & Wang, Y. (2017). Distribution and function of voltage-gated sodium channels in the nervous system. Channels, 11(6), 534–554. https://doi.org/10.1080/19336950.2017.1380758

Wang, X. J. (2001). Synaptic reverberation underlying mnemonic persistent activity. Trends in Neurosciences, 24(8), 455–463. https://doi.org/10.1016/s0166-2236(00)01868-3

Wang, X., Meng, Z., Wang, J., Zhou, H., Wu, Y., & Wu, J. (2018). Enriched environment improves working memory impairment of mice with traumatic brain injury by enhancing histone acetylation in the prefrontal cortex. PeerJ, 6, e6113. https://doi.org/10.7717/peerj.6113

Watson, C., Paxinos, G., & Puelles, L. (2012). The mouse nervous system. ELSEVIER. https://www.sciencedirect.com/book/9780123694973/the-mouse-nervous-system

Wende, H., Lechner, S., Cheret, C., Bourane, S., Kolanczyk, M. E., Pattyn, A., Reuter, K., Munier, F. L., Carroll, P., Lewin, G. R., & Birchmeier, C. (2012). The transcription factor C-MAF controls touch receptor development and function. Science, 335(6074), 1373–1376. https://doi.org/10.1126/science.1214314

Winder, C. V., Wax, J., Serrano, B., Jones, E. M., & McPhee, M. L. (1963). Anti-inflammatory and antipyretic properties of N-(α,α,α-Trifluoro-m-tolyl) anthranilic acid (CI-440; flufenamic acid). Arthritis & Rheumatism, 6(1), 36–47. https://doi.org/10.1002/art.1780060105

Wong, L., Singh, S., Wang, H., Hsu, C., Hu, S., & Lee, W. (2019). FOXG1-Related Syndrome: From clinical to molecular genetics and pathogenic mechanisms. International Journal of Molecular Sciences, 20(17), 4176. https://doi.org/10.3390/ijms20174176

Woolsey, T. A., & Van Der Loos, H. (1970). The structural organization of layer IV in the somatosensory region (S I) of mouse cerebral cortex. Brain Research, 17(2), 205–242. https://doi.org/10.1016/0006-8993(70)90079-x

Wu, D., Deng, H., Xiao, X., Zuo, Y., Sun, J., & Wang, Z. (2017). Persistent Neuronal Activity in Anterior Cingulate Cortex Correlates with Sustained Attention in Rats Regardless of Sensory Modality. Scientific Reports, 7(1). https://doi.org/10.1038/srep43101

Xiang, M. (2019). Serotonin receptors 2A and 1A modulate anxiety-like behavior in post-traumatic stress disordered mice. PubMed Central (PMC). https://www.ncbi.nlm.nih.gov/pmc/articles/PMC6511758/#:~:text=5%2DHT2A%20and%205%2DHT1A%20receptors%20have%20been%20reported%20to,stress%20%5B41%2D43%5D.

Xiang, Z., Thompson, A. D., Jones, C. K., Lindsley, C. W., & Conn, P. J. (2011). Roles of the M1 muscarinic acetylcholine receptor subtype in the regulation of basal ganglia function and implications for the treatment of Parkinson's disease. Journal of Pharmacology and Experimental Therapeutics, 340(3), 595–603. https://doi.org/10.1124/jpet.111.187856

Xu, P., Ai, C., Li, Y., Xing, X., & Lu, H. (2019). Medial prefrontal cortex in neurological diseases. Physiological Genomics, 51(9), 432–442. https://doi.org/10.1152/physiolgenomics.00006.2019

Yan, H., Villalobos, C., & Andrade, R. (2009). TRPC channels mediate a muscarinic Receptor-Induced afterdepolarization in cerebral cortex. The Journal of Neuroscience, 29(32), 10038–10046. https://doi.org/10.1523/jneurosci.1042-09.2009

Yang, S., Shi, Y., Wang, Q., Peng, J., & Li, B. (2014). Neuronal representation of working memory in the medial prefrontal cortex of rats. Molecular Brain, 7(1). https://doi.org/10.1186/s13041-014-0061-2

Yi, J. H., Whitcomb, D. J., Park, S. J., Martinez-Perez, C., Barbati, S. A., Mitchell, S. J., & Cho, K. (2020). M1 muscarinic acetylcholine receptor dysfunction in moderate Alzheimer's disease pathology. Brain Communications, 2(2). https://doi.org/10.1093/braincomms/fcaa058

Yizhar, O., Fenno, L. E., Prigge, M., Schneider, F., Davidson, T. J., O'Shea, D. J., Sohal, V. S., Goshen, I., Finkelstein, J., Paz, J. T., Stehfest, K., Fudim, R., Ramakrishnan, C., Huguenard, J. R., Hegemann, P., & Deisseroth, K. (2011). Neocortical excitation/inhibition balance in information processing and social dysfunction. Nature, 477(7363), 171–178. https://doi.org/10.1038/nature10360

Young, C., & Yang, C. R. (2004). Dopamine D1/D5 Receptor Modulates State-Dependent Switching of Soma-Dendritic Ca2+Potentials via Differential Protein Kinase A and C Activation in Rat Prefrontal Cortical Neurons. The Journal of Neuroscience, 24(1), 8–23. https://doi.org/10.1523/jneurosci.1650-03.2004

Younkin, S. G. (1998). The role of Aβ42 in Alzheimer's disease. Journal of Physiology-paris, 92(3–4), 289–292. https://doi.org/10.1016/s0928-4257(98)80035-1

Yu, W., Appler, J. M., Kim, Y., Nishitani, A. M., Holt, J. R., & Goodrich, L. V. (2013). A Gata3–Mafb transcriptional network directs post-synaptic differentiation in synapses specialized for hearing. eLife, 2. https://doi.org/10.7554/elife.01341

Yuan, Y., Leung, A., Duan, H., Zhang, L., Zhang, K., Wu, J., & Qin, S. (2016). The effects of long-term stress on neural dynamics of working memory processing: An investigation using ERP. Scientific Reports, 6(1). https://doi.org/10.1038/srep23217

Zhang, Z., Matos, S. C., Jego, S., Adamantidis, A., & Séguéla, P. (2013). Norepinephrine Drives Persistent Activity in Prefrontal Cortex via Synergistic α1 and α2 Adrenoceptors. PLOS ONE, 8(6), e66122. https://doi.org/10.1371/journal.pone.0066122

Zhang, Z., & Séguéla, P. (2010). Metabotropic induction of persistent activity in layers II/III of anterior cingulate cortex. Cerebral Cortex, 20(12), 2948–2957. https://doi.org/10.1093/cercor/bhq043

Zhao, Y., Flandin, P., Long, J. E., Cuesta, M. D., Westphal, H., & Rubenstein, J. L. (2008). Distinct molecular pathways for development of telencephalic interneuron subtypes revealed through analysis of Lhx6 mutants. Journal of Comparative Neurology, 510(1), 79–99. https://doi.org/10.1002/cne.21772

Zhou, Y., Song, W. M., Andhey, P. S., Swain, A., Levy, T., Miller, K. R., Poliani, P. L., Cominelli, M., Grover, S., Gilfillan, S., Cella, M., Ulland, T. K., Zaitsev, K., Miyashita, A., Ikeuchi, T., Sainouchi, M., Kakita, A., Bennett, D. A., Schneider, J. A., . . . Colonna, M. (2020). Human and mouse single-nucleus transcriptomics reveal TREM2-dependent and TREM2-independent cellular responses in Alzheimer's disease. Nature Medicine, 26(1), 131–142. https://doi.org/10.1038/s41591-019-0695-9

Zokaei, N., & Husain, M. (2019). Working memory in Alzheimer's disease and Parkinson's disease. In Current topics in behavioral neurosciences (pp. 325–344). https://doi.org/10.1007/7854_2019_103

Zufall, F., Hatt, H., & Keil, T. A. (1991). A Calcium-Activated Nonspecific Cation Channel From Olfactory Receptor Neurones of the Silkmoth Antheraea Polyphemus. The Journal of Experimental Biology, 161(1), 455–468. https://doi.org/10.1242/jeb.161.1.455

Zylberberg, J., & Strowbridge, B. W. (2017). Mechanisms of persistent activity in cortical circuits: possible neural substrates for working memory. Annual Review of Neuroscience, 40(1), 603–627. https://doi.org/10.1146/annurev-neuro-070815-014006